Modern Thermal Power Plants

Aspects on Modelling and Evaluation

Klas Jonshagen

LUND
UNIVERSITY

January 20th 2011
Doctoral thesis
Division of Thermal Power Engineering
Department of Energy Sciences
Lund University
Sweden

Division of Thermal Power Engineering
Department of Energy Sciences
Lund University
Sweden

ISBN 978-91-7473-070-8
ISSN 0282-1990
ISRN LUTMDN/TMHP-10/1075-SE

Printed in Sweden by E-huset Tryckeri
Lund 2010

To Louise

Abstract

The European Union (EU) has laid down very clear objectives for the reduction of greenhouse gases in the hope that it will prevent or mitigate climate change. Political incentives are used to make the power industry adopt changes in order to reach these EU targets. In this thesis, some solutions that could help power companies meet the EU objectives are evaluated. Thermodynamic models have been developed to evaluate the proposed methods. A description of the models and the way in which they are used to model power plant cycles in off-design mode is included in this thesis.

The focus was on combined-cycle power plants, which have the highest efficiency among commercial power plants today. Three ways of adapting power plants so as to meet the EU targets were formulated:

- reduced CO_2 emissions
- increased use of biofuels
- improved part-load abilities

A new method based on using low-grade heat when implementing carbon capture in a combined cycle power plant is presented. The results show that the method can increase the total efficiency and reduce the initial cost of the power plant. The method is applicable for both retrofitting to existing plants and for new plants. The effect of using low-calorific bio-fuels in a combined-cycle power plant was investigated. The results show that below a heating value of about 20-25 MJ/kg the plant quickly departs from its design point. The supply of power to the national grid is expected to be fluctuate more in the future due to the uneven availability of wind and solar power. Therefore, two part-load operation strategies were evaluated. The first involves a strategy that entails less wear on the gas turbine, which could extend the maintenance interval of the unit. The second method combines two well-established part-load strategies for part-load operation of steam-cycle power plants. The combination of the two methods will increase the part-load efficiency of the power plant.

Key words: Combined cycle, CO_2, carbon capture, heat- and mass-balance modelling, T-Q diagram

Populärvetenskaplig sammanfattning

Jordens medeltemperatur har ökat stadigt de senaste hundra åren. Det har skett samtidigt som vårt eget användande av fossila bränslen ökat och många forskare ser paralleller mellan dessa två utvecklingar.

När fossila bränslen förbränns frigörs kol, i form av koldioxid, som sedan miljontals år har varit isolerat från jordens atmosfär. Det gör att koldioxidhalten i atmosfären ökar, vilket påverkar jordens klimat. Koldioxid är en av de så kallade växthusgaserna som finns i jordens atmosfär. Dessa gaser ger upphov till den så kallade växthuseffekten. Växthusgaserna hindrar en del av solens strålar från att nå jorden men reflekterar även tillbaka en del av den strålning som jorden avger. Den totala effekten av växthusgaserna är att jordens globala genomsnittstemperatur ökar. Vårt ekosystem är beroende av växthusgaserna vars effekt höjer medeltemperaturen med cirka 33 °C [1]. Med ökade halter av koldioxid i atmosfären förväntas effekten tillta vilket kan få stora konsekvenser så som stigande havsnivåer och växande ökenområden.

För två år sedan, 2008, stod el- och värmeproduktion för drygt 40% av den koldioxid som vi människor släpper ut [2]. Näst mest kommer från transportsektorn som stod för drygt 20% av utsläppen.

Många globala organisationer har uppmärksammat problemet med de ökande koldioxidutsläppen och den europeiska unionen (EU) har satt upp mycket konkreta mål som bland annat styr hur stora koldioxidutsläppen får lov att vara om tio år.

Att ersätta fossila bränslen med sol och vindkraft är ett effektivt sätt att minska utsläppen av koldioxid men den omställningen kommer att ta tid. För att uppnå en så snabb förändring som EUs målsättningar kräver behövs metoder som gör fossilt eldade kraftverk mer koldioxidneutrala.

I den här avhandlingen presenteras ett par olika metoder för att minska utsläppen från termiska kraftverk d.v.s. kraftverk som innefattar någon sorts förbränning. För att utvärdera de metoderna har en beräkningsmetod som kallas värme- och massbalans modellering använts. Genom termodynamiska ekvationer kan de termodynamiska tillstånden i kraftverkscykler beräknas. Den här typen av modellering gör det möjligt att beräkna till exempel vilken verkningsgrad en kraftverkscykel kommer att få utan att fysiska experiment krävs.

Metoderna för att minska koldioxidutsläppen som behandlas i den här avhandlingen är koldioxidavskiljning, ersättning av naturgas med biogas i ett kombikraftverk och förbättrade dellast egenskaper i kraftverk.

Med koldioxidavskiljning menas att koldioxiden separeras någonstans i processen och sedan trycksätts, kondenseras och pumpas ner i marken där den kan hållas isolerad från atmosfären. Den här avhandlingen fokuserar på en metod för koldioxidavskiljning som kallas "post-combustion" och bygger på att man separerar koldioxiden efter förbränningen. Att separera och trycksätta koldioxiden är energikrävande och kommer konsumera en del av den energi som frigörs när bränslet förbränns. Dessutom är avskiljningsanläggningen dyr.

För att upprätthålla en så hög elproduktion som möjligt när koldioxidavskiljning integreras i ett kraftverk bör integreringen ske så att kraftverket påverkas i så liten utsträckning som möjligt. Oftast hämtas energin till att driva separations-anläggningen genom att tappa av ånga från kraftverkets turbin, vilket gör att det inte går att producera lika mycket el. Den här avhandlingen tar upp en integreringsmetod som bygger på att värme i första hand hämtas tidigare i kraftverkscykeln så att kraftproduktionen inte störs i lika stor utsträckning.

Att ersätta vår användning av fossila bränslen med biobränslen är ett annat sätt att minska nettotillförseln av koldioxid i atmosfären. Biobränslen är förnybara vilket innebär att de naturligt reproduceras i samma takt som de konsumeras. Men eftersom dessa bränslen har helt andra egenskaper jämfört med de fossila motsvarigheterna kan man i moderna kraftverk sällan byta bränsle rakt av. Den här avhandlingen innehåller en studie som visar effekterna i en kraftverkstyp (kombikraftverk) när inblandning av biobränsle ökas från 0-100%.

Utmaningen inför framtiden, då en betydande del av kraftproduktionen kommer från sol- och vindkraft, blir att balansera nätet för upp- och nedgångar i en sådan kraftproduktion. För att klara det krävs snabbreglerande kraftverk. Den här avhandlingen tar upp två typer av regleringsstrategier för kraftverk som kan förbättra dellastegenskaperna för termiska kraftverk.

Papers

This thesis is based on the following papers, which will be referred to in the text by their Roman numerals. The papers are appended at the end of the thesis.

Paper I K. Jonshagen, M. Sammak, M. Genrup
Post-Combustion CO_2 Capture on Combined Cycles Utilizing Hot-Water for Absorbent Regeneration
Submitted to ASME Turbo Expo 2011, GT2011-45678 Vancouver, Canada, June 2011

Paper II K. Jonshagen, N. Sipöcz, M. Genrup
A Novel Approach of Retrofitting a Combined Cycle with Post-Combustion CO_2 Capture
Journal of Engineering for Gas Turbines and Power, January 2011, Vol. 133 / 011703-1

Paper III N. Sipöcz, K. Jonshagen, M. Genrup
Novel High-Performing Single-Pressure Combined Cycle with CO_2 Capture
Journal of Engineering for Gas Turbines and Power, April 2011, Vol. 133 / 041701-1

Paper IV M. Sammak, K. Jonshagen, M. Thern, E. Thorbergsson, T. Grönstedt, A. Dahlquist, M. Genrup
Conceptual Design of a Mid-Sized Semi-Closed Oxyfuel Cycle
Submitted to ASME Turbo Expo 2011, GT2011-46299, Vancouver, Canada, June 2011

Paper V K. Jonshagen, P. Eriksson, M. Genrup
Low-Calorific Fuel Mix in a Large Size Combined-Cycle Plant
Presented at ASME Turbo Expo 2009 in Orlando, Florida, June 2009

Paper VI K. Jonshagen, M. Genrup
Improved Load Control for a Steam Cycle Combined Heat and Power Plant
Energy 35 (2010) 1694-1700

Paper VII K. Jonshagen, P. Eriksson, M. Genrup
Improved Load Control Strategy for Large-Sized Combined Cycles
Presented at ECOS 2009, Foz do Iguaçu, Paraná, Brazil, September 2009

Papers outside thesis

Paper VIII: P. O. Johansson, K. Jonshagen, M. Genrup
Influence of District Heating Temperature Level on a CHP Station
Presented at ECOS 2009, Foz do Iguaçu, Paraná, Brazil, September 2009

Paper IX: P. Eriksson, J. Klingmann, K. Jonshagen, M. Genrup
Re-Sizing of a Natural Gas Fired Two-Shaft Gas Turbine for Low Calorific Gas Operation
Presented at ASME Turbo Expo 2009 in Orlando, Florida, GT2009-60386, June 2009

Paper X: P. Eriksson, K. Jonshagen, M. Genrup, J. Klingmann
Off-Design Performance Investigation Of a Low Calorific Gas Fired Two-Shaft Gas Turbine
Presented at ASME Turbo Expo 2009 in Orlando, GT2009-59067, Florida, June 2009

Paper XI: K. Jonshagen, M. Assadi
Thermodynamic Investigation for Optimal Integration of a Solid Waste Boiler in an Existing Biomass Fueled Plant at ENA Energy
Presented at IGEC-III 2007, Västerås, Sweden June 2007

Contents

Nomenclature

Arabic

Symbol	*Unit*	*Description*
A	[m^2]	Area
C	[...]	Constant
c	[m/s]	Speed
c_p	[kJ/(kg·K)]	Specific heat
C_P	[-]	Pressure recovery coefficient
D	[m]	Diameter
h	[kJ/kg]	Enthalpy
l	[m]	Length
LMTD	[K]	Logarithmic mean temperature difference
n	[rev/s]	Rotational speed
$\dot{m}$	[kg/s]	Mass flow
p	[kPa]	Pressure
Pr	[-]	Prandtl number
Re	[-]	Reynolds number
RNI	[-]	Reynolds number index
S	[kJ/(kg·K)]	Entropy
T	[K]	Temperature
t	[m]	Thickness
U	[W/(K·m^2)]	Heat transfer coefficient
u	[m/s]	Rotor speed
w	[m/s]	Relative speed
y	[kg/kg]	Moisture content
$\dot{Q}$	[kW]	Heat flux

Greek

Symbol	*Unit*	*Description*
α	[W/(K·m^2)]	Heat transfer coefficient
α	[-]	Baumann factor
γ	[-]	Isentropic exponent
Δ	[-]	Difference
λ	[W/(K·m)]	Heat conductivity
Λ	[-]	Stage correction factor
μ	[kg/(m·s)]	Dynamic viscosity
ν	[m^3/kg]	Specific volume
ξ	[-]	Friction coefficient

ρ	[kg/(m^3)]	Density
φ	[-]	Flange efficiency
X	[-]	Parson number

Subscript

0	Stagnation
c	Cold
d	Droplet
des	Design
gen	Generation
h	Hot
i	Inner
in	Inlet
o	Outer
out	Outlet
ref	Reference
s	Static
w	Wall
θ	In rotational direction

Superscript

$\bar{}$	Mean value

Abbreviations

CCPP	Combined cycle power plant
COT	Combustor outlet temperature
EGT	Exhaust gas temperature
FN	Flow number
HRSG	Heat recovery steam generator
ISO	International Organization for Standardization
ISO TIT	ISO Turbine inlet temperature
LHV	Lower heating value
SCOC-CC	Semi-Closed-Oxy-Combusted-Combined-Cycle
SOT	Stator outlet temperature
VIGV	Variable inlet guide vanes

1 Introduction

1.1 Background

Observations of warming of the climate system with increases in global average air and ocean temperatures, melting of snow and ice, and rising global average sea level has caused a considerable concern in society. Much research has focused on finding the cause of this temperature increase. Several theories describing the causes of this observation have been developed, the most generally accepted is that the increase in the Earth's temperature is caused by the emission of carbon dioxide, CO_2, and other so-called greenhouse gases into the Earth's atmosphere.

In response to these theories, the European Union (EU) has announced very clear objectives aimed at reducing the emission of greenhouse gases in the hope that this will prevent or mitigate climate change. Other global organisations have similar objectives, but these have not been expressed as clearly. According to the EU, "Climate change could reach catastrophic levels this century unless we quickly and sharply reduce emissions of greenhouse gases" [3]. Furthermore, "The EU needs more secure energy sources, i.e. less dependence on imports of foreign oil and gas." [3]. The following objectives have been defined by the EU to solve these issues [3] (note that they are unformatted quotations):

- Cutting greenhouse gases by at least 20% of 1990 levels (30% if other developed countries commit to comparable cuts)
- Increasing use of renewables (wind, solar, biomass, etc) to 20% of total energy production (currently ± 8.5%)
- Cutting energy consumption by 20% of projected 2020 levels - by improving energy efficiency

The greenhouse effect is a natural increase in the temperature of Earth as energy from sunlight is trapped by the so-called greenhouse gases. The greenhouse gases absorb thermal radiation from Earth's surface and re-radiate it in all directions. Part of this re-radiation is directed back towards the surface resulting in that energy is encapsulated in the lower part of the atmosphere. As a result, the temperature there

is higher than it would be if direct heating by solar radiation were the only warming mechanism. The greenhouse gases are vital for the life on Earth, without them the mean temperature of the Earths surface would be as low as -19 °C [1].

The greenhouse gases are naturally occurring in the atmosphere but human activities such as combustion increases their amount. With an increased amount of greenhouse gases their effect is magnified and the temperature in the lower part of the atmosphere will increase.

Some greenhouse gases, such as carbon dioxide, are formed when materials containing carbon are combusted. If this material is part of the natural carbon cycle, for instance from renewable resources, there will be no net increase in CO_2 in the atmosphere. A resource is defined as renewable if it is replaced by natural processes at a rate comparable to, or faster than, its rate of consumption by humans. Renewable fuels are fuels produced from renewable resources. Wood is a renewable biofuel and, if no fossil fuels are used to produce and harvest it, its combustion will not increase the net amount of CO_2 in the atmosphere. However, the formation of fossil fuels such as oil and coal takes millions of years, and the carbon that is released when fossil fuels are combusted is therefore not part of the carbon cycle, and will increase the amount of CO_2 in the atmosphere. Increasing amounts of greenhouse gases in the atmosphere will increase the temperature even more.

The work presented in this thesis is concerned with thermal power plants, and the following three factors, leading to the reduction of greenhouse gas emission from such plants, have been identified, based on the objectives set out by the EU:

- reduced CO_2 emissions
- increased use of biofuels
- improved part-load abilities

In 2008, the generation of heat and electricity accounted for 41% of the globally produced CO_2. The other large sectors was transport at 22% and industry at 20% [2]. Two renewable resources are suitable for thermal power plants, namely solar power and biomass. Solar thermal power plants are not a realistic option in Northern Europe, but the availability of biomass is high, offering a more suitable alternative. The third factor mentioned above is not as obviously connected to the EU's objectives which state that 20% of the total energy production should originate from renewable sources such as wind, solar power and biomass. The use of large amounts of wind power and solar power will lead to large fluctuations in the power grid, which must be compensated for. This means that quick response to load changes and high part-load efficiencies will be important in modern power plants.

Therefore, the focus of the work presented in this thesis was on combined-cycle power plants, which have the highest efficiency of commercial power plants in use today. They are usually fuelled by natural gas, which produces less carbon dioxide per unit energy released when combusted than other fossil fuels such as coal and oil.

1.2 Objectives

The aim of this work was to evaluate some conceptual solutions for combined-cycle power plants that could be used to meet the EU's climate goals. The thesis therefore presents studies on the following topics.

1. Post-combustion carbon capture processes and their implementation in combined-cycle power plants
2. Part-load strategies for thermal power plants
3. The effects of introducing bio-gas in the fuel mix of a combined-cycle power plant

1.3 Limitations

The power plants studied were combined-cycle power plants, with one exception (in Paper VI). No economical evaluation or component dimensioning was performed. No efforts were made to simulate the dynamic behaviour of the system, and the modelling was limited to a one-dimensional approach.

1.4 Methods

The tool used to evaluate power plant cycles was the heat- and mass-balance program IPSEpro, developed by SimTech Simulation Technology [4]. SimTechs standard library for power plant modelling "advanced power plant library" has been used. This library has been further developed at the Division of Thermal Power Engineering, and documented in numerous scientific articles and theses [5-8]. The model library was further extended and modified during the course of this work.

1.5 Outline of this thesis

This thesis is based on seven scientific papers, which are appended at the end of this summary. The summary contains seven chapters, which provide an introduction to the subject and put the papers in their context.

Chapter 2 includes a brief introduction to combined-cycle power plants. In the chapter that follows, some methods of analysing and describing combined-cycle power plants are presented. Chapter 4 describes the models used in this work, and how to use them. This chapter also includes the theory of power plant components and their behaviour. Chapter 5 presents a brief introduction to post-combustion carbon capture, which is the topic of four of the papers included in this thesis. Chapter 6 gives a brief description of some power plant part-load control methods. Finally, Chapter 7 gives a very brief introduction to the use of low-calorific fuels in combined-cycle power plants designed for natural gas. Concluding remarks are given at the end of the thesis.

1.6 Acknowledgements

When working on a doctoral thesis, it is important to find the inspiration to work harder and learn more. Inspiration can come from books and publications, but the greatest source of inspiration is from the people one works with. I would, therefore, especially like to thank my supervisor, Magnus Genrup, who has been a source of inspiration; his enthusiasm for the subject was invaluable. I would also like to thank all my colleagues at the Department of Energy Sciences for making it an inspirational place to work. Thanks are also due to Marcus Thern, whose knowledge in thermodynamics has increased my understanding of the subject. His support and help during the writing of this thesis were also very valuable.
The work presented in this thesis was financed by Eon; special thanks to Björn Fredriksson Möller and Fredrik B. Olsson.

2 Combined Cycles

The industrial revolution led to the development of electric power, which quickly became very important to mankind. The need for electric power grew rapidly, and with it more efficient power-producing plants. When it became clear that combustion products had an impact on the environment and that fossil fuel resources are finite, efforts devoted to developing more efficient power plants increased. Several different methods can be used to produce electricity: chemical combustion, nuclear reactions, the exploitation of geothermal energy, kinetic flows such as wind, hydro power, and solar photochemical processes. This thesis deals with chemical combustion, which can be further divided into two types: internal combustion and external combustion.

The steam boiler, or rather the steam cycle, is a typical external combustion engine. A modern power plant based on a steam boiler consists of a boiler and a steam turbine. The majority of these plants are coal fired, especially the larger ones. One major advantage of the steam boiler is that it can be constructed for almost any type of combustible fuel. The main disadvantage is that the high temperature arising from combustion cannot be fully utilized because of material reasons. About 80% of all the electricity generated in the world today is produced by steam turbines.

In an internal combustion engine, combustion takes place inside the engine. Energy, in the form of a fuel, is added to the engine, which increases the temperature of the working fluid. The working fluid then expands and the volume change is used to generate work. There are two main types of internal combustion engines: intermittent and continuous. Examples of intermittent engines are the diesel engine and the Otto engine, while an example of continuous internal combustion engines is the gas turbine. The main advantage of the internal combustion engine is that it is compact, which has made it the natural choice for vehicle propulsion. Its major disadvantage is that it is less flexible with regard to fuel than the steam boiler. It is better at utilizing the high temperature developed during combustion, but at the same time it has hotter exhaust gases and therefore the energy lost with the exhaust is greater.

Various combinations of thermodynamic cycles have been tested with the aim to combine advantages and to avoid disadvantages. The goal is to utilize the strengths

of two thermodynamic cycles and incorporate them into one cycle with high efficiency, power output and flexibility. These cycles are referred to as combined cycles, and are typically defined as any power-producing unit consisting of two or more power-producing cycles. They consist of a topping cycle and a bottoming cycle, where the waste heat from the topping cycle constitutes the heat input to the bottoming cycle. The most common combined cycle consists of a gas turbine (Brayton cycle) as the topping cycle and a steam-turbine-based steam cycle (Rankine cycle) as the bottoming cycle. Plants employing this combination are common, and are normally referred to as a combined-cycle power plant (CCPP).

The CCPP is a popular power producing unit that has a number of desirable features such as high efficiency, low initial cost, relatively short construction time, small footprint and a short start-up time. These desirable features have made the CCPP a common choice for the power industry, and the number of CCPPs has thus increased around the world, from 5% to almost 20% of the total capacity in the past 10 years [9]. The CCPP does have some disadvantages, the major one being that its fuel flexibility is rather limited. For instance, solid fuels require gasification before they can be combusted in a gas turbine. The key feature is the high efficiency which, for a state-of-the-art unit of today is very close to reaching 60%.

Because of its popularity, many books and scientific articles have been written on the CCPP. Three publications giving good scientific descriptions of the CCPP are the book by Kehlhofer [9], the doctoral thesis by Bolland [10] and the book by Horlock [11]. These three authors have also published numerous articles on the subject.

2.1 The components of a CCPP

Figure 1 shows a schematic illustration of a CCPP and its three main components: a gas turbine, a steam turbine and a heat-recovery steam generator (HRSG). The gas turbine operates at a high temperature and pressure where it produces power which is fed to the electric grid. The flue-gases from the gas turbine are relatively hot and contain a large amount of energy. This energy is fed to a HRSG where the flue-gases heat, boil and superheat water to a high temperature under high pressure. The high-temperature steam is delivered to a steam turbine where it expands and produces work. The energy in the exhaust gases, which is by far the major loss in the gas turbine, is thus utilized to produce additional power from a second cycle.

The following sections will briefly describe the different parts of the CCPP. More details can be found in Sections 4.6 and 4.7.

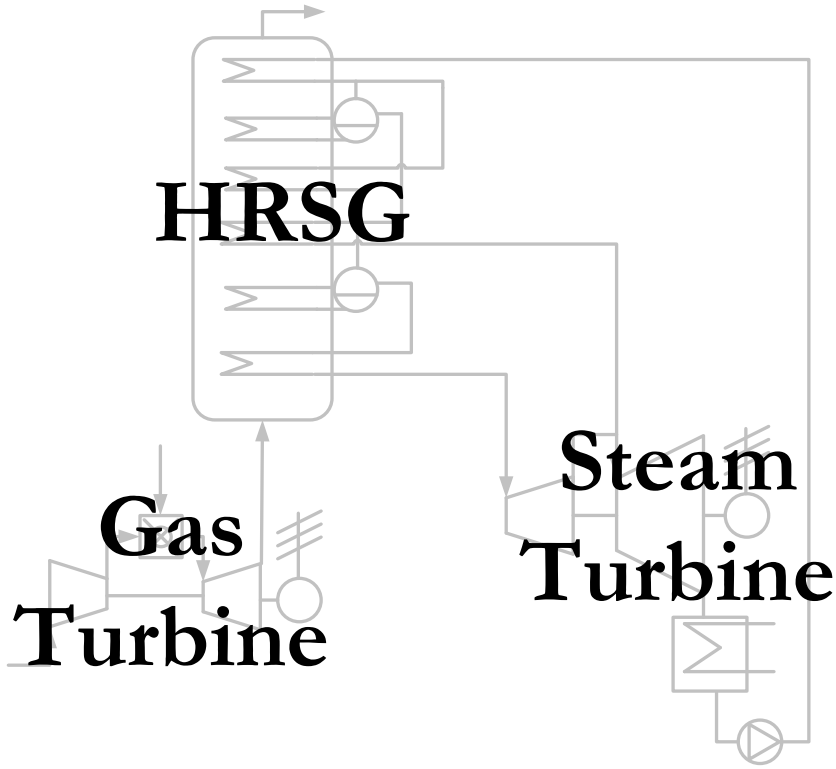

Figure 1: Schematic illustration of a single-pressure CCPP

2.1.1 The gas turbine

The gas turbine is the topping cycle, which is a normal open Brayton cycle with some special features. A simple cycle gas turbine, i.e. a gas turbine not operated in a combined cycle, has maximum efficiency at a high pressure ratio. A high pressure ratio results in a large expansion and hence the temperature of the exhaust gas is low. The low exhaust gas temperature means a reduction in stack loss and therefore a high efficiency. Too high a pressure ratio results in the compressor consuming a large amount of energy in comparison to the energy that can be added with the fuel without exceeding the maximum turbine inlet temperature. When a gas turbine is to be designed for combined-cycle operation it is no longer desirable to have a low flue-gas temperature. A low flue-gas temperature would give a low steam admittance temperature in the bottoming steam cycle, which limits the efficiency and power output. Therefore, the pressure ratio of the gas turbine should be lower than for a single-cycle unit to ensure that the bottoming cycle receives energy at a suitable temperature for steam production. On the other hand, too low a pressure ratio will lead to poor gas turbine efficiency. In today's plants, with combustor outlet

temperatures of 1400-1500 °C and steam turbine inlet temperatures of 565-600 °C, the pressure ratio should be in the range of 17-22 bar. In a sequentially fired gas turbine, the pressure ratio will be higher, with the second combustor at the pressure level of an ordinary combined-cycle gas turbine. In some plants, two or more gas turbines are run in parallel to generate exhaust gases for a large steam cycle. This will give extra flexibility and better part-load performance.

2.1.2 The steam cycle

The bottoming cycle is an ordinary Rankine cycle utilizing water as the working medium. Unlike the topping cycle, the bottoming steam cycle is a closed cycle, i.e. the working fluid never leaves the system. In the simplest possible Rankine cycle, water is boiled and superheated in a boiler. The steam is then passed from the boiler to a steam turbine where it is expanded, producing work. The steam is then condensed in a condenser using an ambient heat sink. Finally, the water is pumped up to the operating pressure and returned to the boiler. In the Rankine cycle, the working fluid is pressurized in the liquid state, which is much less energy consuming than compression in the gaseous state, as in the Brayton cycle. The pressure ratio is therefore not limited by the work consumption but by the two-phase region (gas and liquid) at the end of the expansion. To further increase the pressure of a Rankine cycle the steam can be reheated part of the way of the expansion. This allows a higher admission pressure for a given maximum steam temperature without exceeding the maximum moisture content at the end of the expansion. If the moisture content is too high at the end of the expansion, the steam turbine will suffer from erosion, which drastically shortens its lifetime. This is discussed further in Section 4.6.3. A steam-boiler-based Rankine cycle normally uses a water preheating train prior to the boiler. When reheating is introduced the next limit on admittance pressure is the physical blade length in the high-pressure turbine; especially in small plants. The preheating energy is supplied by steam extracted from the steam turbine at a number of pressure levels. Preheating reduces the amount of fuel required in the boiler. In a combined cycle this is not beneficial because it will reduce the recovery of heat from the exhaust gas.

The pressure at the end of the expansion and in the condenser is well below atmospheric pressure and, therefore, it is inevitable that air will leak into the system. Dissolved oxygen is a major problem because it causes serious corrosion in the system. Water also combines with dissolved carbon dioxide to form carbonic acid, which causes further corrosion. In order to reduce this problem, oxygen and other gases are removed in a deaerator. The principle is based on the fact that the

solubility of gases in saturated water is almost zero. The feedwater is heated to saturation by adding steam in a closed tank. The steam and the gases will rise to the surface where they are cooled, and the gases and some steam are vented out of the system at the top of the deaerator.

The steam turbine in a combined cycle has two special features. Firstly, large-scale combined cycles normally generate steam at more than one pressure level (the reason for this is explained in Section 3.3), and therefore the steam turbine is equipped with steam induction points. Large steam turbines consist of a number of turbine cylinders and the induction point will normally be located between them. The other special feature is the load control method. The steam production will vary with the ambient conditions as a result of the steam cycle being powered by energy from the gas turbine exhaust. To control the steam production, a method called variable pressure control is used in the steam cycle. A conventional steam boiler plant sometimes uses partial-arc control, which has superior part-load efficiency. Partial-arc control utilizes a fixed pressure in the boiler at all loads, giving high part-load efficiency. However, a constant pressure in the boiler is undesirable for the heat recovery in the HRSG. With a fixed evaporation pressure the HRSG becomes stiff, inflexible and inefficient. The part-load efficiency of the turbine is secondary to efficient heat recovery. Instead of using a fixed pressure, the combined-cycle bottoming cycle is controlled by sliding pressure control. Sliding pressure control means that the inlet control valves are always fully open so that the admittance pressure is sliding or floating. When the control valve is open, the inlet volume flow is constant at all loads, resulting in a more or less fixed pressure ratio over the first stage. Therefore, the temperature gradients are much smaller than those in partial-arc control.

Large high-pressure CCPPs have three pressure levels and reheating. Therefore, the steam turbine has induction points for each pressure level. A modern high-performance CCPP of today has a steam admittance pressure of 160-180 bar at 600 °C.

2.1.3 The heat recovery steam generator

The task of the HRSG is to transfer heat from the gas turbine exhaust to the bottoming steam cycle. The HRSG consists of a set of heat exchangers that transfer the heat from the gas to water. The heat transfer in a HRSG mainly consists of convection, unlike the ordinary steam boiler where radiation contributes to the heat transfer. The simplest form of HRSG operates at only one pressure level. This means that water only boils at one pressure. To increase the efficiency of the HRSG

additional evaporators working at lower pressures can be introduced. The reason for the increase in efficiency is discussed in the next section.

The HRSG can be vertical or horizontal. A vertical unit has a small footprint, but the steel structure is more expensive as it has to carry the heat exchangers as well as the drums. In a horizontal unit the heat exchanger tubes are vertical and, therefore, more suitable for a self-circulating boiler. Horizontal tubes are also less sensitive to steam blockage and dry-out.

The plant output can be increased by supplementary firing, which means that a duct burner is placed at the HRSG inlet. The oxygen surplus in the flue-gas is usually sufficient for combustion. Supplementary firing increases the plant output at the expense of efficiency. Supplementary firing was more common in early CCPPs because the gas turbine exhaust was not hot enough for the steam cycle. It is rare to find supplementary firing in a modern plant, but in some cases it is used to increase the flexibility of the power plant.

2.2 Number of pressure levels and configuration

The simplest CCPP includes only one evaporator. This configuration is referred to as the single-pressure configuration and reheating is usually not included.

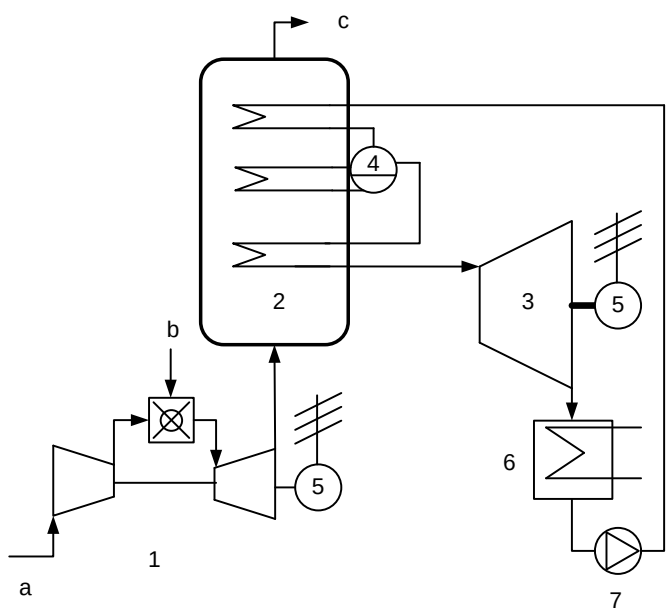

1. Gas turbine
2. HRSG
3. Steam turbine
4. Steam drum
5. Generator
6. Condenser
7. Feedwater pump
a. Air
b. Fuel
c. Flue-gas

Figure 2: Schematic illustration of a single-pressure combined cycle

A typical layout of a single-pressure CCPP is shown in Figure 2. This plant has a rather low pressure to keep the moisture content in the turbine exhaust at an acceptable level. With only one steam drum it will have a relatively small heat storage capacity and will therefore respond quickly to load control and have a short start-up time. Single-pressure plants have a relatively large stack loss, which could be used for co-generation. Typically, co-generation is integrated so that the excess energy from the economizer is utilized for district heating, but the major part must be supplied via a hot condenser heated by steam extracted from the crossover pipe between low- and intermediate-pressure steam turbines.

By introducing a second pressure level in the steam cycle more energy can be recovered from the flue-gas. The reason is explained in Section 3.3. As for the single-pressure cycle, the admittance pressure is limited by the moisture content at the end of the expansion. Introducing a reheating circuit will increase the mean steam temperature without exceeding the maximum temperature. This will allow for a higher admittance pressure, which will significantly increase the efficiency and the power output. Reheating is rare in single-pressure plants because it limits the amount of energy that can be recovered from the flue-gas. The reason for this is explained in Section 3.2.1.

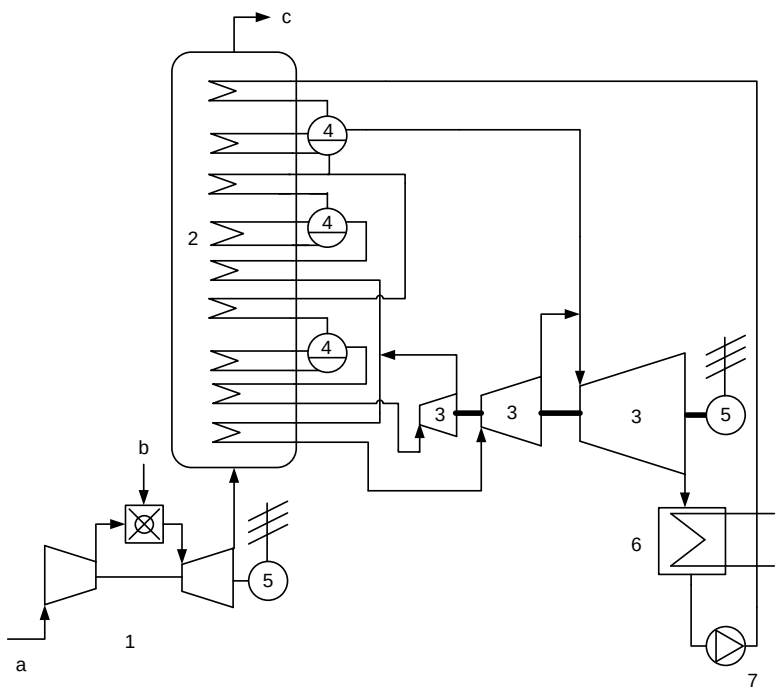

Figure 3: Schematic illustration of a triple-pressure combined cycle with reheating. Component numbering as in Figure 2.

Figure 3 shows the layout of a triple-pressure CCPP with reheating. When comparing Figure 2, showing a single-pressure plant, with Figure 3 it is obvious that the triple-cycle is more complex. The number of steam drums, the number of heat exchangers and the piping of the triple-pressure cycle makes the initial cost higher than for a single-pressure plant.

A steam turbine normally consists of a high-pressure, an intermediate-pressure and a low-pressure cylinder. This means that only two natural induction points are available (excluding the admittance). For a triple-pressure CCPP with reheating this means that the intermediate pressure steam produced in the HRSG should be mixed and superheated with the reheating flow.

Single-pressure CCPPs are used when a short start-up time is important, or if the heat remaining in the flue-gas can be recovered for an external process such as district heating (co-generation). A dual-pressure plant would typically be a medium-sized plant, where a third pressure level is not economically motivated. For a large-scale plant, operated as a base load producer with many hours' operation per year, it is easier to motivate a higher initial cost, and such a plant will include three pressure levels and reheating. Figure 4 shows the net heat-to-power efficiency for four different CCPP configurations. The plants without reheating utilize an admittance pressure and temperature of 100 bar and 565 °C, while the reheating units have a pressure of 160 bar and a temperature of 565 °C.

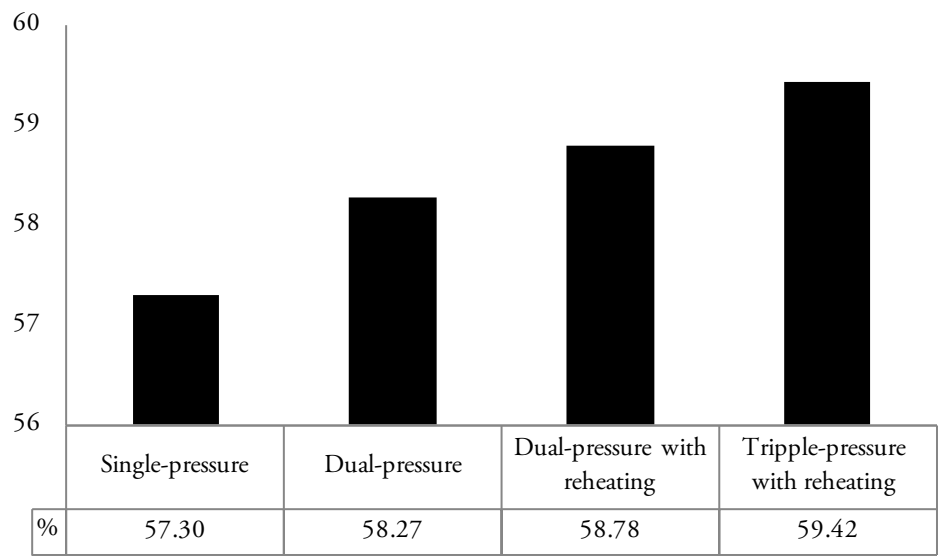

Figure 4: Efficiency of different CCPP configurations without parasitic or step-up transformer losses

3 Analysing Combined Cycle Power Plants

The transfer of heat from the gas turbine exhaust to the steam cycle is vital for the overall efficiency of the CCPP. This is done by the HRSG. It is important to understand the HRSG process, and how it is affected by cycle parameters and cycle features. The process of the HRSG can be visualized in a temperature-to-heat-flux diagram (T-Q diagram). In this chapter the T-Q diagram is explained and it is used to analyse how some cycle features can improve the efficiency of a CCPP.

3.1 The T-Q diagram

The HRSG should be designed with consideration to both the first and second laws of thermodynamics. The most important cycle features determining the behaviour of the HRSG are the number of pressure levels and whether reheating is implemented or not. Other considerations include how and where deaeration is performed and the heat-transfer area, i.e. the magnitude of the pinch point.

The use of T-Q diagram is crucial in understanding and designing combined cycles. Figure 5 shows the T-Q diagram for a single-pressure combined cycle with 100 bar admission pressure and a turbine inlet temperature of 565 °C. The T-Q diagram in Figure 5 originates from a single-pressure CCPP, and shows the temperature profile of the heat recovery process. The smallest temperature difference in the HRSG is called the pinch-point, and is located on the cold side of the evaporator. The upper continuous line, with an almost constant slope, represents the temperature profile of the flue-gas, and the lower line represents the temperature of the water/steam. The HRSG of a single-pressure combined cycle consists of three different sections. Starting at the lowest temperature, the first section is called the economizer, and is where liquid water is heated to the saturation temperature. To avoid evaporation, which could cause steam blockage that may result in “water hammering” [12] in the economizer, the outlet temperature is always kept a few degrees below the saturated state. This temperature difference is called the approach point.

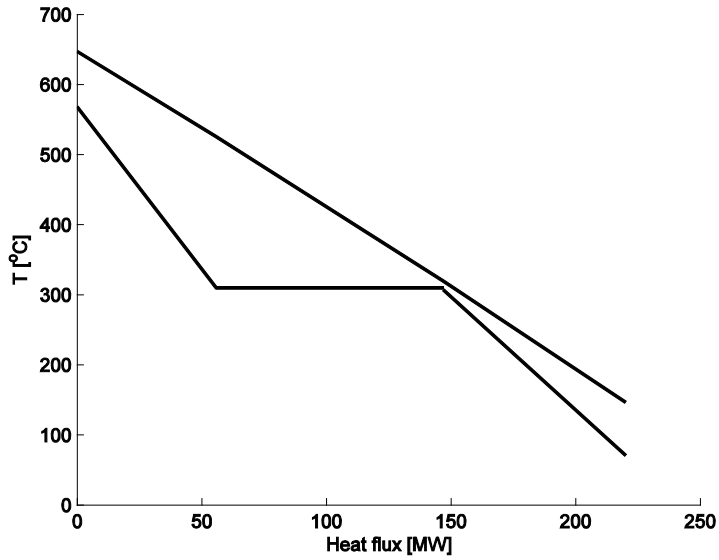

Figure 5: Temperature-to-heat-flux diagram for a single-pressure combined cycle

The second section is the evaporator, in which the water is evaporated at constant temperature. In the third and final section of the HRSG, the superheater, the steam or evaporated water is superheated.

The relation between temperature and heat can be described by:

$$\dot{Q} = \dot{m} \cdot \bar{c}_p (T_2 - T_1) \tag{1}$$

Equation (1) is valid when the working medium does not undergo a phase transition. In the HRSG a phase transition from water to steam occurs in the evaporator, which means that Equation (1) must be replaced by:

$$\dot{Q} = \dot{m} \cdot \Delta h_{evap} \tag{2}$$

where $\dot{Q}$ is the energy transferred and Δh_{evap} is the evaporation enthalpy. If Equation (1) is rearranged it can be seen that the slope of the line in the T-Q diagram is inversely proportional to the mass flow and the specific heat. From Equation (2) it can be understood that the term $\dot{m} \cdot \Delta h_{evap}$ is the length of the evaporation line. These relations are central for the analysis of combined cycle power plants.

At the beginning of this section it was mentioned that the HRSG should be designed taking both the first and second laws of thermodynamics into

consideration. The first law implies that as much heat as possible should be recovered from the flue-gas. The second law, which also embodies a very important factor in the HRSG design, states that the potential or exergy of the flue-gas energy should be utilized as efficiently as possible. In other words, as small an amount of entropy as possible should be generated through the process. To evaluate this, an exergy analysis of the system can be performed, which will quantify the deficiencies of the process. There is a simple way of illustrating the loss of exergy for a HRSG without performing the exergy analysis. If the temperature difference throughout the T-Q diagram is minimized, the process generates a minimum amount of entropy. Horlock [11] reasoned that, theoretically, the temperature difference can be used to drive the Carnot cycle, and is therefore origin of entropy generation and hence, a loss.

A reversible or perfect process is one that can return both the system and the surroundings to their initial conditions with no net work input. A reversible process will never occur in reality since there is no driving force. However, the reversibility of a process can vary, and the irreversibility can be quantified by:

$$I = T_{ref}\left(S_{gen}\right) \tag{3}$$

where I is the irreversibility, T_{ref} is the reference temperature or the "dead state" usually the ambient temperature, and S_{gen} is the entropy generated in the process. For a reversible process no entropy is generated, thus $S_{gen}=0$.

For a heat exchanger, the process is reversible if there is no temperature difference between the hot and cold sides. Thus, the irreversibility increases with increasing temperature difference. Considering the first and second laws of thermodynamics when designing a HRSG means a compromise between the following:

- as much energy as possible should be recovered, i.e., the T-Q diagram should be extended as far as possible along the x-axis, and
- the temperature difference, i.e. the area between the lines in the T-Q diagram, should be minimized.

3.2 The influence of pressure level in a CCPP

First of all, it should be made clear that if the steam admittance pressure in a CCPP is increased the efficiency will increase. In this section the other effects of the cycle

pressure are examined, these effects are the reason why the efficiency does not increase linearly with the pressure.

With a fixed steam turbine inlet temperature, the cycle pressure in a single-pressure CCPP will have two major effects on the HRSG. First, an increase in pressure will change the distribution of heat between the economizer and the superheater. A higher cycle pressure goes hand in hand with a higher evaporation temperature and, hence, the HRSG pinch point is moved up along the flue-gas line in the T-Q diagram. The result is that the heat flux is shifted from the superheater to the economizer. Second, a higher pressure reduces the evaporation energy needed to evaporate water allowing for an increase in mass flow.

If the temperature rise in the feedwater pump is neglected, the feedwater temperature is more or less independent of the cycle pressure. Figure 5 shows that the temperature difference in the economizer is diverging, and that the smallest temperature difference is at the hot end. According to Equation (1) this means that the product $\dot{m} \cdot c_p$ for the water is less than for the flue-gas. If the cycle pressure is reduced, the HRSG pinch point will be situated at a lower temperature due to a reduction in the evaporation temperature.

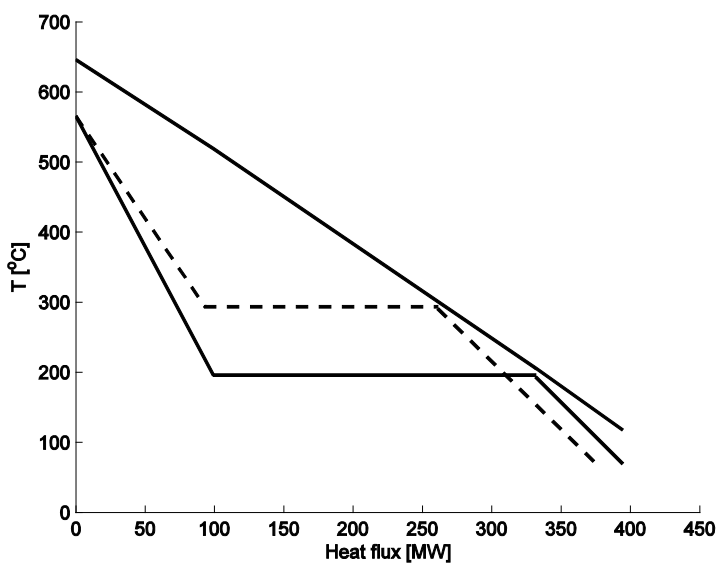

Figure 6: Temperature-to-heat-flux diagram for two single-pressure combined cycles. More energy is recovered in the low-pressure cycle (lower solid line), while less entropy is generated in the high-pressure cycle (dashed line).

This means that the temperature rise in the economizer is reduced and hence there is less scope for the temperature to diverge. With a reduced temperature difference at the outlet and a fixed temperature on the cold side, it can be understood that a

very low pressure will be beneficial for the amount of heat recovered, which fulfils the first law of thermodynamics. In other words, if the evaporation temperature is low more energy can be recovered from the flue-gas. Figure 6 shows the T-Q diagram for a high-pressure CCPP (dashed line) and a low-pressure CCPP (solid line). The low-pressure cycle stretches further along the x-axis, which means that more heat is recovered. However, Figure 6 also shows that the mean temperature difference is greater for the low-pressure cycle and, hence, a large amount of entropy is generated, which is not favourable according to the second law of thermodynamics. It should be mentioned that with a low admittance pressure and a high admittance temperature, the heat lost in the condenser will increase due to the short expansion.

A higher cycle pressure results in a higher evaporation temperature and hence less flue-gas energy can be utilized in the evaporator. Figure 6 shows that for the higher-pressure cycle (dashed line) the HRSG pinch point, which is the starting point of the evaporator, has moved up along the flue-gas line. The reason for this is that the evaporation temperature has increased, which results in less energy being available to the evaporator. However, an increase in pressure also means that the evaporation energy per kilogram of water is reduced. From Equation (2) it can be seen that if the evaporation energy is reduced, a fixed amount of energy will result in a larger mass flow.

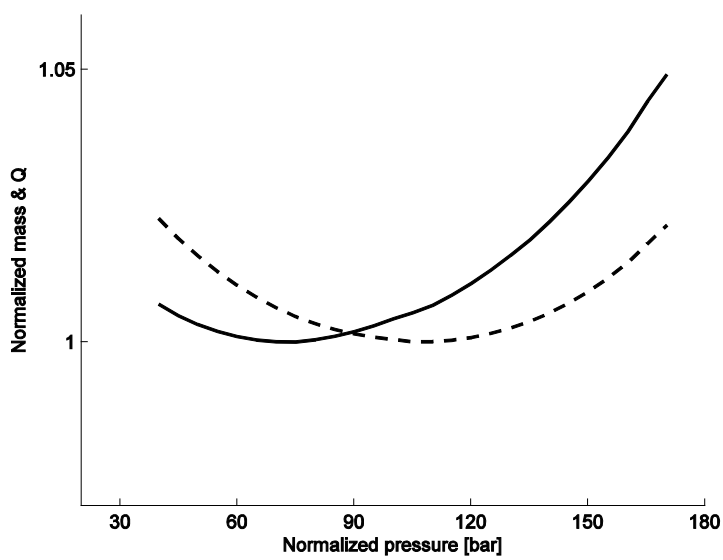

Figure 7: Normalized mass flow (solid line) and recovered heat (dashed line) as function of cycle pressure

Thus, an increase in pressure causes the evaporation energy to decrease, which is positive for the mass flow but, at the same time, less energy will be available in the evaporator, which is negative for the mass flow. Figure 7 shows the mass flow (solid line) as a function of cycle pressure, and it can be seen that the mass flow will have a minimum at a certain cycle pressure. From this pressure level, the reduced evaporation energy dominates the negative effect of less energy being available in the evaporator.

Figure 7 also shows that the total amount of recovered heat has a minimum value at a specific pressure. It was mentioned above that the diverging temperature in the economizer is a problem when the cycle pressure is increased. However, once the mass flow starts to increase the product $\dot{m} \cdot c_p$ for the water side increases, and more energy can be recovered in the economizer.

3.2.1 Reheating

The pressure level of the cycle is limited by factors such as the initial cost of the plant, the volume flow through the high-pressure turbine and the moisture content in the low-pressure turbine exhaust.

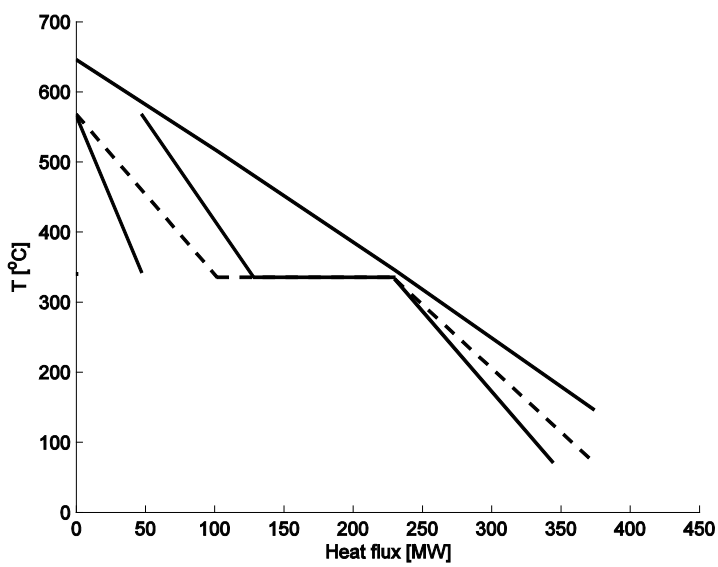

Figure 8: The T-Q diagram of a single-pressure CCPP with (solid line) and without (dashed line) reheating

The initial cost will increases as the piping and other material must be stronger to withstand the higher pressure. A high pressure results in a low volume flow entering the high-pressure turbine, which is a problem especially for small CCPPs. For a

short blade the end-wall losses and tip clearance will become dominant and manufacturing tolerance will also have larger impact as the component size is reduced.

A high moisture content in the low-pressure turbine causes erosion of the blades and reduced efficiency. To limit the moisture content and allow for a further increase in the admittance pressure, reheating can be introduced to the cycle. Reheating means that the steam is reheated in the HRSG before it enters the intermediate turbine. The heat supplied to the reheating steam reduces the available heat for the evaporation, as can be seen in Figure 8, and will therefore reduce the mass flow of the cycle. Figure 8 also shows that the reduced mass flow causes the economizer temperature profile to diverge even more than in the case without reheating.

3.3 Multi-pressure CCPPs

Reheating and a high admittance pressure will lead to a large temperature difference in the economizer. If this temperature difference, or at least part of it, is used to drive a second Carnot cycle the efficiency can be further increased. This can be done by adding an additional low-pressure Rankine cycle, i.e., by dividing the economizer into two sections with a low-pressure evaporator between them, according to the

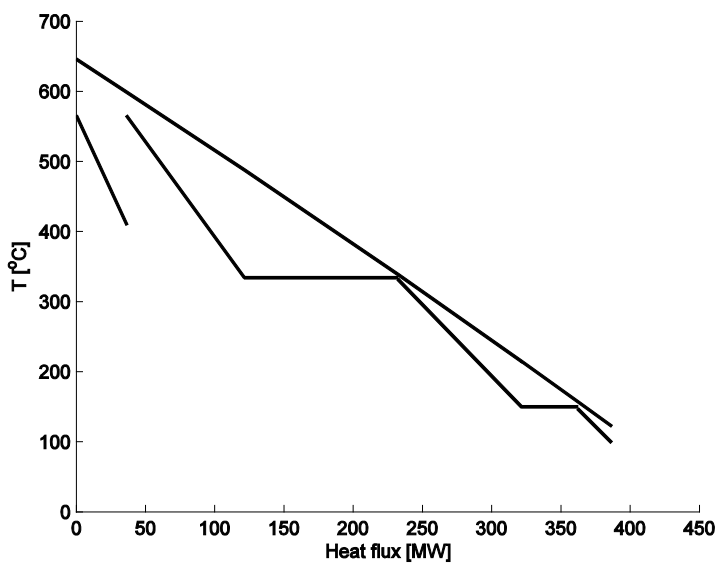

Figure 9: A dual-pressure combined cycle with reheating (Reheating is the last part on the hot end)

T-Q diagram in Figure 9. The cycle in Figure 9 is typical for a dual-pressure CCPP with no superheating of the low-pressure steam. The steam produced in the low-pressure cycle is injected into the steam turbine in the crossover pipe between the intermediate-pressure and low-pressure turbine cylinder. The cycle now has the advantage of recovering a large amount of energy, associated with a low pressure level, while the overall temperature difference and entropy generation are limited.

The higher the cycle pressure, the greater the scope for additional pressure levels. If reheating is used and the cycle pressure is very high the mean temperature difference in the HRSG can be further reduced if a third pressure level is introduced. The amount of heat recovered is also somewhat increased as the total mass flow will be increased and the optimum low-pressure level will be slightly reduced.

In today's market it is economically justifiable to use three pressure levels in a large combined cycle. It was mentioned in Section 2.2 that the turbine is limited to 3 turbine cylinders and, therefore, the reheating pressure of a triple-pressure CCPP will be set to the intermediate pressure level so that it can be inserted at the same position. A four-pressure CCPP would require a fourth turbine cylinder, which would lead to an unrealistically high initial cost of the plant.

3.4 The deaerator

To avoid corrosion of the drum walls and piping of the system the feedwater must be deaerated (see Section 2.1.2). This can be done in a number of ways. If deaeration is performed in the low-pressure drum, no separate deaeration unit is required. To do this, the drum approach temperature must be higher than normal and all the water must be passed through the unit. The higher the approach temperature to the deaerator, the more gases can be removed. The energy consumed in the deaeration process will be supplied from the evaporator, which results in less low-pressure steam being available in the turbine. However, no additional deaerator tank is required, which reduces the initial cost and saves space. From a thermodynamic perspective, it is more beneficial to use energy at a lower temperature for deaeration. For instance, part of the flow from the economizer outlet can be flashed and used in the deaerator. To do this a separate deaeration tank is required.

4 Thermodynamic Power Plant Modelling

Through calculations it is possible to determine the critical parameters of a power plant. In this work, such calculations were carried out to evaluate the impact of changes in the boundary conditions, the introduction of a new component or the modification of a component. One-dimensional steady-state modelling is suitable to study the effects on the whole power cycle. This type of modelling does not provide any details on the dynamic events taking place in the components, but is excellent in giving a more global view of the performance. The principle is that each component has a set of inlets and outlets at which the stagnation properties are calculated using thermodynamic equations.

When designing a computer-based model, the key is to maintain a good balance between the number of inputs and the accuracy. With too many inputs, the model becomes difficult to use and the requirements on the user's experience increase. Also, if information is not available for all the inputs, imprecise estimates may make the model less accurate than a simpler version. The number of inputs needed is generally decided by the operational window of the unit. The most complex unit to model is one that employs different working media under wide variations of temperature and pressure. It is important to evaluate every parameter that is left out and the user should be well aware of the limitations of the model.

Heat and mass balance models can be based on equations or characteristics, i.e. tabulated values or graphs, or both. Simple units are preferably based on equations, but more complex units become too complicated to model with equations only.

4.1 Model components

A large number of equations containing an even larger amount of variables are required to model a power plant. To make modelling more practical, the equations are collected into groups representing separate units or components of the power plant such as heat exchangers, pipes, condensers, and turbine stages. Each component depends on the others and in order to model the complete cycle the

components should be linked together to form a network representing the whole power plant. The number of units differs depending on the purpose of the model, for example, a boiler can be modelled as single unit or as a number of heat exchangers, a drum and a furnace.

Each unit is represented by a number of equations. The number of variables can be greatly reduced by referring or normalizing all values with the design point. This will remove all values that are constants through the load range such as geometries, etc. This is a standard procedure that can be applied to almost all components. It is also important to arrange the equations so that the variables required can be easily measured or obtained.

4.2 Off-design modelling

Off-design operation is sometimes confused with part-load operation, but it involves much more than that. The expression “off-design” means any mode of operation deviating from the design point, including part-load operation. The design point is normally the operation point corresponding to full-load operations at ISO conditions, at a given air humidity with a specified fuel. Changes in any of these variables will result in off-design operation.

4.3 Modelling with characteristics

A component characteristic is a map describing the unit’s behaviour over its operational range. If the hardware of the unit is modified, the entire characteristic must be recalculated or even re-measured. Each point on the map, is unique regarding the behaviour of the unit. There may, however, be several combination of parameter that is valid for a single position in the map. The behaviour of the unit is dependent on several parameters, for example, the thermodynamic properties of the working medium and the physical speed. By using the characteristics of a unit it is possible to predict its performance under various conditions . It is important to keep in mind that when modelling with characteristics the results can never be more accurate than the characteristics.

4.4 Modelling a pressure loss

Pressure losses result from frictional forces on the flowing medium as it passes through a component. Higher velocities are associated with higher pressure losses.

All components suffer from pressure loss; for some components it is sufficient to model them as a fixed pressure drop or as a percentage of the total pressure, but in many cases the pressure loss must be modelled more accurately. The pressure drop in a component can be described by the following equation:

$$\Delta p = \xi \cdot \frac{c^2}{2} \cdot \rho \tag{4}$$

where ξ is the friction coefficient, which is constant for a specific component, c is the mean velocity of the fluid and ρ is the fluid density. If the design value of the pressure drop is known, Equation (4) can be normalized to the design value.

$$\frac{\Delta p}{\Delta p_{des}} = \frac{\xi \cdot \frac{c^2}{2} \cdot \rho}{\xi_{des} \cdot \frac{c_{des}^2}{2} \cdot \rho_{des}} \tag{5}$$

Equation (5) represents the pressure drop at any given conditions in the component, and is related to the design value. In Equation (5), all constant values i.e. values that are equal to the design value, can now be removed:

$$\frac{\Delta p}{\Delta p_{des}} = \frac{c^2 \cdot \rho}{c_{des}^2 \cdot \rho_{des}} \tag{6}$$

Equation (6) shows that the pressure drop is simply a function of the velocity and the density of the fluid at the operating conditions and the design conditions. It is more convenient to work with mass flows in heat balance calculations because these are easily obtained from the continuity equation. Equation (6) is therefore rewritten using the equation of continuity.

$$\frac{\Delta p}{\Delta p_{des}} = \frac{\left(\frac{\dot{m}}{A\rho}\right)^2 \cdot \rho}{\left(\frac{\dot{m}}{A\rho}\right)_{des}^2 \cdot \rho_{des}} = \frac{\dot{m}^2}{\dot{m}_{des}^2} \frac{\rho_{des}}{\rho} \tag{7}$$

In most units the density of the fluid will not deviate significantly from the design value and, therefore, the influence of the mass-flow ratio squared will dominate the equation, and the density ratio can be left out.

$$\frac{\Delta p}{\Delta p_{des}} = \left(\frac{\dot{m}}{\dot{m}_{des}}\right)^2 \tag{8}$$

Equation (12) is thus the final expression for the pressure ratio, and is valid if the density of the fluid can be considered to be constant throughout the load range of the unit.

4.5 Modelling a heat exchanger

The purpose of a heat exchanger is to transfer heat from one fluid to another without the two fluids coming into direct contact. Thermal power plants always contain a large amount of heat exchangers. The purpose of the heat exchangers in the HRSG of a CCPP is to transfer heat from the gas turbine exhaust to the water or steam of the bottoming Rankine cycle. Two methods are commonly used to model heat exchangers, the NTU method and the LMTD method. The NTU method was introduced by Kays and London in 1955 [13], and is suitable when the inlet and outlet temperatures are unknown. For heat- and mass-balance modelling, the LMTD method is more suitable.

The driving force of the heat transfer process in a heat exchanger is the temperature difference between the hot and cold sides. The temperature difference varies non-linearly along the unit, and by assuming that the specific heat of the media is constant, a logarithmic mean temperature difference can be calculated. This is the basis of the LMTD method, and is derived in most textbooks on the subject [14]. For a counter-current heat exchanger the LMTD is calculated as follows:

$$LMTD = \frac{\left(T_{h,out} - T_{c,in}\right) - \left(T_{h,in} - T_{c,out}\right)}{ln\frac{\left(T_{h,out} - T_{c,in}\right)}{\left(T_{h,in} - T_{c,out}\right)}} \tag{9}$$

When the temperature difference at the inlet and outlet of the heat exchanger is equally large, Equation (9) is not solvable. If the temperature differences are almost equal, the mean temperature can be used instead of LMTD.
The total amount of heat transferred is given by:

$$\dot{Q} = U \cdot A \cdot LMTD \tag{10}$$

In Equation (10) the heat transfer coefficient U is dependent on the convective heat transfer on the inside, through the material and on the outside.

$$\frac{1}{U \cdot A} = \frac{1}{A_i \cdot \alpha_i} + \frac{t_w}{\lambda_w \cdot A_i} + \frac{1}{\varphi \cdot A_o \cdot \alpha_o} \tag{11}$$

This equation is difficult to rearrange and requires numerous input parameters, several of which are not easily estimated. It is therefore desirable to simplify the equation thus limiting the number of parameters needed in the model.

The heat conductivity through the heat exchanger material is very good and, therefore, the second term can be excluded. It is common for the heat transfer on one side of a heat exchanger to be much worse than on the other, and thus one term will completely dominate Equation (11), which then can be simplified into Equation (12). This simplification is generally valid for heat exchangers in a steam boiler or a HRSG where the medium is water/steam or evaporating water on one side and flue-gas on the other. Caution should be exercised when employing this simplification as in some cases the flow on the steam side in some off-design scenarios is significantly reduced, causing the heat transfer to decrease.

$$U \cdot A = \varphi \cdot A_o \cdot \alpha_o \tag{12}$$

The heat transfer coefficient α is dependent on the fluid properties, the Reynolds number and the geometry of the unit. In a steam boiler or a HRSG the heat exchangers are normally of shell-and-tube type, and the heat transfer coefficient is given by:

$$\frac{\alpha \cdot d}{\lambda_f} = C \cdot Re^n \cdot Pr^{1/3} \tag{13}$$

where the constant n is dependent on the diameter and configuration of the tubing; in the general case it can be set to 0.6. The Prandtl number (Pr) is a dimensionless number depending only on the fluid properties and state of the fluid. The Prandtl number does not vary greatly for different gases, and the temperature dependency is very small. However there is a pressure dependency, and under some conditions it should be included. If Prandtl number is to be considered Equation (22) can be applied.

The Reynolds number should be calculated for the highest fluid velocity.

$$Re = \frac{\rho \cdot c_{max} \cdot d}{\mu_f} \tag{14}$$

As when modelling a pressure loss, it is now desirable to reduce the number of variables. By combining Equations (12), (13) and (14), and dividing by the design value, the following equation is obtained. The flange efficiency is assumed to be constant throughout the load range.

$$\frac{UA}{U_{des}A} = \frac{\mu_{f,des}(\rho c_{max})^{0.6}}{\mu_f(\rho c_{max})_{des}^{0.6}} \tag{15}$$

The dynamic viscosity (μ) can be omitted in most cases, but if the temperature varies considerably over the operational range of the unit it can be replaced by [15].

$$\left(\frac{\mu_{f,des}}{\mu_f}\right)^{0.6} \approx 1 - (\bar{t}_{des} - \bar{t}) \cdot 5 \cdot 10^{-4} \tag{16}$$

The continuity equation can be applied, and as the flow area is fixed the equation can be simplified so that it is only a function of the ratio of the actual mass flow and the design mass flow:

$$\frac{UA}{UA_{des}} = \frac{\dot{m}^{0.6}}{\dot{m}_{des}^{0.6}} \tag{17}$$

The heat exchanger model can now be constructed from Equations (9), (10) and (17), together with an energy balance, a mass balance and the pressure drop Equation (8). If a heat balance including the heat exchanger is available, the design values that must be set ($U_{des} \cdot A$, $\dot{m}_{des,i}$ $\dot{m}_{des,o}$, $\Delta p_{des,i}$ and $\Delta p_{des,o}$) can be calculated by setting the boundary conditions obtained from the heat balance.

If the heat transfer on both sides is to be considered, the model becomes more complicated, and the following equation can be applied.

$$\frac{1}{U \cdot A} = \frac{1}{\alpha_i \cdot A_i} + \frac{1}{\alpha_o \cdot A_o} = \frac{\alpha_i \cdot A_i + \alpha_o \cdot A_o}{\alpha_i \cdot A_i \cdot \alpha_o \cdot A_o} \tag{18}$$

As in the previous cases, the parameters are normalized to the design value, and the equation rearranged.

$$\frac{U \cdot A}{U_{des} \cdot A} = \frac{\left(\alpha_{i,des} A_i + \alpha_{o,des} A_o\right)\alpha_i A_i \cdot \alpha_o A_o}{(\alpha_i \cdot A_i + \alpha_o \cdot A_o)\alpha_{i,des} A_i \cdot \alpha_{o,des} A_o} =$$

$$= \frac{\frac{A_i \alpha_{i,des} \alpha_i \alpha_o}{\alpha_{i,des} \alpha_{o,des}} + \frac{A_o \alpha_{o,des} \alpha_i \alpha_o}{\alpha_{i,des} \alpha_{o,des}}}{A_i \frac{\alpha_{i,des}}{\alpha_{i,des}} \alpha_i + A_o \frac{\alpha_{o,des}}{\alpha_{o,des}} \alpha_o} \tag{19}$$

From Equations (13) and (14), and if the same fluids are used and the thermodynamic operating range is not very large, the following is valid.

$$\frac{\alpha}{\alpha_{des}} = \frac{\dot{m}^{0.6}}{\dot{m}_{des}^{0.6}} \tag{20}$$

Equation (19) can now be further simplified to give:

$$\frac{UA}{U_{des} A} = \frac{\left(1 + \frac{\alpha_{i,des}}{\alpha_{o,des}}\right)\left(\frac{\dot{m}_i}{\dot{m}_{i,des}}\right)^{0.6}\left(\frac{\dot{m}_o}{\dot{m}_{o,des}}\right)^{0.6}}{\frac{\alpha_{i,des}}{\alpha_{o,des}}\left(\frac{\dot{m}_i}{\dot{m}_{i,des}}\right)^{0.6} + \left(\frac{\dot{m}_o}{\dot{m}_{o,des}}\right)^{0.6}} \tag{21}$$

Compared to Equation (17), Equation (21) appears to be very complicated, however, the only extra factor required for the model is the ratio between the heat transfer on the hot and cold sides at the design conditions. If this value can be obtained, the improved model should be straightforward to use. If one side of the heat exchanger has poorer heat transfer than the other, all efforts to improve the unit should be spent on that side. If possible, the heat exchanger should be designed so that the ratio of the heat transfer on the hot and cold sides equals unity at the design point.

If the Prandtl number is to be included, the following equation can be applied (constant thermal conductivity):

$$\frac{Pr}{Pr_{des}} = \frac{c_p \cdot \mu \cdot \rho}{\left(c_p \cdot \mu \cdot \rho\right)_{des}} \tag{22}$$

4.6 Modelling a fixed-speed steam turbine

The simplest turbine model is based on a fixed isentropic efficiency. However, the efficiency is dependent on the turbine load, and should not be considered to be constant at off-design conditions. When the admittance pressure of a turbine is changed, the volume flow passing through it will naturally be affected. The turbine's ability to swallow a certain mass flow is called the turbine capacity, and is a measure of the turbine size or rather the area of the turbine inlet. The turbine capacity is essential for off-design modelling especially for combined cycles which are operated at sliding pressure. Finally, it is important to consider the moisture content at the outlet of the turbine, as increased moisture will reduce the efficiency.

Steam turbines are normally modelled as a number of turbine sections. The sections are divided by admission or extraction/induction points. This simplifies modelling of both the turbine capacity and the efficiency. In reality, turbines are normally divided into three types of turbine cylinders with different pressure levels, normally referred to as high-pressure turbines, intermediate-pressure turbines and low-pressure turbines. It is possible to make small extractions between stages in one cylinder, but larger extractions must be made between the turbine cylinders. For large plants it is necessary to divide the flow among a number of parallel units; in low-pressure turbines the flow is often divided between at least two identical cylinders. The reason for this is to limit the rotor length in order to restrict the mechanical forces on the blade to an acceptable level. In power production, the turbine is connected to a fixed-speed generator and it is therefore operated at a fixed speed, which simplifies the modelling.

4.6.1 Dry efficiency

The dry efficiency is defined here as the turbine efficiency in the absence of moisture at the end of the expansion. If the expansion enters the wet region of the Mollier chart, the dry efficiency must be corrected for the losses due to the formation of droplets. This is discussed in Section 4.6.3.

The efficiency of a turbine stage is a function of the stage loading. The stage loading affects the velocities and the velocity diagrams. The stage loading can be described by the relationship between the fluid speed and the speed of the rotating blades. To shorten the iteration process the speed obtained by the isentropic heat drop is used rather than the actual heat drop, which depends on the efficiency itself:

$$\eta = f\left(\frac{u}{c_s}\right) \tag{23}$$

The function in Equation (23) is often called the ν number (Nu number). For heat- and mass-balance calculations it is more convenient to express the speed in terms of the enthalpy:

$$\eta = f\left(\frac{u}{\sqrt{2\Delta h_s}}\right) \tag{24}$$

Equation (23) and (24) is only valid for one stage. Different manufacturers use different versions of similar functions to describe the efficiency of a turbine section. One popular version is the Parson number. The Parson number uses the sum of the mean rotor speed for a turbine section:

$$X = \frac{\sum u^2}{\Delta h_s} \tag{25}$$

For a fixed-speed steam turbine the rotor speed u is constant for all loads. When Equation (25) is normalized to the design point the following expression is obtained:

$$\frac{\eta}{\eta_{des}} = f\left(\frac{\Delta h_{s,des}}{\Delta h_s}\right) \tag{26}$$

The function above can be determined from operational data or, if no data are available, a standard function can be used.

4.6.2 Capacity

The turbine capacity is a central part of turbomachine off-design modelling. The capacity of a turbine or swallowing capacity describes the relation between inlet and outlet pressure, inlet temperature and mass flow. At a certain pressure ratio the turbine will choke, and above this the mass flow will be independent of the outlet pressure. Modelling a choked turbine accurately is complicated. In the 1920s, Stodola empirically developed an expression called the steam-cone law [16]. He recognized that the function describing the turbine mass flow as a function of back-pressure at constant inlet pressure was an ellipse. In the 1960s Beckmann thermodynamically derived a more accurate formula, which was used in this work [17].

To understand the basics regarding turbine capacity, a single nozzle, as illustrated in Figure 10, can be studied. The pressure at position 1 is higher than at position 2, so the fluid will flow from 1 to 2.

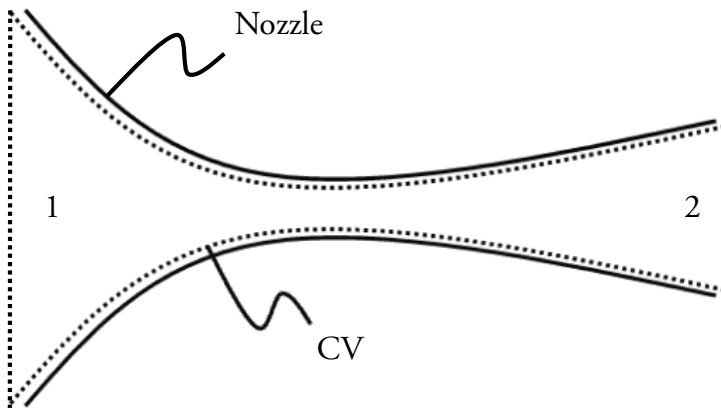

Figure 10: Flow through a nozzle

We start by applying the first law of thermodynamics with a control volume according to Figure 10 and making the following assumptions: the dynamic part at position 1 is negligible ($c_1^2 \ll c_2^2$), the specific heat can be considered to be constant ($c_{p1} = c_{p2}$), and the fluid can be treated as a perfect gas. By setting up an energy balance between position 1 and position 2 and applying the continuity equation and the isentropic relation the following equation can be derived (the derivation is presented in numerous textbooks on turbomachinery [18-19]):

$$\dot{m} = C \cdot A \sqrt{\frac{p_1}{v_1} \cdot \left(\left(\frac{p_2}{p_1}\right)^{\frac{2}{\gamma}} - \left(\frac{p_2}{p_1}\right)^{\frac{\gamma+1}{\gamma}} \right)} \tag{27}$$

where the constant *C* accounts for all losses due to friction, boundary layer blockage, etc. Equation (27) is often divided into two parts, the first part is the flow function, Equation (28), which only depends on the inlet condition, and the second part, Equation (29), is often replaced by the Greek symbol Ψ which depends on the pressure ratio and the isentropic exponent.

$$\dot{m} = \Psi \cdot C \sqrt{\frac{p_1}{v_1}} \tag{28}$$

$$\Psi = \sqrt{\left(\left(\frac{p_2}{p_1}\right)^{\frac{2}{\gamma}} - \left(\frac{p_2}{p_1}\right)^{\frac{\gamma+1}{\gamma}}\right)} \tag{29}$$

If the pressure ratio is varied by changing the outlet pressure (p_2) Equation (27) will give a maximum mass flow at a certain pressure ratio. This pressure ratio is the critical value, and occurs when the Mach number equals unity at the throat of the nozzle. The critical pressure ratio is reached when the ratio of the pressure over the inlet of the nozzle to the pressure over the nozzle throat is:

$$\frac{P_{throat}}{p_1} = \left(\frac{2}{\gamma+1}\right)^{\frac{\gamma}{\gamma-1}} \tag{30}$$

If the pressure ratio exceeds the critical value a shock wave (or a number of shocks) will occur in the nozzle. This shock is a sudden drop in pressure which ensures thermodynamic equilibrium without exceeding the speed of sound (Mach 1) at the throat. Even if the pressure ratio over the nozzle is increased the speed at the nozzle throat will be fixed at the speed of sound. With a fixed speed at the throat, the mass flow will also be fixed. This means that above the critical pressure ratio the outlet pressure has no effect on the capacity and hence Ψ, described in Equation (29), is constant. A shock wave is highly irreversible and therefore Equation (27), which was derived using the assumption of isentropic flow, cannot be used when the critical pressure ratio is exceeded.

The pressure lost as a result of the shock must be considered when calculating the mass flow, and this is not included in Equation (27), which was derived using the isentropic relation. Furthermore, Equation (27) only treats a single nozzle and is not suitable for turbine sections. Beckmann derived a function which is valid and continuous even for choked turbine sections [17]. To make the equation suitable for a turbine section including a number of nozzles, he introduced the stage correction factor, $\bar{\Lambda}$. This resulted in the following expression, which can be used to calculate the capacity of a turbine section:

$$\dot{m} = \tag{31}$$

$$= C\sqrt{\frac{p_1}{v_1}\cdot\frac{\gamma}{\gamma+1}\cdot\left[1-\left(1+2\cdot\frac{\bar{\Lambda}}{\gamma-1}\right)\cdot\left(\frac{1}{\pi}\right)^{\frac{\gamma+1}{\gamma}} - \left(1-\frac{\gamma+1}{\gamma-1}\cdot\left(\frac{1}{\pi}\right)^{\frac{2}{\gamma}}\right)\cdot\bar{\Lambda}\right]}$$

Beckmann's capacity function is used in the steam turbine models in this work. The mass flow plotted against the pressure ratio according to Equation (31) is plotted in Figure 11.

In analogy with the modelling described in this section, all constant values can be omitted when the equation is normalized to the design point. This means that no geometry is required as long as data from one operation point are available.

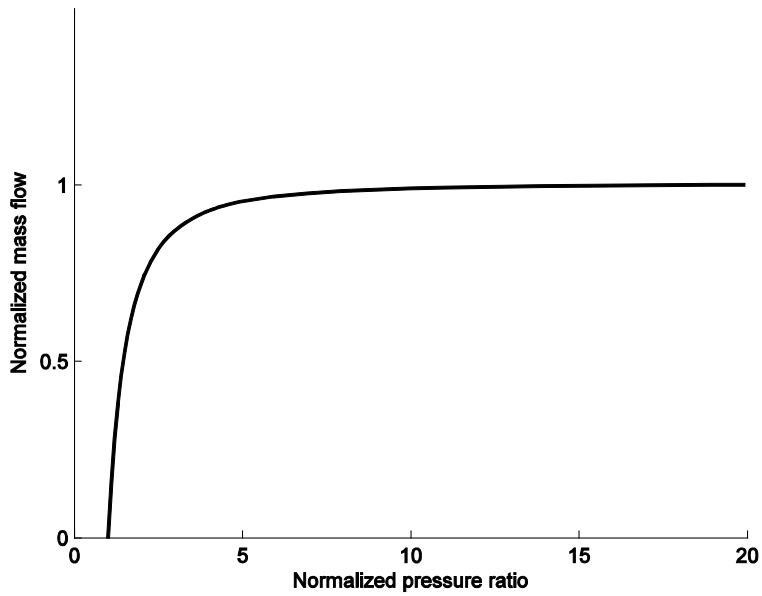

Figure 11: Beckmann's function for steam turbine capacity

The inlet pressure of any intermediate stage is the outlet pressure of the preceding stage. If the flow through the turbine is increased the pressure upstream and downstream of all intermediate stages will therefore increase by the same amount. This means that if no uneven steam extractions are present, the pressure ratio is fixed for intermediate stages during the whole load range. From this reasoning, it is also clear that Ψ, (Equation (29)), which is a function of the pressure ratio, has a constant value if the isentropic exponent is considered constant. Therefore, Equation (28) can be simplified by applying the ideal gas law, and if all the constant values are collected, the following expression is obtained:

$$\dot{m} = C \frac{p_1}{\sqrt{T_1}} \tag{32}$$

Equation (32) shows that if the mass flow is increased by a certain percentage, the inlet pressure of each intermediate stage will increase by the same percentage. Taking logarithm and subsequent differentiation shows that increasing the inlet temperature will reduce the mass flow by half the magnitude. This is because increasing the temperature reduces the density, and when the volume flow is constant the mass flow will be reduced.

The variation in the pressure ratio over the first stage is dependent on the type of control method used. The method called partial-arc control will give a varying pressure ratio over the first stage, while sliding pressure control will not. (Steam turbine control strategies are discussed in Section 6.1.) The pressure in the condenser is, to a first order, independent of the turbine loading and hence the pressure ratio over the last stage will vary significantly over the load range.

The volume flow through the last part of the turbine is reduced when the turbine is operated in the wet region. As steam condenses, the droplets have to be accelerated by the steam flow and therefore the turbine capacity is reduced. To compensate for the moisture at the turbine exhaust, Cotton [18] suggested the following modification to Equation (28) based on laboratory tests:

$$\dot{m} = \Psi \cdot C \cdot \sqrt{1 - Y} \sqrt{\frac{p_1}{v_1}} \tag{33}$$

where Y is the moisture fraction at the outlet of the last stage.

4.6.3 Expansion of wet steam

If a steam turbine is operated in the wet region, below the line of saturation, droplets will start to form. The condensation process itself and the effects of the droplets on the flow will cause the efficiency to decrease significantly. There are several reasons for this, and some of the major causes are described in this section. Traupel discusses it in his textbook [20], and Young has published studies on the subject [21-22].

Wet expansion will not only reduce the efficiency, it will also cause damage to the machine. Erosion is a major problem originating from the fact that the two phases have a large difference in density, resulting in the droplets having a higher momentum than the steam. The droplets will thus not follow the channel, but collide with the rotor. Erosion is normally the factor limiting the amount of moisture that can be tolerated at the end of low-pressure turbines.

There are three major reasons for the reduction of efficiency when operating a turbine in the wet area:

- thermodynamic losses
- braking losses
- frictional losses

4.6.3.1 Thermodynamic losses

When steam expands rapidly into the wet area across the saturation line, the nucleation time is limited and the steam will become subcooled while remaining dry. The steam temperature will therefore undergo the local saturation temperature and will not be at thermodynamic equilibrium, hence, $T < T(p)$. At a certain point called the Wilson point, maximum subcooling is reached and droplets start to form. The Wilson point is not a fixed value, and depends on the rate of expansion. Once condensation has been initiated and the droplet surface is created the process proceeds very rapidly. When droplets are formed, the latent heat produced heats the flow, which speeds up the process of reaching the equilibrium temperature. Sudden condensation leads to a sheet of discontinuity when the volume of the flow is reduced. The event has many similarities with an adiabatic shock wave in ideal gas [23].

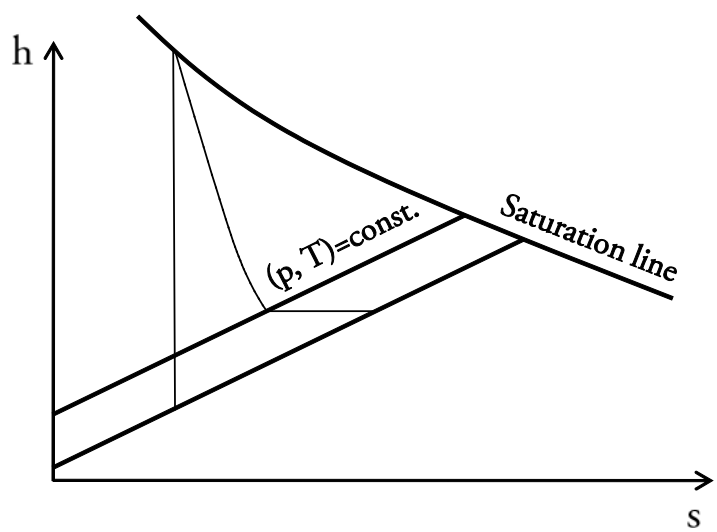

Figure 12: The condensation shock in a h-s diagram

The phenomenon can be illustrated in an enthalpy versus entropy diagram, as shown in Figure 12, but it should be noted that the expansion before the

condensational shock does not take place at equilibrium conditions. For example, the process of moving from the Wilson point to the equilibrium state occurs under constant pressure (if the time gradient is ignored), but not along a constant pressure line in Figure 12. Note that the illustration is a simplification; the true path would be somewhat smoother. If the expansion were to take place at equilibrium state, less entropy would be generated. In Figure 12 this would mean that the end point would be further to the left on the constant pressure line, and more work would be produced, as Δh would be greater.

4.6.3.2 Braking effects

The fog formed by the condensational shock has a small effect on the flow field. However, some of the droplets stick to the blades, forming a film of moisture. The amount of moisture accumulated on the stator is a function of the droplet size. With increasing droplet size, the droplets' ability to follow the flow is reduced due to their increased momentum, i.e. with larger droplets more moisture is collected on the blade surface. This film of moisture formed on the blade travels towards the back end of the vane. Large droplets are then formed on the back of the blade, and eventually they will fall back with a velocity much lower than that of the flow field.

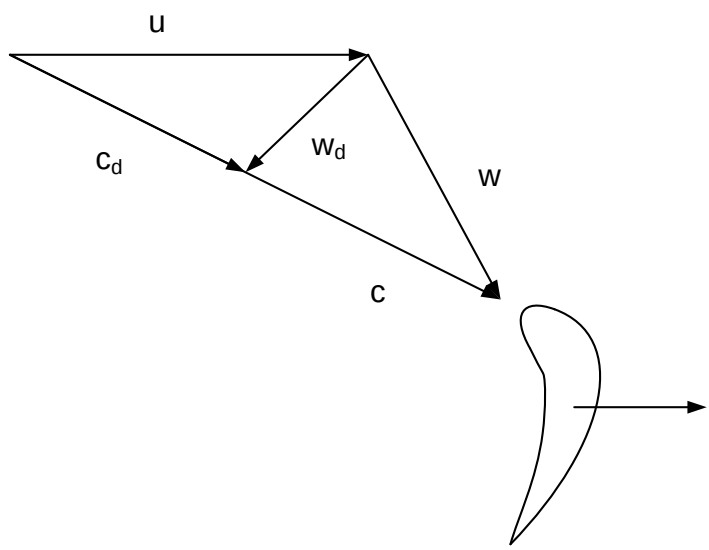

Figure 13: The droplets will travel more slowly and will collide with the back of the rotor (see direction of w_d) causing braking of the rotor

The velocity diagrams are excellent for illustrating the flow in a turbomachine. The velocity diagrams are triangles consisting of three vectors, the fluid velocity, *c*, the fluid velocity relative to the rotor, *w*, and the rotor velocity [24]. The velocity of the

falling drops relative to the rotor will thus have a different direction. In Figure 13 the vector w_d shows the droplets' velocity relative to the blade. These droplets will hit the back of the blade resulting in a braking effect on the rotor.

4.6.3.3 Frictional losses

As the two phases are moving at different velocities, there will be friction between them. This will slow down the steam flow and accelerate the droplets. The erosion caused by droplets will cause an increased surface roughness which will increase the friction.

4.6.3.4 Calculating the wet efficiency

Quantifying all the losses due to wet expansion is complicated. The normal way of doing this is to use the Baumann equation (Equation (34)), which was established through experiments on steam turbines performed by Baumann in the 1920s. The method is described by Traupel [20] and is based on the observation that the wet losses are proportional to the mean moisture content in the turbine section.

$$\eta_w = \eta_{dry} \cdot \left(1 - \alpha \cdot \frac{y_{in} + y_{out}}{2}\right) \tag{34}$$

The Baumann factor α normally has a value between 0.5 and 1, and is larger for a turbine section than for a single stage.

4.7 Modelling a gas turbine

The main components of a gas turbine are a compressor, a combustion chamber and a turbine. There are single- and multi-shaft gas turbines. In a single-shaft gas turbine the compressor is operated on the same shaft as the turbine, while in a multi-shaft gas turbine the compressor and/or the turbine is divided into more than one unit. For example, a two-shaft gas turbine consists of a compressor connected via a shaft to a high-pressure turbine and a low-pressure turbine on a second shaft operating at a different speed. Generally, the single-shaft gas turbine is simpler and cheaper but less flexible than a multi-shaft turbine, although it has some load control advantages.

The behaviour of a gas turbine depends on many parameters. In comparison to the steam turbine which is operated on pure steam, gas turbine will experience different gas compositions which add to the complexity. In this work, all the gas turbine modelling was based on modelling with characteristics, i.e. a number of maps describing the behaviour of the machinery. Modelling the off-design

behaviour of a gas turbine with equations requires a large number of equations and information about the machine geometry and design. A comprehensive description of modelling a gas turbine with characteristics is presented by Walsh and Fletcher [25].

Using the characteristics of the compressor and turbine it is possible to model gas turbines with limited input data. Characteristics are used for both the compressor and the turbine and describe them as whole units and will therefore not give any information about the dynamic events within the components. This is acceptable for cycle studies to a certain degree. When blade temperatures and cooling flows are to be studied more advanced modelling is required, but this is outside the scope of this work.

4.7.1 Stagnation properties

Turbomachines consists of rotating blades and fluid in motion, and should be considered as high-speed flow systems [26]. For calculations this means that the kinetic energy cannot be neglected. All states for a system in motion can be divided into a dynamic and a static part. The sum of these two terms is the total or stagnation state, which is the condition resulting if the fluid is brought to rest with no work or heat transfer.

$$h_0 = h_s + \frac{c^2}{2} \tag{35}$$

This can also be expressed in terms of temperature:

$$T_0 = T_s + \frac{c^2}{2c_p} \tag{36}$$

where the subscript 0 indicates stagnation conditions and s indicates static conditions, c is the fluid velocity and c_p is the specific heat of the fluid. The isentropic relation can be used to find the total and static pressures once the temperatures are known:

$$p_0 = p_s \cdot \left(\frac{T_0}{T_s}\right)^{\frac{\gamma}{\gamma-1}} \tag{37}$$

4.7.2 The Compressor

The behaviour of a compressor is dependent on a large number of parameters. The calculations can be made more manageable by creating parameter groups instead of considering each parameter separately. Not only the calculations are simplified, the use of parameter groups also provides a quick overview of the machine.

The parameter groups can be derived using Buckingham's pi theorem, as is explained in several books [27]. There is however a more physical derivation which gives the same result. The key is that each point on the map should represent a unique flow condition. A unique flow condition will be obtained if the Mach numbers are equal for all vectors in the velocity triangle, the velocity diagrams are uniform and the Reynolds number is constant. This means that if the velocity diagrams are based on Mach numbers rather than actual velocities, a unique flow condition is described. For a stationary machine the influence of the Reynolds number is very small, but a method of including it is presented later in this section. The compressor map is principally formed by the mass flow, pressure ratio and rotational speed. This means that three groups are required for the map. These groups should be derived so that together they fully describe uniform velocity diagrams based on Mach numbers for each point on the map. The method is presented by Lindberg [28] and Kyrklund [29], but the latter is only available in Swedish. Many textbooks do not include the derivation of parameter groups and, therefore, the three parameter groups needed for the compressor map are described below.

4.7.2.1 Mass-flow

The fluid speed, *c*, is included when forming the mass-flow group.

$$\left.\begin{aligned} \dot{m} &= \rho A c \\ c &= Ma_c\sqrt{\gamma RT} \end{aligned}\right\} \dot{m} = \frac{\pi}{4} d^2 \rho Ma_c \sqrt{\gamma RT} \tag{38}$$

The ideal gas law is applied, giving:

$$Ma_c = C\frac{\dot{m}\sqrt{RT}}{d^2 p\sqrt{\gamma}} \tag{39}$$

4.7.2.2 Speed

This group is referred to as the aerodynamic speed and the rotor speed *u* is included:

$$\left.\begin{aligned} u &= n \cdot D \cdot \pi \\ u &= Ma_u \cdot \sqrt{\gamma RT} \end{aligned}\right\} Ma_u = \frac{n \cdot D \cdot \pi}{\sqrt{\gamma RT}} \tag{40}$$

4.7.2.3 Pressure ratio

The pressure ratio group is more complicated, start with the change of enthalpy or "head", which could just as well be used as the parameter group, but most manufacturers use pressure ratio in their characteristics. The component of the fluid speeds in the direction of the rotor is used Figure 14 as well as the rotor speed:

$$\left.\begin{aligned} u \cdot \Delta C_\theta &= \Delta h_0 \\ u &= Ma_u \cdot \sqrt{\gamma RT} \\ c_\theta &= Ma_{c_\theta} \cdot \sqrt{\gamma RT} \end{aligned}\right\} Ma_u \cdot Ma_{c_\theta} = \frac{\Delta h_0}{\gamma RT} \tag{41}$$

As mentioned above, Equation (41) can be used instead of the pressure ratio, but as the pressure ratio is easier to relate to, it is commonly used instead. Equation (41) can be rearranged and the polytropic relation is applied giving the final parameter group for pressure:

$$Ma_u \cdot Ma_{c_\theta} = \frac{\eta_s \left(\pi^{\frac{\gamma-1}{\gamma}} - 1 \right)}{\gamma - 1} \tag{42}$$

The compressor characteristic is based on the three parameter groups from Equations (39), (40) and (42). Each of these equations will have a specific value at every point on the map.

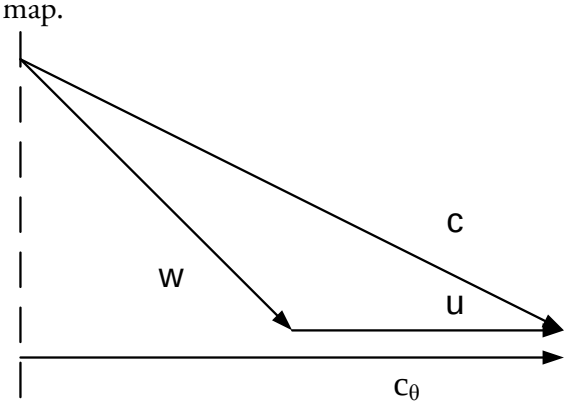

Figure 14: With u, c and c_θ fixed the velocity diagram is fully described

This means that the velocity diagrams based on Mach numbers are fixed. Figure 14 shows that the velocities used to derive the parameter groups, *u, c* and c_θ are

sufficient to fully describe a velocity triangle, which means that the machine behaviour is completely described. It should be borne in mind that the Reynolds numbers also may have an effect, but this will be discussed later.

The characteristic or compressor map is a multi-dimensional table based on the three parameter groups derived above. Each point in the map defines a unique behaviour of the unit. However, multiple combinations of parameters in Equations (39), (40) and (42) are valid for the same point on the map. This means that the machine's behaviour when operated at, for example, a different inlet pressure can be evaluated by changing other parameters to get to the same working point in the characteristics. This is the advantage of using parameter groups; regardless of whether the machine has been operated under certain conditions before, the behaviour can be predicted from the characteristics.

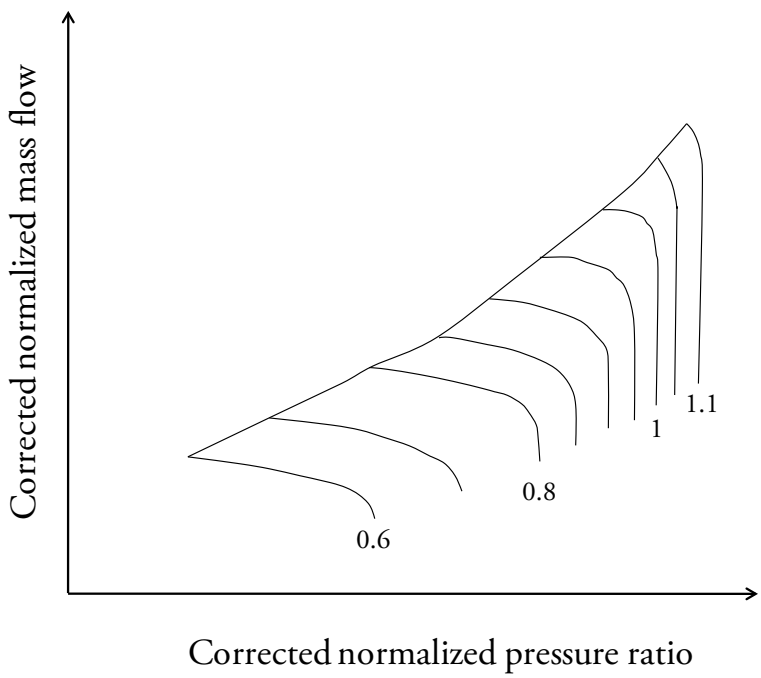

Figure 15: Typical characteristics of a radial flow compressor showing normalized aerodynamic speed lines

The characteristic can be either measured or calculated. For smaller machines the characteristic can be measured in a compressor rig. This is normally done by varying the shaft speed while a valve is used to control the back-pressure of the compressor. The results obtained are corrected for the ambient conditions and the map can be plotted. A typical compressor map is shown in Figure 15. The speed lines in Figure 15 are vertical in some areas of the map, and for some speed lines a certain pressure ratio can give two solutions for the mass flow. To eliminate this problem, auxiliary

coordinates called beta lines, which intersect the speed lines, are introduced. Using the beta lines and the speed lines to read the map, each point will have a unique value.

A reference point is required to define other locations on the map and this usually the design point. It is useful to normalize the map to the design point so that the coordinates (1,1,1) represent the design point. With a normalized map it does not matter which parameters are included in the parameter group. This means that all the parameters that can be assumed to be constant can be omitted. For instance, if only one working fluid is to be used and the isentropic exponent can be considered constant it can be excluded from the calculations.

The procedure for calculations is to determine the parameter groups for a reasonable starting value, divide them by their design value and locate the position on the normalized map. The guessed values are corrected in an iterative process until a solution is found where the value of the three parameter groups match in the map.

4.7.3 Reynolds number effects

The viscous effects, like losses and blockage, are not included when using the three parameter groups derived in Equations (39), (40) and (42). The Reynolds number variation due to load changes is influenced by the temperature, pressure, specific gas constant and the viscosity. For an industrial unit all this parameters only deflects to a certain limit from the design condition and this will normally not influence the behaviour of the machine. However, in aircraft propulsion the inlet pressure will vary significantly and the Reynolds number will have an impact on the engine performance. Below a critical Reynolds number the capacity and efficiency of the gas turbine will be affected.

The effects of Reynolds number have been studied by Wassell [30], and a method of accounting for it in characteristic-based modelling is given by Kurzke [31]. To keep track of the Reynolds number deviation when changing the working media due to exhaust gas recirculation in this work Kurzkes method have been implemented. The method is based on that when the three parameter groups have been calculated the values are corrected whit a factor based on the deviation in Reynolds number. This factor is called Reynolds number index (*RNI*):

$$\left.\begin{aligned} RNI = \frac{Re}{Re_{des}} = \frac{\rho_s \cdot L \cdot c}{\rho_{s,des} \cdot L_{des} \cdot c_{des}} \cdot \frac{\mu_{des}}{\mu} \\ \rho_s = \frac{p_s}{R \cdot T_s} \end{aligned}\right\} \Rightarrow \qquad (43)$$

$$RNI = \frac{p_s}{R \cdot T_s} \cdot \frac{R_{des} \cdot T_{s,des}}{p_{s,des}} \cdot \frac{c}{c_{des}} \cdot \frac{\mu_{des}}{\mu}$$

where c is the fluid speed at the critical position. The index des here refers to any value in the *RNI=1* plane i.e. any point in the map of the design Reynolds number. When the values are corrected for Reynolds number deviation we move on the fourth axis in the map, this means that the Mach numbers are constant. Therefore the ratio of the design Mach number and the actual Mach number are equal.

$$Ma = \frac{c}{\sqrt{\gamma R T_s}} = \frac{c_{des}}{\sqrt{\gamma_{des} R_{des} T_{s,des}}} \tag{44}$$

$$RNI = \frac{p_s}{p_{s,des}} \cdot \frac{c}{\sqrt{\gamma R T_s}} \cdot \frac{\sqrt{\gamma_{des} R_{des} T_{s,des}}}{c_{des}} \cdot \frac{\sqrt{R_{des} \cdot T_{s,des}}}{\sqrt{\gamma_{des}}} \cdot \frac{\sqrt{\gamma}}{\sqrt{R \cdot T_s}} \cdot \frac{\mu_{des}}{\mu} \tag{45}$$

$$RNI = \frac{p_s}{p_{s,des}} \cdot \frac{\sqrt{T_{s,des}}}{\sqrt{T_s}} \cdot \frac{\sqrt{R_{des}}}{\sqrt{R}} \cdot \frac{\sqrt{\gamma}}{\sqrt{\gamma_{des}}} \cdot \frac{\mu_{des}}{\mu} \tag{46}$$

The ratios of static to total pressure and temperature are the same for the case being studied and the reference case since the Mach numbers are the same (assuming a constant isentropic exponent).

$$RNI = \frac{p_s/p_0}{p_{s,des}/p_{0,des}} \cdot \frac{p_0}{p_{0,des}} \cdot \frac{\sqrt{\frac{T_{s,des}}{T_{0,des}} \cdot T_{0,des}}}{\sqrt{\frac{T_s}{T_0} \cdot T_0}} \cdot \frac{\sqrt{R_{des}}}{\sqrt{R}} \cdot \frac{\sqrt{\gamma}}{\sqrt{\gamma_{des}}} \cdot \frac{\mu_{des}}{\mu} = \tag{47}$$

$$= \frac{p_0}{p_{0,des}} \cdot \frac{\sqrt{T_{0,des}}}{\sqrt{T_0}} \cdot \frac{\sqrt{R_{des}}}{\sqrt{R}} \cdot \frac{\sqrt{\gamma}}{\sqrt{\gamma_{des}}} \cdot \frac{\mu_{des}}{\mu}$$

4.7.4 Extractions

The isentropic efficiency will give a straight line between the starting point and end point of the compression. If extractions are included between these points the true expansion path must be determined in order to identify the correct properties of the

extracted fluid. A more accurate path can be calculated by using the polytropic efficiency.

The normal procedure for modelling the amount of cooling extracted is to specify a fixed percentage of the total mass flow. For extreme off-design conditions, where the turbine is operated at pressure ratios far from the design point, the cooling channel could be modelled with a finite capacity, i.e., a higher extraction pressure should give a larger mass flow. In doing this it is assumed that the pressure at the induction point will increase by the same amount as the pressure at the extraction point.

4.7.5 The combustion chamber

The combustion chamber model used in this work has been developed by my predecessors at the department. The model includes several features that have not been explored in the current work, and the model is based on the theory presented by Walsh and Fletcher [25]. The model uses a table which describes how the combustion efficiency varies as a function of the combustor outlet temperature. The unburned fuel and carbon monoxide represent a very small fraction of the flue-gas and was therefore not included in the outgoing stream.

4.7.6 The turbine

Modelling the turbine with the use of characteristics has many similarities to the compressor modelling. There are two types of turbine characteristics depending on whether the turbine chokes in the first stator, as displayed in Figure 16a or in the first rotor, as in Figure 16b. The two maps show different results for each speed line before the turbine chokes. This is due to the fact that the static density and the static pressure relative to the blade differ for different aerodynamic speeds and, therefore, the pressure distribution between the stator nozzles and rotor nozzles is dependent on the aerodynamic speed. For a turbine that chokes in the first stator the capacity is the same for all the aerodynamic speed lines in the choked area, which is explained by the fact that the capacity is set by the first nozzle before reaching the rotors. When a section is choked the pressure behind it does not have any effect on the mass flow (see the section on capacity in Section 4.6.2.

If the first rotor is choked, the capacity is dependent on the aerodynamic speed. As the relative speed increases, the relative static density decreases and hence the capacity is reduced. Likewise, a higher relative aerodynamic speed results in a lower relative static pressure and, therefore, the pressure ratio at which choke occurs is higher.

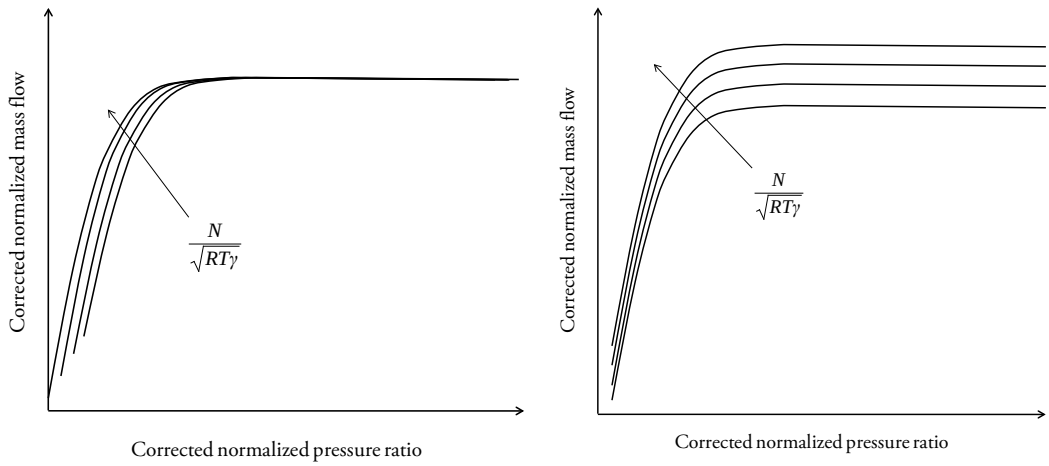

Figure 16: Typical characteristics for an axial flow turbine, where choking occurs in the stator (a) or in the first rotor (b).

The number of cooled stages can, to some extent, be reduced by the first stage loading. With a high first stage loading the succeeding stages will experience a lower temperature. Therefore, turbines are designed with a high loading in the first stage which results in that turbines generally choke in the first stage.

4.7.7 Cooling

Large modern gas turbines use air cooling. The air is extracted from the compressor and injected into the turbine via channels on the inside of the blades. The blades have small holes allowing the air to flow through and cool the blades. Sometimes film cooling is used, which means that the cooling air forms a film on the blade surface. The bleed of cooling air into the expansion path makes the expansion path rather complicated. One method of dealing with this when the turbine is modelled as a single unit is to introduce all the cooling before the turbine and find the isentropic efficiency that corresponds to the correct end point of the expansion. The stator outlet temperature (SOT) is obtained by assuming constant total pressure and mixing in the stator cooling air, thereafter the remaining cooling is injected. The temperature after all cooling is mixed with the main flow, as defined by the International Organization for standards ISO, is called the turbine inlet temperature (ISO TIT). Both SOT and ISO TIT are important temperatures when modelling gas turbines. Figure 17 shows the real expansion line as well as the simplified expansion via the ISO TIT.

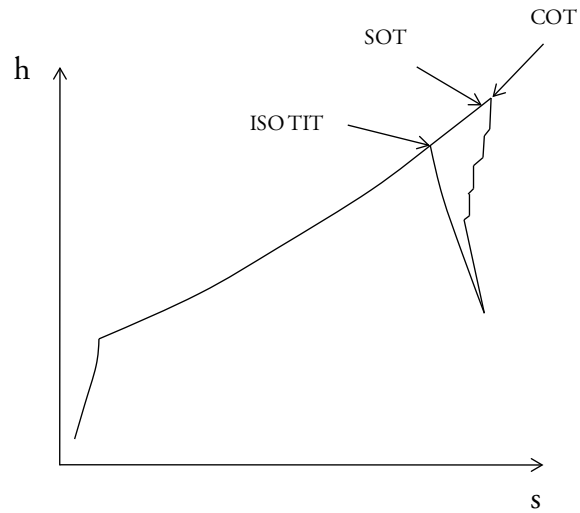

Figure 17: Temperature vs. entropy diagram for the Brayton cycle showing the method used to model turbine cooling modelling

4.7.8 The turbine diffuser

The diffuser's ability to recover kinetic energy is described by its pressure recovery coefficient, C_P:

$$C_P = \frac{p_{2s} - p_{1s}}{p_{01} - p_{1s}} \tag{48}$$

The pressure recovery coefficient is a function of the outlet swirl angle from the turbine. By using a table for C_P as a function of turbine swirl angle an easy to use diffuser model can be attained. To find the turbine static outlet pressure, p_{1s}, and the swirl angle the turbine outlet flow area and the design point swirl angle are required. The turbine outlet flow area can be estimated by assuming a value of the area times the rotational speed squared (AN^2) at the design point. AN^2 quantifies the rotor centrifugal pull force, and atypical design value can be found in the text book by Moustapha [32].

5 Post-Combustion Carbon Capture

The EU's objective of reducing the emission of greenhouse gases by at least 20% of 1990 levels in 2020 requires drastic action. Part of this reduction can be achieved by increasing the amount of power produced from renewable resources, but in the timeframe of 10 years it will be necessary to employ carbon capture at fossil fuel power plants.

Carbon dioxide emissions from fossil fuel power plants can be reduced by implementing technology for carbon dioxide capture. The idea is to separate the carbon dioxide produced and permanently store it underground. The emission of carbon dioxide can be avoided or mitigated either by removing the carbon before the combustion process, i.e. pre-combustion techniques, or by collecting the carbon dioxide from the flue-gases after combustion, i.e. post-combustion techniques. Pre-combustion can be performed with membrane technology and chemical looping or with fuel-upgrading processes using physical or chemical absorption. Post-combustion can be divided into two categories: oxy-fuel cycles and conventional cycles.

The principle of the oxy-fuel cycle is that nitrogen is removed from the air before combustion so that the flue-gas consists mainly of CO_2 and water. After the steam generator (a boiler or a HRSG), the steam is separated by condensation of the water vapour in the flue-gases.

The other post-combustion method is based on the separation of CO_2 using an absorbent, where the CO_2 is separated after the power plant. Compared with the other CO_2 capture techniques, post-combustion absorbent-based CO_2 capture does not require a new power plant concept, and the technique can be applied to existing plants. This and the fact that the method is suitable for retrofitting of existing power plants has made post-combustion absorbent based CO_2 capture a hot topic in the research field, numerous publication are available both on CCPPs [5, 33-40]and on regular coal-fired power plants [41-45]. The absorption process can be divided into reversible and irreversible processes. In a reversible absorption process the absorbent can be regenerated and reused. Two absorbents are discussed in this thesis, namely monoethanolamine (MEA) and ammonia. MEA has been proven to be a useful absorbent, while ammonia is one of the promising less proven alternatives.

5.1 Oxy-fuel CCPPs

When organic fuels such as natural gas are combusted in air the flue-gas will consist mainly of CO_2, N_2, water and small amounts of argon. The nitrogen originates from air and is not formed during combustion. If the nitrogen is removed from the air before combustion, the flue-gas will only consist of CO_2, water and argon. This means that the CO_2 can be removed by condensing the water. The small amount of argon in the CO_2 will be separated during the compression process. In normal combustion the temperature is limited by nitrogen, which adsorbs a proportion of the energy released. To limit the temperature developed in oxy-fuel combustion, CO_2 and/or steam is recirculated from the flue-gas.

Two main concepts based on oxy-fuel combustion have emerged in combined-cycle power plants: the semi-closed-oxy-combusted-combined-cycle (SCOC-CC) and the Graz cycle. Both these cycles include an air separation unit (ASU) which removes nitrogen from the air using cryogenic, membrane or adsorption techniques. Cryogenic separation, based on condensation of the gases at low temperature, is the best choice in large-scale separation, but this does not normally include the separation of argon.

The Graz cycle was invented by Jericha and first presented at the CIMAC Conference in Oslo, Norway in 1985. The gas turbine is cooled with steam from the bottoming steam cycle. Part of the heat generated from the compression of CO_2 prior to storage is recovered in the Rankine cycle [46]. The Graz cycle was not considered in this work, and will not be discussed further.

The SCOC-CC is promising due to its relative simplicity compared with other oxy-fuelled cycles. This cycle has many similarities with a normal combined cycle, however the topping gas turbine cycle differs. Firstly, the working fluid in the compressor is CO_2 (diluted with small amounts of argon and steam). Secondly, the combustion chamber is operated under conditions close to stoichiometric conditions, with pure oxygen as the oxidizer and CO_2 as the coolant.

Figure 18 shows an illustration of a SCOC-CC. CO_2 enters the compressor where it is compressed to about 40 bar. After compression, the CO_2 enters the combustion chamber where the temperature increases as oxygen reacts with the fuel. Some excess oxygen is required to ensure complete combustion, i.e. high combustion efficiency. The turbine is cooled with CO_2 extracted from the compressor.

The pressure ratio of a SCOC-CC gas turbine is about 40, which is much higher than in a normal combined-cycle gas turbine. This is a result of that CO_2 has a lower isentropic exponent than nitrogen According to the isentropic relation,

Equation (37), this results in a smaller decrease in temperature for a given pressure ratio. Thus, in order to achieve a temperature suitable for the steam generator, the gas turbine pressure ratio must be higher. The HRSG does not differ physically from that in a normal CCPP, neither does the steam cycle. After the HRSG the exhaust gas must be cooled before further treatment. This is done by direct contact with water, which is sprayed in at the top of a column in the opposite direction to the exhaust gas. The steam in the exhaust gas will then condense and drain away with the cooling water at the bottom of the column. The main part of the exhaust is recirculated to the compressor inlet. The remaining exhaust, which corresponds to the amount of CO_2 formed in the combustion process, is then ready to be compressed for storage.

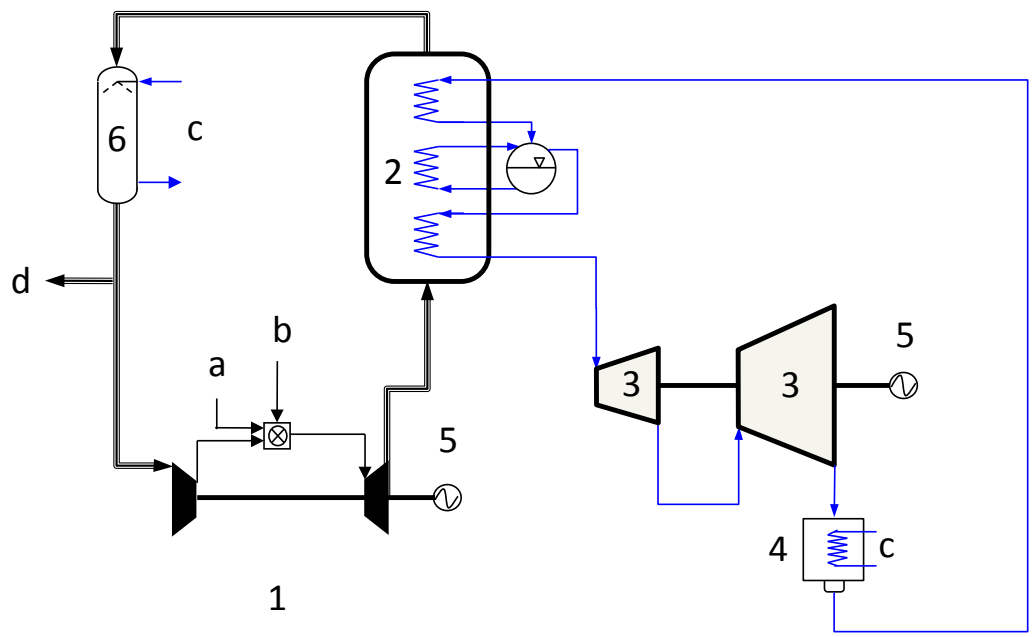

1. Gas turbine **4. Condenser** **a. Oxygen** **d. CO_2 to further treatment**
2. HRSG **5. Generator** **b. Fuel**
3. Steam turbine **6. Flue-gas condenser** **c. Cooling water**
Figure 18: Schematic illustration of a SCOC-CC

Figure 19 shows the difference in specific heat, c_p, of the flue-gas from a SCOC-CC and a conventional combined cycle. The specific heat of the CO_2-rich flue-gas produced in the SCOC-CC is higher at high temperatures, but falls quickly at lower temperatures. When comparing a dual-pressure SCOC-CC with a normal dual-pressure CCPP, the mass flow of steam is higher in the high-pressure section but lower in the low-pressure section. Furthermore, due to the low specific heat of the

flue-gas in the economizer, the temperature profile will be tighter and hence the HRSG outlet temperature difference will be smaller. The latter results in the flue-gas temperature after the HRSG lower than for a conventional CCPP. Therefore, the gain of using a third pressure level is small. The dual-pressure SCOC-CC bottoming steam cycle will have about 1% higher efficiency than the same cycle in a normal CCPP.

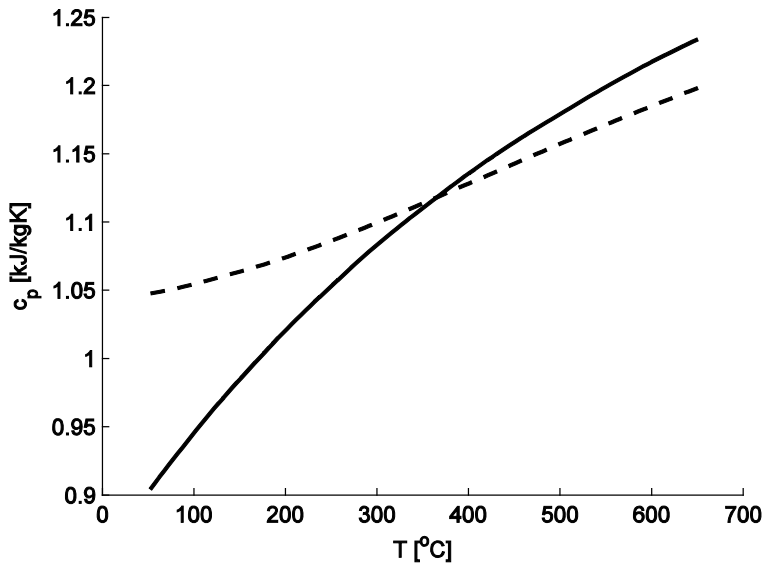

Figure 19: Specific heat, c_p, as a function of temperature for the flue-gas from an SCOC-CC (solid line) and a normal CCPP (dashed line)

5.2 Absorbent-based CO_2 capture

Absorption processes for gas purification can be divided into different categories based on whether the gas is chemically or physically absorbed and whether the process is reversible or not. The methods used in the present work are reversible, meaning that CO_2 is released from the absorbent. This means that the absorbent can be regenerated and used again in the process. The absorbents used in this work, MEA and ammonia, absorb CO_2 chemically.

The most simple post-combustion absorbent-based carbon capture unit consists of two columns, as shown in Figure 20. In the first column, the absorber, the liquid absorbent absorbs the CO_2 from the flue-gas. The flue-gas enters at the bottom of the column in the opposite direction to the absorbent solution. The treated flue-gas is released into the atmosphere from the top of the column. At the bottom of the absorber the now CO_2-rich absorbent is pumped through a heat exchanger, in which it is heated by the lean absorbent, to the top of the other column, called the

regenerator or stripper. The CO_2 is released from the absorbent by breaking the chemical link between them. This process is endothermic, which means that it requires heat. This heat is supplied externally from the reboiler at the bottom of the column. Before the CO_2 leaves the system at the top of the regenerator for further treatment it is cooled and dried in a cooler. From the reboiler, the lean absorbent is fed to the heat exchanger and back to the absorber to close the cycle.

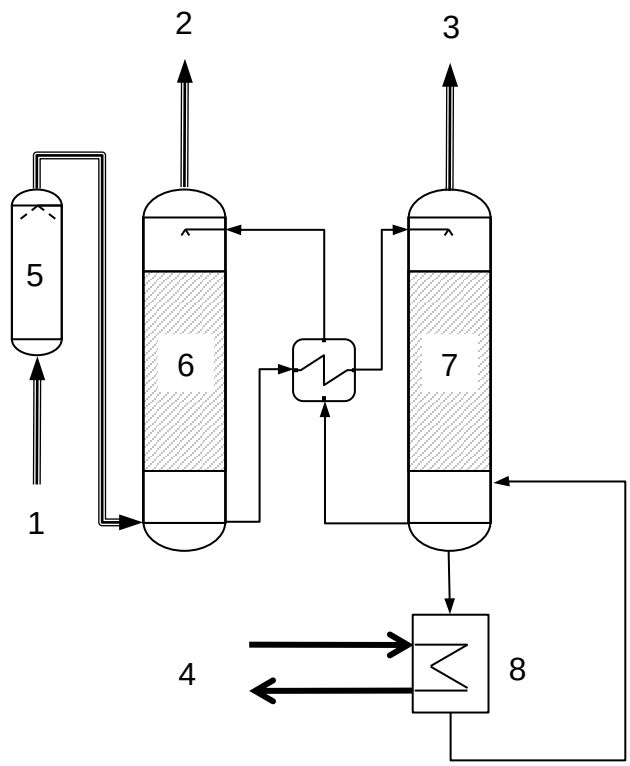

1. Flue-gas **3. CO_2** **5. Flue-gas condenser** **7. Regenerator**
2. Lean gas **4. External heat** **6. Absorber** **8. Reboiler**

Figure 20: Schematic illustration of an absorption CO_2 separation unit

The pressure in the absorber is normally just above atmospheric, and the temperature depends on the absorbent used. The pressure in the regenerator plays an important role in the energy consumption of CO_2 compression before final storage. A high pressure increases the possibility of raising the pressure of the CO_2 solved in the liquid state in the absorbent. This means that the gaseous CO_2 leaving the regenerator will require less energy for compression to the final storage pressure. However, several parameters limit the pressure in the regenerator. The absorbent is often sensitive to high temperatures, and a higher pressure results in a higher

evaporation temperature, and hence a higher regenerator temperature. The regenerator pressure also affects the energy required to separate the CO_2 from the absorbent. The gain in terms of reduced compressor work must be weighed against the increase in the energy required to release the CO_2 from the absorbent.

5.2.1 The reboiler

The purpose of the reboiler is to re-evaporate the CO_2. This is done by supplying heat from an external source. This heat is usually carried by steam which is condensed in a tube bundle in the reboiler, according to Figure 21.

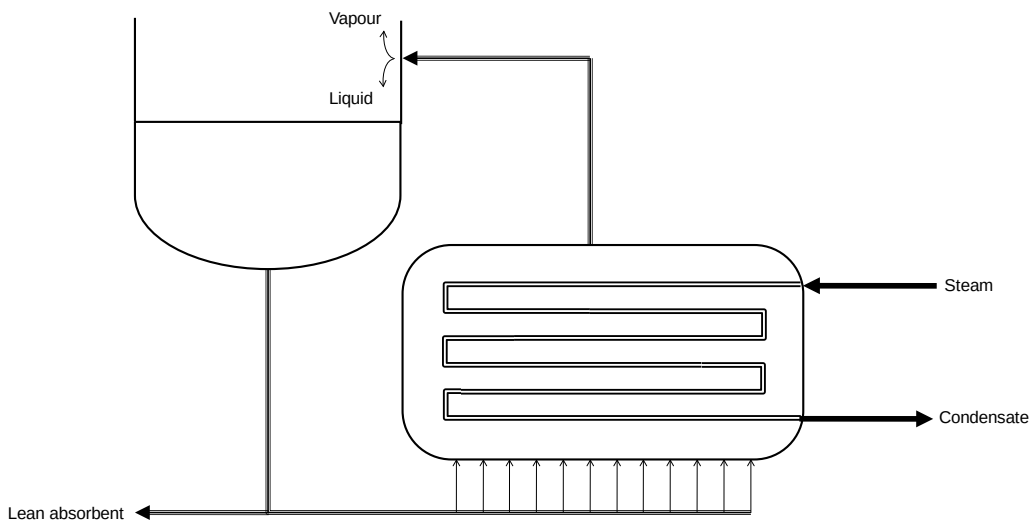

Figure 21: Schematic illustration of the reboiler

The steam is preferably saturated at the inlet of the reboiler to minimize the temperature difference and avoid local hot spots and overheating of the absorbent. Usually, not only the CO_2 is evaporated in the reboiler, but part of the absorbent solvent as well. If the evaporated absorbent is condensed inside the regenerator it mixes with the liquid absorbent and flows down to the bottom of the column where it is collected in the reboiler again. However, some of the gaseous absorbent is likely to leave the regenerator and must be condensed and returned to the system, which results in energy loss.

5.2.2 Amine-based carbon capture unit

The MEA process is currently the most developed industrial process for capturing CO_2 at ambient pressure. It has been known since the 1930's, and has been used,

for instance, for enhancing oil recovery and upgrading natural gas. The process is described in detail in the textbook by Kohl [47]. The demand for high efficiency in the power industry has increased interest in finding better processes. A key aspect is the amount of energy required to regenerate the absorbent, but the CO_2 loading capacity of the absorbent is also of relevance. Other amines are available, but the amount of well documented experience of the use of MEA led to the decision to focus on it in this work.

The absorbent usually consists of 30%wt MEA and 70%wt water. The flue-gas is cooled by an ambient heat sink to about 40 °C before it enters the absorber. The regenerator temperature is approximately 100-120 °C, resulting in a pressure of about 1.6 bar [48].

One limitation of MEA and other amines is their sensitivity to high temperatures, which causes them to degrade quickly. This limits the pressure in the regenerator column since a high pressure increases the evaporation temperature. A higher pressure in the regenerator reduces the energy required for CO_2 compression as it allows for a higher pressure rise in the pump between the absorber and the regenerator.

5.2.3 The chilled ammonia process

An interesting alternative for the absorption of CO_2 is ammonia. Less energy is required to release the CO_2 and the problem of degradation can be avoided. However, ammonia absorbs CO_2 at a lower temperature than amines, and therefore refrigeration is required in the absorber. Furthermore, ammonia is both caustic and toxic and release to the atmosphere must be avoided.

A CO_2 separation method based on ammonia, called the chilled ammonia process, was patented in 2006 by Eli Gal [49]. The absorption temperature range is 0-20 °C, but preferably not above 10 °C, according to the patent. This low temperature prevents ammonia from evaporating in the absorber. To avoid the release of ammonia to the atmosphere, the lean flue-gas is washed with cold water and an acid solution before leaving the system at the top of the absorption column. As with MEA, the absorbent is water based, and the mixture ratio depends on the configuration of the plant. The rich absorbent leaving the absorption column is a slurry, containing both liquid and solid phases. The temperature in the regenerator is between 50 and 200 °C, preferably 100-150 °C, according to the patent. To prevent ammonia and water from evaporating in the regenerator the pressure should be between 2 and 136 bar [50]. The energy required for desorption of the CO_2 is lower than for MEA, and the energy required for compression is also lower as the

CO_2 leaves the system at a higher pressure. However, cooling of the absorption column requires large amounts of energy and, as the regeneration column works at a higher temperature, the CO_2 leaving the system contains more energy which will be lost.

5.2.4 Integration of absorbent-based CO_2 capture with a CCPP

Regardless of which absorbent is used, a large amount of heat is required for desorption of CO_2. The best way to supply this heat is to extract it from the power plant, and the method of integration is thus important for the total power output. The most straightforward method is to extract steam before the low-pressure turbine. A significant amount of steam must be extracted from the steam cycle to cover the heat requirement of the carbon capture plant. This steam is returned at a much higher temperature than the feedwater returned from the main condenser, resulting in an increased feedwater temperature. The effect of this is that less energy can be recovered from the flue-gas. In a T-Q diagram this can be visualized by cutting off the last part of the economizer as shown by the hatched area in Figure 22.

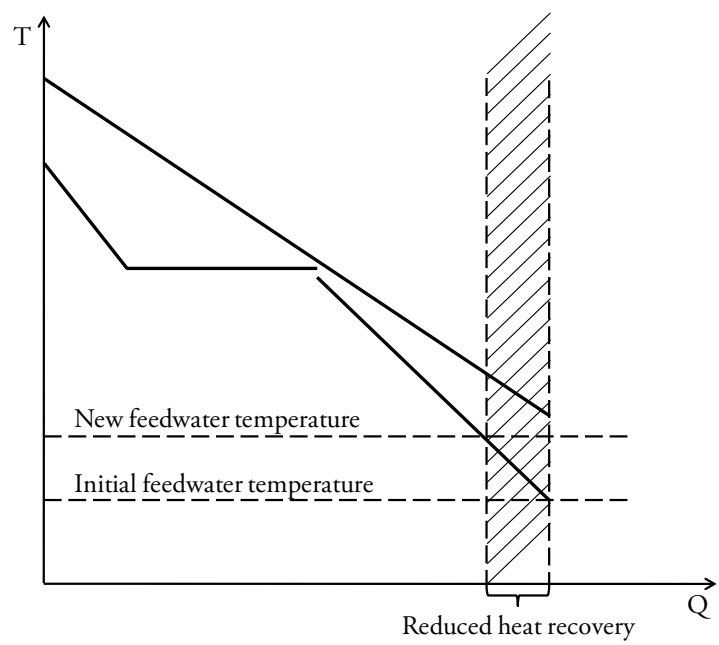

Figure 22: Less energy can be recovered from the flue-gas when the feedwater temperature is increased. The hatched area shows the reduced heat recovering due to the warmer feedwater.

In an attempt to reduce the amount of steam that has to be extracted, different configurations have been evaluated. Jassim and Rochelle [48] used the heat from the intercooling of the CO_2 compression process to provide the reboiler with additional energy. The amount of heat above the reboiler temperature available here is very limited. The number of compressor stages could be reduced to supply more energy, but this would increase the amount of energy required for CO_2 compression. Chinn et al. [51] suggested a concept based on integration of the reboiler with the HRSG. By pumping 75% of the rich absorbent (in this case MEA) through a heat exchanger in the HRSG, the exergetic losses due to a second heat carrier are avoided. However, amines are sensitive to high temperatures and are also corrosive, which may cause problems in the HRSG.

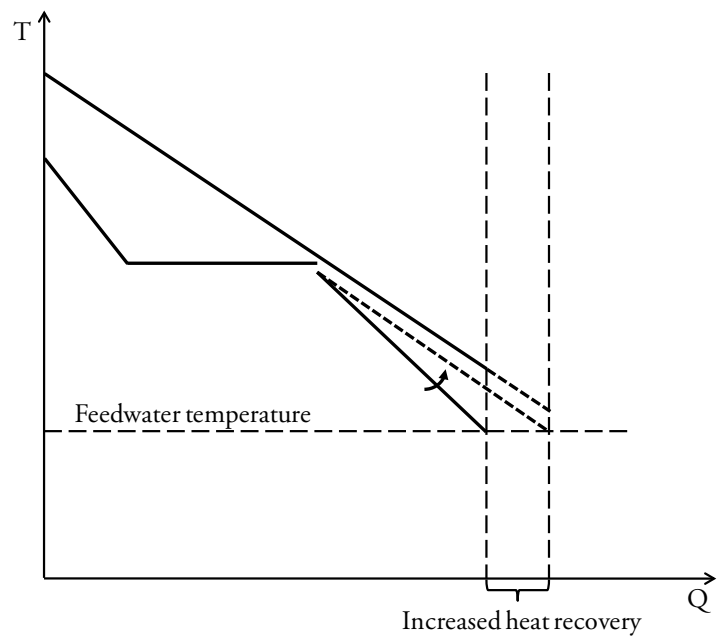

Figure 23: The amount of excess energy recovered in the economizer to provide part of the reboiler heat duty, illustrated in a T-Q diagram

Equation (1) in section 3.1 showed that if the mass flow through the economizer is increased, the slope of the water side in the T-Q diagram will be reduced. In the studies presented in Paper I-Paper III a water circuit was introduced between the economizer and the CO_2 separation plant. This loop allows for more heat to be recovered from the flue-gas and supplied to the reboiler so that less steam needs to be extracted from the steam turbine. The result is that the economizer mass flow is increased while the feedwater temperature remains more or less constant. By increasing the mass flow sufficiently, the lines representing the water and flue-gas in

the T-Q diagram become parallel. The result is that more energy can be recovered from the flue-gas, according to Figure 23.

A number of important criteria must be considered when designing an economizer:

- suitable approach point
- sufficiently high surface temperature on the gas side, and
- sufficient heat transfer area

The process in a heat exchanger is driven by the temperature difference between the hot and cold side. This means that in order to reduce the temperature difference it is necessary to increase the heat transfer area.

In a conventional CCPP, the economizer heat transfer area is large enough to give a sufficient approach point on the hot side. The approach point is defined as the difference between the evaporation temperature in the drum and the economizer outlet temperature. The heat exchanger surface temperature on the hot side is also an important parameter for the economizer. If it falls below a critical value there is a risk of flue-gas condensation on the tubes which may cause corrosion. To control surface temperature in the tubes a part flow of water is recirculated through the economizer.

Using an economizer-reboiler loop the approach point can be controlled by the mass flow through the reboiler. This means that the heat transferring area should be as large as possible. The amount of reboiler duty that is supplied by the economizer-reboiler loop is thus an economical question. The mass flow to the reboiler can be increased by increasing the heat transfer area of the economizer, reducing the temperature difference at the cold side of the HRSG.

When a carbon capture unit is used, the temperature of the metal on gas side of the economizer is much higher than in a conventional CCPP, and there will be no risk of flue-gas condensation on the tubes. When the plant is operated without the capture unit the economizer-reboiler loop can be bypassed so that part of the flow of water is recirculated from the economizer outlet to control the temperature of the tube surface.

5.2.5 Dual-pressure regenerator

As mentioned in section 5.2.1, the purpose of the reboiler is to evaporate CO_2 solved in the absorbent. The process can be considered to have a constant temperature, although the temperature may be influenced by the fact that the mixture ratio of the absorbent is varying slightly through the process of evaporation.

If condensing steam, which is extracted from a steam turbine, supplies heat to the reboiler, the temperature on the hot side of the reboiler also is constant. On the other hand, if the heat is supplied from the economizer-reboiler loop the temperature on the hot side will vary through the process. If an absorbent that tolerates high temperature regeneration is used the potential of the high temperature arising from the economizer-reboiler coupling can be better utilize. By dividing the regenerator into two columns using different regeneration temperatures, the heat can be better utilized. The temperature in the regenerator is a function of the pressure and by using a high pressure column and a low pressure column according to Figure 24 the temperature difference can be reduced. By desorbing part of the CO_2 at a higher pressure the compression work before final storage of CO_2 is reduced.

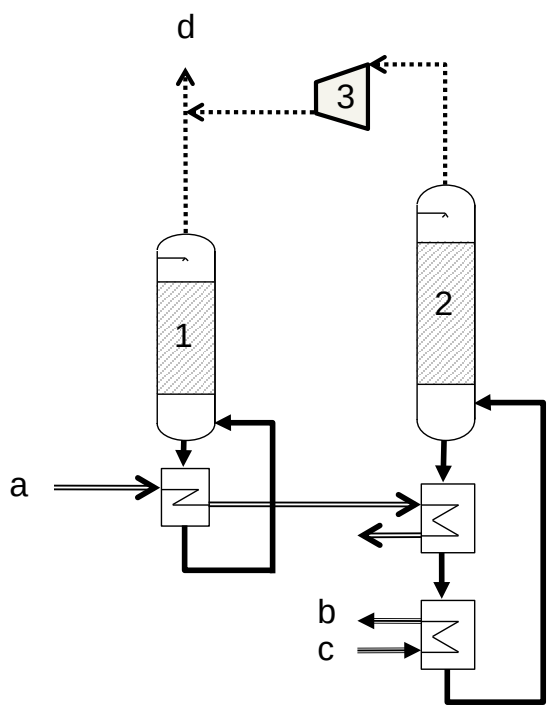

1. High pressure regenerator **3. Compressor** **b. Steam** **d. CO_2**
2. Low-pressure regenerator **a. Hot water** **c. Condensate**
Figure 24: Configuration of the dual-pressure regenerator

The heat carried with the water extracted from the economizer first passes the high-pressure reboiler and thereafter it is fed into the low-pressure reboiler, the T-Q diagram is shown in Figure 25. The remaining reboiler heat duty is supplied to the low-pressure regenerator with steam extracted from the turbine. By providing all

steam extracted from the turbine to the low-pressure regenerator this configuration can utilize the hot water without increasing requirements on the steam extraction.

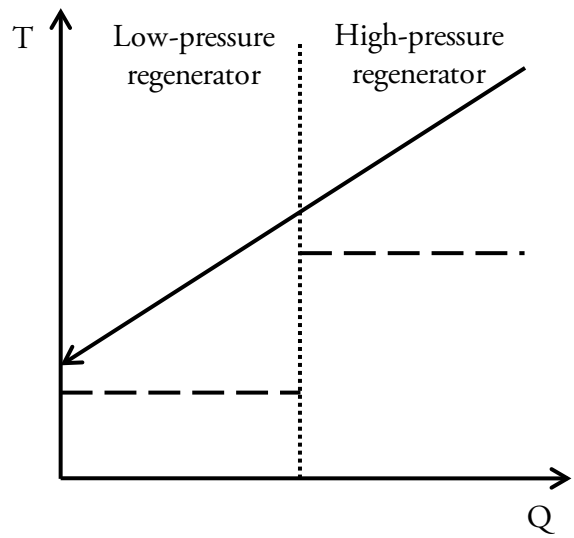

Figure 25: T-Q diagram of the economizer-reboiler part of the dual-pressure regenerator. Dashed line represent the absorbent and solid line is the hot water supplied from the economizer

5.3 Summary of the results on post-combustion-based CO_2 capture

Paper I, Paper II and Paper III uses the economizer-reboiler loop described in section 5.2.4 to integrate absorbent based CO_2 capture on CCPPs. In Paper I and Paper II CCPPs are specially designed for good implementation of the method while Paper III retrofits a triple-pressure CCPP with CO_2 capture.

The maximum amount of reboiler heat can be supplied if the temperature rise in the economizer is as large as possible in combination with a low feedwater mass flow. This will give a large amount of excess energy in the economizer which is available for the reboiler, see Figure 23. A high economizer water outlet temperature and a relatively low feedwater mass flow is typical features of a single-pressure CCPP with reheating. If MEA is the absorbent the regenerator temperature is limited and a too high reboiler heating source results in large temperature differences and entropy generation. A dual-pressure CCPP offers the possibility to optimize the low-pressure to fit the reboiler temperature. The results show that the most suitable CCPP for a

MEA carbon capture unit is a dual-pressure plant with reheating and a relatively high low pressure level.

When using the economizer-reboiler method for retrofitting a triple-pressure CCPP with carbon capture the best result is achieved if the entire low-pressure section is replaced by a large economizer. However this requires large modifications and reduces the efficiency when the plant is operated without the capture unit. Even if only the minimum effort is done to implement the method the results shows potential.

Paper IV presents a conceptual design for an SCOC-CC. A single-shaft gas turbine was designed and the main conclusion was that it was limited by the turbine outlet Mach number. A dual-shaft gas turbine offers the possibility to use a lower speed on the low-pressure turbine and is therefore probably more suitable for this cycle.

6 Part-Load Operation

Power production will have to be more flexible as more and more power is produced by wind and solar energy to compensate for the uneven energy production from these resources. In Paper VI, an alternative load control strategy for a bio-fuelled combined heat and power plant (CHP) is evaluated, and in Paper VII a new load control strategy for a CCPP is evaluated. This chapter gives a brief introduction to some of the methods available for load control of steam turbines and CCPPs.

6.1 Load control of steam turbines

Under part-load operation the mass flow through the steam turbine is reduced. The load on a steam turbine can be controlled by throttling sliding pressure, as described by Cotton [18] and Silvestri [52].

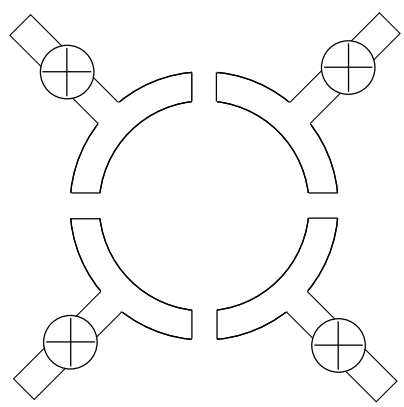

Figure 26: Schematic illustration of the partial-arc turbine inlet

When using throttling control the pressure in the boiler is maintained at a constant high level. A high pressure in the boiler results in less entropy being generated. The simplest method of throttling control is to throttle the total flow using a number of control valves, but a more advanced method is partial-arc control, which uses a control stage. In a partial-arc control stage, the annulus inlet area is divided into arcs each controlled by a separate valve, as illustrated in Figure 26. When all the valves are fully open or closed there are no throttling losses and the efficiency is very high.

Sliding pressure control is based on the concept of maintaining a constant volume flow through the turbine admittance. This is done by reducing the cycle pressure at part load. A reduction in the pressure in the steam generator increases the evaporation energy per unit mass. However, a control stage is not needed, and the turbine efficiency at full load is thus higher. Furthermore, the pressure ratio will be evenly distribution throughout the turbine, leading to reduced temperature gradients.

Equation (28) from Section 4.6.2 describes the mass flow as a function of the pressure ratio. Partial-arc control can be thought of as a method of controlling the inlet flow area. The inlet flow area is included in the constant C in Equation (28), and hence partial-arc control means manoeuvring the constant C, while sliding pressure control involves controlling the inlet pressure, p_1, to reduce the mass flow.

$$\dot{m} = \Psi \cdot C \sqrt{\frac{p_1}{v_1}} \tag{28}$$

6.2 Load control of a CCPP

Paper VII discusses the load control of a CCPP based on a single-shaft gas turbine without sequential combustion. Even if the gas turbine is operated at full throttle the bottoming steam cycle will experience different loads during the course of a day. The reason for this is that when the ambient temperature falls, the volume flow through the gas turbine increases, which increases the pressure ratio. This means that the exhaust gas (energy) available for the steam cycle is at a lower temperature, but the mass flow is increased. To cope with the varying energy supply, sliding pressure control is applied to the steam turbine. This makes the HRSG flexible and good heat recovery will be possible at part loads.

When the CCPP is operated at part load, the load of the topping gas turbine is controlled and the bottoming steam cycle follows with its sliding pressure. The load of a single-shaft gas turbine can be controlled by the variable inlet guide vanes (VIGV) or he variable stator vanes (VSV), and the amount of fuel burnt, i.e. the firing temperature [53].

Reducing the firing temperature has considerable effects on the gas turbine efficiency, and should be avoided if possible. The VIGV and/or VSV control the mass flow through the compressor by controlling the angle of the stators. The number of stators that are variable differs between machines. When the flow is

reduced the pressure ratio will fall, and hence the turbine outlet temperature will increase. When the exhaust temperature has reached its maximum value, the firing temperature must be reduced as the VIGV and/or VSV continue to close. When the VIGV and/or VSV have reached their maximum position, the firing level is the only option for further load reduction. Figure 27 shows the exhaust gas temperature (EGT) as a function of load. The initial part starting from full load (from the right side) of Figure 27 shows where the VIGV and/or VSV are starting to close. When the maximum EGT is reached the firing temperature is reduced as the VIGV and/or VSV continue to close to maintain a constant EGT. The final part of the curve shows the region where the VIGV and/or VSV are at their maximum position, and the firing temperature is further reduced.

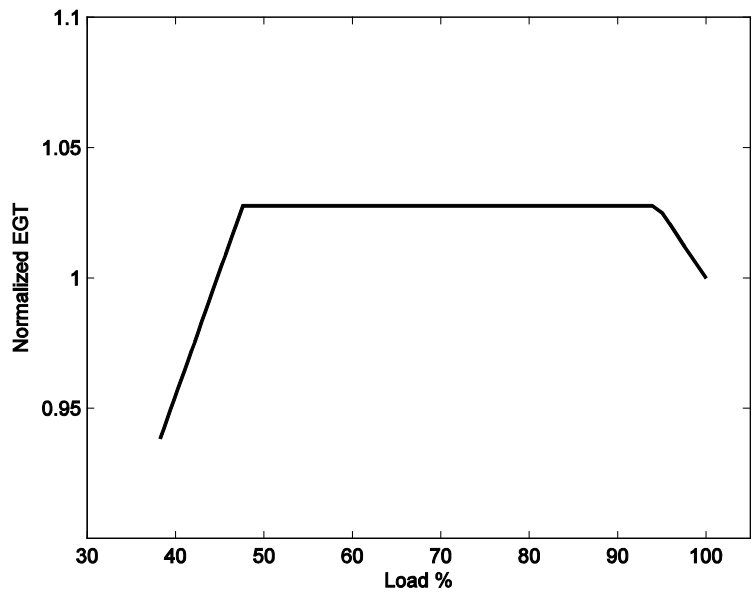

Figure 27: A typical load curve for a CCPP, normalized EGT as a function of load

6.3 Summary of the results on part-load operation

Paper VI evaluates the advantage of using hybrid control in a combined heat and power steam cycle based power plant. The advantages of the two methods can be highlighted by combining partial-arc control and sliding pressure control. Partial-arc control is inefficient when the valves are partly closed, but the efficiency can be improved by using sliding pressure control to get between the valve positions where all valves are fully open or closed. Just below full load it is advantageous to use

partial-arc control, but at lower loads when several arcs are closed it is beneficial to use sliding pressure control, which also leads to less wear of the turbine.

Paper VII discusses a method of load control of CCPPs that causes less wear on the gas turbine than the conventional method. The conventional method involves operation at the highest possible exhaust gas temperature, which will require spray cooling in the HRSG to keep the superheating temperature below its maximum value. By reducing the firing temperature so that no spray cooling is required in the steam cycle, the gas turbine can be operated at lower temperatures with almost the same total plant efficiency. A lower firing temperature also extends the maintenance interval.

7 Low Calorific Fuels in CCPPs

Resources of fossil fuels are finite, and their combustion leads to an increase in the amount of CO_2 in the atmosphere. There are thus economic and environmental reasons for finding alternative fuels. Consequently, gas turbine manufacturers are making efforts to increase the fuel flexibility of their products.

Paper V discusses how a CCPP designed for natural gas reacts to operation with low calorific gas in the fuel mix. There are several articles on CCPPs with integrated gasifiers and hence low calorific fuel operation [54-55]. When a pressurized gasifier is integrated into the cycle, air can be extracted after the compressor of the gas turbine, which offers an efficient and gentle method of operating a natural gas turbine on low calorific fuels. Gas turbine fuel flexibility and the requirements for low calorific fuel operability are described by Rahm et al. and Foster et al. [56-57].

When gaseous fuels are produced from biomass they contain inert gases. If the fuel is produced by air-blown gasification it will contain nitrogen and carbon dioxide. If pure oxygen is used as the oxidizer, or if heat is added externally, the amount of nitrogen can be reduced. If the fuel is produced by anaerobic digestion or fermentation of biomass it will contain carbon dioxide. The inert gases can be removed, but this is an energy-consuming process and should be avoided if possible.

If a gas turbine is operated at a fixed firing temperature and the amount of inert gases in the fuel is increased, the distribution of mass flow between the compressor and the turbine will be disturbed. A higher pressure ratio is required to force the increased mass flow through the turbine. This places a strain on the compressor which will be operating closer to the surge line.

Apart from the modifications required to the combustor and the fuel supply system, a gas turbine redesigned for operation with a low lower heating value (LHV) fuel has a different size matching between the compressor and turbine. Figure 28 shows how much the turbine flow number must be increased as the fuel is diluted with CO_2 if the compressor is to be operated at its design point without any other modifications to the unit. The gas turbine flow number corresponds to the capacity of steam turbines and is thus a measure of the turbine size or its ability to swallow a certain mass flow. The flow number can be increased to a certain extent by changing

the angle of the first stator. Larger changes would require the turbine to be redesigned.

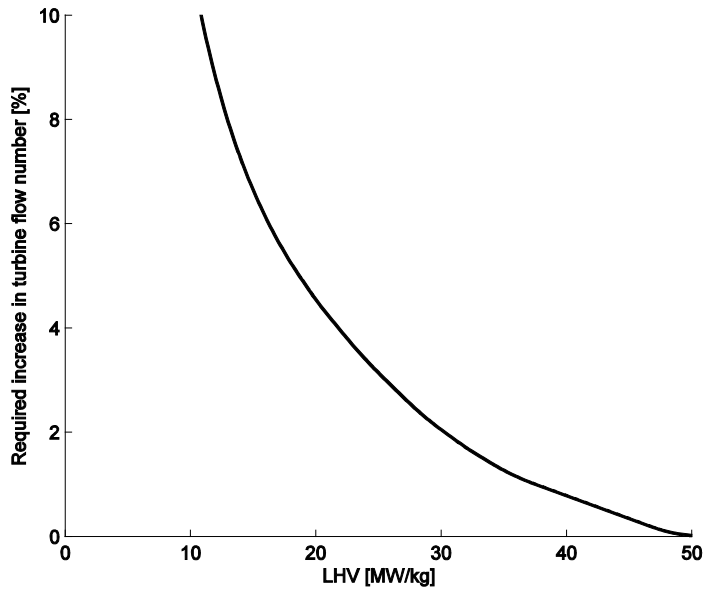

Figure 28: The required increase in turbine flow number to maintain the compressor at the design point when the fuel is diluted with CO_2

When the compressor is operated at a high pressure ratio the first stage does not experience any significant difference in the flow and it will deliver about the same mass flow. However, in the last stage the high pressure will have reduced the volume flow and therefore also the axial velocity. A low axial velocity results in a change in the direction of the relative velocity and hence an increased incidence angle. The high positive incidence angle will eventually cause the flow to separate from the suction surface. This phenomenon is called stall and is acceptable to a certain degree. However, if it becomes severe the stage will no longer be able to support the upstream pressure gradient and the flow will reverse. The compressor will recover quickly, but if nothing is done to reduce the pressure ratio the phenomenon will be repeated at a high frequency. This is called surge and will lead to engine damage.

7.1 Summary of the results on low calorific fuels in CCPPs

Paper V discusses the effects of operating a CCPP on low calorific fuels. The results indicate that the turbomachine is not drastically affected by operation down to a heating value of to 20-25 MJ/kg. Below this level the engine will experience a rather steep response in terms of a decrease in surge margin, engine thrust balance, power increase and associated shaft torque levels. The steam cycle will receive more energy as more inert ballast is introduced. Although the pressure ratio is increased in the gas turbine the flue-gas temperature increases. This is explained by the large amount of CO_2 in the fuel, which has a lower isentropic exponent. The increased amount of energy in the flue-gas will increase the steam production and hence the steam cycle power output.

8 Concluding Remarks

The objective of the work presented in this thesis was to evaluate methods that can help power companies to meet the climate change objectives of the European Union. Three factors summarizing the requirements on future thermal power plants were identified:

- reduced CO_2 emissions
- increased use of biofuels
- improved part-load abilities

The method of utilizing low-grade heat for post-combustion CO_2 capture described in Section 5.2.4 and Paper I - Paper III can be used in fossil fuel power plants in order to fulfil the first requirement. If the method is implemented so that the number of pressure levels in the CCPP is reduced, this will improve the part-load ability, therefore fulfilling the third requirement. Paper IV is concerned with SCOC-CC power plants which employ a cycle designed for post-combustion CO_2 capture. This power plant cycle fulfils the first requirement. Paper V shows how a CCPP reacts if the fuel heating value is reduced by adding low calorific fuels to the fuel mix. Using fuels produced from renewable resources reduces the CO_2 emissions and replaces fossil fuel, satisfying the first and second requirements. Paper VI and Paper VII evaluate load control strategies related to the third requirement. These two methods can be applied to power plants fulfilling the other requirements.

9 Summary of papers

Paper I K. Jonshagen, M. Sammak, M. Genrup
Post-Combustion CO_2 Capture on Combined Cycles Utilizing Hot-Water for Absorbent Regeneration
Submitted to ASME Turbo Expo 2011, GT2011-45678 Vancouver, Canada, June 2011

The author made the necessary modifications and improvements in the heat- and mass-balance models required for this publication. The heat- and mass-balance calculations were done by the author. Majed Sammak made the ASPEN simulations. The publication was written by the author.

Paper II K. Jonshagen, N. Sipöcz, M. Genrup
A Novel Approach of Retrofitting a Combined Cycle with Post-Combustion CO_2 Capture
Journal of Engineering for Gas Turbines and Power, January 2011, Vol. 133 / 011703-1

The author and Magnus Genrup developed the simulation models and made the necessary modifications and improvements to the components. The calculations were performed by the author. Nikolett Sipöcz parameterized the carbon capture plant. The backbone of the publication was written by the author.

Paper III N. Sipöcz, K. Jonshagen, M. Genrup
Novel High-Performing Single-Pressure Combined Cycle with CO_2 Capture
Journal of Engineering for Gas Turbines and Power, April 2011, Vol. 133 / 041701-1

The author and Nikolett Sipöcz developed the simulation model. The author made the necessary modifications and improvements to the components. Nikolett Sipöcz parameterized the carbon capture plant. The calculations were performed by Nikolett Sipöcz. Nikolett Sipöcz wrote the backbone of the publication.

Paper IV M. Sammak, K. Jonshagen, M. Thern, E. Thorbergsson, T. Grönstedt, A. Dahlquist, M. Genrup
Conceptual Design of a Mid-Sized Semi-Closed Oxyfuel Cycle
Submitted to ASME Turbo Expo 2011, GT2011-46299, Vancouver, Canada, June 2011

The author developed the calculation model. The heat- and mass balance calculations where performed by Majed Sammak. Magnus Genrup, Thomas Grönstedt, Majed Sammak and Egill Thorbergsson designed the gas turbine components. Egill Thorbergsson programmed the link between IPSEpro and refprop. Marcus Thern assisted in developing the real gas calculations.

Paper V K. Jonshagen, P. Eriksson, M. Genrup
Low-Calorific Fuel Mix in a Large Size Combined-Cycle Plant
Presented at ASME Turbo Expo 2009 in Orlando, Florida, June 2009

The author performed the calculations. Magnus Genrup, the author and Pontus Eriksson developed the models. The author wrote backbone of the publication.

Paper VI K. Jonshagen, M. Genrup
Improved Load Control for a Steam Cycle Combined Heat and Power Plant
Energy 35 (2010) 1694-1700

The author performed the calculations. Magnus Genrup and the author developed the models and wrote the publication.

Paper VII K. Jonshagen, P. Eriksson, M. Genrup
Improved Load Control Strategy for Large-Sized Combined Cycles Presented at
ECOS 2009, Foz do Iguaçu, Paraná, Brazil, September 2009

The author performed the calculations. The author and Magnus Genrup developed the models and wrote the publication.

References

[1] Le Treut, H., R. Somerville, U. Cubasch, Y. Ding, C. Mauritzen, A. Mokssit, T. Peterson and M. Prather, 2007, "Historical Overview of Climate Change. In: Climate Change 2007: The Physical Science Basis. Contribution of orking Group I to the Fourth Assessment Report of the Intergovernmental Panel on Climate Change [Solomon, S., D. Qin, M. Manning, Z. Chen, M. Marquis, K.B. Averyt, M. Tignor and H.L. Miller (eds.)].", Cambridge University Press, Cambridge, United Kingdom and New York, NY, USA.

[2] Tanaka, N., 2010, "CO_2 Emissions from Fuel Combustion 2010 - Highlights, " International Energy Agency, IEA, Annual Publication.

[3] 2010, "European Commission, Climate Action, Energy for a Changing World", http://ec.europa.eu/climateaction/index_en.htm.

[4] IPSEpro, 2003, "SimTech Simulation Technology (SimTech)",Graz, Austria.

[5] Fredriksson Möller, B., 2005, "A Thermoeconomic Evaluation of CO_2 Capture with Focus on Gas Turbine-Based Power Plants", PhD Thesis, Lund University, Lund, Sweden.

[6] Genrup, M., 2005, "On Degradaition and Monitoring Tools for Gas and Steam Turbines", PhD Thesis, Lund University, Lund, Sweden.

[7] Lorentz, M., 2004, "Modeling and Off Design Simulation of the Evaporative Gas Turbine", MSc thesis, Lund Universite, Lund.

[8] M.Truedsson, 2004, "Systemstudie av Västhamnsverket i Helsingborg", MSc thesis, Lund Universite, Lund.

[9] Kehlhofer, R., 2009, Combined-cycle gas & steam turbine power plants, Fairmont Press; Distributed by Prentice-Hall, Lilburn, GA Englewood Cliffs, NJ ISBN 0881730769 (FP): 0131514814 (PH).

[10] Bolland, O., 1990, "Analysis of combined and integrated gas turbine cycles", PhD thesis, NTH, Trondheim.

[11] Horlock, J. H., 1992, Combined power plants including combined cycle gas turbine (CCGT) plants, Pergamon Press, Oxford, England ; New York : ISBN 0080405029 (HC) :.

[12] Rao, K. R., 2008, Companion Guide to the ASME Boiler & Pressure Vessel Code, ASME Press, ISBN 9780791802717

[13] Kays, W. M., and London, A. L., 1984, Compact heat exchangers, Krieger Publishing Company, ISBN 1575240602.

[14] Martin, H., 2005, VDI-Wärmeatlas, Springer, Düsseldorf ISBN 3-540-25503-6.

[15] Kehlhofer, R. H., 1978, "Calculation for part-load operation of combined gas / steam turbine plants", Brown Boveri Rev., 10, pp. 672-679.

[16] Stodola, A., and Loewenstein, L. C., 1945, Steam and gas turbines, P. Smith, New York, ISBN.

[17] Beckmann, G., 1961, "Eine allgemeine theori der mengendruckgleichung", PhD-thesis.

[18] Cotton, K. C., 1993, Evaluating and improving steam turbine performance, Cotton Fact, Rexford, N.Y. ISBN 0963995502.

[19] Schobeiri, M., 2005, Turbomachinery flow physics and dynamic performance, Springer, Berlin ISBN 3540223681 (acid-free).
[20] Traupel, W., 1977, Thermische Turbomaschinen, Springer-Verlag, Berlin; New York ISBN 0387079394 (v. 1).
[21] Young, J. B., 1984, "Semi-analytical techniques for investigating thermal non-equilibrium effects in wet steam turbines", International Journal of Heat and Fluid Flow, 5(2), pp. 81-91.
[22] A. Guha, J. Y., 1994, "The effect of flow unsteadiness on the homogeneous nucleation of water droplets in steam turbines", Philosophical Transactions: Physical Sciences and Engineering, 349(1691), pp. 445-472.
[23] Guha, A., 1994, "A unified theory of aerodynamic and condensation shock waves in vapor-droplet flows with or without a carrier gas", Physics of fluids, 6(5), pp. 1893-1913.
[24] Glassman, A. J., 1972, Turbine design and application, Nasa Sp-290, Scientific and Technical Information Office, National Aeronautics and Space Administration: For sale by the Supt. of Docs., Washington, ISBN NA.
[25] Walsh, P. P., Fletcher, P., 2004, Gas turbine performance, Blackwell Science, Malden, MA ISBN 063206434X (alk. paper).
[26] Çengel, Y. A., and Boles, M. A., 2002, Thermodynamics: an engineering approach, McGraw-Hill, Boston ISBN 0072383321
0071121773 (ISE).
[27] Dixon, S. L., and Hall, C. A., 2010, Fluid mechanics and thermodynamics of turbomachinery, Butterworth-Heinemann/Elsevier, Burlington, MA ISBN 9781856177931 (alk. paper) 1856177939 (alk. paper).
[28] Lindberg, G., 1975, "Accurate determination of gas turbine performance under different operational conditions",PhD Thesis, Lund University, Lund.
[29] Kyrklund, B., 1977, "Ett gasturbinaggregat för bas- och spetslast", Stal-Laval, Finnspång, p. 104.
[30] Wassell, A. B., 1968, "Reynolds Number Effects in Axial Flow Compressors," Journal of Engineering for Power, pp. 149-156.
[31] Kurzke, J., 2007, "GasTurb 11 - Design and Off-Design Performance of Gas Turbines", http://www.gasturb.de.
[32] H. Moustapha, M. F. Z., N. C. Baines, D. Japikse, 2003, Axial and Radial Turbines, Concepts NREC, White River Junction, Vermont, USA ISBN 0-933283-12-0.
[33] Bolland, O., Mathieu, P., 1998, "Comparison of two CO_2 removal options in combined cycle power plants", Energy Conversion and Management, 39(16-18), pp. 1653-1663.
[34] Botero, C., Finkenrath, M., Bartlett, M., Chu, R., Choi, G., and Chinn, D., 2009, "Redesign, Optimization, and Economic Evaluation of a Natural Gas Combined Cycle with the Best Integrated Technology CO_2 Capture", Energy Procedia, 1(1), pp. 3835-3842.
[35] Chiesa, P., and Consonni, S., 2000, "Natural Gas Fired Combined Cycles With Low CO_2 Emissions", J. Eng. Gas Turbines Power, 429(3), p. 8.
[36] Finkenrath, M., Ursin, T. P., Hoffmann, S., Bartlett, M., Evulet, A., Bowman, M. J., Lynghjem, A., and Jakobsen, J., "Performance and cost analysis of novel gas turbine cycle with CO2 capture", Proc. ASME Turbo Expo.
[37] Jack, A. R., Audus, H., and Riemer, P. W. F., "The IEA greenhouse gas R&D programme", Energy Conversion and Management, 33(5-8), pp. 813-818.
[38] Kvamsdal, H. M., Jordal, K., and Bolland, O., 2007, "A quantitative comparison of gas turbine cycles with CO_2 capture", Energy, 32(1), pp. 10-24.

[39] Mimura, T., Shimojo, S., Suda, T., Iijima, M., and Mitsuoka, S., "Research and development on energy saving technology for flue gas carbon dioxide recovery and steam system in power plant", Energy Conversion and Management, 36(6-9), pp. 397-400.
[40] Zachary, J., and Titus, S., "CO_2 capture and sequestration options: Impact on turbo-machinery design", Proc. ASME Turbo Expo.
[41] Desideri, U., and Paolucci, A., 1999, "Performance modelling of a carbon dioxide removal system for power plants", Energy Conversion and Management, 40(18), pp. 1899-1915.
[42] Oexmann, J., Hensel, C., and Kather, A., 2008, "Post-combustion CO_2-capture from coal-fired power plants: Preliminary evaluation of an integrated chemical absorption process with piperazine-promoted potassium carbonate", International Journal of Greenhouse Gas Control, 2(4), pp. 539-552.
[43] Romeo, L. M., Bolea, I., and Escosa, J. M., 2008, "Integration of power plant and amine scrubbing to reduce CO_2 capture costs", Applied Thermal Engineering, 28(8-9), pp. 1039-1046.
[44] Romeo, L. M., Espatolero, S., and Bolea, I., 2008, "Designing a supercritical steam cycle to integrate the energy requirements of CO_2 amine scrubbing", International Journal of Greenhouse Gas Control, 2(4), pp. 563-570.
[45] Singh, D., Croiset, E., Douglas, P. L., and Douglas, M. A., 2003, "Techno-economic study of CO_2 capture from an existing coal-fired power plant: MEA scrubbing vs. O_2/CO_2 recycle combustion", Energy Conversion and Management, 44(19), pp. 3073-3091.
[46] Jericha, H., Sanz, W., Göttlich E., Neumayer, F, 2008, "Design Details of a 600 MW Graz Cycle Thermal Power Plant for CO_2 Capture", ASME Paper GT2008-50515, ASME Turbo Expo 2008Berlin, Germany.
[47] Kohl, A. L., and Nielsen, R. B., 1997, Gas Purification 5th ed., Gulf Publishing Co., Houston USA ISBN.
[48] Jassim, M. S., and Rochelle, G. T., 2005, "Innovative Absorber/Stripper Configurations for CO2 Capture by Aqueous Monoethanolamine", Industrial & Engineering Chemistry Research, 45(8), pp. 2465-2472.
[49] Gal, E., 2006, "Ultra Cleaning Of Combustion Gas Including The Removal Of CO_2", A. P. Inc, ed.US.
[50] V. Dardea, K. T., W.J.M. van Wellb, E.H. Stenbya, 2009, "Chilled ammonia process for CO_2 capture", Energy Procedia 1 (2009) 1035–1042.
[51] Chinn, D., Choi, G. N., Chu, R., and Degen, B., 2005, "Cost efficient amine plant design for post combustion CO_2 capture from power plant flue gas", Greenhouse Gas Control Technologies 7, E. S. Rubin, D. W. Keith, C. F. Gilboy, M. Wilson, T. Morris, J. Gale, and K. Thambimuthu, eds., Elsevier Science Ltd, Oxford, pp. 1133-1138.
[52] G. J. Silvestri Jr. O. J. Aanstad, J. T. B., 1972, "A Review of Sliding Throttle Pressure for Fossil Fueled Steam-Turbine Generators", American Power Conference, Large Turbine Engineering Westinghouse Electric Corp., Chicago, Illinois.
[53] D. Balevic, R. B., D. Forry, 2004, "Heavy-Duty Gas Turbine Operating and Maintenance Considerations", GE Energy.
[54] Jaber, J. O., Probert, S. D., and Williams, P. T., 1998, "Gaseous fuels (derived from oil shale) for heavy-duty gas turbines and combined-cycle power generators", Applied Energy, 60(1), pp. 1-20.

[55] Rodrigues, M., Walter, A., and Faaij, A., 2007, "Performance evaluation of atmospheric biomass integrated gasifier combined cycle systems under different strategies for the use of low calorific gases", Energy Conversion and Management, 48(4), pp. 1289-1301.
[56] A. D. Foster, h. E. v. D., M. B. Hilt, 1983, "Fuels Flexibility in Heavy Duty Gas Turbines", GE Power, Schenectady, New York.
[57] S. Rahm, J. G., M. Molière, A. Eranki, 2009, "Addressing gas turbine fuel flexibility", GE Power, Schenectady, New York.

I

Proceedings of ASME Turbo Expo 2011
GT2011
June 6-10, 2011, Vancouver, Canada

GT2011-45678

Post-Combustion CO_2 Capture for Combined Cycles Utilizing Hot-Water Absorbent Regeneration

Klas Jonshagen*
Dept. of Energy Sciences
Lund University
SE-22100 Lund
Sweden
klas.jonshagen@energy.lth.se

Majed Sammak
Dept. of Energy Sciences
Lund University
SE-22100 Lund
Sweden
majed.sammak@energy.lth.se

Magnus Genrup
Dept. of Energy Sciences
Lund University
SE-22100 Lund
Sweden
magnus.genrup@energy.lth.se

ABSTRACT
The partly hot-water driven CO_2 capture plant offers a significant potential for improvement in performance when implemented in a combined-cycle power plant (CCPP). It is possible to achieve the same performance with a dual-pressure cycle as in a triple-pressure unit. Even a single-pressure plant can attain an efficiency competitive with that achievable with a triple-pressure plant without the hot-water reboiler. The underlying reasons are better heat utilization in the heat recovery unit and less cross-over extraction to the absorbent regenerating unit(s).

In this paper, the design criteria for a combined cycle power plant utilizing hot-water absorbent regeneration will be examined and presented. The results show that the most suitable plant is one with two pressure levels. The low-pressure level should be much higher than in a conventional combined cycle in order to increase the amount of heat available in the economizer. The external heat required in the CO_2 capture plant is partly supplied by the economizer, allowing temperature optimization in the unit. The maximum value of the low-pressure level is determined by the reboiler, as too great a temperature difference is unfavourable.

We have evaluated the benefits of coupling the economizer and the reboiler in a specially designed CCPP. In the CO_2 separation plant both monoethanolamine (MEA) and ammonia are evaluated as absorbents. Higher regeneration temperatures can be tolerated in ammonia-based plants than in MEA-based plants. When using a liquid heat carrier the reboiler temperature is not constant on the hot side, which results in greater temperature differences. The temperature difference can be greatly reduced by dividing the regeneration process into two units operating at different pressures.
The possibility of extracting more energy from the economizer to replace part of the extracted steam increases the plant efficiency. The results show that very high efficiencies can be achieved without using multiple pressure-levels.

INTRODUCTION
Carbon dioxide emissions can be reduced by implementing technology for carbon dioxide capture. The emission of carbon dioxide can be avoided or mitigated either by removing the carbon from the combustion process, i.e. pre-combustion techniques, or by collecting the carbon dioxide from the flue gases after combustion, i.e. post-combustion techniques. Pre-combustion can be performed with different types of fuel-upgrading processes such as membrane technology and chemical looping. Post-combustion can be divided into two categories: oxy-fuel cycles and conventional cycles.

The principle of the oxy-fuel cycle is that nitrogen is removed from the air before the process so that the flue gas consists mainly of CO_2 and water. After the steam generator (a boiler or a heat-recovery steam generator (HRSG)), the steam is separated by condensation of the water vapour in the flue gases. Two major concepts for oxy-fuel cycles have emerged: the semi-closed oxy-fuel combined cycle [1-3] and the Graz cycle [4].

The other post-combustion method is absorbent-based CO_2 separation. Compared with the other CO_2 capture techniques, absorbent-based CO_2 capture does not require a new power plant concept; hence proven technology can be used. This makes the method very suitable for retrofitting to existing plants. Two absorbents were investigated in this study: monoethanolamine (MEA) and ammonia.

Monoethanolamine is an alkanolamine that has been used for many years in the petroleum industry. Kohl and Nielsen have described the method of CO_2 capture with MEA [5], and there are numerous publications concerning the integration of MEA with CCPPs [6-14].

*Corresponding author

Eli Gal developed and patented the method of using ammonia to capture carbon dioxide, referred to as the chilled ammonia technique [15]. The patent is today owned by Alstom power. Darde has presented a detailed study of the chilled ammonia process [16], and Dave later compared the performance of chilled ammonia and MEA [17]. Common to all post-combustion techniques is that heat is required to regenerate the absorbent. In previous studies in this field steam extracted from the turbine has been used to regenerate the absorbent.

This paper describes a method of utilizing low-grade energy to regenerate the absorbent. The theoretical study was designed to investigate the utilization of low-grade energy in two post-combustion CO_2-sequestration processes employing chilled ammonia and MEA. A single-pressure cycle with and without reheat, a dual- and a triple-pressure cycle including reheat has been tested with a MEA capture plant. The single-pressure reheat cycle has also been tested with a chilled ammonia capture unit. The purpose of the study was to evaluate the benefits of recovering excess energy from the economizer to provide a part of the reboiler heat duty.

ABBREVIATIONS AND ACRONYMS

CCPP	Combined Cycle Power Plant
EGR	Exhaust Gas Recirculation
GT	Gas Turbine
HP	High-Pressure
HRSG	Heat Recovery Steam Generator
IP	Intermediate-Pressure
LP	Low-Pressure
MEA	Monoethanolamine

CARBON CAPTURE ON A CCPP

The flow of flue gas per unit power produced in a CCPP is much higher than that from a steam-boiler-based power plant as combustion is performed in the former with a large surplus of air. This results in a need for very large, and thus very expensive, absorption columns. The volume of the columns can be reduced by utilizing exhaust gas recirculation (EGR), which is described in a later section. The size of the column is determined by the maximum possible velocity of the flue gas. This is to ensure that none of the liquid absorbent is swept away with the flue gas at the top of the column.

A post-combustion CO_2 capture plant requires heat to regenerate the absorbent (to break the CO_2–absorbent bonds). The temperature required for absorbent regeneration depends on the absorbent used. If a higher temperature can be used, the pressure in the regenerator can be increased. A high regenerator pressure means that the absorbent can absorb the CO_2 at ambient pressure, and then be pumped to a higher pressure. The result of this is that the energy required for the compression of gaseous CO_2 can be reduced.

The energy required in the carbon capture plant is generally supplied by steam from the low-pressure part of the steam cycle. In a combined cycle there is no other low-temperature heat sink than the feedwater from the condenser. If part of the water is condensed at a higher pressure, and hence at a higher temperature, the heat sink will be reduced. The result of this is that less energy can be recovered from the gas turbine exhaust gas.

Exhaust gas recirculation, EGR

The working principle of a gas turbine with large amount of excess air in the combustion results in that the concentration of CO_2 in the exhaust gas is lower than for a conventional steam boiler. This, in combination with the higher specific flue gas flow for the gas turbine, makes the separation plant large and costly. (The specific flue gas flow in a gas turbine plant is of the order of 1.5 kg/MWs, compared with approximately 0.95 kg/MWs for a normal steam boiler.) To limit the flow, the concentration of carbon dioxide in the gas turbine working fluid can be increased by utilizing EGR. This will reduce the volume of flue gas to be treated in the separation plant. It should be noted that the energy required in the CO_2 capture plant, apart from some minor pumping requirements, consists of the absorbent regeneration energy, which is not affected by the concentration of CO_2 in the flue gas. In other words, the amount of CO_2 dissolved in the absorbent determines the energy required, and this is the same regardless of whether EGR is used or not. The limit on how much EGR can be utilized is, in principle, determined by the combustor. The limitation is in general caused by a lack of oxygen, which reduces the efficiency of the combustor, resulting in high CO levels [9, 18].

Experimental studies by Elkady et al. showed that the dry low NO_X (DLN) combustor used in General Electric's F-class, heavy-duty gas turbines can be operated at 30–35 % EGR without modification, and they predicted that such turbines could be operated with EGR levels above 40% with only minor modifications [18]. Bolland and Mathieu used an EGR rate of 40% in a GE-109FA gas turbine. This was possible provided that the concentration of O_2 before the combustion can be kept above 16 %vol.

We have previously theoretically investigated the effects of EGR on the turbomachinery, in terms of Mach numbers, resulting from changes in the gas properties of the working fluid [19]. We found that the change in Mach number was very small at 40 % EGR.

The current model gives a CO_2 concentration of just below 8 %vol with 40 % EGR, which corresponds to the value suggested by Elkady et al. for the GE 109FB burner [18], therefore, 40 % EGR was used in this work. EGR requires exhaust gas cooling in order to reduce the temperature at the compressor inlet. This is done with water at ambient temperature, which is sprayed through the exhaust in an exhaust gas condenser.

THERMODYNAMIC MODELLING

This study is based on a combined cycle using the General Electric 109FB gas turbine, a 300 MW, single-shaft machine, as topping cycle. With no available data from using EGR it was necessary to use an off-design gas turbine model. The gas turbine model is modelled as described by Walsh and Fletcher

[20] and uses fully dimensionless parameter groups. The compressor map is based on a publication by General Electric [21]. The map is actually for a Frame 7 unit, which is the 60 Hz version of the Frame 9 type. It is assumed that the Frame 9 compressor is a direct scale-up of the smaller Frame 7 unit. The turbine uses a standard turbine map (choking occurs in the stator).

The purpose of this study is not to make a retrofit but to design a new CCPP, therefore the steam turbine calculation only will concern the design point. The wet efficiency is modelled according to Baumann as described by Traupel [22] and the exhaust loss in the low-pressure turbine is set to 30 kJ/kg. Parasitic losses and transformed step-up losses are not included in the presented efficiencies. The heat- and mass-balance program IPSEpro by simtech [23] have been used for the calculation.

CO_2 capture plant modelling

Two types of absorbent-based CO_2 separation techniques were studied. In both cases the capture rate was set to 90 %vol. The first separation plant uses MEA as absorbent. The separation unit model was developed by Fredriksson Möller [6], based on the concept described by Kohl and Nielsen [5]. The absorbent consists of a solution of 30 %wt MEA and 70 %wt water. The absorbent regeneration temperature is set to 120 °C to limit the degradation of the amine.

The second separation unit is based on the chilled ammonia concept developed by Alstom. This process involves many different chemical reactions, and the reaction path depends on the process settings. ASPEN was used to generate the tables needed to make a simplified model in the heat- and mass-balance program IPSEpro [21]. The tables required for the IPSEpro model were created by fixing most of the process parameters in ASPEN and varying the pressure in the regenerator column. This limited the model to one particular solvent mixture. The purpose here was to test the possibility to utilize a higher temperature for regenerating the absorbent which characterized the choice of mixing ratio of the solvent. To evaluate a chilled ammonia separation unit in a CCPP which supplies the reboiler with energy at a lower temperature, a different solvent should be used and this has not been done in this work.

The rich solvent used consisted of 11 %wt ammonia, 88 %wt water and 95 ppm CO_2. The lean solvent consisted of 11 %wt ammonia, 63 %wt water and 26 %wt CO_2. The separation unit includes an absorption column, a low-pressure and a high-pressure regeneration column, and an ammonia stripper. The ammonia stripper prevents ammonia from escaping to the atmosphere. It was assumed that an ambient heat sink could be used to cool the absorption process to 20 °C and that an electric refrigerator with a coefficient of performance (COP) of 4 was used for further cooling to 5 °C. The energy required for electric cooling was calculated to be 21.2 MW.

INTEGRATION OF CO_2 CAPTURE

The transfer of heat from the gas turbine exhaust to the steam cycle is essential for the efficiency of a CCPP. When absorbent-based CO_2 capture is integrated with the cycle the heat recovery unit will inevitably be drastically affected. A significant amount of steam is extracted from the steam cycle to cover the heat requirement of the carbon capture plant. This steam is returned at a much higher temperature than the feedwater returned from the main condenser.

The design of any CCPP is a compromise between the first and second law of thermodynamics. The first law states that as little energy as possible should leave the system, i.e. the stack temperature should be as low as possible. The condensation temperature of the flue gas limits this temperature. To avoided condensation in the economizer, some of the water is circulated to increase the surface temperature on the gas side. The second law states that the amount of entropy generated in the process should be minimized. This means that the irreversibility of the process should be as small as possible. For an HRSG this means that the mean temperature difference on the hot and cold side should be minimized.

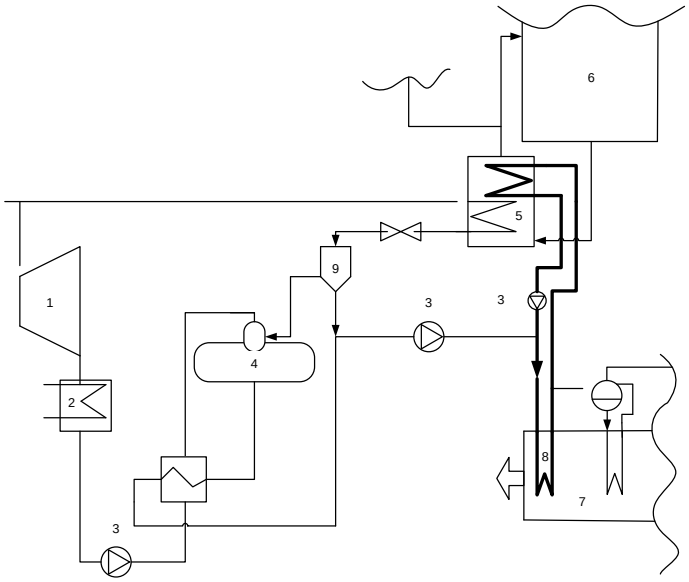

1. LP Steam Turbine *4. Deaerator* *7. HRSG*
2. Condenser *5. Reboiler* *8. Economizer*
3. Pump *6. Stripper* *9. Separator*

Figure 1: The proposed circuit between the economizer and the reboiler

The most straightforward method of integrating a CO_2 separation unit into a CCPP would be to supply the heat via steam extraction. The condensate returned from the reboiler outlet of the separation plant is mixed with the feedwater before it enters the HRSG. This result in the water entering the HRSG being warmer, and thus less heat can be recovered from the flue gas.

HOT WATER ABSORBENT REGENERATION

The nature of a CCPP is such that the temperatures on the sides of the economizer differ. By applying the equation below to both sides of the economizer, it can be seen that if the mass flow on the cold side is increased the temperature difference will be smaller.

$$\dot{Q} = \dot{m}\bar{c}_p(T_2 - T_1)$$

By introducing a water loop between the economizer and the reboiler, according to figure 1, to cover part of the reboiler duty, more energy can be recovered. The reboiler consists of two heating coils, one heated by pressurized water and one by condensing steam. The energy supplied by the economizer replaces some of the steam extracted from the turbine, and more power will be produced in the low pressure steam turbine. When more heat is recovered from the flue gas, the requirement of exhaust gas cooling prior to the EGR and the carbon capture plant is reduced.

The control strategy for the economizer–reboiler loop is that the mass flow is regulated so that the temperature of the water at the economizer outlet is close to the saturated state at all loads. This will provide extra control, preventing evaporation and drying-out of the economizer.

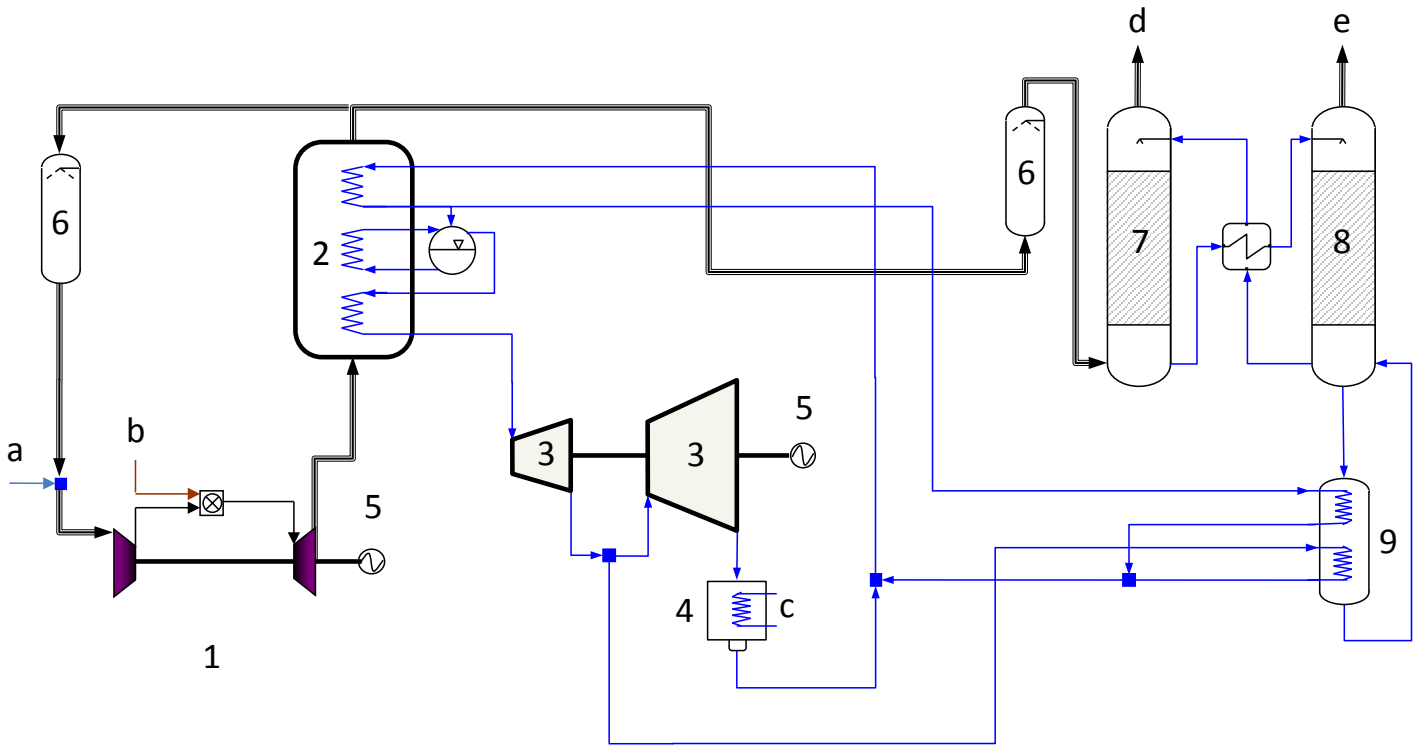

1. Gas Turbine
2. HRSG
3. Steam turbine
4. Condenser
5. Generator
6. Flue gas condenser
7. Absorber
8. Regenerator
9. Reboiler
a. Air
b. Natural gas
c. Water
d. Lean gas
e. CO_2

Figure 2: Schematic simplified picture of the CCPP with CO_2 capture utilizing the economizer-reboiler loop

DESIGNING A CCPP WITH CO_2 CAPTURE

When the carbon capture plant is integrated into the CCPP and the economizer-reboiler loop is used, some new aspects should be considered in the plant design. The extra mass flow through the economizer reduces the temperature difference at the exit of the HRSG. This means that the first law of thermodynamics is fulfilled, more or less independently of the temperature rise in the economizer. Thus, the low-pressure level of the plant can be increased, and the benefit of introducing multiple pressure levels is significantly reduced. In the configuration used in this work the condensate leaving the reboiler is flashed and used for deaeration see figure 1, and the pressurized water leaving the water circuit of the reboiler is used to preheat the fuel (not shown in figure 1).

In the first case a single-pressure CCPP is designed with a carbon capture unit utilizing a MEA with an absorbent solution of 30 % MEA and 70 % water regenerated at 122 °C. Figure 2 shows a schematic picture of the plant and the characteristics of the CCPP are given in table 1.

The compression of CO_2 is performed with 8 compressor stages with intercooling to 25 °C. The CO_2 leaving the capture unit has a pressure of 1.4 bar, and is compressed to 200 bar. The power consumption for compression is 300 kJ/kg CO_2.

Table 1: Key parameter of the single-pressure cycle

Admittance pressure	100.0	bar
η_{HP}	85.0	%
η_{IP}	90.0	%
η_{LP} *(wet)*	83.4	%
η_{GT}	37.7	%
$\eta_{CC,net}$ *excl.* CO_2 *comp.*	52.36	%
Compression work per kg CO_2	300	kJ/kg
$\eta_{CC,net}$ *incl.* CO_2 *comp.*	50.80	%
Pressure loss in HRSG	40	mbar
Evaporator pinch point	8	°C
Temperature difference in economizer	10	°C

Figure 3 shows a temperature vs. heat flux diagram for a single-pressure CCPP in which the proposed water-reboiler loop, described in figure 1, has been integrated. The small temperature difference between the hot and cold side of the economizer results in that more heat can be recovered from the exhaust and very efficient heat recovery. A reduced temperature difference in the economizer means that the thermodynamic driving force is reduced and thus an increased heat transferring area is required. The temperature difference used in the cycles in this work is 10 °C. The approach point i.e. the margin to the boiling point at the economizer is maintained at all loads by controlling the flow in the economizer-reboiler loop. The output of the Rankine cycle is limited by a pressure of 100 bar, which was set to keep the moist content at the LP outlet at a reasonable level.

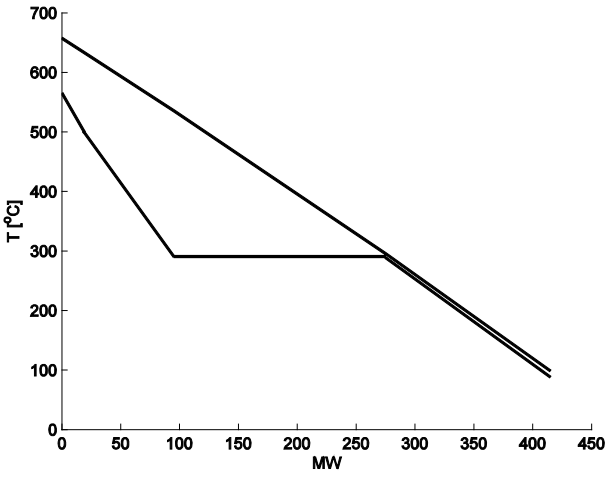

Figure 3: Temperature vs. heat flux for the single-pressure CCPP with carbon capture and the economizer–reboiler loop. Note the small temperature difference in the economizer

By introducing a reheat circuit between the HP and LP turbine the moist pressure can be increased further. Reheat circuit will increase the mean temperature of the supplied heat, which is beneficial for the Rankine cycle, but at the same time will reduce the cycle mass flow. The reheat heat is extracted before the evaporator and will therefore restrict the energy available for steam production. In a conventional CCPP, a reduction in mass flow would result in less energy being recovered in the economizer, and therefore more energy would be lost in the stack. This is the reason why it is very rare to see single-pressure plants with reheat Rankine cycles. However, this is not a problem with the economizer–reboiler loop as the excess energy is supplied to the reboiler. Thanks to the proposed coupling, the temperature difference in the economizer is not affected when a reheat circuit is introduced. This means that the amount of recovered energy in a single-pressure CCPP is almost independent of if a reheat circuit is used or not. The amount of energy recovered from the flue gas is slightly reduced due to the increase in mass flow in the economizer–reboiler loop, resulting in an increase in the economizer inlet water temperature.

The optimum pressure for the reheat is 110 bar, but this gives a pressure ratio of 1.45 in the high-pressure turbine, which would only allow the turbine to have one stage. A single-stage HP turbine would be very expensive, and therefore the reheat pressure is set to 50 bar, which gives a pressure ratio of 3.2. The steam turbine consists of three sections and is configured so that the steam required for the regeneration of the absorbent is extracted from the cross-over pipe between the intermediate and low pressure turbines. The results for the single-pressure CCPP with reheat are presented in table 2.

Table 2: Key parameters for the single-pressure cycle with reheat

Admittance pressure	160.0	bar
η_{HP}	85.0	%
η_{IP}	90.0	%
η_{LP} *(wet)*	84.8	%
η_{GT}	37.7	%
$\eta_{CC,net}$ *excl.* CO_2 *comp.*	53.06	%
$\eta_{CC,net}$ *incl.* CO_2 *comp.*	51.50	%
Compression work per kg CO_2	300	kJ/kg
Pressure loss in HRSG	40	mbar
Evaporator pinch point	8	°C
Temperature difference in economizer	10	°C

With the new heat exchanger, i.e. the reboiler, another temperature difference must be considered. The cold side in the reboiler is the absorbent/water solution in which some of the water is evaporated at an essentially constant temperature. The implication of this is that the temperature difference will increase when water is used on the hot side instead of condensing steam. Therefore, it is necessary to make a trade-off between increasing the pressure to produce steam which is allowed to expand through part of the turbine, and increasing the cycle pressure so that more energy is available in the

economizer. For a single-pressure plant the distribution of heat carried by steam and water is determined by the cycle pressure. A dual-pressure plant has an extra degree of freedom in the additional pressure, which can be adjusted to suit the temperature difference in the reboiler. The steam turbine already consists of three cylinders due to the large volume of steam extracted to supply heat to the reboiler. A fourth turbine cylinder is not an option for economical reasons, and therefore steam at the second pressure level in inserted at the point of the reheat in the dual-pressure plant. For the GE 109FB gas turbine and a steam cycle with an admittance pressure of 160 bar with reheat and a final superheating temperature of 565 °C, optimal efficiency is obtained at a low pressure of 50 bar. The cycle parameters are presented in table 3, and the corresponding temperature vs. heat flux diagram is shown in figure 4.

Table 3: Key parameters for the dual-pressure cycle with reheat

Admittance pressure	160.0	bar
η_{HP}	*85.0*	*%*
η_{IP}	*90.0*	*%*
η_{LP} *(wet)*	*84.7*	*%*
η_{GT}	*37.7*	*%*
$\eta_{CC,net}$ *excl.* CO_2 *comp.*	*53.35*	*%*
$\eta_{CC,net}$ *incl.* CO_2 *comp.*	*51.81*	*%*
Compression work per kg CO_2	*300*	*kJ/kg*
Pressure loss in HRSG	*40*	*mbar*
Evaporator pinch point	*8*	*°C*
Temperature difference in economizer	*10*	*°C*

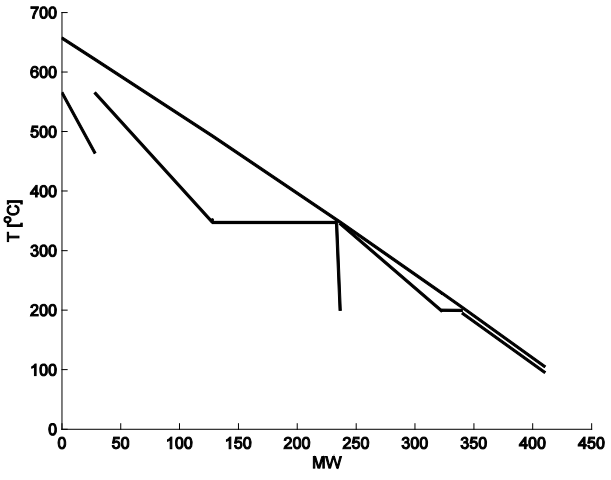

Figure 4: Temperature vs. heat flux for the dual-pressure reheat CCPP with carbon capture and the economizer–reboiler loop

Although it is unrealistic, a fourth turbine cylinder was introduced to show theoretical maximum efficiency. The fourth cylinder allows the low pressure level to be chosen independently of the reheat pressure. The result show a maximum if the low pressure is set to 21 bar, which is much higher than in a conventional dual-pressure CCPP, which would have a low pressure of 3–8 bar. The efficiency of this rather unrealistic cycle is 51.88 %, including the compression of CO_2.

CHILLED AMMONIA

One limitation of a MEA-based separation unit is its sensitivity to high temperatures, which limits the pressure in the regeneration column. A higher pressure in the regenerator reduces the energy required for CO_2 compression as it allows for pumping between the absorber and the regenerator. However, it also requires heat at a higher temperature. The economizer–reboiler loop makes high-temperature heat available, especially if the CCPP is a single-pressure unit.

Table 4: Key parameters for the single-pressure cycle with reheat using chilled ammonia

Admittance pressure	160.0	bar
η_{HP}	85.0	%
η_{IP}	90.0	%
η_{LP} *(wet)*	84.8	%
η_{GT}	37.7	%
$\eta_{CC,net}$ *excl.* CO_2 *comp.*	52.88	%
$\eta_{CC,net}$ *incl.* CO_2 *comp.*	52.27	%
Pressure in HP regenerator	21	bar
Pressure in LP regenerator	10	bar
Electric cooling duty	21221	kW
Compression work per kg CO_2*,HP*	84	kJ/kg
Compression work per kg CO_2*,LP*	136	kJ/kg
Mass flow CO_2*, HP*	14.8	kg/s
Mass flow CO_2*, LP*	24.5	kg/s
Pressure loss in HRSG	40	mbar
Evaporator pinch point	8	°C
Temperature difference in economizer	10	°C

With the chilled ammonia process, a higher temperature and a higher pressure can be used in the regeneration column. One drawback of including the economizer–reboiler loop in a single-pressure reheat plant using MEA was the large temperature difference in the reboiler. If a chilled ammonia unit is used instead, the high-temperature water can be utilized in a high-pressure regenerator, and further regeneration can then be performed in a regenerator at a lower pressure with additional steam. The ammonia stripper in which ammonia is recovered from the lean gas (exhaust) is operated at ambient pressure. The energy for ammonia stripping is supplied by the condensate complemented with steam. The configuration of the heat supply to the reboilers is shown in figure 5. The pressure level for steam extraction is set to suit the temperature in the low pressure regenerator. Therefore, it is preferable to use a low regeneration temperature in the low-pressure column.

The dual-pressure chilled ammonia CO_2 separation unit was investigated in the same single-pressure reheat plant as for the MEA unit (described in table 2). The energy required to compress the CO_2 from the LP regenerator is 136 kJ/kg CO_2, and for the HP column 84 kJ/kg CO_2. The temperature in the reboiler is a function of the ammonia/water ratio in the absorbent solution and the amounts of CO_2 in the lean and rich absorbent table 4 gives some of the most important results. For a large-scale plant the height of the columns is a problem, and both the absorber and the regeneration columns are usually divided into two or more units (including two regenerators at different pressures does not necessarily increase the initial plant cost).

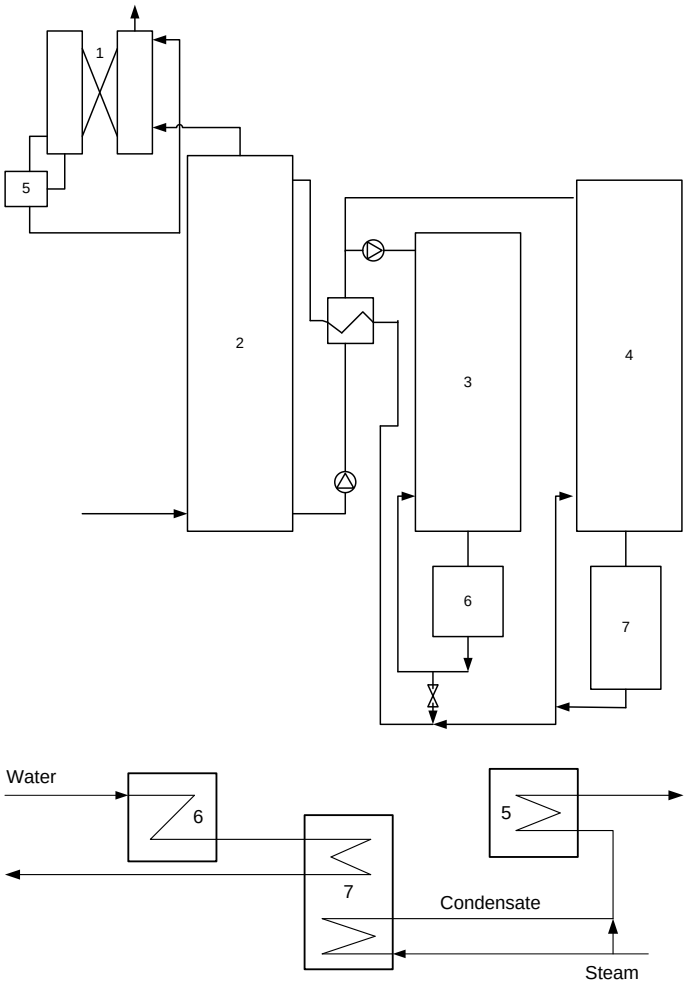

1. Ammonia stripper *4. LP regenerator* *7. Reboiler 3*
2. Absorber *5. Reboiler 1*
3. HP regenerator *6. Reboiler 2*

Figure 5: The chilled ammonia CO_2 separation unit and the reboiler heat configuration

Summary of results

Combined-cycle power plants have been modelled to accommodate absorbent-based CO_2 capture using hot water to partly cover the reboiler duty. When the economizer–reboiler loop was included, the mean temperature difference in the economizer was reduced. The result of this is that the HRSG efficiency is no longer dependent on the number of pressure levels. On the other hand, if the CO_2 separation unit employs an absorbent that cannot withstand high temperatures, a second pressure level can improve the total efficiency. This is a consequence of the increasing amount of entropy generated in the reboiler with increasing temperature difference. The low pressure of such a plant should be much higher than in a conventional dual-pressure CCPP.

If the absorbent can be regenerated at a higher temperature, a single-pressure CCPP is preferable. By dividing the regeneration column into a high- and a low-pressure section, the steam extracted from the turbine can still be extracted at a low pressure level. A chilled ammonia separation unit offers the possibility of using a high regenerator temperature.

The possibility of better utilizing the potential of the hot water in a chilled ammonia CO_2 separation unit appears very promising. To fully evaluate the possibilities and the problems that may be associated with a chilled ammonia unit using a dual-pressure regenerator, more work should be devoted to finding the appropriate composition of the absorbent, i.e. the water/ammonia ratio and lean/rich CO_2 loading.

DISCUSSION

The economizer–reboiler loop provides hot water for the regeneration of the absorbent. The hot water is supplied by the economizer and does not affect the steam production. However, on the other side of the process, i.e. in the reboiler, a liquid heat carrier will not provide heat at a constant temperature. Therefore, it is better for the heat to be supplied at two stages at different temperatures. This will give a process in which less entropy is generated, according to the second law of thermodynamics.

MEA decomposes rapidly when heated above about 120 °C, and lowering the temperature would result in reduced pressure in the regenerator column. This will lead to a large expensive column and increased consumption of power in the compression of CO_2. Ammonia is not as sensitive to high temperatures, and a higher temperature can be used in the reboiler, allowing the regeneration column to be divided into a high-pressure and a low-pressure unit. The amount of energy required to regenerate the absorbent in the chilled ammonia process increases with increasing pressure. This must be weighed against the saving in the energy required for compression as the CO_2 is pumped in a liquid state dissolved in the absorbent.

The concept of a dual-pressure regeneration process has, to the best of the author's knowledge, not previously been modelled in the open literature. The configuration investigated here is such that the concentration of ammonia in the solvent is the same in both columns. Therefore, the concentration is a compromise between the concentrations most suitable for the two regeneration pressures/temperatures. The same applies to the CO_2 loading. In order to find the optimal CO_2 separation

plant for the proposed configuration more modelling in ASPEN is required.

The results show that the dual-pressure plant with reheat has the highest efficiency. From figure 4 it can be seen that the scope for an additional pressure level is very small, but this was investigated for the sake of completeness. To provide a comprehensive overview of the potential of the proposed method, the efficiencies of a single-pressure and a triple-pressure plant with a conventional steam-heated reboiler were calculated. Figure 6 shows the efficiency of a number of CCPPs with carbon capture. All the values include CO_2 compression to 200 bar and care was taken to make the comparisons as fair as possible. A conventional triple-pressure CCPP with same losses has an efficiency of 59.44 % (parasitic losses and transformer step-up losses not included).

A single-pressure plant is much cheaper to construct than a multi-pressure plant, and it is also more flexible. With only one steam drum, the plant is quicker to start, and responds more rapidly to load variations. This is an important factor in the power market today. The carbon capture process consists of chemical reactions and has a large heat storage capacity, and is therefore very sluggish to control. The single-pressure plant has the ability to adapt to very rapid load changes when operated without the CO_2 separation unit, and is still able to compete with regard to efficiency when the CO_2 separation plant is in operation.

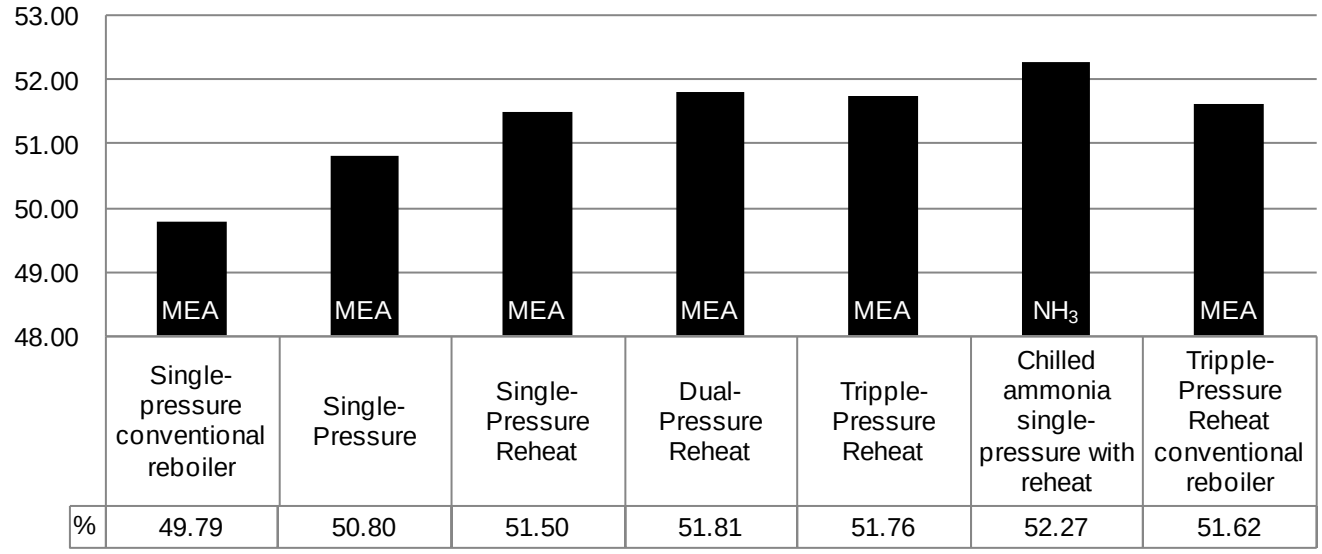

Figure 6: Efficiencies of different CCPP with CO_2 capture. The pile to the most left and to the most right does not use the economizer-reboiler coupling. All plants except the sixth from the left uses MEA as absorbent

CONCLUSIONS

This study shows the benefits of using excess energy from the economizer to regenerate the absorbent in a combined cycle with post combustion CO_2 capture. It has been shown that by using the economizer-reboiler loop high efficiencies can be achieved without the need of a third pressure level. If a MEA carbon capture unit is used the highest efficiency is achieved with a dual-pressure reheat plant. The single-pressure reheat plant only suffers 0.3 % units to the dual-pressure reheat plant.

The single-pressure reheat plant supplies high temperature water to the reboiler and this can be better utilized by a chilled ammonia separation unit. By designing a chilled ammonia separation unit using a dual pressure regenerator the hot water could be better utilized. The result shows that the chilled ammonia process greatly benefits from the economizer-reboiler coupling and shows higher cycle efficiencies than the MEA unit

A single-pressure plant is much cheaper to construct and offers better flexibility in terms of rapid response to changes in load. The latter is an important feature when the plant is operated without CO_2 capture.

ACKNOWLEDGMENTS

The authors acknowledge Dr. Marcus Thern for valuable discussions during this work. Furthermore, we would like to thank Dr. Björn Fredriksson Möller for the development of the MEA CO_2 separation model.

REFERENCES

[1] Hammer, T., Keyser, J., and Bolland, O., 2009, "Natural gas oxy-fuel cycles--Part 2: Heat transfer analysis of a gas turbine," Energy Procedia, 1(1), pp. 557-564.

[2] Rezvani, S., Bolland, O., Franco, F., Huang, Y., Span, R., Keyser, J., Sander, F., McIlveen-Wright, D., and Hewitt, N., 2009, "Natural gas oxy-fuel cycles--Part 3: Economic evaluation," Energy Procedia, 1(1), pp. 565-572.

[3] Woollatt, G., and Franco, F., 2009, "Natural gas oxy-fuel cycles--Part 1: Conceptual aerodynamic design of turbo-machinery components," Energy Procedia, 1(1), pp. 573-580.
[4] Sanz, W., Jericha, H., and Bauer, B., 2008, "Qualitative and Quantitative Comparison of Two Promising Oxy-Fuel Power Cycles for CO_2 Capture," Journal of Engineering for Gas Turbines & Power, 130(3), pp. 021-032.
[5] Kohl, A. L., and Nielsen, R. B., 1997, Gas Purification 5th ed., Gulf Publishing Co., Houston USA.
[6] Fredriksson Möller, B., 2005, "A Thermoeconomic Evaluation of CO_2 Capture with Focus on Gas Turbine-Based Power Plants," PhD thesis, Lund University, Sweden.
[7] Finkenrath, M., Ursin, T. P., Hoffmann, S., Bartlett, M., Evulet, A., Bowman, M. J., Lynghjem, A., and Jakobsen, J., "Performance and cost analysis of novel gas turbine cycle with CO_2 capture," Proc. ASME Turbo Expo.
[8] Botero, C., Finkenrath, M., Bartlett, M., Chu, R., Choi, G., and Chinn, D., 2009, "Redesign, Optimization, and Economic Evaluation of a Natural Gas Combined Cycle with the Best Integrated Technology CO_2 Capture," Energy Procedia, 1(1), pp. 3835-3842.
[9] Bolland, O., and Mathieu, P., 1998, "Comparison of two CO_2 removal options in combined cycle power plants," Energy Conversion and Management, 39(16-18), pp. 1653-1663.
[10] Chiesa, P., and Consonni, S., 2000, "Natural Gas Fired Combined Cycles With Low CO_2 Emissions," J. Eng. Gas Turbines Power, 429(3), p. 8.
[11] Jack, A. R., Audus, H., and Riemer, P. W. F., "The IEA greenhouse gas R&D programme," Energy Conversion and Management, 33(5-8), pp. 813-818.
[12] Kvamsdal, H. M., Jordal, K., and Bolland, O., 2007, "A quantitative comparison of gas turbine cycles with CO_2 capture," Energy, 32(1), pp. 10-24.
[13] Zachary, J., and Titus, S., "CO_2 capture and sequestration options: Impact on turbo-machinery design," Proc. ASME Turbo Expo, 2008, Berlin, Germany.
[14] Mimura, T., Shimojo, S., Suda, T., Iijima, M., and Mitsuoka, S., "Research and development on energy saving technology for flue gas carbon dioxide recovery and steam system in power plant," Energy Conversion and Management, 36(6-9), pp. 397-400.
[15] Gal, E., 2006, "Ultra Cleaning Of Combustion Gas Including The Removal Of CO_2," A. P. Inc, ed.US.
[16] Darde, V., Thomsen, K., van Well, W. J. M., and Stenby, E. H., 2009, "Chilled ammonia process for CO_2 capture," Energy Procedia, 1(1), pp. 1035-1042.
[17] Dave, N., Do, T., Puxty, G., Rowland, R., Feron, P. H. M., and Attalla, M. I., 2009, "CO_2 capture by aqueous amines and aqueous ammonia-A Comparison," Energy Procedia, 1(1), pp. 949-954.
[18] Elkady, A. M., Evulet, A. T., Brand, A., Ursin, T. P., and Lynghjem, A., 2008, "Exhaust Gas Recirculation in DLN F-class Gas Turbines for Post-Combustion CO_2 Capture," Proceedings of GT 2008, pp. 9-12.
[19] Jonshagen, K., Sipocz, N., and Genrup, M., 2011, "A Novel Approach of Retrofitting a Combined Cycle With Post Combustion CO_2 Capture," Journal of Engineering for Gas Turbines and Power, 133(1), pp. 011703-011707.
[20] Walsh, P. P., and Fletcher, P., 2004, Gas turbine performance, Blackwell Science, Malden, MA.
[21] Gülen, S. C., Griffin, P. R., and Paolucci, S., 2002, "Real-Time On-Line Performance Diagnostics of Heavy-Duty Industrial Gas Turbines," Journal of Engineering for Gas Turbines and Power, 124(4), p. 12.
[22] Traupel, W., 1977, Thermische Turbomaschinen, Springer-Verlag, Berlin ; New York.
[23] IPSEpro, 2003, "SimTech Simulation Technology (SimTech),,"Graz, Austria.

II

Klas Jonshagen
Department of Energy Sciences,
Faculty of Engineering,
Lund University,
P.O. Box 118,
SE-221 00 Lund Sweden
e-mail: klas.jonshagen@energy.lth.se

Nikolett Sipöcz
Department of Mechanical and Structural
Engineering and Material Science,
University of Stavanger,
Kitty Kiellands hus,
Rennebergstien 30,
4021 Stavanger, Norway
e-mail: nikolett.sipocz@uis.no

Magnus Genrup
Department of Energy Sciences,
Faculty of Engineering,
Lund University,
P.O. Box 118,
SE-221 00 Lund Sweden
e-mail: magnus.genrup@energy.lth.se

A Novel Approach of Retrofitting a Combined Cycle With Post Combustion CO_2 Capture

Most state-of-the-art natural gas-fired combined cycle (NGCC) plants are triple-pressure reheat cycles with efficiencies close to 60%. However, with carbon capture and storage, the efficiency will be penalized by almost 10% units. To limit the energy consumption for a carbon capture NGCC plant, exhaust gas recirculation (EGR) is necessary. Utilizing EGR increases the CO_2 content in the gas turbine exhaust while it reduces the flue gas flow to be treated in the capture plant. Nevertheless, due to EGR, the gas turbine will experience a different media with different properties compared with the design case. This study looks into how the turbomachinery reacts to EGR. The work also discusses the potential of further improvements by utilizing pressurized water rather than extraction steam as the heat source for the CO_2 stripper. The results show that the required low-pressure level should be elevated to a point close to the intermediate-pressure to achieve optimum efficiency, hence, one pressure level can be omitted. The main tool used for this study is an in-house off-design model based on fully dimensionless groups programmed in the commercially available heat and mass balance program IPSEPRO. The model is based on a GE 109FB machine with a triple-pressure reheat steam cycle.
[DOI: 10.1115/1.4001988]

1 Introduction

Large-sized combined cycles will contribute to a great part of the future electricity market due to their relatively low investment cost and short construction time. Future legislation and political incentives may render that fossil fuel power plant owners would be forced to either implement carbon capture and storage (CCS) or switch to biofuels. For large-sized (~400 MW) gas turbine-based combined cycle power plants, the latter would result in consumption of enormous amounts of biomass, which would require great areas for growing and may cause logistical issues, therefore, CCS might be more suitable.

To integrate a CO_2 capture plant into an existing NGCC, will require some major modifications to the plant. The main issue is that about 60% of the steam is condensed at a higher pressure level and, therefore, the last section of the HRSG becomes inefficient due to a reduced flow on the cold side.

The near-term implementation of CO_2 capture in terms of post-combustion capture into natural gas-fired power plants has been a hot topic in the power plant research field for the last couple of years [1–10]. These studies, along with the numerous ones completed on coal-fired power plants [11–15] using chemical absorption, have all pointed out the high efficiency penalties associated with this technology due to solvent regeneration. Thus, analysis considering alternatives that could reduce the reboiler duty is one of the most important research topics within this field [16–18]. Studies evaluating different integration methods of the capture process in conventional power plants have also been carried out in the recent past. These have revealed that the optimal option in order to fulfill the reboiler requirements is to utilize saturated steam with a pressure corresponding to a steam saturation temperature of approximately 132°C, depending on the boiler pinch point [19].

The objective of this present paper is to evaluate the possibility of recovering excess energy from the last part of the HRSG from a triple-pressure natural gas-fired combined cycle to cover part of the reboiler duty. The plant utilizes exhaust gas recirculation and CO_2 separation using an amine-based absorption process with MEA. The essence of the idea is to, the greatest possible extent, utilize saturated economizer water to provide heat for the regeneration of the solvent. This results in a better deployment of the heat available in the flue gases and, consequently, reduces the large power loss in the steam turbine due to steam extraction for the reboiler.

2 The Gas Turbine

This study is based on a combined cycle using the General Electric 109FB, a 300 MW single-shaft gas turbine, as toping cycle. The machine, by virtue of its size, is directly connected to a 50 Hz generator running at a fixed speed of 3000 rpm. The exact details for the GE unit are not published but the model is based on available data. The compressor and turbine characteristics are normally not available outside the OEM's domains. In this case, the compressor map is based on a publication by General Electric [20]. The map is actually for a frame 7 unit, which is the 60 Hz version of the frame 9 type. It is assumed that the frame 9 compressor is a direct scale-up of the smaller frame 7. There are only relative values on the published characteristics and the reference points are assumed to be the same for both cases. The actual values are based on the ISO condition.

3 Exhaust Gas Recirculation

By virtue of the gas turbine working principle, the CO_2-content in the exhaust is less than for a normal steam boiler. This, in combination with higher specific flows for the gas turbine, makes the separation plant bulky and costly. The specific flue gas flow is on the order of 1.5 kg/MW s, in contrast to approximately 0.95 kg/MW s for a normal steam boiler. The remedy is to use EGR for higher concentrations of carbon and reduce the flow to be treated in the separation plant. The limit to how much EGR that can be utilized is, in principle, set by the combustor. The problems are, in general, caused by lack of oxygen that reduces combustor efficiency, resulting in high CO levels [4,21].

Contributed by the International Gas Turbine Institute (IGTI) of ASME for publication in the JOURNAL OF ENGINEERING FOR GAS TURBINES AND POWER. Manuscript received April 12, 2010; final manuscript received April 22, 2010; published online September 17, 2010. Editor: Dilip R. Ballal.

Table 1 Reduction in isentropic exponent and gas constant due to change of working fluid (in percent)

	γ (%)	R (%)
Compressor inlet	0.32	0.85
After combustor	0.50	0.79
Turbine outlet	0.59	0.80

In Ref. [21], experimental works proved that the dry low NO_x (DLN) combustor currently employed in GE-109FB can operate on 30–35% EGR without modifications and it is predicted that with only minor modification, it can be operated with EGR levels beyond 40%. Reference [4] used an EGR rate of 40% in a GE-109FA. This is based on that; the concentration of O_2 before the combustion should be kept above 16%.

The current model obtains a CO_2 concentration of just below 8 vol % with 40% EGR, which corresponds with what Ref. [21] suggested should be possible with the GE 109FB burner, therefore, a 40% EGR rate is used in this work.

4 The Calculation Model

Most of the modeling in this work has been performed in the commercially available heat and mass balance program IPSEPRO by SimTech [22]. IPSEPRO has the capacity of introducing new and modified components in a very straight-forward and flexible manner. The gas turbine model is described in Ref. [23], the steam turbine models are described in Ref. [24], and the CO_2 capture plant is presented in Ref. [1].

The behavior of a compressor or a turbine is dependent on a larger number of base parameters. By creating parameter groups consisting of a number of the base parameters, the overview of the machine behavior is drastically simplified. These parameter groups, in combination with the machine characteristics, make it possible to create accurate desktop studies at off-design operations.

It is possible to predict the behavior under different working media by introducing rigorous parameter groups. The word rigorous means that the fluid properties are kept in nondimensional parameter groups. It is, thereby, possible to calculate the normal cycle behavior into different mediums [25].

5 EGR Effects on the Turbomachinery

The calculations in this section show that the changes in the gas turbine performance are minute, possibly even smaller than what is measurable in a real engine. In the calculations, the fluid properties have been included when addressing the working point in the compressor and turbine map but the secondary order losses has been considered constant. Also, the deviation of Reynolds number has been calculated, however, the changes are very small and will not affect the efficiencies nor the pumping/swallowing capacities.

The increased concentration of CO_2 in the gas turbine working fluid achieved by EGR alters the gas properties. Table 1 lists the changes of specific gas constant (R) and isentropic exponent (γ) at three different engine stations while an EGR rate of 40% is utilized. The changes are very small, however, as they affect the machine in a multi dimensional manner and one parameter affects the other the overall result is not easily predicted. The gas constant at the compressor inlet gas mixture is reduced from 288.6 kJ/kgK to 286.2 kJ/kgK or by 0.85%. The isentropic exponent for CO_2 differs more from air at higher temperatures which explains why the inlet is less affected as can be seen in Table 1.

Due to the reduction in the isentropic exponent, the temperature after both the compressor and turbine will increase in accordance with the polytropic expression

$$\frac{p_1}{p_2} = \left(\frac{T_1}{T_2}\right)^{(\gamma \cdot \eta_p/\gamma - 1)} \tag{1}$$

A higher temperature at the turbine outlet corresponds to a larger exhaust gas loss. However, in a CCPP, the energy in the exhaust gas is recovered in the steam cycle and reduced GT efficiency due to elevated exhaust gas temperature is not an important factor. More important is that the gas turbine has a maximum temperature allowed in the exhaust and this has to be considered, especially at high ambient temperatures and at part-load operation.

With a higher temperature after the compressor, the temperature difference over the combustion chamber is reduced. Nevertheless, the specific heat capacity of the working fluid has increased due to the higher concentration of CO_2 and the overall effect is that the amount of fuel is increased.

Equations (2)–(4) show the parameter group related to the mass flow, pressure ratio, and speed. Each of them includes the isentropic exponent and will be affected when the working fluid is changed.

$$\mathrm{FN} = \frac{\dot{m} \cdot \sqrt{\dfrac{T}{T_{\mathrm{ref}}}}}{\dfrac{p}{p_{\mathrm{ref}}} \sqrt{\dfrac{\gamma \cdot R_{\mathrm{ref}}}{\gamma_{\mathrm{ref}} \cdot R}}} \tag{2}$$

$$\pi^* = \left[\frac{((\pi_{\mathrm{rel}} \cdot (\pi_{\mathrm{ref}} - 1) + 1)^{\gamma_{\mathrm{ref}} - 1/\gamma_{\mathrm{ref}}} - 1)}{\dfrac{\gamma_{\mathrm{ref}} - 1}{\gamma - 1}} + 1 \right]^{(\gamma/\gamma - 1)} \tag{3}$$

$$\mathrm{aerospeed} = \frac{\mathrm{speed}}{\sqrt{\dfrac{T}{T_{\mathrm{ref}}}}} \sqrt{\frac{\gamma_{\mathrm{ref}}}{\gamma}} \tag{4}$$

Some of the effects cancel each other out, e.g., what is gained in the compressor is lost in the turbine and vice versa. The main difference is that the exhaust gas temperature is increased by 4.4°C, the mass flow is increased with 5.5 kg/s, and the most important result is that more energy is available to the bottoming cycle.

The increased flow will increase the axial velocity through the machine and, in combination with reduced speed of sound (5), this will render in increased Mach numbers (Ma).

$$a = \sqrt{\gamma \cdot R \cdot T} \tag{5}$$

To obtain an estimate of how much this will affect the machine, two key positions are studied; the inlet of the compressor and the outlet of the turbine. To calculate the compressor inlet Mach number, geometry is needed and this is normally not available outside the manufacturer domains. To get an applicable estimate of the geometry, a published cross-section [26] of the 107FB machine, which is the scaled down 60 Hz version of the 109FB, was used to find the hub tip ratio. By assuming that the machine is designed with an inlet Ma at the tip of the first rotor of 1.3 at ISO-condition and using the hub tip ratio from Ref. [26], the inlet area could be estimated. The outlet geometry is obtained by assuming that the annulus area times the squared speed (AN_2) is 55×10^6 at design conditions together with an absolute exit Mach number of 0.6.

By not considering the exact figures but only relative changes in percent, the results should provide relevant accuracy. The inlet Ma relative to the tip of the first rotor increases with 0.23% and the outlet Ma relative to the last rotor tip increases with 0.7%. The changes are indeed small and should not be an issue when compared with the combustion system.

6 Amine-Based Carbon Capture Plant

An amine-based carbon capture plant consists of two columns. In the first column called the absorber, the liquid amine mixture chemically absorbs the CO_2 from the flue gas. The flue gas enters at the bottom of the column and faces the countercurrent amine solution. At the top of the column, the treated flue gas is let out into the atmosphere. At the bottom of the absorber, the now CO_2-rich amine mixture is pumped via a heat exchanger in which it is heated by the lean amine to the top of the other column called the stripper. In the stripper, the CO_2 is released from the amine as the chemical link between them is broken. This process requires heat, which is added through the condensation of steam. The CO_2 leaves the stripper for further treatment at the top of the column. As the steam condenses, it mixes with the amine and pores down to the bottom of the column where it is collected in the reboiler. In the reboiler, heat is added from an external source to evaporate some of the water content and provide steam to the stripper. From the reboiler, the lean amine is fed to the heat exchanger and back to the absorber to close the cycle. The choice of the process solution is determined by the pressure and temperature conditions of the gas to be treated; for this case, monoethanolamine (MEA) is selected. The model used for CO_2 separation is based on the calculation model proposed by Kohl and Nielsen [27] and was developed by Fredriksson Möller [1]. The calculation of the heat requirement and power needed for the capture process is dependent on the capture rate and level of regeneration at a given temperature. Hence, an initial condition of the simulations has been to capture 90% of CO_2 produced by means of an aqueous solution of MEA with 30% MEA by weight at a regeneration temperature of 120°C. Selection of the reboiler temperature has been made meeting the limiting temperature level of 122°C above which thermal degradation of MEA and corrosion becomes intolerable [19].

7 CO_2 Compression

The CO_2 compression part presented here is included in order to give a comprehensive estimation of the total efficiency penalty for the power plant with CO_2 capture for which compression is an essential part. Several studies [28–30] have evaluated the feasibility of different compression options and this will not be further discussed here. For a more extensive outline, the reader is referred to [28–30].

There are several viable options for the compression of CO_2 where the main categories are compression only, compression and condensing with water at ambient temperature and pumping and, finally, compression and condensing using a refrigerant and pumping. To find the most suitable method, the refrigeration process library package in IPSEPRO has been used. To simplify the calculations, the substance used was assumed to be pure CO_2, in reality the CO_2 stream contains fractions of argon and moisture, which might affect the available intercooling levels (preventing liquid knock-out) and compressor work. CO_2 and ammonia were tested as refrigerants. The ammonia cycle calculations showed superior performance over CO_2. Among the available options, the method using water at ambient conditions for condensing was found to be the least energy-consuming and, hence, the most preferable.

The CO_2 compression is performed in a six stage intercooled compressor after which the CO_2 is condensed at pressure of 60 bars by utilizing water with a temperature of 15°C and then finally cryopumped up to the final pressure of 200 bars (see Table 2).

The result is very dependent on the cooling source, for example, if the intercooling and condensing temperature would be increased to 25°C, the pressure for the condensation would increase to 65 bars. This would favor the compression-only alternative even though the option with water intercooling and final pumping to final pressure is less energy intensive. (327.5 kW/kg compared with 321.1 kW/kg).

Table 2 Compression data

	Value	
Compressor efficiency	85.0	%
Pump efficiency	50.0	%
Intercooling level	20.0	°C
Power consumption per kg CO_2	310.2	kW/kg

8 Integration of CO_2 Capture

The reference case used in this study is a standard three-pressure reheat combined cycle plant without supplementary firing as shown in Fig. 1. The plant is based on a General Electric frame 9 gas turbine. To minimize the greenhouse gas emissions, the plant includes a MEA capture unit and utilizes EGR. After the HRSG, 40% of the flue gas is fed to an exhaust gas condenser and cooled to 20°C and then returned via a flue gas fan to the gas turbine inlet. The remaining flue gas is treated in another flue gas condenser where it is cooled to 30°C before it enters the carbon capture unit.

In the steam cycle, the HP and RH steam are superheated to 565°C and the pressure levels are 150/24/2.8 bars. The LP-pressure level is set to fit the carbon capture plants steam requirements of 130°C (including a reboiler pinch point of 8°C). The plant also includes fuel preheating to 200°C by utilizing IP-economizer water. Losses in heat exchangers, ducts, etc., are estimates based on past experience. The cycle has no separate feed water tank and the feed water is instead degassed in the condenser hot-well and the low-pressure drum. The latter is posing limits in terms of temperature difference between the saturation level at the LP-pressure and the feed water after the economizer for efficient deaeration.

The heat needed for regenerating the amine in the carbon capture plant is extracted from before the LP turbine at a pressure of 2.7–2.8 bars corresponding to the saturation temperature at the outlet of the reboiler. For this system, which is using MEA, the temperature of the amine leaving the regenerator is 120°C. Approximately 60% of the low-pressure steam is required for the reboiler. After condensation, the condensate is returned to the HRSG at a temperature of 130°C. The water can either be mixed with the cold condensate after the main condenser or it could be mixed in after a first economizer at a corresponding temperature. Efficiencywise, the result is the same in this work; the condensate from the reboiler is mixed in after the second economizer. Therefore, the flow in the last section of the HRSG (below 130°C) is very limited. Figure 2 shows a temperature-to-heat flux diagram of the HRSG. The reduced flow in the last section occurs as a steep slope in accordance with the relation between heat and temperature differences at the cold side of the heat exchanger.

$$\dot{Q} = \dot{m} c_p (T_2 - T_1) \tag{6}$$

The result of the low flow in the last section of the HRSG is that the flue gas exit temperature is much higher compared with the non-CO_2 capture case. The high temperature at the HRSG outlet indicates that there is a potential of recovering more energy in the last sections. A MEA CO_2 capture unit, as well as the use of EGR, requires cooling of the flue gas; hence, a high HRSG exit temperature is not only coupled to poor heat recovering but also a larger need of cooling water in the exhaust gas condenser. The efficiency of the reference case is 50.17% including the compression of CO_2 (51.78% without CO_2 compression).

As mentioned earlier, the reboiler heat is extracted from the turbine at a pressure of 2.7–2.8 bars. For a conventional multi-pressure combined cycle, especially if it includes reheat, the steam will be superheated at this pressure level. For the evaporating process in the reboiler, the temperature difference becomes large if superheated steam is used; hence, it is not optimal in a thermo-

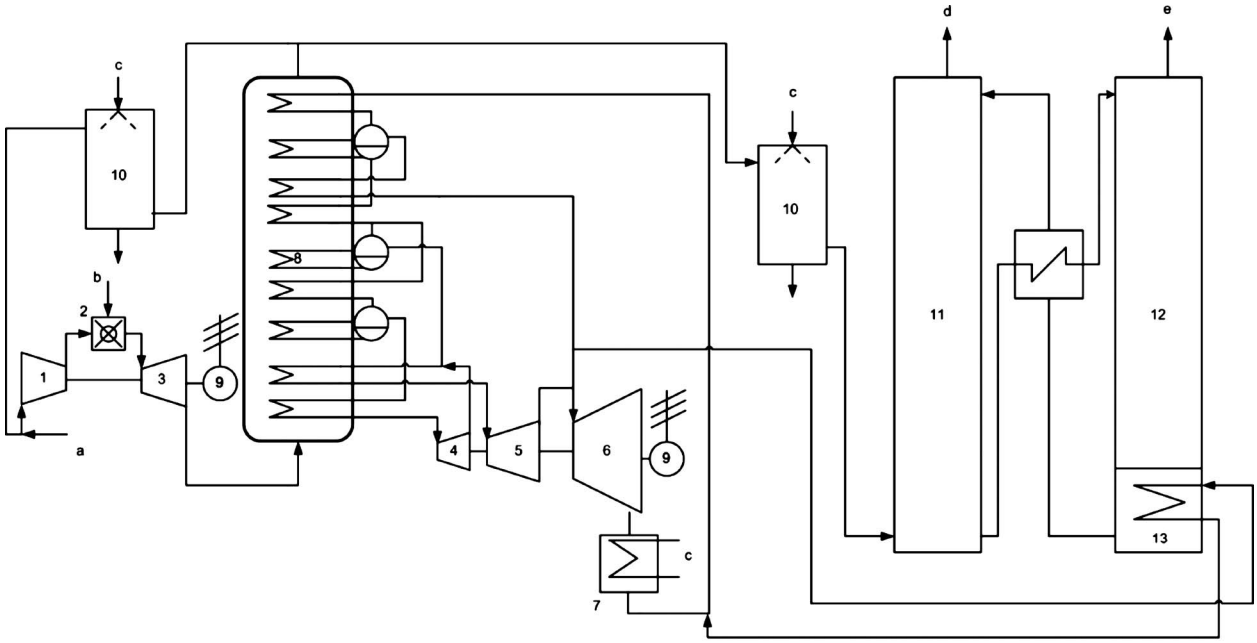

1. Compressor *4. LP Turbine* *7. Condenser* *10. Exhaust gas condenser* *13. Reboiler* *c. Cooling Water*
2. Combustor *5. IP Turbine* *8. HRSG* *11. CO_2 absorber* *a. Air* *d. Exhaust*
3. Turbine *6. HP Turbine* *9. Generator* *12. Stripper* *b. Fuel* *e. CO_2 to be compressed*

Fig. 1 Schematic figure of the reference plant (CO_2 compression not included)

dynamic prospective. The potential of superheated steam can be better utilized in the steam turbine rather than in the reboiler.

9 Cycle Improvements

By dedicating the steam produced in the LP section of the HRSG to the reboiler, the LP superheater becomes redundant and removing it exposes more energy to the other sections, allowing especially the IP mass flow to increase. However, the low-pressure section only produces a fraction of the required heat for the reboiler and the main part still needs to be extracted from the turbine. This is controlled by means of a control valve before the low-pressure turbine, maintaining nominal reboiler pressure.

The first economizer (last part of the HRSG) flow is very small due to the fact that about 60% of the steam is condensed at a higher temperature in the reboiler and returned to the HRSG before the second economizer. This miss-balance in the HRSG results in a high flue gas exit temperature, see Fig. 2. By reducing the temperature of the water from the reboiler before it enters the HRSG, the miss-matched section can be reduced. This can, for example, be done by using the hot water for fuel preheating. The reference case uses saturated water extracted from the intermediate drum for fuel preheating to 200°C and if this is done in two stages; preheating to 125°C with the reboiler water and topping it in a second part with IP-water, the flue gas temperature can be reduced.

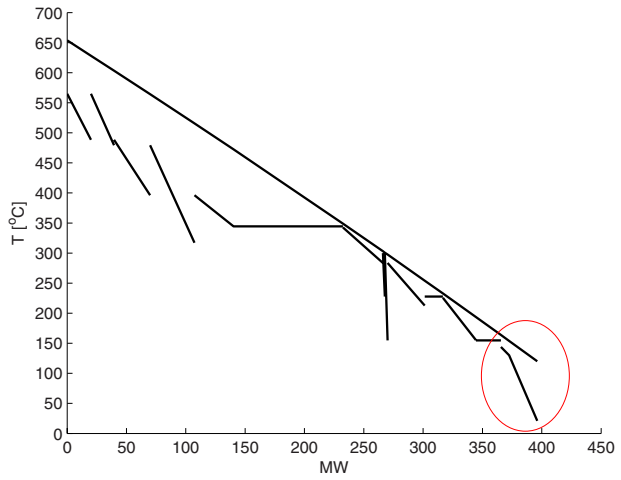

Fig. 2 Temperature to heat flux diagram of the reference case with the economizer highlighted

In the reference case, the deaeration is performed in the low-pressure drum utilizing saturated LP steam. By flashing the water from the reboiler, it can be used for deaeration and thereby, more LP steam is available for the turbine and the economizer flow is increased as a knock-on effect. The deaeration is preferably performed above atmospheric pressure. In this case, a pressure of 1.2 bars is chosen and the approach temperature is set to 11°C for adequate degassing.

Figure 3 illustrates the effect of the changes made that include removing the low-pressure superheater and adding condensate driven fuel preheating and a new deaeration set-up. The HRSG exit temperature is reduced from 120°C for the reference case to 108°C for the efficiency, resulting in an increase from 50.17% to 50.37% (51.78–51.99% without CO_2 compression). The reduced temperature after the HRSG results in that; the required flue gas cooling water is reduced by 257 kg/s or 6% compared with the reference case.

The temperature differences in the last section of the HRSG are despite the improvements made large and the exit temperature of 108°C requires large amount of cooling prior to the carbon capture process.

10 Hot Water Driven Reboiler

The purpose of the reboiler is to provide saturated steam for the absorption column by evaporating part of the water content in the

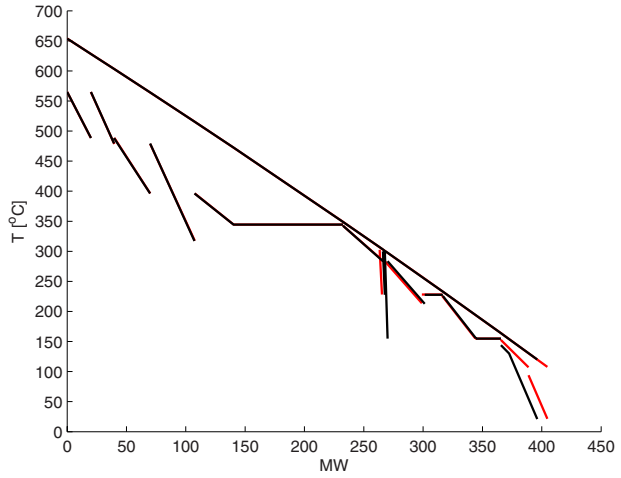

Fig. 3 Temperature to heat flux diagram of the plant after removing the low-pressure superheater, adding condensate driven fuel preheating and a new deaeration set-up

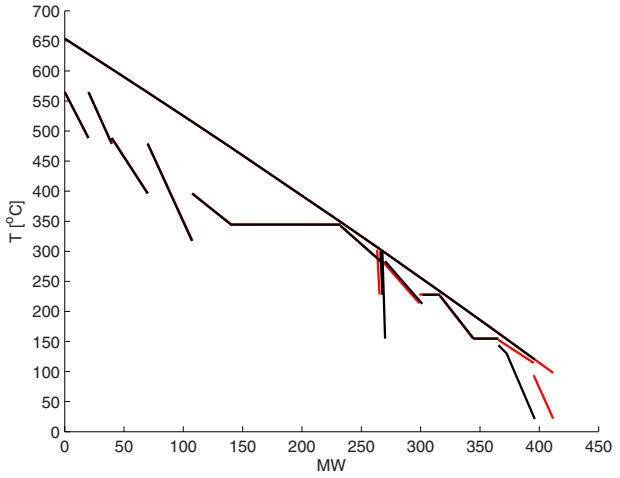

Fig. 4 Temperature to heat flux diagram of the CCPP plant with CO_2 capture when the excess energy from the second economizer is utilized for regenerating the amine

amine mixture at the bottom of the stripper. The temperature of the amine mixture should not exceed 122°C to ensure that no thermal degradation of the amine occurs [19]. In previous studies, heat has been added through condensation of steam extracted from the turbine; however, from the TQ diagram shown in Fig. 2, it can be seen that in this result, the energy extracted from the economizer becomes too low relative to the rest of the HRSG, resulting in a high flue gas exit temperature.

A solution could be to use pressurized hot water extracted from the LP-economizer exit to supply the reboiler with heat. The amount of excess energy available in the economizer will not cover the entire heat required in the reboiler and steam is still needed. With this solution, a part of the regeneration heat can be extracted from the flue gas without interfering with any other section of the HRSG.

With the modifications made, the reboiler consists of two sections: one heated by hot water and one heated by condensing steam from the turbine. The water section only provides 4% of the total reboiler energy consumption. However, since this heat was wasted in the exhaust gas condenser in the reference case, the positive effect is obvious. The improvement of the economizer reduces the flue gas exit temperature from 108°C to 95.3°C. This and the fact that more steam expands through the LP-turbine, results in an efficiency increase from 50.37% to 50.51% (51.99–52.12% without CO_2 compression for comparison). Figure 4 shows the new temperature-to-heat flux diagram.

In order to increase the hot water section in the reboiler further, a valve is introduced at the outlet of the LP segment in the HRSG. By raising the LP-pressure, the drum temperature will increase and the amount of energy extracted in the LP-economizer can, thereby, be extended. An optimization of the LP pressure with respect to the efficiency shows that the pressure should be increased as far as possible, which is to the level of the IP pressure. In view of the fact that the LP-steam was already dedicated to the reboiler, this maneuver only changes part of the heat carrier from LP-steam to pressurized water. This is providing some relief of the thermal miss-mach in the HRSG.

Figure 5 shows the temperature-to-heat flux diagram when the LP section has been removed and the second economizer preheats the feed water from 113°C to 229°C. By supplying the reboiler with all the available excess energy, the temperature difference in the second economizer can be minimized. With this configuration, the hot water section contributes to 13.5% of the total heat supply in the reboiler and the steam extraction is reduced with 8.2 kg or 12.3%. The plant efficiency has now reached 50.74% (52.36% without CO_2 compression) and the flue gas cooling water is reduced by 11.5%.

11 Summary of Results

Table 3 shows the impact from every modification alone (i.e., only one modification at the time for clarity). The last row requires the rest for practical reasons. In the "ecoreboiler" case, the

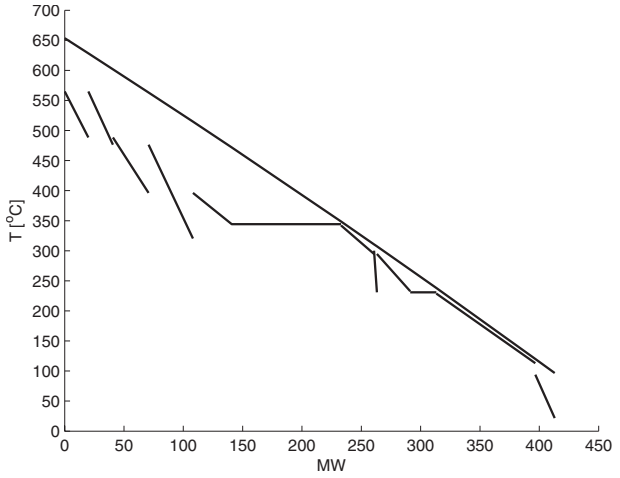

Fig. 5 Temperature to heat flux diagram of the CCPP plant with CO_2 capture, one pressure level has been omitted to enlarge the economizer and thereby, the energy available for amine regenerating

Table 3 Results

	Power increase (MW)	Efficiency increase (%)	Cooling water flow reduction (%)	HRSG exit temperature reduction (°C)
Deaerator	1.2	0.3	4.1	8.1
Fuel preheat	0.0	0	2.1	4.2
No LP superheater	0.3	0	0	0
Ecoreboiler	2.2	0.5	8.8	17.4
Two pressure	4.5	1.1	11.5	23.4

deaeration is performed in the LP-drum and, therefore, the pressure cannot be increased even though this would be beneficial for the efficiency.

12 Analysis

This work has shown that the effects of EGR to the turbomachinery are not posing any major issues. The main difference is that the exhaust gas temperature will increase and this is indeed a limiting factor. When the exhaust gas reaches the maximum allowed temperature, the firing level needs to be reduced and this is not beneficial for the cycle power density. The 40% EGR rate used here increases the CO_2 concentration in the exhaust from 4 vol % to 8 vol % and reduces the flow to be treated in the capture plan by 40%.

The MEA capture plant will introduce a large return flow of 130°C condensate from the reboiler. This amount of low-grade heat will make the exhaust gas utilization less efficient. This manifests itself through less flow in the first part of the LP-economizer. To mitigate this effect, the water from the carbon capture plant can be used for fuel preheating and deaeration. Utilizing hot water for deaeration is advantageous; however, if a plant is to be retrofitted, this will probably require a new feedwater tank. Although finding space for this rearrangement might be tough.

The highest potential is gained by removing the LP-drum and using saturated IP water for supplying part of the heat to the amine regenerator in the carbon capture plant. If a plant is to be retrofitted, this will require major changes to the economizer/LP part of the HRSG and will require a new deaeration arrangement, however for the calculated example the output is increased by 4.5 MW and the cooling water in the exhaust gas condenser is reduced by 11.5%.

The results show that a CCPP with two pressure levels will out-perform a three-pressure plant if economizer water is utilized in the regenerator. The reason for multiple pressure levels is to obtain good heat recovery and a low stack temperature. By extracting the excess energy from the economizer to power the CO_2 capture plant, the heat recovery becomes efficient without the additional pressure levels. This logic indicates that it is probably possible to achieve as good output with a single pressure plant.

With fewer pressure levels in the HRSG, the plant becomes less complex, less costly to construct and quicker to start.

13 Conclusions

The following points were concluded.

- EGR will not pose major issues to the turbomachinery in terms of Mach number levels.
- EGR will cause the exhaust gas temperature to raise and increase the mass flow slightly.
- The potential of utilizing economizer water to cover part of the heat needed in the reboiler is significant.
- The heat recovery is improved, e.g., more energy is recovered from the flue gas.
- Less steam has to be extracted from the steam turbine, e.g., more power is produced at higher efficiency.
- By utilizing hot water to cover part of the reboiler duty, a more efficient heat recovery could be achieved without the necessity of multiple pressure levels.

Acknowledgment

The authors wish to acknowledge Dr. Björn Fredriksson Möller for developing the CO_2 capture model and Drs. Raik C. Orbay and Andre Hildebrandt for early work with the off-design models. The authors would also like to acknowledge Professor Mohsen Assadi of UoS for discussion and feedback during this work.

Nomenclature

A = area (m^2)
Δ = difference
$R = c_p - c_v$ = gas constant (kJ/(kg K))
$\gamma = c_p / c_v$ = isentropic exponent
$\mathrm{Ma} = u / \sqrt{\gamma \cdot R \cdot T}$ = Mach number
$\dot{m}$ = mass flow (kg/s)
η_p = polytropic efficiency
P = pressure (Pa)
$\pi = p_1 / p_2$ = pressure ratio
u = velocity/speed (m/s)

Subscripts

ref = design point value
rel = value normalized to the design point

Superscripts

* = dimensionless parameter group

Abbreviations and Acronyms

CCS = carbon capture and storage
DLN = dry low NO_x
EGR = exhaust gas recirculation
FN = flow number
GT = gas turbine
HP = high-pressure
HRSG = heat recovery steam generator
IP = intermediate-pressure
LP = low-pressure
Ma = Mach number
MEA = monoethanolamine
RH = reheat

References

[1] Fredriksson Möller, B., 2005, "A Thermoeconomic Evaluation of CO_2 Capture With Focus on Gas Turbine-Based Power Plants," Ph.D. thesis, Lund University, Sweden.
[2] Finkenrath, M., Ursin, T. P., Hoffmann, S., Bartlett, M., Evulet, A., Bowman, M. J., Lynghjem, A., and Jakobsen, J., eds., 2007, Performance and Cost Analysis of Novel Gas Turbine Cycle With CO_2 Capture, ASME Paper No. GT2007-27764.
[3] Botero, C., Finkenrath, M., Bartlett, M., Chu, R., Choi, G., and Chinn, D., 2009, "Redesign, Optimization, and Economic Evaluation of a Natural Gas Combined Cycle With the Best Integrated Technology CO_2 Capture," Energy Procedia, **1**(1), pp. 3835–3842.
[4] Bolland, O., and Mathieu, P., 1998, "Comparison of Two CO_2 Removal Options in Combined Cycle Power Plants," Energy Convers. Manage., **39**(16–18), pp. 1653–1663.
[5] Chiesa, P., and Consonni, S., 2000, "Natural Gas Fired Combined Cycles With Low CO_2 Emissions," ASME J. Eng. Gas Turbines Power, **429**(3), pp. 8.
[6] Jack, A. R., Audus, H., and Riemer, P. W. F., 1992, "The IEA Greenhouse Gas R&D Programme," Energy Convers. Manage., **33**(5–8), pp. 813–818.
[7] Kvamsdal, H. M., Jordal, K., and Bolland, O., 2007, "A Quantitative Comparison of Gas Turbine Cycles With CO_2 Capture," Energy, **32**(1), pp. 10–24.
[8] Zachary, J. and Titus, S., eds., 2008, "CO_2 Capture and Sequestration Options—Impact on Turbomachinery Design," Bechtel Technology Journal, **1**(1), pp. 1–20.
[9] Mimura, T., Shimojo, S., Suda, T., Iijima, M., and Mitsuoka, S., 1995, "Research and Development on Energy Saving Technology for Flue Gas Carbon Dioxide Recovery and Steam System in Power Plant," Energy Convers. Manage., **36**(6–9), pp. 397–400.
[10] Sipöcz, N., and Assadi, M., 2009, "Combined Cycles With CO_2 Capture: Two Alternatives for System Integration," ASME Paper No. GT 2009-59595.
[11] Desideri, U., and Paolucci, A., 1999, "Performance Modelling of a Carbon Dioxide Removal System for Power Plants," Energy Convers. Manage., **40**(18), pp. 1899–1915.
[12] Singh, D., Croiset, E., Douglas, P. L., and Douglas, M. A., 2003, "Techno-Economic Study of CO_2 Capture From an Existing Coal-Fired Power Plant: Mea Scrubbing vs. O_2/CO_2 Recycle Combustion," Energy Convers. Manage., **44**(19), pp. 3073–3091.
[13] Romeo, L. M., Espatolero, S., and Bolea, I., 2008, "Designing a Supercritical Steam Cycle to Integrate the Energy Requirements of CO_2 Amine Scrubbing," Int. J. Greenhouse Gas Control, **2**(4), pp. 563–570.
[14] Romeo, L. M., Bolea, I., and Escosa, J. M., 2008, "Integration of Power Plant and Amine Scrubbing to Reduce CO_2 Capture Costs," Appl. Therm. Eng., **28**(8–9), pp. 1039–1046.
[15] Oexmann, J., Hensel, C., and Kather, A., 2008, "Post-Combustion CO_2-Capture From Coal-Fired Power Plants: Preliminary Evaluation of an Integrated Chemical Absorption Process With Piperazine-Promoted Potassium Carbonate," Int. J. Greenhouse Gas Control, **2**(4), pp. 539–552.

[16] Tobiesen, A., Svendsen, H. F., and Hoff, K. A., 2005, "Desorber Energy Consumption Amine-Based Absorption Plants," International Journal of Green Energy, **2**, pp. 201–215.
[17] Abu-Zahra, M. R. M., Schneiders, L. H. J., Niederer, J. P. M., Feron, P. H. M., and Versteeg, G. F., 2007, "CO_2 Capture From Power Plants: Part I. A Parametric Study of the Technical Performance Based on Monoethanolamine," Int. J. Greenhouse Gas Control, **1**(1), pp. 37–46.
[18] Aroonwilas, A., and Veawab, A., 2007, "Integration of CO_2 Capture Unit Using Single- and Blended-Amines Into Supercritical Coal-Fired Power Plants: Implications for Emission and Energy Management," Int. J. Greenhouse Gas Control, **1**(2), pp. 143–150.
[19] Alie, C. F., 2004, "CO_2 Capture With MEA: Integrating the Absorption Process and Steam Cycle of an Existing Coal-Fired Power Plant," MSc. thesis, University of Waterloo, Waterloo, Ontario, Canada.
[20] Gülen, S. C., Griffin, P. R., and Paolucci, S., 2002, "Real-Time On-Line Performance Diagnostics of Heavy-Duty Industrial Gas Turbines," ASME J. Eng. Gas Turbines Power, **124**(4), pp. 910–921.
[21] Elkady, A. M., Evulet, A. T., Brand, A., Ursin, T. P., and Lynghjem, A., 2008, "Exhaust Gas Recirculation in DLN F-Class Gas Turbines for Post-Combustion CO_2 Capture," Proceedings of GT 2008, pp. 9–12.
[22] IPSEpro v.4.0, 2003, Simtech Simulation Technology (Simtech), Graz, Austria.
[23] Jonshagen, K., Eriksson, P., and Genrup, M., 2009, "Low-Calorific Fuel Mix in a Large Size Combined Cycle Plant," ASME Paper No. GT 2009-59329.
[24] Jonshagen, K., and Genrup, M., 2010, "Improved Load Control for a Steam Cycle Combined Heat and Power Plant," Energy, **35**(4), pp. 1694–1700.
[25] Walsh, P. P., and Fletcher, P., 2004, *Gas Turbine Performance*, 2nd ed., Bleckell, Oxford, UK.
[26] Eldrid, R., Kaufman, L., and Marks, P., 2001, "The 7fb: The Next Evolution of the F Gas Turbine," Technical Report No. 4194, Schnenectady, NY.
[27] Kohl, A. L., and Nielsen, R. B., 1997, *Gas Purification*, 5th ed., Gulf, Houston, TX.
[28] Botero, C., Finkenrath, M., Belloni, C., and Bertolo, S., D'ercole, M., Gori, E., and Tacconelli, R., 2009, "Thermoeconomic Evaluation of CO_2 Compression Strategies for Post-Combustion CO_2 Capture Applications," *Proceedings of ASME Turbo Expo 2009*.
[29] Moore, J. J., Nored, M. G., Gernentz, R. S., and Brun, K., 2007, "Novel Concepts for the Compression of Large Volumes of Carbon Dioxide," Technical Report, Southwest Research Institute.
[30] Romeo, L. M., Bolea, I., Lara, Y., and Escosa, J. M., 2009, "Optimization of Intercooling Compression in CO_2 Capture Systems," Appl. Therm. Eng., **29**(8–9), pp. 1744–1751.

III

Novel High-Performing Single-Pressure Combined Cycle With CO_2 Capture

Nikolett Sipöcz
Department of Mechanical and Structural Engineering and Material Science, University of Stavanger, N-4036 Stavanger, Norway

Klas Jonshagen
Division of Thermal Power Engineering, Department of Energy Sciences, Lund University, P.O. Box 118, S-221 00 Lund, Sweden

Mohsen Assadi
Department of Mechanical and Structural Engineering and Material Science, University of Stavanger, N-4036 Stavanger, Norway

Magnus Genrup
Division of Thermal Power Engineering, Department of Energy Sciences, Lund University, P.O. Box 118, S-221 00 Lund, Sweden

The European electric power industry has undergone considerable changes over the past two decades as a result of more stringent laws concerning environmental protection along with the deregulation and liberalization of the electric power market. However, the pressure to deliver solutions in regard to the issue of climate change has increased dramatically in the last few years and has given rise to the possibility that future natural gas-fired combined cycle (NGCC) plants will also be subject to CO_2 capture requirements. At the same time, the interest in combined cycles with their high efficiency, low capital costs, and complexity has grown as a consequence of addressing new challenges posed by the need to operate according to market demand in order to be economically viable. Considering that these challenges will also be imposed on new natural gas-fired power plants in the foreseeable future, this study presents a new process concept for natural gas combined cycle power plants with CO_2 capture. The simulation tool IPSEpro is used to model a 400 MW single-pressure NGCC with post-combustion CO_2 capture using an amine-based absorption process with monoethanolamine. To improve the costs of capture, the gas turbine GE 109FB is utilizing exhaust gas recirculation, thereby, increasing the CO_2 content in the gas turbine working fluid to almost double that of conventional operating gas turbines. In addition, the concept advantageously uses approximately 20% less steam for solvent regeneration by utilizing preheated water extracted from heat recovery steam generator. The further recovery of heat from exhaust gases for water preheating by use of an increased economizer flow results in an outlet stack temperature comparable to those achieved in combined cycle plants with multiple-pressure levels. As a result, overall power plant efficiency as high as that achieved for a triple-pressure reheated NGCC with corresponding CO_2 removal facility is attained. The concept, thus, provides a more cost-efficient option to triple-pressure combined cycles since the number of heat exchangers, boilers, etc., is reduced considerably.
[DOI: 10.1115/1.4002155]

1 Introduction

The current crisis in the world's financial markets has caused prices in the energy supply market to fall dramatically. Nevertheless, future projections indicate that this decline is only temporary and that the sharp increase in fossil fuel and raw material prices from 2003 until its all-time high in 2008 will return, bringing the costs for new power plants and electricity generation up again over the long term [1]. Adding the huge investment needed for the replacement and upgrade of the world's aging power plants, many of which are already running well beyond their originally designed lifespan in conjunction with the possible implementation of the Kyoto measures to reduce the world's carbon footprint, will give rise to a greater challenge than ever before for the power industry.

Natural gas-fuelled power plants will remain a vital component in the mix of future power generation in both Europe and the U.S. due to their high efficiency, short construction lead times, low emissions, and quick starting and stopping capability. The latter is particularly important in relation to an increase in bio-based, wind-based, and solar-based production in which replacement capacity is required. One original equipment manufacturer (OEM) has introduced a commercially available concept based on a single-pressure once-through boiler with a rapid starting capacity. This configuration is typically a couple of points lower in efficiency, although from the perspective of running at minimum load, e.g., overnight, should be able to provide a reasonable compromise. The new generation of H-class gas turbines (GT) has recently reached the stage of commercial implementation, driving the overall thermal efficiencies of combined cycles well beyond 60%. However, the approval of appropriate legislation to limit CO_2 emissions from stationary power plants by including carbon capture and storage (CCS) in the post-Kyoto agreement will lower the efficiencies for natural gas-fired combined cycle (NGCC) to levels achieved by the best GT and steam turbine (ST) technology available at the beginning of the 1990s. Therefore, if natural gas is to remain a viable and competitive fuel source, innovative solutions are required, which efficiently utilize natural gas for power generation while minimizing CO_2 emissions.

The efficiency improvement of combined cycles over the last few decades has been driven by utilizing higher turbine inlet temperatures (TIT), which has also allowed for the extensive application of multiple-pressure reheat combined cycles. Accordingly, studies considering the near-term implementation of CO_2 capture in terms of post-combustion capture into natural gas-fired power plants have exclusively been conducted on dual-pressure and triple-pressure combined cycles with reheat [2–11]. Many theses, along with numerous studies completed on coal-fired power plants [12–16] that use chemical absorption, have all pointed out the high efficiency penalties associated with this technology due to solvent regeneration. Thus, an analysis, which considers alternatives that could reduce reboiler duty, is one of the most important research topics within this field [17–19]. Studies evaluating various integration methods of the capture process into conventional

Contributed by the International Gas Turbine Institute (IGTI) of ASME for publication in the JOURNAL OF ENGINEERING FOR GAS TURBINES AND POWER. Manuscript received April 13, 2010; final manuscript received May 3, 2010; published online November 22, 2010. Editor: Dilip R. Ballal.

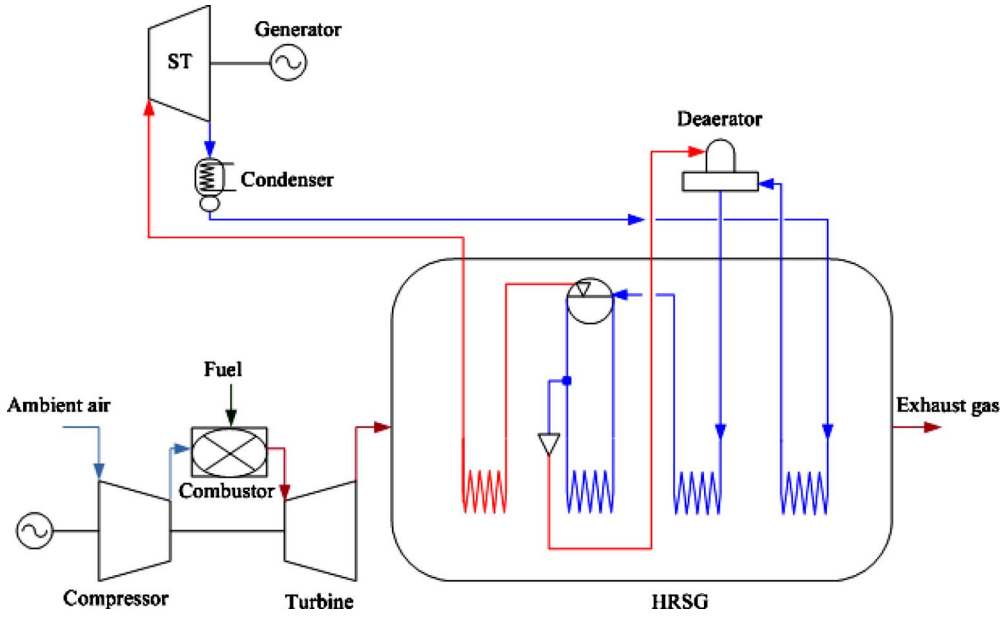

Fig. 1 Schematic figure of the reference CC

power plants have also been conducted in the recent past, revealing that the optimal option in order to fulfill reboiler requirements is to utilize saturated steam with a pressure corresponding to a steam saturation temperature of approximately 132°C, depending on the boiler's pinch point [20].

Since both efficiency and cost of the CO_2 separation process strongly depend on the concentration of CO_2 and the volumetric flow of the gas to be treated, increasing the CO_2 concentration by means of exhaust gas recirculation (EGR) allows for CO_2 separation at an elevated partial pressure, thereby, reducing the efficiency penalty and equipment costs. A large sized combined cycle plant has a flue gas flow of approximately 1.5 kg/MW_s (without recirculation) compared with 0.95 kg/MW_s for a hard coal plant. EGR has emerged as a technology, which enables an increase in the CO_2 concentration of the flue gas stream of gas-fuelled power plants and recent experimental studies performed with an existing dry low NO_x GE gas turbine burner have demonstrated that EGR levels of up to 40% and beyond could be feasible with only minor modifications of existing combustion technology [21,22]. However, the main limitation is the low oxygen concentration, which has a negative impact on the oxidation of CO to CO_2.

The objective of the present paper is to evaluate the design of a novel single-pressure NGCC with EGR and CO_2 separation using an amine-based absorption process with monoethanolamine (MEA). The essence of the idea is to utilize saturated water with high pressure to the greatest possible extent in order to provide heat for the regeneration of the solvent. This results in a better deployment of the available heat in the flue gases, which consequently reduces the large amount of power lost in the ST due to the steam extraction of the reboiler.

One can argue as to whether a direct MEA loop in the heat recovery steam generator (HRSG) should provide an optimum solution. Unfortunately, MEA has a narrow temperature span between the minimum regeneration temperature and severe thermal decomposition. Because of this, an intermediate circuit is necessary for accurate control under all operating modes.

This plant configuration also provides for a rapid start-up capability for flexible midmerit production in which an operator has the option to separate the carbon emissions.

2 Cycle Concept

The main reason for multiple-pressure levels in a combined cycle (CC) power plant is to achieve maximum efficiency. A single-pressure CC power plant typically has stack temperatures in the range of 100–110°C while a triple-pressure plant can obtain stack temperatures as low as 70–80°C. The corresponding gain in efficiency is about three percentage points. However, when amine-based CO_2 capture is to be integrated, heat recovery becomes disturbed by the fact that amine regeneration requires a great portion of the generated heat. In Ref. [23], it was concluded that by using the excess energy from the economizer, good heat recovery can be obtained without using multiple-pressure levels; therefore, this work will use this feature to create an optimal plant using only one pressure level.

The topping cycle consists of general electric's gas turbine GE109FB, which is a 50 Hz and 300 MW class single-shaft gas turbine. As previously mentioned, the bottoming cycle is a single-pressure steam cycle and a layout of the reference cycle is shown in Fig. 1. The main problem with a single-pressure steam cycle is that the energy needed in the economizer is not enough to recover the available heat from the flue gas, thus, resulting in large stack losses. By choosing a low steam pressure, the economizer section becomes small and the heat recovery is satisfactory, but with a low steam pressure, the evaporating energy is large, which therefore limits the mass flow through the cycle. By increasing the pressure, the mass flow will increase, so, at a certain point, this becomes a more important factor than the fact that the economizer is increased. What is more important than the stack losses though is the fact that a higher pressure will always yield more power output from the steam cycle. The limiting factors of how high the pressure can be are moist content in the ST exhaust, volume flow at the ST inlet (blade length), and, of course, the total cost of the plant.

High levels of exhaust moisture will result in an asymptotic erosion process in the last rotor, meaning that levels above 16% should be avoided for an acceptable lifting of the last rotor. There is no certain absolute maximum moisture level since one can have several design features such as a Stellite™-coated leading edge, suction slits, etc. The moisture content could be reduced by intro-

Table 1 Assumptions for the reference single-pressure CC

Parameter	Value	Unit
Ambient air temperature	15	°C
Evaporator pinch point	5	°C
HRSG pressure drop hot side	0.06	bars
Steam superheating temperature	565	°C
TIT	1370	°C
GT total pressure ratio	18.6	–
Exhaust gas mass flow	663	kg/s

Table 2 Settings for the CO_2 separation plant

Parameter	Value	Unit
Pressure drop absorber	0.15	bar
Reboiler pinch point	10	°C
Amine regeneration temperature	120	°C
Heat of reaction MEA	85	kJ/mol_{CO_2}
Lean/rich amine HTX pinch point	10	°C
Absorber amine inlet temperature	40	°C

ducing reheat, which would further improve cycle performance as the live steam pressure could be increased. A high level of moisture also lowers the attainable turbine efficiency levels since the droplets need to be accelerated and are prone to subcooling. The droplets will only contain approximately half of the main stream velocity and due to the relative motion of a blade, they will hit the pressure side. Droplet subcooling is a pure thermodynamic effect in which the amount of subcooling is governed by the time derivative of the pressure drop.

Initially, the selection of 142 bars/565°C admission has been made as higher levels either result in moisture issues or more costly turbine and HRSG due to the necessity of reheat and high pressure resistant steel, etc.

The water condenser operates at a water cooling temperature of 15°C with a corresponding condenser pressure of 0.026 bars. Since it is preferable to carry out deaeration above atmospheric pressure, the deaerator has been integrated by splitting the economizer into two sections and performing deaeration after the first preheater in order to suit the selected pressure of 1.2 bars. The approach temperature is set to 11°C and steam is supplied by flashing a part of the saturated water from the bottom of the drum. These operational conditions together with the assumptions presented in Table 1 lead to a net power output of 438 MW and a net efficiency of 57.8% and all calculations are based on the lower heating value of natural gas (48.16 MJ/kg).

2.1 Integration of CO_2 Capture. The CO_2 separation is assumed to be incorporated into a greenfield power plant, meaning that the power cycle including the CO_2 capture process along with all the components have been designed and optimized to operate under prevailing plant specific conditions. The integration of the post-treatment of the flue gases into a power plant by means of chemical absorption together with the additional required compression of the CO_2 product gas results in a reduction in the net power output due to the extraction of steam from the low pressure part of the ST and the additional requirement of power to auxiliaries, such as solvent pumps and flue gas blowers, in order to compensate for pressure losses in the subsequent capture system. In the current study, it is assumed that the location of the power plant is such that it enables the use of seawater at a temperature of 15°C to satisfy the needs for cooling in both the capture process and the compression stage. Nevertheless, a further demand for power to attain the cooling necessities would be inevitable without the power plant site considered here.

The combined cycle studied in this work features a state of the art post-combustion chemical absorption removal process. The model used for CO_2 separation is based on the calculation model proposed by Kohl and Nielsen [24] and developed by Möller [2]. The model has been used in several studies of gas turbine-based power plants with CO_2 capture and is not further described here [2,25]. The calculation of the heat requirement and power needed for the capture process is dependent on both the capture rate and the level of regeneration at a given temperature. Hence, an initial condition of the simulations has been to capture 90% of the CO_2 produced by means of an aqueous solution of MEA with 30% MEA by weight at a regeneration temperature of 120°C. The selection of the reboiler temperature has been made to meet the limiting temperature level of 122°C above which the thermal degradation of MEA and corrosion becomes intolerable [20]. Information about the flue gas, such as composition, flow rate, and the pressure needed for the prediction of the reboiler requirements, are given input data to the capture model. A summary of the assumptions for the CO_2 separation plant can be found in Table 2.

2.2 EGR. As post-combustion capture has grown as being the most feasible near-term alternative in reducing CO_2 emissions; a simultaneous development within the GT industry has been to explore the possibility of reducing costs for gas-fuelled power plants utilizing this type of CO_2 abatement technology by the recirculation of exhaust gases. The advantages of EGR have been shown by several theoretical studies [3–5,11] and it is a well-known method that has been previously used for anti-icing purposes [26] in compressors as well as an option for the reduction in NO_x emissions in internal combustion engines [27,28]. The verification of these previous studies along with issues considering the actual levels of recirculation that could be met with current technology have been the most recent works conducted within this field [21,22]. Due to the consideration that EGR will be a necessary add-on for NGCCs with post-combustion capture, the reference cycle studied in this work has been modeled with a fraction of the exhausts recycled back to the GT inlet and the maximum level of recirculation is limited by combustion-related effects such as flame stability, incomplete oxidation of CO, etc. An upper maximum recirculation level of 35–40% has been shown to be manageable both from a real operational point of view [21] and based on the recommendations by Bolland and Mathieu [5], meaning that EGR levels of less than 40% are acceptable in reaching a minimum oxygen concentration (MOC) of 16–18% in the combustion air. Accordingly, a rate of 40% has been considered (after condensation of the water content) in this study with a corresponding MOC value of 16 vol%, which results in an initial CO_2 content increase in the flue gas from 4.0 vol % to 7.2 vol %.

In order to maintain a high GT power output, the recirculated flue gas is cooled down to 20°C in a flue gas condenser (FGC), which gives an inlet temperature of approximately 17°C in the compressor after being mixed with ambient air (15°C).

The cooling of the exhaust gas for the purpose of recirculation in the direct contact condenser will cause pressure losses that would call for an additional blower in order to bring the pressure up to ambient air conditions.

The modified combined cycle with EGR has a higher total power output than the reference cycle as a result of an increased working mass flow. The cycle efficiency is slightly higher due to an increase in the power production of the steam cycle, which is superior to the increased fuel consumption and reduction in the power output from the gas turbine. However, these advantages are at the expense of the large amounts of cooling water needed (50 MW_{th}) to bring down the exhaust temperature from 95°C to 20°C.

The changes from having a different working media on the gas turbine turbomachinery components are minute. The combustor issues are the limiting factor since, e.g., changes in critical turbo-

Table 3 Settings for the CO_2 compression train

Parameter	Value	Unit
Compressor efficiency	85.0	%
Pump efficiency	50.0	%
Intercooling temperature	20.0	°C

machinery Mach number levels are on the order of 1%. The details are discussed in Ref. [23] in which a large single-shaft unit is used as a vehicle for the analysis.

2.3 CO_2 Compression. In addition to capture, carbon capture and storage (CCS) involves two other major components: transport and storage. As none of these will be realized without the constraints being solved for each and every one of them, one of the primary concerns for transportation and storage derived from the economical and technical limitations related to the capture process is the requirement of a more purified CO_2 stream than what is achievable to meet the specifications posed by operation and safety. Therefore, in terms of dehydration, compression, and purification, post-treatment will most likely be an essential topic debited the power generation process. Since there is no general agreement on the purification level of the CO_2 to be stored, any evaluation of purification options and their possible consequences, such as energy and/or water demand, would probably be based on theoretical assumptions and are therefore not taken into account in this study. Concerning CO_2 compression, several studies have evaluated the feasibility of different compression options [29–31]; hence, this part of the study is only included in order to show a comprehensive estimation of the total efficiency penalty for the power plant with CO_2 capture for which compression will be an essential part. For a more extensive outline, the reader is referred to Refs. [28–30].

There are several viable options for the compression of CO_2 and the main categories are: compression only, compression and condensing with ambient temperate water and final pumping, and compression and condensing with a refrigerant and final pumping. To find the most suitable method, the refrigeration process library package in IPSEpro has been used. The calculations have been simplified by assuming the treated flow to be pure CO_2 along with the further assumptions, as shown in Table 3. As previously mentioned, in reality, the CO_2 stream will contain a fraction of argon, nitrogen, oxygen, etc., which will affect the thermodynamic properties of the fluid and, consequently, the intercooling levels and compression work. For an assessment of the option of using refrigerants to perform the condensation, both CO_2 and ammonia were examined, and, as expected, ammonia was found to be the most efficient and preferable for this application. However, the option with water intercooling and condensation was found to be superior to both the compression only alternative and to the one using condensation with ammonia as a refrigerant ($310.2\ \mathrm{kJ/kg_{CO_2}}$).

The CO_2 compression was performed in a six-stage intercooled compressor, after which the CO_2 was condensed at a pressure of 60 bars by utilizing water with a temperature of 15°C and then, finally, pumped up to the final pressure of 200 bars.

The cooling temperature has been pointed out earlier as being an important parameter that has a considerable effect on both efficiency and power output in the context of EGR. Apparently, its influence on the compression work is inevitable and an increase in the intercooling water temperature of 5°C would force the pressure for condensation up 65 bars, which, in turn, would favor the compression only alternative. Nevertheless, the option with water intercooling and final pumping is less energy intensive ($327.5\ \mathrm{kJ/kg_{CO_2}}$ compared with $321.1\ \mathrm{kJ/kg_{CO_2}}$).

2.4 Interaction Between HRSG and Reboiler. The large amount of thermal energy needed for amine scrubbing is one of the main drawbacks of solvent-based CO_2 capture. The conventional method for the integration of the capture plant into a power cycle is by extracting steam prior the low pressure (LP) section of the ST. For a natural gas power plant with a 285 MW gas turbine as is the 9FB considered here, the thermal energy required for the CO_2 separation with the specified conditions, as presented in Table 2, is approximately $3.9\ \mathrm{GJ/tons_{CO_2}}$. The extraction point is chosen to satisfy the regeneration temperature and pressure of the solvent; in this case, the extracted steam has to have a pressure of approximately 2.8 bars. To extract the steam with the specified conditions, the ST expansion is divided into two sections and the required amount is dedicated to the CO_2 separation process. The condensate leaving the CO_2 separation plant has a temperature of 130°C and is returned back to the HRSG. This result in a reduced heat transfer in the first economizer compared with the case without CO_2 capture, thereby, leaving the exhaust gas at a temperature of 145°C. This difference is illustrated in Fig. 2, which demonstrates the poor performance of the last part of the HRSG when CO_2 capture is applied. The great temperature differences between the hot and cold side of the economizer as well as the high HRSG flue gas exit temperature indicate that a significant amount of excess energy could be recovered. Figure 2 also shows that the increased exhaust gas temperature has allowed for a larger steam mass flow, appearing as a reduced slope for the heat transfer in the superheater and a prolonged line for the evaporator.

In order to reduce the low heat utilization in the last part of the HRSG, as shown in Fig. 2, a part of the saturated water leaving the CO_2 capture plant can be used for deaeration. This is done by flashing a part of the condensate, leaving the CO_2 separation unit, thus reducing throttle losses as the reduction in pressure down to 1.2 bars are considerably lower compared with the reference case for which the corresponding is accomplished by using saturated water from the bottom of the drum. The condensate not employed for deaeration is used for the preheating of the fuel before being returned back to the HRSG. These improvements result in a gain of 0.3 percentage points in cycle efficiency.

2.5 Alternative Reboiler Utilizing Hot Water. The main purpose of the reboiler at the bottom of the desorber/solvent regenerator is to provide vapor, so when it comes into contact with the rich amine stream strips, the CO_2 gas from the liquid flows down the column. The reboiler is usually a shell and tube heat exchanger of the kettle type and the heat for vaporization is provided by using LP steam condensed in the reboiler. However, the fluid transferring the heat does not necessarily have to be steam as long as the fluid provides the energy required to vaporize the liquid, diluting the CO_2 gas and reversing the chemical reactions by releasing the bound CO_2. The reversed chemical reactions in the desorber benefit from the increased temperature but a maximum temperature due to the thermal degradation of MEA, as described earlier, limits the regeneration temperature to a maximum of 122°C.

As shown in Fig. 2, there is a huge potential for extracting more energy from the economizer part of the HRSG. By taking advantage of this heat, a considerable part of the reboiler duty could be covered without interfering with the rest of the steam production; therefore, the efficiency penalty associated with solvent-based CO_2 capture could be reduced. This has been introduced in this work by adding a closed high pressure saturated water loop prior to the drum, so as to provide the greatest amount of energy for regeneration using this water. Since the amount of water is limited by the recoverable heat available in the exhausts and only a part of the LP steam could be compensated for, the reboiler has to be split into two separate sections. The pressure of the water is 142.3 bars and has been selected in accordance with the pressure in the steam cycle. Figure 3 illustrates the temperature to heat flux (TQ) diagram for the regular steam reboiler compared with the new configuration. By utilizing the excess energy in the economizer for the reboiler, more energy can be recovered from the exhaust gas.

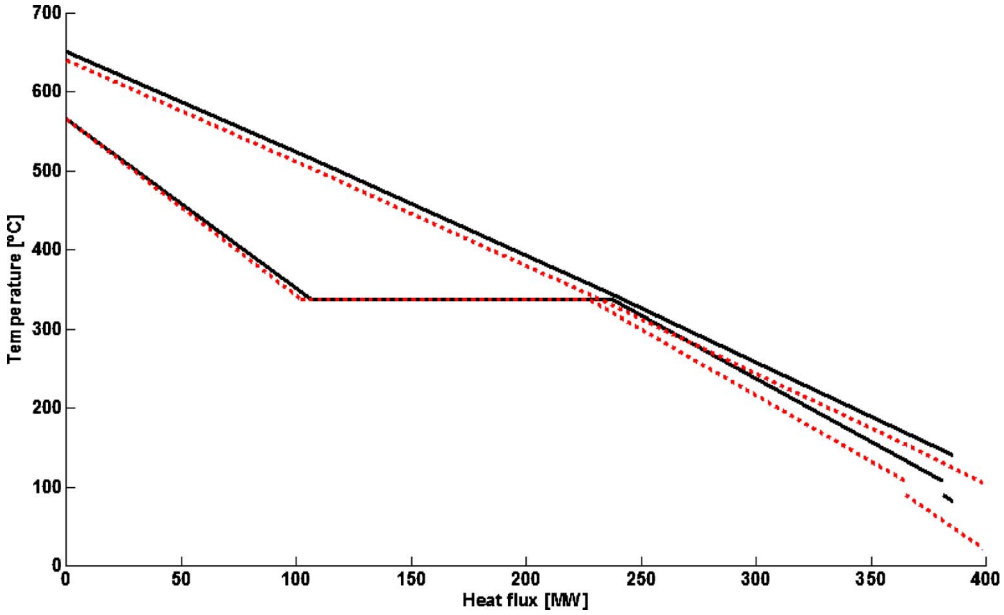

Fig. 2 Temperature to heat flux diagram of the single-pressure cycle with (solid line) and without CO_2 capture (dotted line)

This can be seen in Fig. 3 in which the diagram has been prolonged on the right side. The temperature difference in the second economizer is very small, thus, demonstrating that the process is close to optimal.

The new arrangement of the reboiler results in an 18% reduction in the steam extracted from the ST, i.e., the pressurized water represents 17.7% of the total reboiler duty. Consequently, the increased steam mass flow in the steam cycle compared with the option with the regular steam reboiler increases the power output by 8 MW (376–384 MW).

The reboiler duty covered by the water could be increased by increasing the economizer, which could be accomplished by raising the live steam pressure. As previously described, the cycle pressure has been set to a maximum level limited by the moisture content at the ST outlet. Hence, a further increase is only possible by increasing the admission temperature, which is already considerably high (565°C) or by adding reheat.

Since the last option mentioned is the most reasonable, it has been selected and the reheat temperature has been set to the level at which the moisture content at the end of the ST reaches 16%. In the context of reheat, it should also be mentioned that flow accelerated corrosion (FAC), which achieves its maximum at approximately 150°C and typically manifests itself as an unsuitable area in the h-s chart, is effectively avoided. Nevertheless, reheat renders the possibility for further increasing the pressure, although there is another limitation influencing an elevation, namely the length of the first row of blades in the ST. At a certain pressure

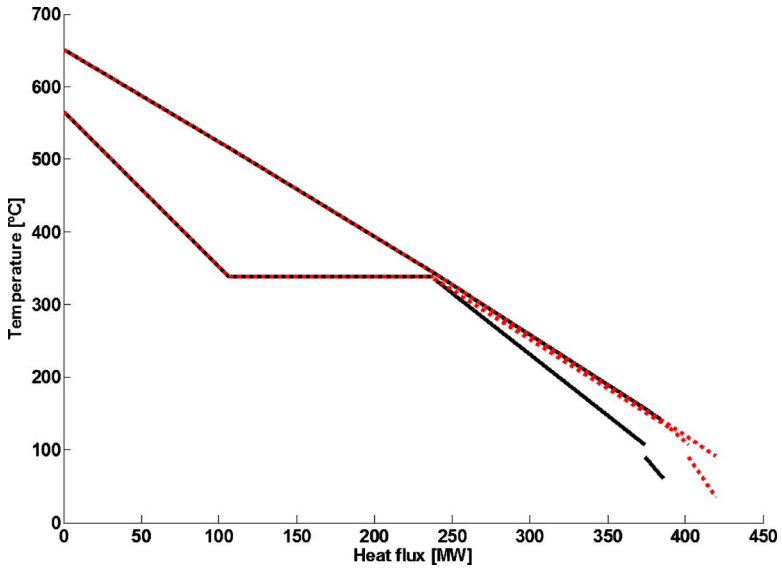

Fig. 3 Temperature to heat flux diagram of the single-pressure cycle with CO_2 capture and regular steam boiler (solid line) and with the water and steam reboiler (dotted line)

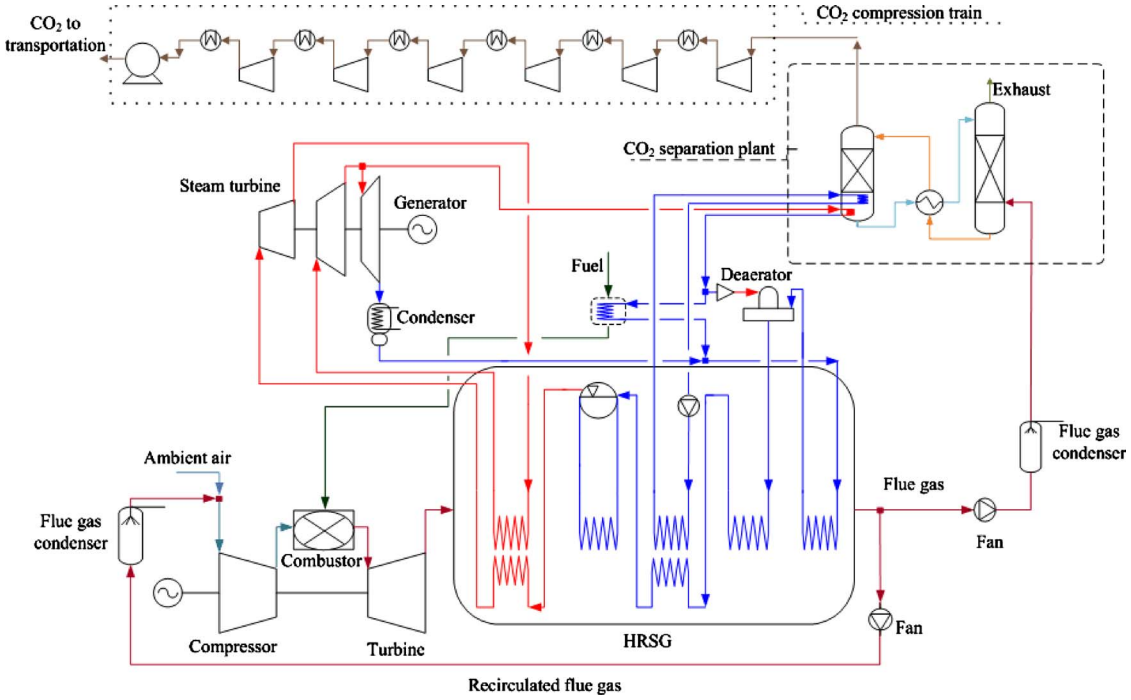

Fig. 4 Schematic figure of the single-pressure CC with CO_2 capture and compression

level, they become too small than what is reasonable from a manufacturing and efficiency point of view. The calculation of the blade length has been made by first estimating the median diameter D_m of the ST inlet based on the blade speed U and the rotational speed N. The first stage flow function is set to 0.4 in order to provide a suitable level of axial velocity. The number is not arbitrarily set and reflects a balance between the blade height and losses due to turning. Denton [32] gave an exhaustive treatment on this topic. The inlet annulus area can be calculated and by knowing the inlet mass flow and specific volume, the length of the blade is derived. The governing equations are as follows:

$$l = \frac{A}{\pi \cdot D_m} \tag{1}$$

$$\frac{U}{C_{\text{axial}}} = 0.4 \tag{2}$$

At 160 bars, the blade length is 20 mm and set as an upper limit and although 160 bars is high, it is not above current practice. The power output is increased marginally but the elevated pressure increases the economizer outlet temperature by 11 °C, thereby ini-

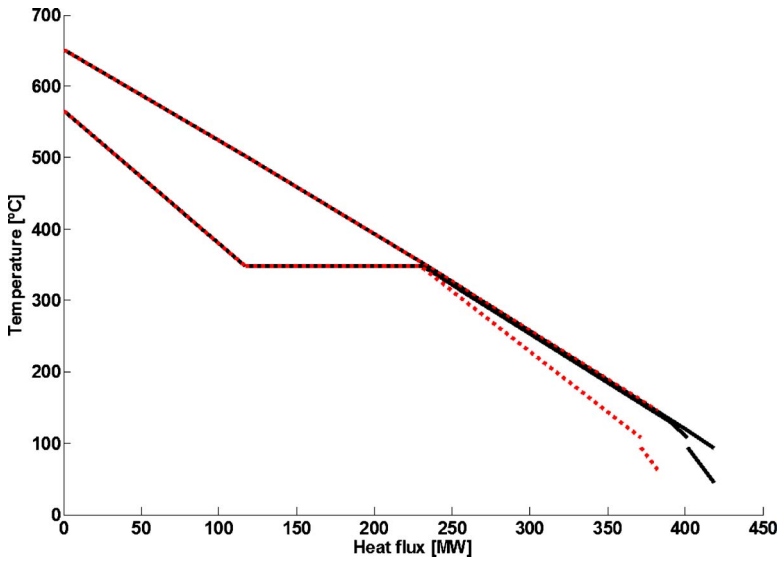

Fig. 5 Temperature to heat flux diagram of the two cases with regular steam supported reboiler (dotted line) and the case with water/steam-driven reboiler (solid line)

Table 4 Performance results

Parameter	Ref. NGCC	NGCC with CCS steam reboiler	NGCC with CCS new reboiler	Unit
Net power output	438	378	390	MW
Net LHV efficiency	57.80	49.60	50.95	%
ST shaft power	157	128	133	MW
GT shaft power	285	284	284	MW
Live steam pressure	142.3	160	160	bars
EGR rate		40	40	%
EGR power		2.58	1.85	MW
Capture plant power		13.92	11.67	MW
Compression power		12.28	12.28	MW
Cooling duty EGR		63.42	49.86	MW_{th}
Cooling duty capture		223.13	204.16	MW_{th}
Cooling duty compression		22.89	22.89	MW_{th}

tially increasing the energy provided by the highly pressurized water to the reboiler from 17.7% to 19%. The schematic outline of the cycle is shown in Figs. 4 and 5 presents the TQ diagram for the final cycle. For comparative reasons, the option with the regular steam reboiler is also included.

3 Results and Discussion

The results of the performance simulations of the redesigned and optimized single-pressure NGCC with reheat, EGR, integrated CO_2 capture, and subsequent CO_2 compression train are presented in Table 4. To give a comprehensive and nonbiased presentation of the results, the performance of the reference cycle and the cycle with integrated CO_2 capture but with conventional steam-driven reboiler are also included.

The results reveal the clear benefit of the new configuration using highly pressurized water to cover part of the reboiler duty. In this case, the extracted steam is reduced by approximately 19% compared with the conventional alternative with the entire duty supplied by LP steam. The, consequently, increased amount of steam expanded through the ST increases the ST power output, thus, reducing the efficiency penalty by 1.35 percentage points compared with the steam only option. A further benefit for this novel cycle concept is the significantly lower thermal energy needed for cooling purposes in addition to power for the blowers, as the new economizer configuration with the added pressurized water stream results in a lower exhaust gas temperature at 93°C compared with 144°C in the case without water. Figure 5 illustrates the temperature to heat flux diagram for the two cases. As can be seen, the heat utilization in the HRSG is considerably better with the new reboiler configuration with an almost optimal heat transfer process in the second economizer indicated by a very small temperature difference. One of the main topics in regard to post-combustion CO_2 capture with chemical solvents is the large increase in cooling water requirements, which is certainly a big barrier and constraint for the implementation of this technology, particularly in countries with limited recourses of water. Therefore, any configuration that can lower the thermal cooling requirements along with the development of solvents that can withstand higher temperatures, as well as having a lower heat reaction than that of MEA ($85\ kJ/mol_{CO_2}$), is crucial for the large deployment of this technology.

The current reboiler design is based on the use of one heating fluid, of which steam is the most common. The simultaneous use of pressurized water and steam would require two separate tube zones within current reboiler configurations. The cost and layout of possible changes in the current design have not been further considered in this work but would not be a major obstacle according to the authors.

In a coherent study made on a triple-pressure combined cycle with the same gas turbine and CO_2 capture and compression facility, the corresponding efficiency was estimated at 50.51% (for further details, please see Ref. [23]). This means that the studied single-pressure CC with CO_2 capture and compression offers major advantages over multiple-pressure cycles not only in terms of efficiency but also from the fact that single-pressure cycles are less costly and have operational benefits, which are underpinned by their minor complexity. The new reboiler configuration also allows for a faster supply of approximately 20% of the reboiler duty since heating up water is significantly faster than that of steam. This means that the capturing process could most probably be taken into operation more quickly than comparable power plants with a conventional steam reboiler.

Nevertheless, the fast start-up of single-pressure cycles is a major advantage since this results in lower total emissions compared with those emitted by multiple-pressure CC as a long start indicates a longer period of time in off-design operation under which the emissions are elevated due to a lower efficiency compared with those under full-load operation.

To fully evaluate the benefits and efficiency over time, i.e., a return of capital for the single-pressure CC with CO_2 capture, an economical analysis taking into consideration measures, such as capital costs, fuel costs, price of electricity, operational costs, emission taxes, etc., has to be made and compared for a corresponding analysis of a multiple-pressure NGGC. This has not been included in this study, although the technical performance parameters indicate a scope for major profitable advantages.

4 Conclusions

A single-pressure NGCC power plant was designed and optimized for the integration of a post-combustion CO_2 capture process using a solution of aqueous MEA. As a possibility to reduce capture costs and improve the forces managing the chemical reactions for the separation of CO_2, a fraction of the exhausts leaving the HRSG has been cooled and recycled back to the GT. EGR has the negative effect of reducing the power output from the gas turbine cycle due to the increased compressor inlet temperature, which is an inevitable consequence of the mixing of ambient air and the cooled exhaust that will, most certainly, always provide a temperature increase because of limitations posed by cooling with ambient temperate water. From a power output and efficiency perspective, EGR has a positive contribution, though these benefits are at the expense of the cooling requirements of 50 MW_{th}.

The integration of CO_2 capture results in a big return flow to the HRSG by means of condensate at a temperature of 130°C. This low-grade heat results in a reduced heat transfer in the last part of the HRSG, thereby leaving the exhaust gas at a temperature of 145°C.

The main focus of this study has been to evaluate the new concept of utilizing pressurized water to meet as much reboiler duty as possible by adding a closed water loop ahead of the evaporator. This new configuration has been shown to be highly efficient as the stream extracted from the power plant to cover the heat needed for solvent regeneration could be reduced by almost 18% for a cycle with the same live steam pressure as the reference cycle. However, it has been shown that by introducing reheat, the live steam pressure could be elevated to 160 bars, increasing the share of heat provided by the pressurized water to cover almost 20% of the total duty. This results in cycle efficiency for the power cycle, including both capture and compression of approximately 50.95%, which is 0.4 percentage points higher than for a corresponding triple-pressure NGCC [23]. Since single-pressure combined cycles are less costly than multiple-pressure cycles, the proposed cycle configuration offers economical benefits that should be of major importance for any newly built NGCC power plant owner if CO_2 capture regulations come into practice, as predicted.

Acknowledgment

The authors wish to acknowledge Dr. Björn Fredriksson Möller for developing the CO_2 capture model and Drs. Raik C. Orbay and Andre Hildebrandt for their early work with gas turbine models.

Nomenclature

A = area
C = absolute flow velocity
D_m = diameter at median
l = blade length
N = rotational speed
U = blade speed

Subscript

th = thermal

References

[1] International Energy Agency (IEA), 2009, *World Energy Outlook*.
[2] Möller, B. F., 2005, "A Thermoeconomic Evaluation of CO_2 Capture With Focus on Gas Turbine-Based Power Plants," Ph.D. thesis, Lund University, Sweden.
[3] Finkenrath, M., Ursin, T. P., Hoffmann, S., Bartlett, M., Evulet, A., Bowman, M. J., Lynghjem, A., and Jakobsen, J., 2007, "Performance and Cost Analysis of Novel Gas Turbine Cycle With CO_2 Capture," ASME Paper No. GT 2007-27764.
[4] Botero, C., Finkenrath, M., Bartlett, M., Chu, R., Choi, G., and Chinn, D., 2009, "Redesign, Optimization, and Economic Evaluation of a Natural Gas Combined Cycle With the Best Integrated Technology CO_2 Capture," Energy Procedia, **1**, pp. 3835–3842.
[5] Bolland, O., and Mathieu, P., 1998, "Comparison of Two CO_2 Removal Options in Combined Cycle Power Plants," Energy Convers. Manage., **39**(16–18), pp. 1653–1663.
[6] Chiesa, P., and Consonni, S., 2000, "Natural Gas Fired Combined Cycles With Low CO_2 Emissions," ASME J. Eng. Gas Turbines Power, **122**, pp. 429–436.
[7] IEA Greenhouse Gas R&D Programme, 2005, Retrofit of CO_2 Capture to Natural Gas Combined Cycle Power Plant.
[8] Kvamsdal, H. M., Jordal, K., and Bolland, O., 2007, "A Quantitative Comparison of Gas Turbine Cycles With CO_2 Capture," Energy, **32**, pp. 10–24.
[9] Zachary, J., and Titus, S., 2008, "CO_2 Capture and Sequestration Options: Impact on Turbo-Machinery Design," ASME Paper No. GT 2008-50642.
[10] Mimura, T., Shimojo, S., Suda, T., Iijima, M., and Mitsuoka, S., 1995, "Research and Development on Energy Saving Technology for Flue Gas Carbon Dioxide Recovery and Steam System in Power Plant," Energy Convers. Manage., **36**, pp. 397–400.
[11] Sipöcz, N., and Assadi, M., 2009, "Combined Cycles With CO_2 Capture: Two Alternatives for System Integration," ASME Paper No. GT 2009-59595.
[12] Desideri, U., and Paolucci, A., 1999, "Performance Modelling of a Carbon Dioxide Removal System for Power Plants," Energy Convers. Manage., **40**, pp. 1899–1915.
[13] Singh, D., Croiset, E., Douglas, P. L., and Douglas, M. A., 2003, "Techno-Economic Study of CO_2 Capture From an Existing Coal-Fired Power Plant: MEA Scrubbing vs O_2/CO_2 Recycle Combustion," Energy Convers. Manage., **44**, pp. 3073–3091.
[14] Romeo, L. M., Espatoleroa, S., and Bolea, I., 2008, "Designing a Supercritical Steam Cycle to Integrate the Energy Requirements of CO_2 Amine Scrubbing," Int. J. Greenh. Gas Control, **2**, pp. 563–570.
[15] Romeo, L. M., Espatoleroa, S., and Bolea, I., 2008, "Integration of Power Plant and Amine Scrubbing to Reduce CO_2 Capture Cost," Appl. Therm. Eng., **28**, pp. 1039–1046.
[16] Oexmann, J., Hensel, C., and Kather, A., 2008, "Post-Combustion CO_2-Capture From Coal-Fired Power Plants: Preliminary Evaluation of an Integrated Chemical Absorption Process With Piperazine-Promoted Potassium Carbonate," Int. J. Greenh. Gas Control, **2**, pp. 539–552.
[17] Tobiesen, A., Svendsen, H. F., and Hoff, K. A., 2005, "Desorber Energy Consumption Amine-Based Absorption Plants," International Journal of Green Energy, **2**, pp. 201–215.
[18] Abu-Zahra, M. R. M., Schneiders, L. H. J., Niederer, J. P. M., Feron, P. H. M., and Versteeg, G. F., 2007, "CO_2 Capture From Power Plants: Part I. A Parametric Study of the Technical Performance Based on Monoethalonamine," Int. J. Greenh. Gas Control, **1**, pp. 37–46.
[19] Aroonwilas, A., and Veawab, A., 2007, "Integration of CO_2 Capture Unit Single- and Blended-Amines Into Supercritical Coal-Fired Power Plant: Implications for Emission and Energy Management," Int. J. Greenh. Gas Control, **1**, pp. 143–150.
[20] Alie, C., 2004, "CO_2 Capture With MEA: Integrating the Absorption Process and Steam Cycle of an Existing Coal-Fired Power Plant," MS thesis, University de Waterloo, Canada.
[21] Elkady, A. M., Evulet, A., Brand, A., Ursin, T. P., and Lynghjem, A., 2008, "Exhaust Gas Recirculation in DLN F-Class Gas Turbines for Post-Combustion CO_2 Capture," ASME Paper No. GT 2008-51152.
[22] Evulet, A. T., Elkady, A. M., Brand, A. R., and Chinn, D., 2009, "On the Performance and Operability of GE's Dry Low NO_x Combustors Utilizing Exhaust Gas Recirculation for Post-Combustion Carbon Capture," Energy Procedia, **1**, pp. 3809–3816.
[23] Jonshagen, K., Sipöcz, N., and Genrup, M., 2010, "Optimal Combined Cycle for CO_2 Capture With EGR," ASME Paper No. GT2010-23420.
[24] Kohl, A. L., and Nielsen, R. B., 1997, *Gas Purification*, 5th ed., Gulf, Houston, TX.
[25] Möller, B. F., Assadi, M., and Linder, U., 2003, "CO_2 Free Power Generation—A Study of Three Conceptually Different Plant Layouts," ASME Paper No. GT 2003-38413.
[26] Loud, R. L., and Slaterpryce, A. A., 1991, "Gas Turbine Inlet Air Treatment," GE Power Generation.
[27] Maiboom, A., Tauzia, X., and Hétet, J.-F., 2008, "Experimental Study of Various Effects of Exhaust Gas Recirculation (EGR) on Combustion and Emissions of an Automotive Direct Injection Diesel Engine," Energy, **33**, pp. 22–34.
[28] Hountalas, D. T., Mavropoulos, G. C., and Binder, K. B., 2008, "Effect of Exhaust Gas Recirculation (EGR) for Various EGR Rates on Heavy Duty DI Diesel Engine Performance and Emissions," Energy, **33**(2), pp. 272–283.
[29] Botero, C., Finkenrath, M., Belloni, C., Bertolo, S., D'Ercole, M., Gori, E., and Tacconelli, R., 2009, "Thermoeconomic Evaluation of CO_2 Compression Strategies for Post-Combustion CO_2 Capture Applications," ASME Paper No. GT2009-60217.
[30] Moore, J. J., Nored, M. G., Gernentz, R. S., and Brun, K., 2008, "Novel Concepts for the Compression of Large Volumes of Carbon Dioxide," ASME Paper No. GT2008-50924.
[31] Romeo, L. M., Bolea, I., Lara, Y., and Escosa, J. M., 2009, "Optimization of Intercooling Compression in CO_2 Capture Systems," Appl. Therm. Eng., **29**(8–9), pp. 1744–1751.
[32] Denton, J., 1999, *Developments in Turbomachinery Design*, Wiley, New York.

IV

Proceedings of the ASME Turbo Expo 2011: Power for Land, Sea and Air
GT 2011
June 06-10, 2011, Vancouver, Canada

GT2011-46299

CONCEPTUAL DESIGN OF A MID-SIZED, SEMI-CLOSED OXY-FUEL COMBUSTION COMBINED CYCLE

[*] Majed Sammak, Klas Jonshagen, Marcus Thern, Magnus Genrup
Lund University
SE-221 00 Lund, Sweden
**Corresponding author. Tel: +46 76 236 3637*
E-mail address: majed.sammak@energy.lth.se

Egill Thorbergsson, Tomas Grönstedt
Chalmers University of Technology
SE-412 96 Gothenburg, Sweden

Adrian Dahlquist
Siemens Industrial Turbomachinery AB
SE-612 83 Finspong, Sweden

ABSTRACT
This paper presents the study of a mid-sized semi-closed oxy-fuel combustion combined cycle (SCOC-CC) with net power output around 134 MW. The paper describes not only the power balance and the performance of the SCOC-CC, but also the conceptual design of the SCOC turbine and compressor. A model has been built in the commercial heat and mass balance code IPSEpro to estimate the efficiency of semi-closed dual-pressure oxy-fuel combustion combined cycle using natural gas as a fuel. In order to obtain the real physical properties of the working fluids in IPSEpro, the code was linked to the NIST Reference Fluid Thermodynamic and Transport Properties Database (REFPROP).

The oxy-fuel turbine was modeled with the in-house Lund University package LUAX-T. Important features such as stage loading, loss modeling, cooling and geometric features were included to generate more accurate results. The oxy-fuel compressor has been modeled using a Chalmers in-house tool for conceptual design of axial compressors. The conceptual design of the SCOC-CC process has a net efficiency of 49%. The air separation unit and CO_2 compression reduce the efficiency by 8 and 2 percentage points, respectively.

A single-shaft configuration was selected for the gas turbine simplicity. The rotational speed chosen was 5200 rpm and the turbine was designed with four stages. All stage preliminary design parameters are within ranges of established industrial axial turbine design limits. The main issue is the turbine exit Mach number – the stage must be lightly loaded in terms of pressure ratio to maintain the exit Mach number below 0.6. The compressor designed with 18 stages. The current value of the product of the annulus area and the blade rotational speed squared (AN^2), was calculated and found to be $40 \cdot 10^6$.

Keywords: SCOC-CC, Oxy fuel, gas turbine, mid-sized dual pressure combined cycle, CO_2.

NOMENCLATURE

A	Area [m^2]
C	Blade chord [m]
Cm	Meridional velocity [m/s]
CCS	Carbon capture and storage
D	Diffusion factor [-]
HP	High pressure
HRSG	Heat recovery steam generator
HTC	Heat transfer coefficient [$W/m^2.K$]
LP	Low pressure
L	Blade length [m]
$\dot{m}$	Mass flow [kg/s]
m^*	Dimensionless mass flow [-]
M	Molecular mass [kg/kmol]
N	Rotational speed [rpm]
P	pressure [bar]
PR	Pressure ratio [-]
R	Gas constant [kJ/kg ^oC]

SCOC-CC	Semi-closed oxy-fuel combustion combined cycle
T	Temperature [°C or K]
U	Blade speed [m/s]

Greek symbols

γ	Gamma [-]
ε	Cooling effectiveness [-]
η	Efficiency [%]
ρ	Density [kg/m^3]
σ	Solidity (chord blade spacing)
φ	Flow coefficient [-]
ψ	Blade loading coefficient [-]

Subscripts

d	Discharge
i	Inlet
p	Polytropic
rel	Relative

INTRODUCTION

Secure, reliable and affordable energy supplies are needed for economic growth. However, the increase in the carbon dioxide (CO_2) emissions associated with oil, coal and natural gas is a cause of major concern. Over the past decade, reducing carbon emissions and their impact on climate change has become the major focus of researchers and scientists. One option that has broad potential is CO_2 capture and storage however; considerable development is needed to enable scale-up for industrial applications, and to make it more economical.

A number of power plant concepts for CO_2-neutral power production have been developed. All have advantages and disadvantages, and no single technique has shown to be superior in terms of performance and cost.

One promising candidate for the separation of carbon dioxide emitted by power plants is the semi-closed oxy-fuel combustion combined cycle (SCOC-CC). The concept is based on replacing air with oxygen in the combustion of the fuel so that the main products of combustion will be carbon dioxide and water. The steam is condensed in the flue gas condenser, while the CO_2rich flue gas is separated into two streams. The main stream is re-circulated to the gas turbine, while the much smaller bleed stream, containing the "new" CO_2, is compressed for transport and storage [1].

The choice of capture technology is determined largely by the process conditions under which it must operate. Current carbon dioxide capture systems for power plants have the potential to capture some 85-95% of the CO_2 produced [1]. However, carbon capture and compression come at a price, namely a decrease in performance of the plant.

The two of the more efficient oxy-fuel cycles are the Graz cycle [2] and the SCOC-CC [2], the latter being the subject of this paper. The issues of air separation and CO_2 transport and storage are not discussed, although their impact is taken into consideration in the cycle assessments.

The change in the working fluid, from air to CO_2, requires a number of important changes in the properties for the design of the gas turbine compressor, combustion chamber, and turbine.

Table 1 presents the main thermodynamic properties of air and carbon dioxide at 15°C and 1 bar.

Table 1: Thermodynamic properties of air and carbon dioxide at 15°C and 1 bar [3].

Thermodynamic properties	*Units*	*Air*	*Carbon dioxide*
C_p	kJ/kg °C	1.005	0.846
C_v	kJ/kg °C	0.718	0.657
R	kJ/kg °C	0.287	0.189
γ	-	1.4	1.289
ρ	kg/m^3	1.2	1.84
M	kg/kmol	28.9	44.01

From Table 1 it can be seen that the carbon dioxide has a lower value of gamma γ and a higher density than air. The speed of sound in the denser gas will be slower, and this will have a profound impact on the design of the gas turbine. Issues such as Mach numbers in the turbomachinery components and maintaining a high performance in the bottoming cycle will have to be addressed.

All land-based gas turbines categorized as single-, twin- or three-shaft units. The two- and three-shaft units can be either "normal" or compound configurations. The choice between single- and multi-shaft turbines is mainly governed by the application, and also to various extents grid-code regulations or synchronous condensation operation. The single-shaft configuration is less complex, but has poor torque characteristics for mechanical drive. The gas turbine mass flow can be controlled using a fixed-speed, single-shaft turbine by means of the compressor variable geometry. This means that part-load operation can be achieved with a, more-or-less, nominal firing level, maintaining a high exhausts temperature over a wide range of loads. This feature results in high combined-cycle performance. A multi-shaft unit typically has about twice the full-load torque at starting speed, and is capable of satisfy both electric power and mechanical drive applications. Thus, a SCOC-CC plant should preferably be based on a single-shaft turbine.

THE SEMI-CLOSED OXY-FUEL COMBSTION COMBINED CYCLE PROCESS

Figure 1 illustrates the SCOC-CC cycle, which consists of five main parts: the topping cycle, the bottoming cycle, the air separation unit, the CO_2 compression and the flue gas condenser.

A brief description of the proposed SCOC-CC is given below.

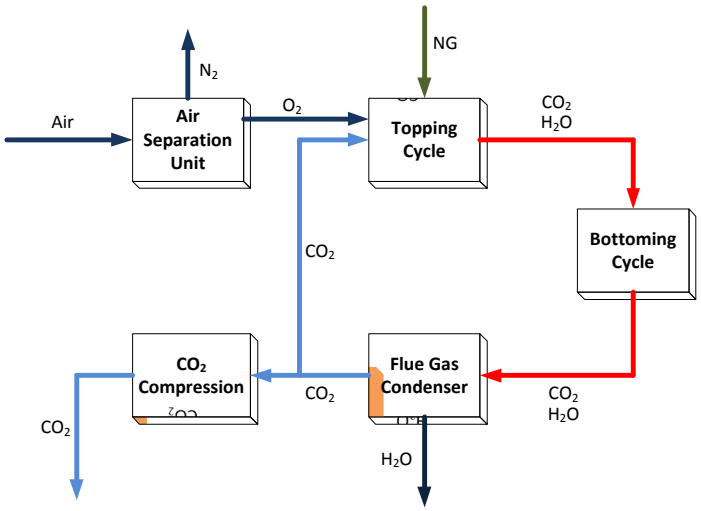

Figure 1: Illustration of the SCOC-CC.

The topping cycle consists of a compressor, a combustion chamber and a turbine

Compressor: The compressor working fluid consists mainly of CO_2 re-circulated from the flue gas condenser. (The flue gas is divided into two streams; about 94% being returned to the compressor.) As a direct consequence of the high CO_2 content, the pressure ratio in the SCOC-CC is chosen to 40, which is higher than the operating pressure ratio for a conventional industrial gas turbine.

Combustion Chamber: In the SCOC-CC, combustion of hydrocarbons is performed in oxygen with a purity of 95–99% at close to the stoichiometric conditions. The oxygen is obtained from the air separation unit. This generates a quite different working fluid leaving the combustion chamber. The outlet temperature from the combustion chamber is set to 1400°C. The actual flame temperature may reach 3500°C [1]. This is considerably higher than any state-of-the-art gas turbine can handle, and must be addressed in subsequent design phases.

Turbine: Due to the high temperature at the turbine inlet the turbine is cooled with CO_2 from the compressor. The mass flow of the cooling CO_2 is about 30% of the turbine inlet mass flow. The flue gas is expanded in the turbine to a pressure of 1.06 bar (including the diffuser loss), resulting in a temperature of 620°C.

The bottoming cycle main components are the heat recovery steam generator (HRSG) and the steam turbine. The heat recovery system employs two pressure levels. A third level would probably give better performance, but is not considered here due to the cost. The heat recovery steam generator has a standard configuration including economizers, a low-pressure (LP) evaporator, a low-pressure superheater, a high-pressure (HP) economizer, a high-pressure evaporator and finally a high-pressure superheater. The HP inlet steam temperature is set at 565°C and a pressure of 127 bar. The static pressure of the condenser is set to 0.042 bar, assuming a cooling water temperature of 19°C. The performance of the steam turbine has been assessed in detail with the Siemens in-house design code for steam turbines, however, due to the proprietary nature of this information; no details can be given here. The deaerator is operating at 105°C and the energy is taken from the LP-economizer. The deaerator outgoing water is cooled by the incoming condensate, to approximately 50°C. The temperature is limited by the requirement of a temperature difference of 13° for efficient deaeration. This configuration increases the temperature of the inlet water in the economizer which prevents flue-gas condensation. The flue-gas exit temperature from the HRSG is 66°C is lower than for a regular dual-pressure combined cycle and this is due to that the specific heat of the flue gas is lower than in a conventional cycle.

The flue gas condenser is assumed to be a packed column. The purpose of this is to condense water from the exhaust gases and remove pollutants and non-condensed gases from the flue gas. The flue gas leaving the condenser consists mainly of CO_2 with a temperature around 20°C. Most of the CO_2, around 94%, is recycled to the compressor, while the remainder is bled off and compressed for storage.

CO_2 is compressed and liquefied at a pressure of 200 bar to enable transport and storage as a super-critical fluid.

There are three commercially available methods of separating air, namely; cryogenic separation, pressure swing absorption, and membranes [4,5]. The very large quantities of oxygen required in oxy-fuel combustion can only be produced economically using cryogenic separation [4,5].

MODELING AND PROCESS SIMULATION

All thermodynamic and process simulations were performed using the commercial software IPSEpro, developed by SimTech Simulation Technology [6]. This software allows the implementation of user-defined fluid properties to simulate the real gas properties of the working fluids. The physical properties of water and steam were calculated using the standard IAPWS-IF97 formulations in IPSEpro [6]. IPSEpro was linked to the NIST Reference Fluid Thermodynamic and Transport Properties Database (REFPROP) to obtain more realistic results [7].

Modeling of e.g. turbomachinery components becomes more intricate with rigorous-state models. Standard definitions of parameters such as the polytropic efficiency of the compressor should not be used, since they are typically derived from semi-perfect gas models. Instead, one should use the basic state equations for such process.

The Mallen-Saville model [8] was implemented in this study.

$$T\,\mathrm{ds/dT} = constant \qquad (1)$$

$$\Delta H_p = \Delta H - (S_d - S_i)(T_{td} - T_{ti})/\ln(T_{td} - T_{ti}) \quad (2)$$

$$\eta_p = \Delta H_p / \Delta H \quad (3)$$

The polytropic efficiency calculated by the model was 92%. Figure 2 illustrates the principle flow scheme of the simulated dual-pressure, semi-closed oxy-fuel combustion combined cycle.

The SCOC-CC was designed as a mid-sized plant. Such a plant would typically have two pressure levels in the bottoming cycle, in contrast to larger plants with three pressure levels and reheat. Choosing a smaller plant offers the possibility of using geared gas- and steam turbines, hence allowing compact parts to be used. Bolland and Mathieu found that the difference between dual- and triple-pressure steam cycles was very small [5].

The work necessary to obtain oxygen with a 95% purity from air has been estimated to be approximately 900 kJ/kg O_2 [2]. The energy required for CO_2 compression from 1 to 200 bar for transport and storage has been estimated to be 325 kJ/kg CO_2 [2].

The thermodynamic states and compositions of the streams are given in Tables 2 and 3 respectively. Table 4 lists the main cycle parameters.

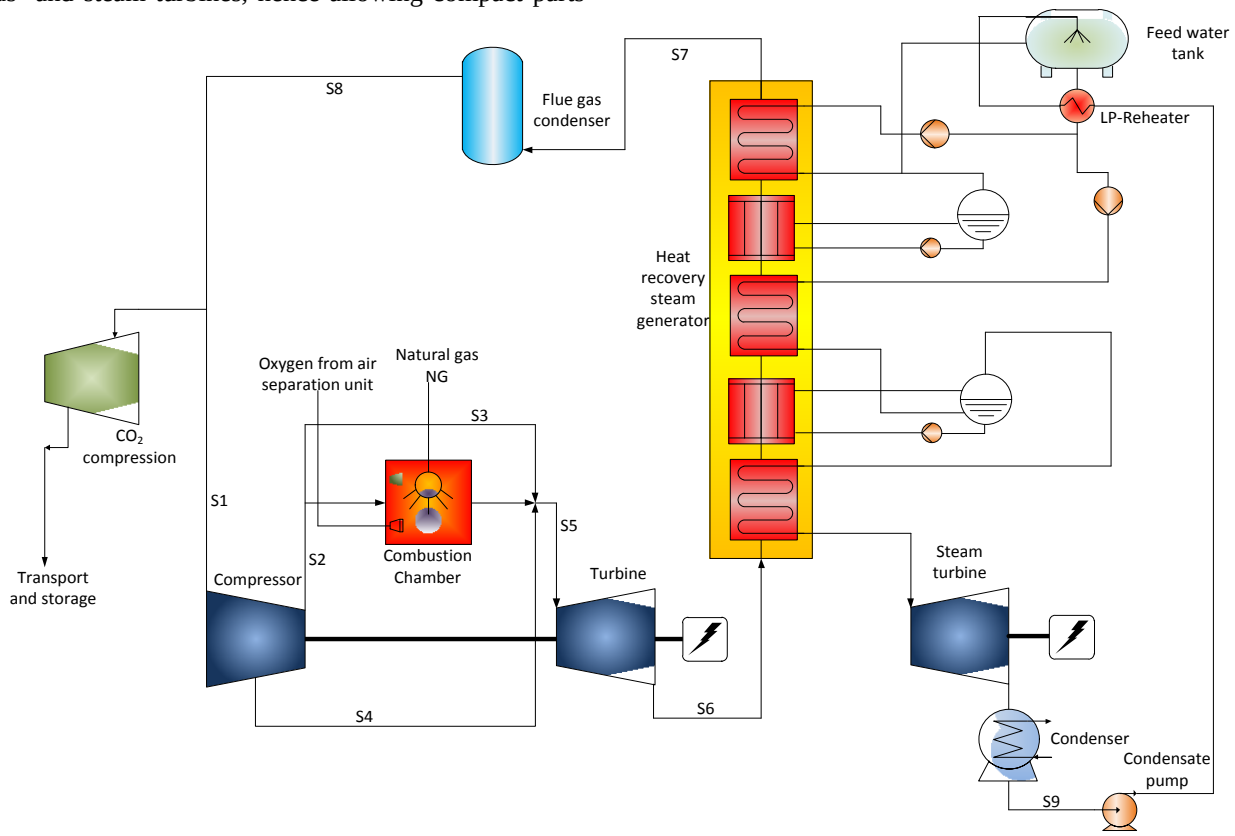

Figure 2: Principle flow scheme for SCOC-CC.

Table 2: Composition of streams S1-S4.

Stream	*Unit*	*S1*	*S2*	*S3*	*S4*
T	°C	20	390	390	261
P	bar	1.013	39.8	39.8	14
m	kg/s	190	172	33	18
CO_2	%	94.5	94.5	94.5	94.5
N_2	%	0.15	0.15	0.15	0.15
Ar	%	4.09	4.09	4.09	4.09
H_2O	%	0.97	0.97	0.97	0.97
O_2	%	0.11	0.11	0.11	0.11

Table 3: Composition of streams S5-S9.

Stream	*Unit*	*S5*	*S6*	*S7*	*S8*	*S9*
T	C	819	620	66	20	30
P	bar	4	1	1	1	0.042
m	kg/s	213	213	213	203	39
CO_2	%	90	90	90	94.6	0
N_2	%	0.145	0.145	0.145	0.152	0
Ar	%	3.9	3.9	3.9	4.9	0
H_2O	%	5.44	5.44	5.44	0.96	100
O_2	%	0.11	0.11	0.11	0.117	0

Table 4: SCOC-CC cycle power balance.

Compressor mass flow	kg/s	190
Compressor pressure ratio	-	41
Combustor outlet temp.	^{o}C	1400
Gas turbine power without comp.	MW	155
Total heat input	MW	227
Steam turbine	MW	47
Total power	MW	134
O_2 generation	MW	17
CO_2 compression to 200 bar	MW	4.5
Net power output	MW	112
Net efficiency	%	49

The designed process has a net effect of 134 MW and a net efficiency of 49%. The penalties for air separation and CO_2 compression accounted for 8 and 2 percentage points, respectively.

CONCEPTUAL DESIGN OF THE SCOC-CC GAS TURBINE

As with the compressor, the working fluid in the turbine is mainly CO_2, with a purity of almost 94%. Changing the fundamental physical properties of the working fluid will have a significant impact on the design of the turbine. The standard set of design rules for a normal gas turbine can therefore not be directly applied to the design of an SCOC cycle. The SCOC-CC turbine has been modeled with the Lund University in-house turbine design tool [1]LUAX-T. The code is a reduced-order throughflow tool which is capable of designing highly cooled turbines. The code uses the [2]AMDC-KO-MK loss model and fundamental equations for momentum, energy and continuity for assessing losses due to cooling, purging and packing flows.

The chosen layout is a straight forward CO_2-cooled single shaft unit. As mentioned the principal reasons for a single shaft are the simplicity and related low cost. Furthermore, a single shaft unit offers significantly less complexity in terms of shaft and bearing systems. Since there is no need for a collector with cold-end drive a more efficient exhaust system could be designed. A conical diffuser can reach a recovery level of 0.8 in comparison to 0.6-0.7 for a system with a 90° bend [9]. Figure 3 presents turbine exhaust diffuser performance which presents the relation between the pressure recovery coefficient and the static/total outlet pressure. A single shaft unit has typically a beam type rotor whereas the twin-shaft needs bearings within the high pressure section of the gas turbine. Before describing the features of a SCOC turbine, it is instructive to discuss the design of a conventional (air and flue gas) single-shaft unit.

[1] LUAX-T is freely available for academic work outside Lund University.

[2] AMDC-KO-MK: Ainley+Mathieson+Dunham+Came-Kacker+Okapuu-Moustaoha+Kacker [12]

One of the most critical design choices is the speed level since it has a profound impact on the stage count and cost.

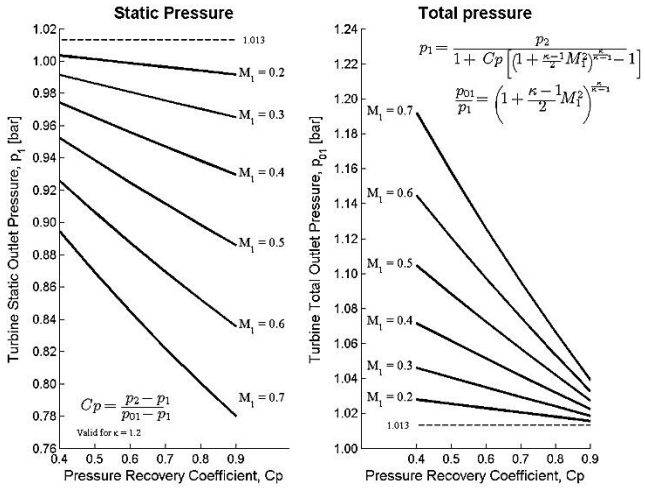

Figure 3: Turbine exhaust diffuser performance.

The SCOC-CC Turbine design

The rotational speed is typically set by either the exhaust Mach number at a maximum available AN^2 (~root stress level) or the relative tip Mach number at the first compressor rotor. The importance of the AN^2 parameter cannot be overemphasized since a reduction from e.g. $50 \cdot 10^6$ to $40 \cdot 10^6$ may translate into two additional compressor stages. The exit Mach number is preferable within the range of 0.5-0.6 while the maximum tip Mach number is in the order of 1.3 [10]. The meridional Mach number should be less than 0.7 at the compressor inlet.
The heavy gas introduces issues with the last stage loading due to the low speed of sound. For reasonable exit losses, the last turbine stage should be designed with an exit Mach number below 0.6 (see figure 3).

The pressure ratio of the last stage needs to be low, but still give sufficient rotor turning to keep blade frequency high enough in order to avoid rotor dynamic difficulties. One can argue whether a twin-shaft unit should provide a better platform. The additional freedom of having another speed level would be advantageous in terms of optimizing the loading distribution. The speed level was set to 5200 rpm and the first turbine stage rim speed 380 m/s. The relative tip Mach number of the first compressor stage does not pose any limitations at the chosen speed level. Efficient gears are available exceeding 100 MW. The associated losses are approximately 1.2% and 0.6% for normal and vacuum respectively.

The first stage has almost no inner wall hade, while the later has about eight degrees. The first two rotors are cylindrical to satisfy minimum running clearance requirements. The outer wall hade was set to a maximum of 25° to maintain a maximum opening of approximately 35°. These values are somewhat

arbitrary, but well within current practice. The actual limitations must be assessed in a later, more detailed design phase. With these design constraints, the exit Mach number is 0.60 and the value of AN^2 is close to $40 \cdot 10^6$. The last rotor has a mid-span turning exceeding 65°. A three-stage design would not be realistic, even at higher speed, due to the inherent limitation on the exit Mach number. Figure 4 presents the annulus of a four stages SCOC designed turbine.

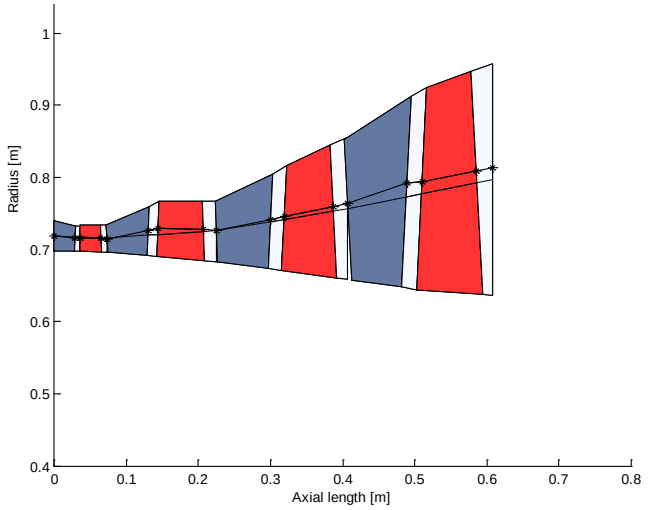

Figure 4: Annulus of the conceptual design of the SCOC turbine.

The designed four stages SCOC turbine flow coefficients, stage loading coefficients and reactions degree are presented in Table 5.

Table 5: Turbine design data.

	Stage 1	*Stage 2*	*Stage 3*	*Stage 4*
$\Delta h_0/U^2$	1.7	1.3	1.1	1.0
$\bar{\psi}$		1.30		
C_m/U	0.39	0.39	0.42	0.44
PR	2.57	2.32	2.34	2.74
Λ_p	0.30	0.38	0.38	0.40
$\varepsilon_{str}/\varepsilon_{rtr}$	0.47/0.4	0.28/0.16	0.05/0	-

The combustor outlet temperature was set to 1400°C to obtain high power density and good cycle performance. This level of firing requires an efficient cooling system. The firing level alone is not sufficient to describe the required cooling, and the cooling effectiveness must be used to describe the cooling duty (ε). At first glance, the values of the cooling effectiveness are low – and well within common practice. The cooling flows can be assessed with the standard m-star model [12].

$$\varepsilon = \frac{T_{gas.rel} - T_{metal}}{T_{gas.rel} - T_{cool.rel}} \qquad \varepsilon = \frac{m^* \eta_{cool}}{1 + m^* \eta_{cool}} \qquad m^* = \frac{\dot{m}_{cool} \cdot c_{p.cool}}{HTC \cdot 2.2 \cdot C \cdot l} \qquad (5)$$

Equations (5) provide a link between the thermodynamic properties of the cycle, the maximum metal temperature, the level of technology and the velocity triangles. All temperatures should be relative, since both the inlet temperature and coolant temperature are dependent on the velocity triangles. The relative inlet temperature can be controlled effectively by lowering the reaction level. Another possibility is to reduce the relative inlet velocity by using a lower value of C_m/U, resulting in lower local heat transfer at the first part of the blade. However, it is not possible to assess this heat transfer with a mid-span code. The present version of LUAX-T has three different ways of mixing coolant into the main stream, namely: (i) film, (ii) trailing-edge ejection, and (iii) packing and cavity purge flows. Losses due to coolant- and packing flows are assessed by conservation of momentum and energy. The mixing routines result in a non-linear system that must be solved iteratively for conservation of mass. Film losses are assessed through a generic free stream velocity distribution and the Hartsel mixing method. The generic velocity distribution assumes a certain loading distribution and suction-side diffusion level. Injection positions, angles and momentum ratios are typical in terms of normal showerhead and profile configurations. Common practice is not to have film after the throat point – driven by that the loss scales with Mach number squared.

The total cooling flow, including 1.5% per disc cooling and packing, is 50.8 kg/s or 26.7% of the compressor inlet flow. This figure is rather high, and must be further investigated. The specific heat ratio between air and carbon dioxide is about 1.2, and a corresponding influence on cooling consumption is to be expected by virtue of the medium alone. It should be borne in mind that the m-star model typically underestimates the total cooling flow for highly fired engines. It is common to introduce an adjustment factor which is dependent on the firing level. Early profiling and a heat transfer code should be able to verify the coolant consumption in a later design stage. The drop in combustion pressure is a limiting factor in terms of the pressure difference for film cooling of the first vane. For a normal gas turbine, the pressure drop should not fall below 3% to ensure sufficient film pressure drop. It is not uncommon to use double feeds for the first guide vane (halving the velocity gives one quarter of the pressure drop), when the pressure drop is low. The entire cooling and secondary air system must be analyzed before any firm conclusions can be drawn.

The SCOC-CC compressor design

As mentioned previously the design of the SCOC-CC compressor is constrained by the relative tip Mach number of the first rotor. To allow a high blade speed and keep first stage transonic losses down an inlet guide vane is employed. Here, a 15° swirl was selected. This was a sufficient level for the relatively moderate Mach number that resulted from the design process described below.

Reducing the flow coefficient at the first stage will help to keep the first stage specific work up. For a given hub tip ratio reducing flow speed will increase speed at the blade mid allowing a higher first stage temperature rise to be achieved for

a given stage loading parameter ψ. However, it is usually desirable to reduce axial flow speed and the flow coefficient through the compressor to allow a relatively low flow coefficient at the compressor exit. This makes the process of establishing a desirable surge margin easier. In fact, it is possible to select a somewhat higher first stage flow factor and simultaneously obtain close to a minimal tip Mach number, i.e. close to the minima of the family of curves presented in Figure 5. This will reduce the transonic losses incurred in the first stage rotor. Here, a first stage hub tip ratio of 0.483 is selected together with a flow factor of 0.65.

To keep blade lengths at a reasonable level and thereby limit tip leakage losses in the last stages of the compressor the hub-tip ratio must be kept at a reasonable number. Here a constraint of 0.92 in exit hub tip ratio has been imposed together with an axial exit Mach number of 0.25. Together with the mass flow, the compressor efficiency and the pressure ratio the hub tip ratio limit will define the compressor exit tip and hub radius; here these numbers turn out to be 0.374 and 0.345 meters respectively.

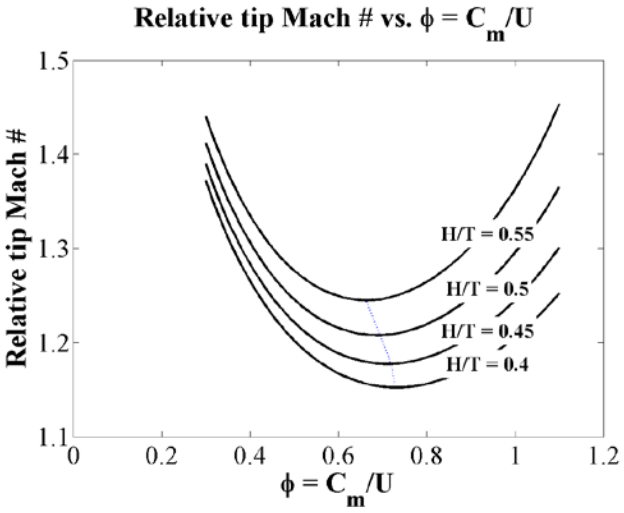

Figure 5: First stage rotor relative tip Mach number as a function of flow coefficient for a range of hub-tip-ratios (0.4, 0.45, 0.50, 0.55).

To ensure that accurate thermodynamic gas properties are obtained the Chalmers in-house tool for conceptual compressor design couples the REFPROP tool [7] to the compressor design process. The original REFPROP code has the drawback that the execution speed is slow due to the reading of a large number of gas property tables for each call. Work has been performed to remove this unnecessary step increasing the speed of execution for the conceptual compressor design tool substantially. The code now executes close to the speed of a conventional table look-up procedure.

The resulting compressor is an 18-stage design. It should be noted that the initial assumption of a first stage rotor hub-tip ratio of 0.50 and the limiting hub tip ratio of 0.92 at the compressor exit produced an annulus very close to a constant hub design after the first stage. Data on axial flow velocities, blade speeds at blade mid, flow coefficients, stage loading coefficients, stage hub tip ratio, relative tip Mach numbers and stage pressure ratios have been collected in Table 6. A cross sectional drawing of the compressor annulus is reproduced in Figure 6.

The design studies carried out strongly suggest that the number of stages and the feasibility of a one stage compressor is quite sensitive to the exit hub tip ratio. Reducing the allowable exit hub tip ratio to 0.90 typically adds 2-4 stages on the compressor due to the reduced blade speed. This gives some insight into how the selection of single shaft compressor architecture imposes restrictions on the pressure ratio of the cycle. Increasing the pressure ratio further will necessitate that the annulus is allowed to move to lower radii, a decreasing hub radius design, to allow the shorter blades arising from the increased pressure and density to stay within the hub tip ratio bound. This will add stages rapidly making the single shaft design less attractive for very high cycle pressure ratios.

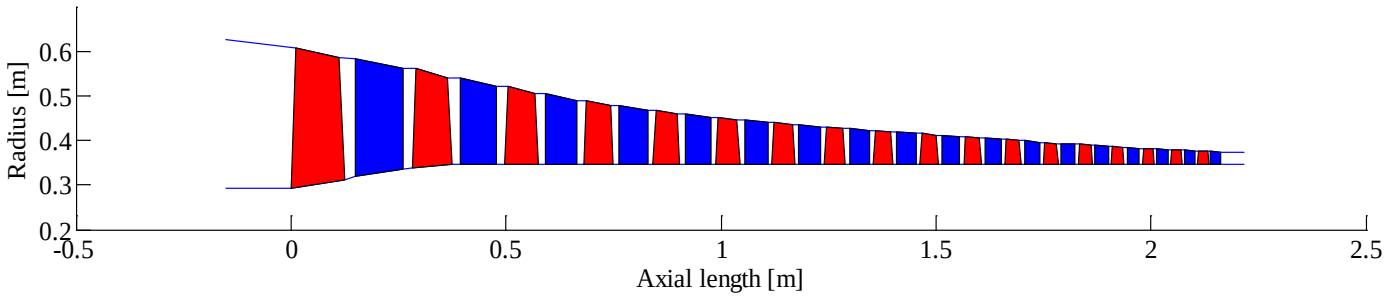

Figure 6: Annulus of the conceptual design of the SCOC compressor.

Table 6: SCOC-CC compressor data.

Stage		*1*	*3*	*5*	*7*	*9*	*11*	*13*	*15*	*17*	*18*
C_{ax}	[m/s]	155	138	127	117	106	100	100	100	100	100
U_m	[m/s]	246	232	219	212	208	204	201	199	197	196
φ_m	-	0.63	0.60	0.58	0.55	0.51	0.49	0.50	0.50	0.51	0.51
ψ_m	-	0.45	0.45	0.45	0.45	0.45	0.45	0.45	0.45	0.45	0.45
Htr	-	0.55	0.68	0.75	0.79	0.83	0.85	0.88	0.90	0.91	0.92
M_{reltip}	-	1.12	0.85	0.73	0.65	0.60	0.56	0.53	0.50	0.48	0.47
PR	-	1.52	1.37	1.28	1.23	1.19	1.17	1.15	1.14	1.13	1.12

CONCLUSION

This paper presents the conceptual design of a mid-sized, semi-closed dual-pressure oxy-fuel combustion combined cycle and the conceptual design of a SCOC turbine and compressor. The SCOC-CC model was based on the heat and mass balance code IPSEpro. The physical properties of the gases were calculated using values determined by NIST software REFPROP.

The designed SCOC-CC process has a net power of 134 MW and 49% efficiency. Note that all values exclude parasitic losses and step-up transformer losses. The air separation unit reduces the net efficiency by 8 percentage points while the CO_2 compression reduces it by another 2 percentage points.

The overall compressor pressure ratio is 40 which is higher than the operating pressure ratio for a conventional industrial gas turbine. The combustion outlet temperature is set to 1400^{o}C. The turbine requires an efficient cooling system to maintain blade metal temperature within the limits. The total calculated cooling flow is 50.8 kg/s or 26.7% of the compressor inlet flow.

A four-stage, single-shaft gas turbine configuration was chosen for simplicity. The rotational speed selected was 5200 rpm. The turbine exit Mach number was maintained below 0.60. The compressor designed with 18 stages. The current value of AN^2 was found to be $40 \cdot 10^6$.

The last stage loading issue together with the relative low compressor rotor inlet Mach number suggests that a twin-shaft unit is a better candidate for optimal turbomachinery operation. Furthermore a two spool design would allow the gas generator to operate at a higher speed level making the compressing system more compact as well as providing an optimized power turbine at a lower speed level. However, the advantages of a dual spool design must always be weighed against retaining the inherent simplicity and low cost of the simple cycle.

ACNOWLEDGEMENTS

This research has been funded by the Swedish Energy Agency, Siemens Industrial Turbomachinery AB, Volvo Aero Corporation and the Royal Institute of Technology through the Swedish research code TURBO POWER, the support of which is gratefully acknowledged. The authors would also like to acknowledge David Olsson and Jonas Svensson for developing the LUAX-T turbine design tool. The steam turbine calculations would not have been possible without the assistance from Specialist Åke Göransson (Siemens).

REFERENCES

[1] Metz B., Davidson O., de Coninck H., Loos M., Meyer L., 2005, "IPCC Special Report on Carbon Dioxide Capture and Storage", Cambridge University, ISBN-13 978-0-521-86643-9.

[2] Sanz W., 2005, "Qualitative and Quantitative Comparison of Two Promising Oxy-Fuel Power Cycles for CO2 Capture", Journal of Engineering for Gas Turbines and Power, **130**.

[3] A. Cengel Y, A. Boles M, 2002, "Thermodynamics an engineering approach", 4th ed, ISBN 0-07-112177-3

[4] Allam R., White V., 2005, "The oxyfuel baseline: revamping heaters and boilers to oxyfiring by cryogenic air separation and fuel gas recycle", Carbon dioxide capture for storage in deep geologic formations, **1**.

[5] Bolland O., Mathieu P., 1998, "Comparison of two CO_2 removal options in combined cycle power plants", Energy Convers. Mgmt, **39**, (16-18), pp. 1653-1663.

[6] IPSEpro, 2003, SimTech Simulation Technology (SimTech), Graz, Austria.

[7] REFPROP, Version 8, Standard Reference Data Code, National Institute of Standard and Technology.

[8] Ronald H. Aungier, 2003, "Axial-Flow Compressor", ISBN 0-7918-0192-6.

[9] Japikse D., Baines N. C., 1997, "Introduction to Turbomachinery", Concepts ETI, ISBN 0-933283-10-5.

[10] Walsh P.P., Fletcher P., 1998, "Gas Turbine Performance", ISBN 0-632-04874-3.

[11] Wennerstrom A. J., 2000, “Design of highly loaded axial-flow fans and compressors”, Concepts ETI, ISBN 0-933283-11-3.

[12] Moustapha H., Zelesky M F., Baines N. C. , Japikse D., 2003, “Axial and Radial Turbine”, Concepts ETI, ISBN 0-933283-12-0.

V

Proceedings of ASME Turbo Expo 2009: Power for Land, Sea and Air
GT2009
June 8-12, 2009, Orlando, Florida, USA

GT2009-59329

LOW-CALORIFIC FUEL MIX IN A LARGE SIZE COMBINED CYCLE PLANT

Klas Jonshagen[1*] **Magnus Genrup[1]**
Pontus Eriksson[2]

[1]Department of Energy Sciences, Lund University, Sweden, klas.jonshagen@energy.lth.se
[2]Volvo Aero Corporation, Sweden

ABSTRACT

This paper will address the effects of mixing low-calorific fuel in to a natural gas fuelled large size combined cycle plant. Three different biofuels are tested namely; air blown gasification gas, indirect gasification gas and digestion gas. Simulations have been performed from 0-100% biofuel – natural gas mixtures.

The biofuel impacts on the full cycle performance are discussed. Some more in-depth discussion about turbo-machinery components will be introduced when needed for the discussion.

The compressors pressure ratio will increase in order to push the inert ballast of the low calorific fuels trough the turbine. Despite the increased expansion ratio in the gas turbine, the exhaust temperature raises slightly which derives from changed gas properties.

The work is based on an in-house advanced off-design model within the software package IPSEPro.

Sweden's newest plant "Öresundsverket", which is a combined heat and power (CHP) plant, is used as a basis for the investigation. The plant is based on a GE Frame-9 gas turbine and has a triple-pressure reheat steam cycle.

INTRODUCTION

In previous work at the department of Energy Sciences at Lund University the effects of using low calorific gases in gas turbines have been studied in both single shaft [1] and two-shaft [2] industrial gas turbines. In this work, a broader approach, looking at the whole picture of a combined cycle rather than focus on machine parts, is kept. There are a limited number of references on introducing low-calorific biomass produced fuels in a certain combined cycle plant. When a specific plant with its fixed components is operated with a different fuel, then the problem has to be treated as an off-design analysis case. This work is based on an off-design model for the complete power plant with its gas turbine, HRSG, steam turbine and condenser. Most of the previously published work focused on the gas turbine alone, see [1][2][5][6] or on fuel [3]. Bio fueled combined cycles are discussed in [4], where the discussion is limited to a single pressure plant and the main focus is, however, on the gas turbine.

Environmental concerns drive plant owners to either use capture technology or renewable fuels. Capture technology will probably, at least, initially seek its way into the power industry in large coal-fired plants and at a later stage combined cycle plants. The reasoning behind this is simply the higher level of carbon emission from a coal-fired plant due to its fuel, and the limited amount of excess air. A typical coal-fired boiler has 1 - 2 percent excess air in the flue gas and the mass flow is on the order of 0.95 kg/s per MW. A gas turbine based plant has less carbon emission per produced power unit by virtue of its hydrogen-rich fuel and significantly higher plant efficiency – hence a smaller benefit from CCS than from a coal fired plant per produced power unit. One scenario could be to replace the non-renewable natural gas by fairly CO_2-neutral low-LHV biofuel. Low-LHV biofuel firing in a gas turbine introduces several issues throughout the machine. It may, however, be impractical to fully replace the natural gas on plants by virtue of their sizes – a 300 MW unit will need some 750 MW fired power. That amount of bio-fuel cannot be locally manufactured nor transported within reason. One can therefore argue that purely bio-fuelled units should be small and that only low ratio mixing is reasonable for large units.

NOMENCLATURE

Area	A	[m^2]
Specific heat at constant pressure	C_P	[J/(kg·K)]
Specific heat at constant volume	C_v	[J/(kg·K)]
Density	ρ	[kg/m3]
Efficiency	η	[-]
Gas Constant	$R = C_p - C_v$	[kJ/(kg·K)]
Isentropic Exponent	$\gamma = \frac{C_p}{C_v}$	[-]
Mach number	$Ma = \frac{u}{\sqrt{\gamma \cdot R \cdot T_{in}}}$	[-]

*Corresponding author

Mass flow	$\dot{m}$	[kg/s]
Pressure	p	[Pa]
Pressure ratio, *for compressor*	$\pi = \frac{P_{out}}{P_{in}}$	[-]
for turbines	$\pi = \frac{P_{in}}{P_{out}}$	[-]
Temperature	T	[K]
Wobbe-index	$WI = \frac{HHV}{\sqrt{SG}}$	[MJ/nm^3]
Difference	Δ	[-]
Coefficient	K	[-]
Combustor section cold Δp coef.	K_C	[-]
Combustor section hot Δp coef.	K_H	[-]
IGV stagger angel	ξ	[º]
Velocity/Speed	u	[m/s]
Parson number	χ	[-]
Average stage loading	$\bar{\psi} = \frac{\Delta h_0}{u^2}$	[-]
Polytropic Exponent	$n = \ln(p_1/p_2)/\ln(v_2/v_1)$	[-]
θ	$\frac{T}{288.15}$	[-]
Overall heat transfer coef.	U	[kW/m^{2}K]

Subscripts

act	Actual value
des	Design value
1	inlet
2	outlet
0	total state
CC	Combustion chamber
IGV	Inlet guide vane
CHIC	compressor characteristic

Abbreviations and acronyms

LHV	Lower heating value
HHV	Higher heating value
OEM	Original equipment manufacturer
SOT	Stator outlet temperature
GT	Gas Turbine
ST	Steam Turbine
HPT	High pressure turbine
HRSG	Heat recovery steam generator

The Fuels

The tested fuels are all biological fuels, produced by biological or thermal breakdown of organic matter. The composition of the gas depends on how it has been produced. Three different gases are used for the calculations; each is named by the method of production. It should be noted that the given figures are typical numbers and may very well vary within certain ranges. These ranges are dependent on the actual bio-source and type of production plant. Table 1 displays the gas compositions and their lower heating value (LHV).

The air blown gasification gas is produced from biomass which is gasified and partly combusted as air is blown trough it, referred to as thermal gasification of biomass. The air blown gasification gas contains a lot of nitrogen and has the lowest heating value of the tested gases.

The indirect gasification gas is also produced by thermal gasification of biomass but rather than adding oxygen to burn some of the biomass the heat is added externally. The indirect gasification gas contains large amounts of carbon monoxide.

The digestion gas or biogas is produced by anaerobic digestion of organic material. The product contains only carbon dioxide and methane and has the highest heating value of the three gases.

Table 1: Fuel composition (kg/kg) and LHV (MJ/kg)

	H_2O	CO	CO_2	N_2	O_2	H_2	CH_4	LHV
Air Blown	0.0%	18.5%	27.2%	49.7%	0.0%	0.9%	3.7%	4.8
Indirect	0.0%	32.8%	47.9%	4.7%	0.0%	3.9%	10.7%	13.4
Digestion	0.0%	0.0%	64.6%	0.0%	0.0%	0.0%	35.4%	17.7

All described fuels have different properties, figure 1 shows how the Wobbe-index decreases as more biofuel is added to the natural gas. Wobbe-index is a gauge of the energy flux through a certain area – which can be thought of as the fuel nozzles or any restriction in the fuel system. Most manufacturers have a range of allowable Wobbe- indices for their engines where they can be offered without limitations. In Figure 1 the lower Wobbe-index limit for two different engines are shown. As an immediate conclusion, the difference in range is quite evident.

The lower line actually reflects only the fuel system whilst the upper line is valid for the whole package. The details and manufacturers are not disclosed in the paper and the reader is referred to different manufacturers' information. The fuel Wobbe-index is certainly not the only limiting factor in terms of suitability for a certain fuel. There are other important issues associated with fuels with e.g. inert ballast, flame speed, corrosion etc. Low calorific fuels have typically high amounts of inert ballast (N_2 and CO_2) causing a miss-match between the cold- and hot end of the gas turbine.

It is assumed that the fuel is prepared in an upstream blending station and should be considered as a homogenous fuel when entering the system boundary.

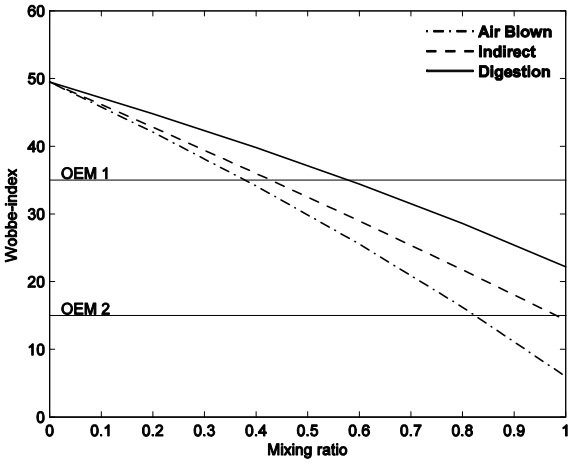

Figure 1: Wobbe-index as a function of mixing ratio of fuels

Operational strategy

The strategy used in this work is to maintain the combustor outlet temperature and keep the inlet guide vanes (IGV) fully open. This approach is rather aggressive to the machine but gives a high efficiency and energy output, and is therefore preferable as long as the equipment allows for it. Other strategies for firing low-calorific strategies could be to reduce the compressor airflow with the IGV's, reduction of turbine inlet temperature or redesigning the turbine inlet section, all described in [1] and [6]. All these methods are, however, less optimal from a pure thermo-economical perspective. Some of these issues are discussed in a later section dealing with firing low-calorifics.

Practical limitations

The aim of the simulations is to illustrate how a natural gas fuelled combined cycle reacts to low calorific fuels. One can argue whether it is possible to operate a gas turbine of this size with biofules alone. It is probably not possible to produce the large amount of biofuel (~820MW) within a reasonable geographical area. Furthermore, most gas turbine designed for natural gas cannot be operated purely on any of the tested biofuels. There are several issues which are likely to set the fuel LHV limit of a gas turbine. Each engine has its own set of limitations and it is not possible to discuss this in general terms. This is reflected in the wide range of allowable lower levels set by each manufactured for their specific engine types. The plots in this work illustrates the calculated results from having biofuel mixtures, and do not consider the limitations of the machine.

Biofuels are likely to contain impurities, especially when it is produces via gasification, which will foul and corrode gas path components. To avoid reaching the acid dew point of the flue gas the exit temperature of HRSG will increase. These problems are not further discussed in this work.

The fuel system and combustor have to be redesigned so the fuel can be introduced to the engine and the combustor with acceptable pressure drops or velocities.

The increased power output may introduce other issues, for example shaft torque and alternator rating. Torque increases in proportion of the power by virtue of having a fixed speed machine.

THE COMBINED CYCLE

The combined cycle is a standard three-pressure reheat (three admissions) plant without supplementary firing. The cycle has no separate feed water tank and the feed water is degassed in the condenser and the low-pressure drum. The latter is posing limits in terms of temperature difference between the saturation level at the LP-pressure and the feed water after the first economizer. There is a minimum LP drum pressure for low level of O_2 in the feed water and the temperature difference should not be less than 11°C.

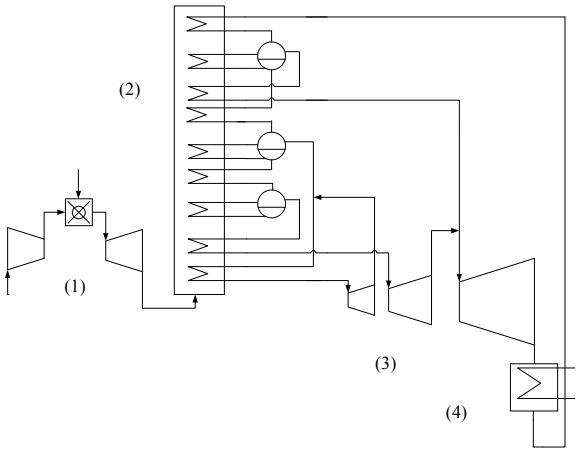

Figure 2: Schematic figure of the plant

1. Turbine
2. HRSG
3. Three-pressure steam turbine
4. Condenser

The gas turbine

The gas turbine is a General Electric Frame-9, a 300MW single shaft machine. The gas turbine is, by virtue of its size, directly connected to a 50 Hz generator running at a fixed speed of 3000 rpm. The exact details for the GE unit are not published but the model is based on available data. The compressor and turbine characteristics are normally not available outside the OEM's domains. In this case, the compressor map is based on a publication by General Electric [7]. The map is actually for a Frame 7 unit, which is the 60 Hz version of the Frame 9 type. It is assumed that the Frame 9 compressor is a direct scale-up of the smaller Frame 7. There are only relative values on the published characteristics and the reference points are assumed to be the same for both cases and the actual values are based on the ISO condition. The used isentropic efficiency is based on an assumed polytropic design efficiency of 90 percent.

The gas turbine Modeling

The gas turbine is a standard single-shaft unit with the following components:

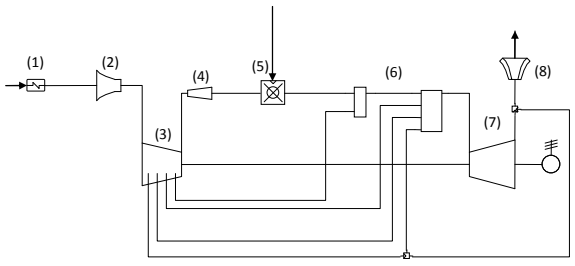

Figure 3: The gas turbine model

1. Anti icing
2. Compressor bellmouth
3. Compressor
4. Compressor diffuser
5. Combustion section
6. Cooling mixers
7. Turbine
8. Turbine diffuser

The inlet pressure drop is simply modeled as a standard off-design pressure drop, where it is assumed that a dynamic component scales on:

$$\frac{\Delta p}{p} = K\left(\frac{\dot{m}\sqrt{T_1}}{p_1}\right)^2 \quad (1)$$

The preceding equation is valid for all adiabatic ducts and hence also used for the bellmouth and compressor diffuser. The bellmouth model also comprises a heat-release model for taking into account condensation in the bellmouth. Bellmouth condensation is an issue itself and outside the scope of this paper. Loosely stated, the increased velocity from some 20 m/s to Ma = 0.5-0.55 will cause a depression of the inlet flow at the compressor bellmouth. The depression will reduce both the static temperature and the static pressure and the exceeding water vapor must be condensed with an associated release of latent heat.

The compressor is modeled with the map as a reference for pressure ratio, mass flow, efficiency and referred speed:

$$f\left(\pi, \frac{\dot{m}\sqrt{\theta}}{\delta}, \eta_s, \frac{N}{\sqrt{T}}, \xi, \gamma, R\right) = 0 \quad (2)$$

The diffuser after the compressor is modeled as described in equation 1.

The combustor section is straight forward and modeled more or less with the standard model in IPSEpro. The combustor pressure drop is modeled as a combined dump/friction and fundamental pressure drop. The latter is the standard Rayleigh pressure drop associated with the momentum change from the changed density due to the temperature increase. The total (or combined) combustor section loss is calculated according to the equation [10]:

$$\frac{\Delta p_{0CC}}{p_{01}} = \left(\frac{\dot{m}_1\sqrt{T_{01}}}{p_{01}}\right)^2 \left[K_C + K_H\left(\frac{T_{01}}{T_{02}} - 1\right)\right] \quad (3)$$

It is normally impossible to evaluate the cold and hot loss separately and the assumption is that the hot loss coefficient is 20 percent of the cold loss coefficient. It is then possible to calibrate the combustor pressure loss model at the design by assuming a certain level of e.g. 4 percent and still have relevant off-design modeling accuracy.

$$\frac{\Delta p_{0CC}}{p_{01}} \approx \left(\frac{\dot{m}_1\sqrt{T_{01}}}{p_{01}\cdot A_{CC}}\right)^2 K\left[1 + 0.2\left(\frac{T_{01}}{T_{02}} - 1\right)\right] \quad (4)$$

The turbine is modeled with its efficiency- and capacity characteristics. Cooling air is mixed into the mainstream before the actual expansion and the coolant mixing losses are embedded in the efficiency. There are essentially two methods for cooled turbine off-design performance namely: mixing all cooling before the actual expansion or add a fraction of the air before and after the turbine. In this work, the first method has been adopted since it simplifies tuning to available data. The detailed procedures are published in e.g. Bitterlich et al. [11] whilst the second method is well described by Walsh and Fletcher in ref [10]. The turbine diffuser is modeled separately, using the model by Japikse [12]. This model takes into account e.g. recovery of the swirl component, inlet turbulence etc and is more advanced than e.g. the previous published data by Sovran and Clomp.

Both for the compressor and turbine, the refereed parameters needed for modeling are based on the rigorous form (in a sense that γ and R are included) of the expressions. This gives the possibility to calculate component performance under a wide range of media compositions. The maps are also non-dimensional and the value of unity represents the design point.

The gas turbine model has been tuned to fit published data of the actual engine [8].

Steam turbine modeling

The steam turbine is based on partial turbines rather than detailed stage-by-stage calculation. The latter requires detailed geometrical data which normally are not known outside the OEM. Instead, the turbines are characterized by their efficiency and swallowing capacity. The efficiency of a section is typically a function of its loading, which can be described by the parson number:

$$\chi = \frac{\sum_{i=1}^{n} u_i^2}{\Delta h_s} \quad (5)$$

In a power production (hence fixed speed application), the off-design case simplifies even further. It is possible to assume that the dry efficiency scales in a certain fashion with the relative Parson number alone. This makes it possible to cancel out the numerator and one is left with the inverse of the ratio of isentropic section heat drop which can easily be evaluated if the node pressures are known. Node pressures are calculated with a swallowing capacity model that essentially gives the relation between flow and pressure. There are several methods, with indeed varying accuracy [13], at hand. Early work by Stodola resulted in the steam cone rule and laid the foundation for most models used today. The more improved model by Beckmann is used in this work:

$$\dot{m}_{1-2} = C_{T,1-2}(1+\bar{\psi})\sqrt{\frac{p_1}{v_1\cdot\bar{\psi}}F} \quad (6)$$

$$F = \frac{n}{n+1}\left\{1 - \left[1 - \frac{2\bar{\lambda}}{n-1}\right]\left(\frac{p_1}{p_2}\right)^{-\frac{n+1}{n}} - \left[1 - \frac{n+1}{n-1}\left(\frac{p_1}{p_2}\right)^{-\frac{2}{n}}\right]\bar{\lambda}\right\} \quad (7)$$

Where:

$\bar{\lambda}$ is a function of number of stages in the section, see e.g. Cordes [13] for further information.

$\bar{\psi}$ is the average stage loading and can in most stages (except the last and an eventual control stage) be assumed to be on the order of unity for a 50 percent reaction turbine.

The exhaust loss is evaluated with the DIN 1943 method. An OEM would have access to a more advanced model of the turbine and would have performed the calculation on a stage-by-stage approach. In this case, the flow angles (hence meridional velocity component) are known and the mass flow is evaluated based on geometry. Loss due to incidence is also evaluated and added to the overall stage loss level. A detailed description of these procedures is outside the scope of this paper and the reader is referred to e.g. Schobeiri [14] for an exhaustive treatment.

Firing low calorifics in a gas turbine

Due to a higher content of inert ballast in the fuel, the balance of flows between the compressor and the turbine will be distorted. The larger flow from the combustor will require a higher pressure in order to pass the turbine; therefore the pressure ratio of the compressor will increase. As the compressor rear stages are operated with an increased positive incidence, the working point moves towards the surge line. This engine behavior can approximately be expressed analytically as:

$$\underbrace{\frac{\Delta\pi}{\pi}}_{(A)} \approx \underbrace{\frac{\Delta\dot{m}_T}{\dot{m}_T}}_{(B)} - \underbrace{\frac{\Delta FN}{FN}}_{(C)} + \underbrace{\frac{1}{2}\frac{\Delta COT}{COT}}_{(D)} + \underbrace{\frac{1}{2}\left(\frac{\Delta R}{R} - \frac{\Delta\gamma}{\gamma}\right)}_{(E)} \qquad (8)$$

The preceding equation is derived from a logarithmic differentiation of the engine pressure ratio described in terms of the turbine capacity and the compressor inlet pressure. Term (A) represents the change in engine pressure ratio due to added mass through term (B) and changed composition in terms (E). There are a couple of strategies available to maintain the engine pressure ratio but the details are outside the scope of this work further detail can be found in [1][2]. The firing temperature (D) can be reduced to counteract the effect from having an increased flow passing the turbine section and restore surge margin (A). Operation with reduced firing level is normally not considered as optimum, since both the gas turbine power density as well as the available heat to the steam cycle is reduced. The cycle efficiency will also be penalized from this strategy. It should, however, be noted that the equation only is valid for first order approximation since e.g. an increased pressure ratio (A) would have reduced the compressor capacity and reducing (B) unless the engine is operated in choke.

An increased pressure ratio will increase the loading of the rear compressor stages and may introduce further issues when the engine is operated in cold climate. The loading is shifted towards the rear stages since the inlet section of the compressor may restrain the meridional velocity at the rear stages, when operated in choke. There are other issues than aerodynamic instability and eventually surge associated with increased pressure ratio, regardless of the type of engine. Aero-elastic phenomena's like flutter may be severe issues, especially when operated in low ambient temperatures. Flutter is a combination of self-induced blade oscillations and reduced aerodynamic damping that may result in high-cycle fatigue problems. An exhaustive treatment is outside the scope of the present work and the reader is referred to e.g. [9] for further information.

The most common practice in modeling the cooling extractions from the compressor is to maintain it as a fixed percentage of the total flow regardless of off-design conditions [10]. The increased pressure ratio is, however, expected to raise the flow through the cooling bleed channels; to consider this in the calculations an extra factor, f_{bleed}, given by equation 9:

$$f_{bleed} = 1 + \frac{\mathrm{p_{act}} - \mathrm{p_{des}}}{\mathrm{p_{des}}} - \frac{1}{2}\frac{\mathrm{T_{act}} - \mathrm{T_{des}}}{\mathrm{T_{des}}} \qquad (9)$$

The basis of equation 9 is the assumption that the driving pressure drop (or ratio) for the coolant is essentially constant and it is derived from the normal compressible flow functions. An OEM would have used their detailed in-house secondary air system (SAS) code to assess the changed coolant feed pressure. The actual secondary flow system (SAS) is normally complicated to mimic without a very detailed model of the engine with its swirl generators, seals, types of cavities and cavity flow models, etc.

The results indicate, however, that the modification of the cooling model with equation 9 alone is insufficient and some additional air is introduced to maintain the stator outlet temperature (SOT) at the datum level.

Another aspect of the secondary air system is the engine thrust balance. Higher pressure ratio may increase the bearing loading (towards the turbine exhaust) and a modification of e.g. balance pistons may become necessary.

Heat recovery steam generator modeling

The heat recovery steam generator (HRSG) is modeled with standard convective relations. Each section of the HRSG is initially calculated with certain pinch and approach points and values of $U \cdot A$ are evaluated through the boiler. It is then assumed that the value of $U \cdot A$ scales with $Re^{0.6}$ on the gas side when solving the off-design cases. Pressure drops are assumed to scale on velocity squared (c^2) and should provide relevant accuracy at this level of calculation.

The maximum HP- and IP admission temperatures are maintained with the normal sprays.

GAS TURBINE CALCULATION RESULTS

Figure show the compressor map with the working point for each fuel displayed. Since it is a 50 Hz fixed speed machine the $3000/\sqrt{\theta}$ rpm[1] speed line is the working line. The referred or aerodynamic speed is in this case the same as the physical speed since the unit is operated at 15°C. Clearly, the machine

[1] $n^* = \frac{n}{\sqrt{\theta}}\sqrt{\frac{\gamma_{ref} \cdot R_{ref}}{\gamma \cdot R}}$

cannot run on 100% air blown gasification gas since the compressor at this point has reached the surge line. The sheer size of the fuel plant and amount of raw material would pose an effective limitation to the produced amount of fuel. However, to display the tendencies, all calculations are made from 0% to 100% biofuel.

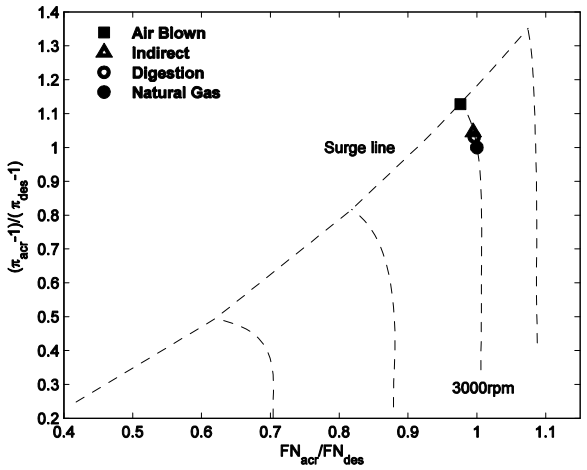

Figure 4a: Compressor map displaying working points for each fuel

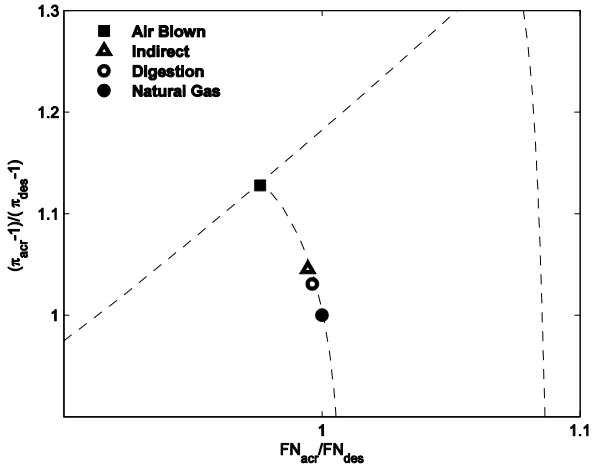

Figure 4b: Working point area enlarged

As the biofuel fraction is increased, the compressor working point moves up along the 3000 rpm speed line towards the surge line. Figure 5 shows how the compressor ratio increases as the heating value is decreased by the blend in of biofuel. The curve indicates that gas turbines designed for natural gas probably never will run on fuels with a lower LHV than 20 - 25 MJ/kg without major redesign of the engine.

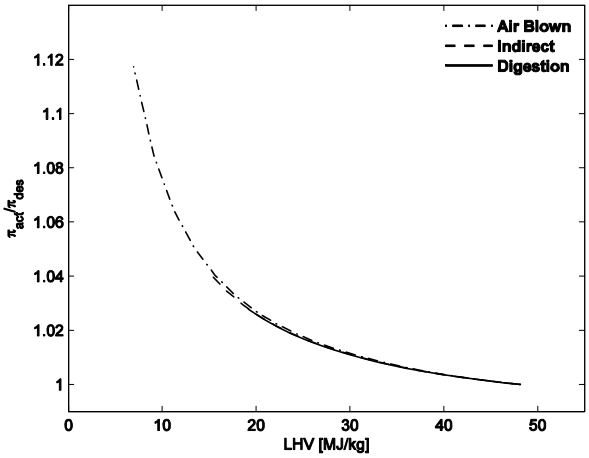

Figure 5: Compressor pressure ratio as a function of LHV

The higher pressure increases the expansion ratio in the turbine which, together with the increased mass flow, results in a higher power output as displayed in Figure 6. The integrated mean specific heat change is an order less than the change in mass flow and expansion ratio.

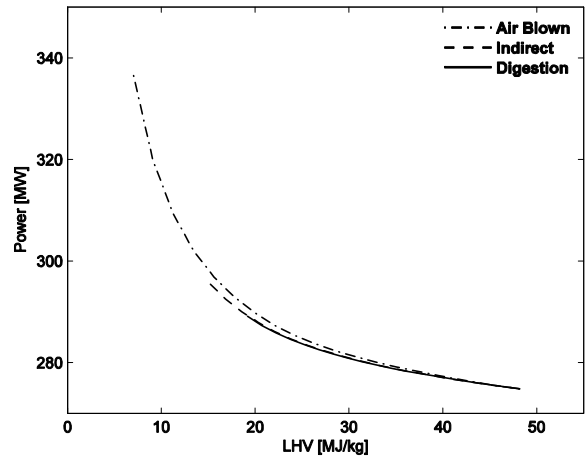

Figure 6: GT power output as a function of LHV

Figure 6 show that the power output increases as the heating value decreases, the extra output largely originate from the compressed inert ballast in the biofuel. When compression of the biofuels is included, the result appears quite different as displayed in Figure 7. Moving towards lower heating values, the mass flow of biofuel required increases exponentially. This affects both the turbine output as well as the fuel compressor power consumption. The behavior makes the calculations for very low LHV (10MJ/kg and less) sensitive for small calculation errors and is probably less accurate and is therefore not shown on Figure 7.

The indirect gasification gas has a 37 percent and 34 percent higher gas constant (R) than the air blown gasification

gas and digestion gas. The high gas constant makes it more energy consuming to pressurize.

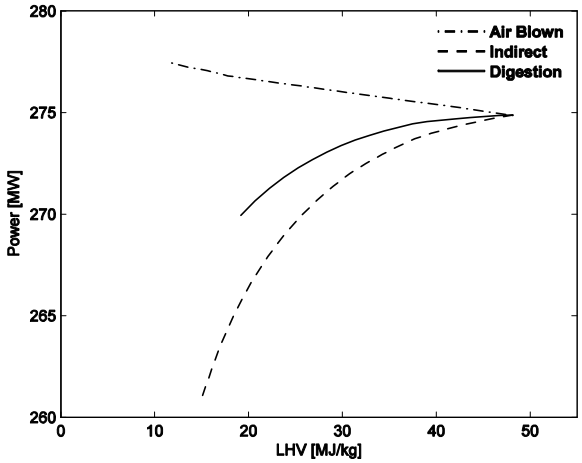

Figure 7: GT power output with biofuel compression included

All the extra inert gases need to be heated to the nominal firing temperature, which means that more energy is needed. Figure 8 show how the amount of chemical energy increases in order to heat the extra inert ballast.

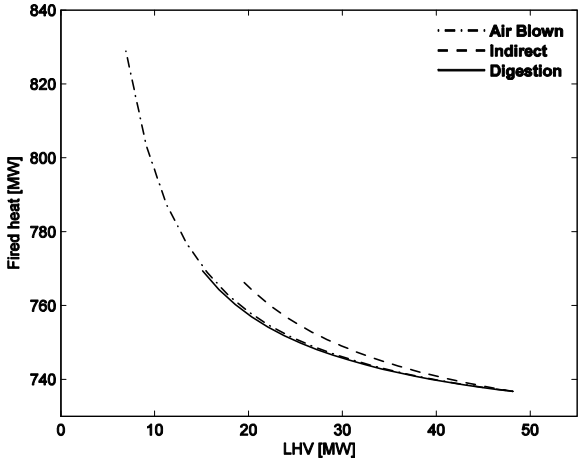

Figure 8: Required Fuel energy as a function of LHV

STEAM CYCLE CALCULATION RESULTS

The steam cycle consists of a triple pressure steam turbine with reheat, a HRSG unit, a district heating condenser and a seawater fed cold condenser.

The increased mass flow through the gas turbine increases the amount of available energy in the HRSG. Figure 9 show the exhaust energy flux as a function of fuel mix heating value.

As shown earlier, the expansion ratio trough the turbine will increase as more biofuel is added to the fuel. With a larger pressure ratio, the exhaust temperature would be expected to decrease, but this is not the case. Figure 10 show how the exhaust temperature increases as more biofuels are added to the natural gas.

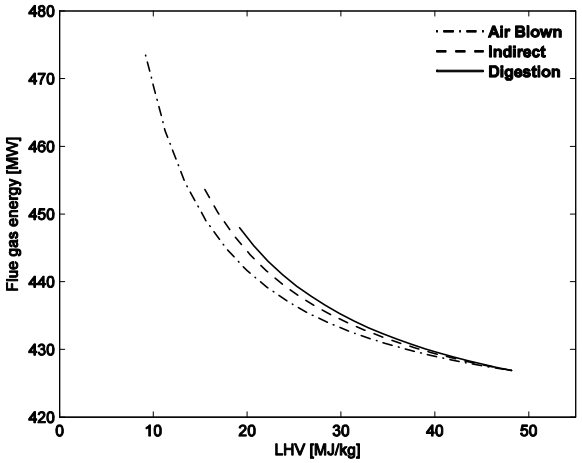

Figure 9: Exhaust energy as a function of LHV

The flue gas produced from the biofuels contains larger parts of CO_2 compared to the one from natural gas. CO_2 has a smaller isentropic exponent (γ) compared to the other large components i.e. N_2, O_2 and H_2O. Table 2 shows the flue gas composition for the fuels studied. Note that the flue gas produced from Air Blown gasification gas contains 65% more CO_2 than the one produced from Natural gas.

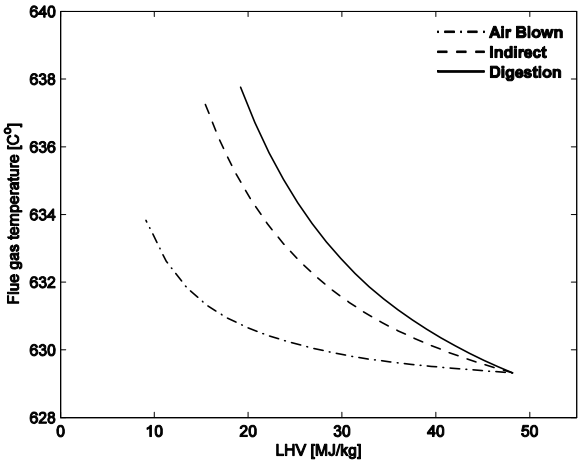

Figure 10: Exhaust temperature as a function of LHV

Table 2: Flue gas composition (kg/kg) and gas properties

	AR	CO_2	H_2O	N_2	O_2	γ	R
Air Blown	1.1%	13.4%	5.8%	70.5%	9.2%	1.31	0.2875
Indirect	1.2%	12.1%	6.6%	69.3%	10.9%	1.31	0.2895
Digestion	1.2%	11.9%	6.8%	70.0%	10.1%	1.31	0.2902
Natural Gas	1.3%	8.1%	6.6%	73.0%	11.1%	1.32	0.2936

In the case studied the difference in the isentropic exponent between the flue gases from natural gas and air blow gasification gas is 0.5%, this will, for the same pressure ratio

and firing temperature, increase the exhaust gas temperature by 10ºC for the bio gas. Figure 11 show how the isentropic exponent depends on the temperature of the flue gases.

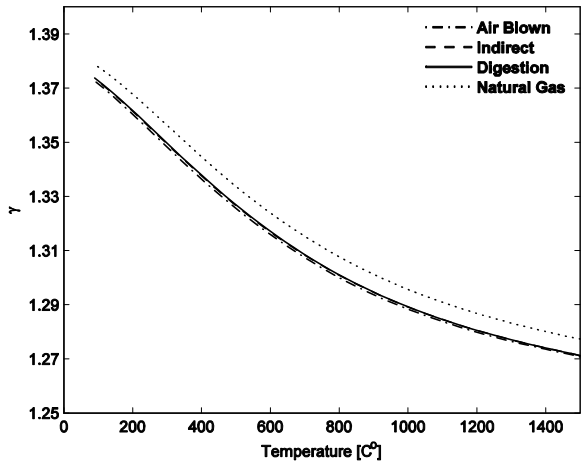

Figure 11: Isentropic exponent (γ) as function of flue gas temperature

Not only does the isentropic exponent differ for the flue gas when biofuel is fired, also the gas constant (R) deviates. The gas constant of the flue gas decreases with 2.1% for air blown, 1.4% for indirect and 1.2% for digestion. The combined effect of increased mass flow and higher density (through lower gas constant) still results in a higher volumetric flow and hence higher pressure drop in the HRSG. The higher back-pressure slightly reduces the increased expansion ratio through the gas turbine.

The increased temperature and mass flow of flue gas will increase the steam production without losing superheat temperature. Figure 12 shows how much the steam mass flow through the HPT will increase. The flow in the intermediate section will follow exactly the same trend.

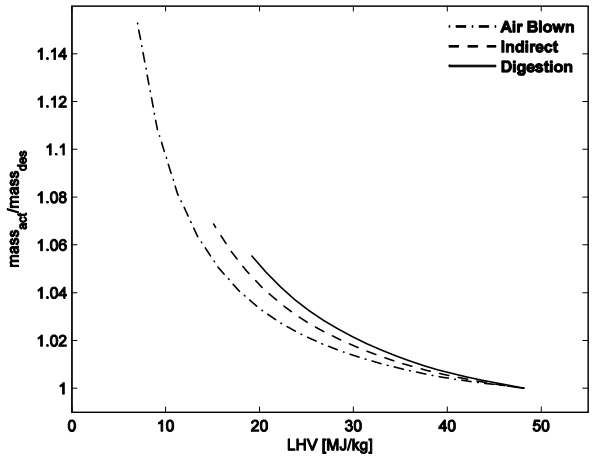

Figure 12: HPT mass flow increase as a function of LHV

As seen in equation 6 and 7, the pressure before a turbine section is, from a practical point of view, directly proportional to the passing mass flow. Figure 13 show how the pressure increases in front of the HPT. Again, the behavior of the intermediate section pressure level is following the same trend.

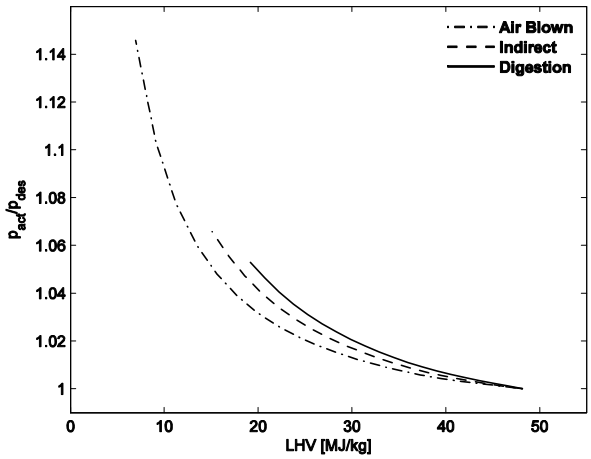

Figure 13: HPT pressure increase as a function of LHV

An increased pressure will alter e.g. the steam turbine thrust balance and it may not be practical to increase the admission pressure above the design point without modifications to the unit. In Cotton [15], there is an excerpt from GE (IEC 45) stating that one cannot increase the admission pressure without reducing the mass flow. This is, however, impractical in this case since one cannot run the steam turbine at de-rated flow without actually decreasing the admission pressure. The calculations show that the volumetric flow through the last LP-stages stays more or less constant, hence the leaving loss is unchanged. The section pressure ratios and hence isentropic heat drops stays at the same level and the section efficiency stays at the design level.

THE COMBINED CYCLE

As discussed, the output of the cycle will increase significantly if the engine is operated at its nominal firing temperature and IGV setting. If the engine is to be operated with the lowest fuel quality, the increase in output is some 25 percent. An increase of this magnitude is certainly outside the limits for an actual plant. A re-rating of a power plant, at this magnitude, is major and may result in other bottle necks like step-up transformers etc. Figure 14 shows the total cycle output as a function of LHV, this is the calculated result, and at some level the mechanical limitations will set a limit.

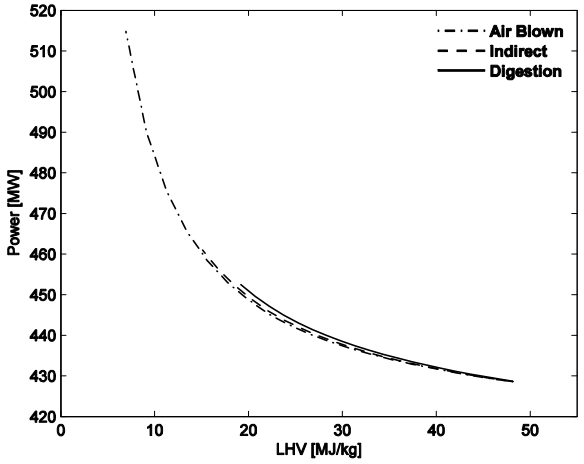

Figure 14: The total cycle output as a function of LHV

In Figure 15 the biofuel compression was not included, it is not obvious if this energy should be seen as a part of the fuel production or the power production side.

In Figure 15 the biofuel compression is included and the result looks quite differently compared to Figure 15. As mentioned before the gas constant differs greatly between the fuels, the indirect gasification gas has a much higher value making it more energy consuming to pressurize.

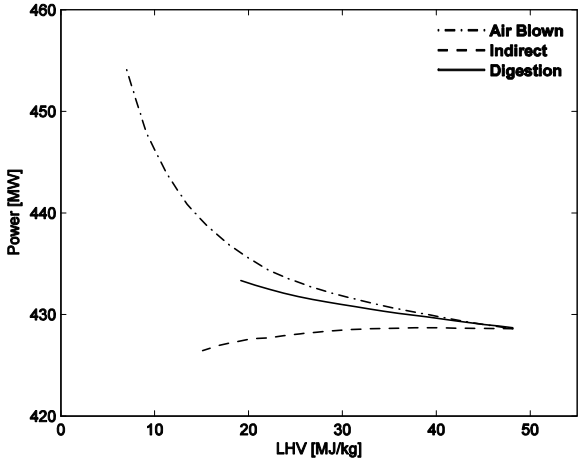

Figure 15: The total cycle output including the biofuel compression as a function of LHV

ANALYSIS

Most results indicate a rather mild response from having a low-calorific fuel down to 20 - 25 MJ/kg. Below this level the engine will experience a rather steep response in terms of drop in surge margin, engine thrust balance, power increase and associated shaft torque levels. The first manufacturer in figure 1 indicates that it should be possible to have a mixing ratio on the order of 40-60 percent depending on the fuel. This corresponds approximately to a fuel mix of 35 MJ/kg. The second indicates 85-100 percent depending on the fuel. The latter is, however, limited to the combustion section and does not reveal any data related to the complete gas turbine. If the bio gases are delivered unpressurised, the compression will consume a significant part of the gained power output.

The steam cycle will, in all cases, receive more energy as more inert ballast is introduced. This will increase the steam production, resulting in a higher steam pressure and more power produced. The flue gas composition and properties will change when different fuels are fired. Increased amount of CO_2 increases the gas constant R and decreases the isentropic exponent (γ). A reduced γ will lower the temperature drop over the expander and hence increase the flue gas temperature at the inlet to the HRSG. Moreover, the increased R will have a beneficial reduction of the pressure losses in the HRSG.

CONCLUSIONS

The results of this work indicate that it may be feasible to use low-calorific fuels or fuel mixes down to 20 - 25 MJ/kg without major modifications to the plant.

In the gas turbine, the distortion in mass flow between the compressor and turbine is a limiting factor. The compressor will be strained as the cycle pressure rises to allow for the larger flow through the turbine. Below a LHV of approximately 20 MJ/kg, the fuel mass flow increases dramatically which indicates that it is not realistic to operate a standard gas turbine below this level.

The calculated results are valid from a compressor stability point of view and do not state anything about the combustor, fuel system, shaft torque, fuel supply system or effects by impurities in the biofuel.

The bottoming cycle will be operated at an elevated power level at higher pressure levels. Both may be severe issues and the steam turbines may have to be re-designed for the new rating.

A pure biofuel plant of this size is probably not feasible and the actual calorific level is probably much higher hence alleviating some of the reported issues.

ACKNOWLEDGMENTS

The authors wish to acknowledge E·ON for supplying background material and funding for this research. The authors also acknowledge Dr Raik C. Orbay, Dr Andre Hildebrandt, Markus Truedsson and Marco Lorenz for the early development of the off-design models.

REFERENCES

[1] Orbay, R., C., Genrup, M., Eriksson P., Klingmann, J., "Off-Design Performance Investigation of a Low Calorific Value Gas Fired Generic-Type Single-Shaft Gas Turbine", Journal of Engineering for Gas Turbines and Power, May 2008, Vol 130

[2] Eriksson, P., Genrup, M., Jonshagen, K., Klingmann, J., ”Off-Design Performance Investigation of a Low Calorific Value Gas Fired Two-Shaft Gas Turbine” ASME TURBO EXPO 2009, Orlando, USA

[3] Moliere, M., “Benefiting From the Wide Fuel Capability of Gas Turbines: a Review of Application Opportunities”, GT-2002-30017, ASME TURBO EXPO 2002, Amsterdam, The Netherlands

[4] Rodrigues, M., Walter, A., Faaij, A., “Performance evaluation of atmospheric biomass integrated gasifier combined cycle systems under different strategies for the use of low calorific gases” Energy and Management 48 (2007) 1289-1301

[5] D.M. Todd, “Gas Turbine Improvments Enhance IGCC Viability” 2000 Gasification Technologies Conference San Fransisco, California, October 8 – 11, 2000

[6] M.S. Johnson, “Prediction of Gas Turbine On- and Off-Design Performance When Firing Coal-Derived Syngas” Journal of engineering for gas turbine and power, April 1992, Vol. 114 / 385

[7] Gülen, S. C., Griffin, P. R., Paolucci, S., “Real-Time On-Line Performance Diagnostics of Heavy-Duty Industrial Gas Turbines” Journal of Engineering for Gas Turbines and Power, October 2002, Vol. 124 / 911

[8] Möller, B. F., Genrup, M., Assadi, M., “On the off-design of a natural gas-fired combined cycle with CO2 capture”, Energy 32 (2007) 353–359, Elsevier, October 2005

[9] Wennerstrom, A., J., “Design of highly loaded axial-flow fans and compressors”, 2000, Concepts ETI, Inc. ISBN 0-933283-11-3

[10] Walsh, P.P., Fletcher, P., “Gas Turbine Performance 2nd ed.”, 2004, Blackwell Science Ltd. ISBN 0-632-06434-X

[11] Bitterlich, W., Ausmeier, S., Lohmann, U., “Gasturbinen und gasturbinenanlagen – Darstellung und berechnung”, 2002, B.G. Teubner GmbH, ISBN 3-519-00384-8

[12] Japikse, D., Baines, C., N., Zelesky F.,M., Moustapha, H., “Axial and radial turbines” 2003, Concepts NREC, ISBN 0-933283-12-0

[13] Cordes, G., “Strömungstechnik der gasbeaufschlagen Axialturbine”, 1963, Springer-Verlag

[14] Schobeiri M., “Turbomachinery Flow Physics and Dynamic Performance”, 2005, Springer Berlin Heidelberg New York, ISBN 3-540-22368-1

[15] Cotton, K.C. “Evaluating and Improving Steam Turbine Performance 2nd ed.”, 1998, Cotton Fact Inc., ISBN 0-9639955-1-0

VI

Energy 35 (2010) 1694–1700

Contents lists available at ScienceDirect

Energy

journal homepage: www.elsevier.com/locate/energy

Improved load control for a steam cycle combined heat and power plant

K. Jonshagen*, M. Genrup

Department of Energy Sciences, Lund University, P.O. Box 118, SE 22100, Sweden

ARTICLE INFO

Article history:
Received 31 October 2008
Received in revised form
9 December 2009
Accepted 14 December 2009
Available online 18 January 2010

Keywords:
Partial arc control
Sliding pressure control
Hybrid control
CHP

ABSTRACT

The problem of optimum load control of steam power plants has been dealt within many technical papers during the last decades. Deregulation of the power markets and close to the (bio-) fuel source thinking has lead to a trend of small scale combined heat and power plants. These plants are usually operated according to the heat demand and therefore they spend a significant time on partial load. The load control of such plants is in general done by partial arc control. This work applies a hybrid control strategy, which is a combination of partial arc control and sliding pressure control. The method achieves further improvement in performance at partial load. Hybrid control itself is not novel and has earlier been used on traditional coal-fired condensing plants. This has, to the author's knowledge, not earlier been applied on combined heat and power plants. The results show that there is a potential for improved electricity production at a significant part of the load range.

1. Introduction

Steam cycle based combined heat and power (CHP) plants achieve total efficiencies of about 90 percent. Efficient heat utilization is achieved by producing superheated steam which is converted into electric power and later on condensed in a hot water condenser supplying heat to a district heating (DH) network. Typically, a small or midsized CHP plant has no cold condensing tail and cannot be operated at any other load level other than dictated by the heat demand. This means that the turbine is governed by the heat requirement and will spend a significant part of its operation at partial load. It is therefore common practice to have partial arc admission to provide some relief. The reason for this is discussed in detail in a later section. Basically, this results in less throttling losses compared to a single valve unit at part load. The situation is reversed at the full load (the normal design point) where the single valve unit has a higher efficiency compared to the partial arc admission turbine.

When operated at partial load, the steam flow through the unit is reduced. There are several practical methods available to reduce the flow. However, whatever the method, two fundamental conditions, less pressure or reduced flow area, are applicable. One important parameter for a CHP plant is the power to heat ratio (α – value) which is more relevant than the electrical efficiency. The α – value is suitable for plants where the focus is directed towards heat production and hence a convenient gauge of how much electricity could be produced per unit of heat.

This study aims to improve the α – value at partial load operation for a typical Nordic CHP plant by combining partial arc control and sliding pressure control. This combination is referred to as hybrid control and is briefly discussed in [1] and [2]. Reference [3] applies hybrid control to large-sized coal fired power units. In reference [4] a comparison of throttle control and sliding pressure control in terms of exergy is performed on a 210 MW coal fired unit. Reference [5] uses the first and second law of thermodynamics to show the benefits of hybrid control mode. However, none of the previous references are applied on district heating units.

2. The plant

The calculations are performed on a 25 MW_{el} biomass fueled CHP in Enköping, Sweden, the configuration and size of this plant is of a standard type and the result is applicable to other small/midsized CHP plants. A typical layout for a plant of this size is shown in Fig. 1. The condenser is normally split into 2 units at different pressure levels in order to obtain flexible and efficient heat utilization, see Fig. 2. The preheating consists of a mixing-heater after the condenser followed by a low-pressure preheater, a deaerator and a high-pressure preheater. The final feed water temperature for the specific plant is slightly higher than 200 °C at full load.

3. Partial arc control

Partial arc admission has been used ever since the pioneering work by deLaval for improving partial load performance. This

* Corresponding author. Tel.: +46 462224771; fax: +46 462224717.
E-mail addresses: klas.jonshagen@energy.lth.se (K. Jonshagen), magnus.genrup@energy.lth.se (M. Genrup).

0360-5442/$ – see front matter © 2009 Elsevier Ltd. All rights reserved.
doi:10.1016/j.energy.2009.12.019

Nomenclature

A	Area [m^2]
C_T	Turbine constant [m^2]
C	Absolute Velocity [m/s]
k_v	Loading correction [-]
$\dot{m}$	Mass flow [kg/s]
n	Polytropic exponent [-]
n_{stg}	Number of stages [-]
p	Pressure [Pa]
u	Rotor Periphery Speed [m/s]
w	Relative velocity [m/s]
α	Power to heat rate [-]
$\bar{\lambda}$	Stage number correction factor [-]
π	Pressure drop [-]
κ	Isentropic exponent [-]
υ	Specific volume [m^3/kg]
μ	Stage loading [-]

Abbreviations

CHP	Combined Heat and Power
C-stage	Control Stage
DH	District Heating
FWT/DEAE	Feed Water Tank/Deaerator
G	Generator
HP	High Pressure Turbine
LP	Low Pressure Turbine
MW	Megawatt

Index

1	Rotor inlet
2	Rotor Outlet
i	Turbine section inlet
j	Turbine section outlet
avg	average
th	Thermal
el	electricity

method controls the steam admittance into the turbine control stage with several valves (usually 4) operating in a special sequence. The first stage stationary blades are divided into a number of sections or arcs each controlled by a valve as illustrated in Fig. 3. The control stage is of an impulse design type, i.e. the entire pressure drop for the stage occurs in the stator. This minimizes the circumferential pressure gradient in the rotor allowing the flow from each arc to pass the rotor relatively unmixed. The impulse design will also keep the unsteady forces, from passing in or out from the admitted sectors on the rotor, at a reasonable level.

The steam flow in each arc is controlled by the control valves, which are shut sequentially. When the first valve is fully closed, the second one closes and finally the two remaining ones are closed simultaneously to limit the forces to the shaft [2].

Partial arc control requires good valve authority, therefore the absolute loading, i.e. enthalpy drop, is typically higher than for a normal repeating stage. For maintaining the stage loading ($\Delta h_0/u^2$), a higher radius is required compared to the rest of the high pressure section. An additional advantage is that the resulting rapid drop in pressure gives a lower temperature at the following stages. This means that the steam temperature can be increased from typically 500–520 °C to approximately 540 °C without introducing advanced materials. A normal control stage typically has lower efficiency than an intermediate stage. Low reaction will result in low rotor acceleration and hence higher secondary loss. There also will be aerodynamic losses associated with the sectors, namely filling- and ventilation losses. Filling losses are the momentum loss that occurs when the rotor passage is filled with steam. The ventilation losses are when the rotor passes the void sectors with no flow which sets up complex unsteady flow structures and recompresses the steam. Other losses include disc ventilation and "swan neck" loss. The latter is due to the change in radius and associated wet surface at high velocity levels. There is also a strong pressure gradient upstream the first repeating stage due to the streamline curvature. When adding up the different losses associated with a control stage, one can expect some 10 percent lower stage efficiency compared to the first "normal" stage.

Initially when a valve begins to close, the throttled flow is a relative large part of the total mass flow, since when the first valve starts to close, 25 percent of the total mass flow flows through this

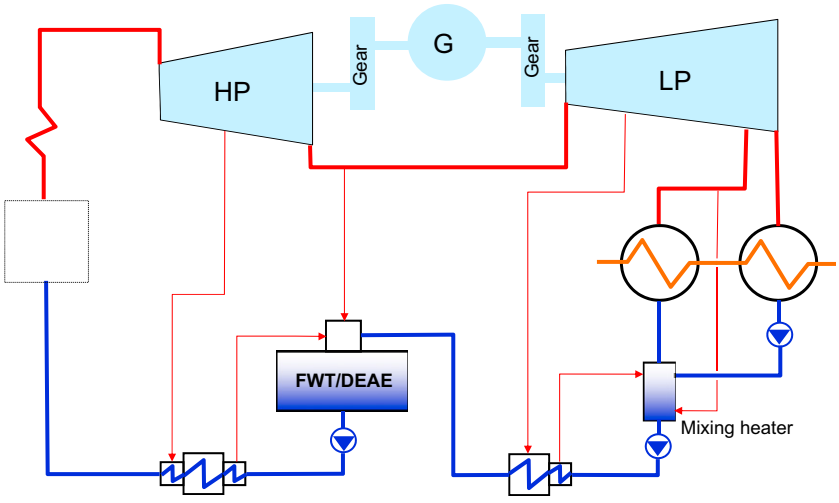

Fig. 1. Typical CHP plant layout.

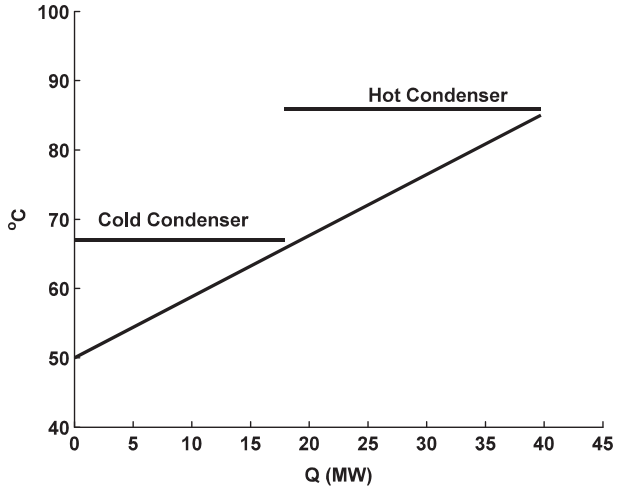

Fig. 2. Condensers Heat–Temperature diagram.

section. As the valve reduces the flow, the throttled flow represents less and less of the total flow. Hence, the influence of the throttling losses is great when a valve starts to close, but decreases as the flow diminishes. This effect is to be balanced with the higher throttle loss when the valve pressure drop increases. These two effects combined gives the typical form of the efficiency vs. flow (or load) curve. When the two first valves have been closed, the remaining two valves close simultaneously in order to keep the shaft force even. This behavior is the same as for normal throttling control.

Partial arc admission can be thought of as an effective means of controlling the admission area to the turbine, whilst maintaining the pressure. [6].

4. Sliding pressure control

In contrast to the partial arc control, sliding pressure control lowers the admission pressure (at constant admission area) in order to control the flow to the turbine.

This will, to a first approximation, maintain the volumetric flow constant without additional throttling losses in the cycle. The method reduces the boiler pressure, i.e. the control stage inlet pressure, with maintained temperature at part loads which results in a more stable volumetric flow. This is beneficial for the isentropic turbine efficiency. By virtue of having lower cycle pressure, the feed pump power will be reduced. For this particular case, at 50 percent load the feed water pump has almost 40 percent less power consumption compared to partial arc control.

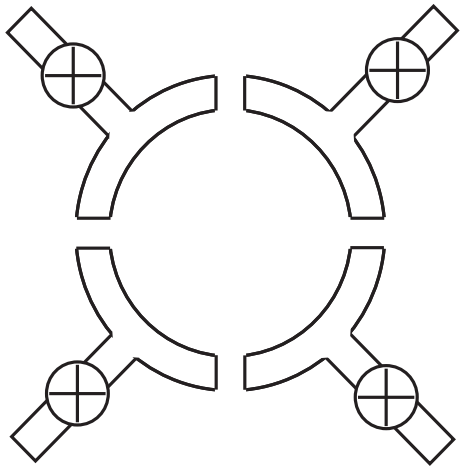

Fig. 3. Schematic representation of the four arcs upstream of the controlling stage.

Reducing the boiler pressure has the draw-back of decreasing the mean temperature of heat supply to the cycle. This has a negative effect on the steam cycle efficiency.

Sliding pressure mode introduces issues related to the boiler pressure, or specifically, the gradients in steam pressure. Normally this has to be constrained to an appropriate level in order not to disturb the boiler circulation or introduce extensive carry-over of impurities like silica oxide etc. This makes the control method slower compared to partial arc control and instant load changes are not possible.

5. Modeling of turbine capacity

The calculations in this work are performed in the commercially available heat- and mass balance program IPSEpro [7]. This section describes the main equations used for the modeling.

The empirical Stodola steam cone rule in this form is usually applied:

$$\dot{m}_{i-j} = C_{T,i-j}\cdot\sqrt{\frac{p_i^2 - p_j^2}{p_i v_i}} = C_{T,i-j}\cdot\sqrt{\frac{p_i}{v_i}}\cdot\sqrt{1-\frac{1}{\left(p_i/p_j\right)^2}} \tag{1}$$

$$\dot{m}_{i-j} = C_{T,i-j}\cdot\sqrt{\frac{p_i}{v_i}} \tag{2}$$

The turbine constant, C_T, can be thought of as an equivalent area and has the unit square meter. Equation (1) has been widely used to describe the relation between flow and pressure. It can be reduced to eq. (2) if $p_i >> p_j$, which is normally the case for condensing turbines. The pressure ratio over a non-reheat steam turbine train may be as high as 3500:1. Equation (1) will not work very well for highly loaded or choked stages, since it cannot accurately model the capacity. Beckmann [8] resolved this and improved the results substantially for single stages or high-loaded sections. This approach is more involved, but is better at taking into account when the turbine gets choked as a function of polytropic exponent (n)[1], number of stages (n_{stg}), stage loading[2] and pressure ratio:

$$\dot{m}_{i-j} = C_{T,B}(1+\mu)\cdot\sqrt{\frac{p_i}{v_i\mu}F} \tag{3}$$

$$F = \frac{n}{n+1}\left\{1-\left[1+\frac{2\bar{\lambda}}{n-1}\right]\left(\frac{p_i}{p_j}\right)^{-\frac{n+1}{n}} - \left[1-\frac{n+1}{n-1}\left(\frac{p_i}{p_j}\right)^{-\frac{2}{n}}\right]\bar{\lambda}\right\} \tag{4}$$

$$\bar{\lambda} = f\left(n_{stg}\right) \tag{5}$$

Fig. 4 shows the comparison between the two models when the stages within the section are lightly loaded and the agreement is fairly good. The agreement for a highly loaded section is poorer, as seen in Fig. 5. The reader is referred to the authoritative textbook by Cordes [9] for an exhaustive treatment. Most off-design modeling is done at a level where partial turbines are calculated instead of

[1] $n = \ln(p_i/p_j)/\ln(v_j/v_i)$.

[2] $\mu = -\int v dp/u^2 \approx \Delta h/\eta_{pol}\cdot u^2$.

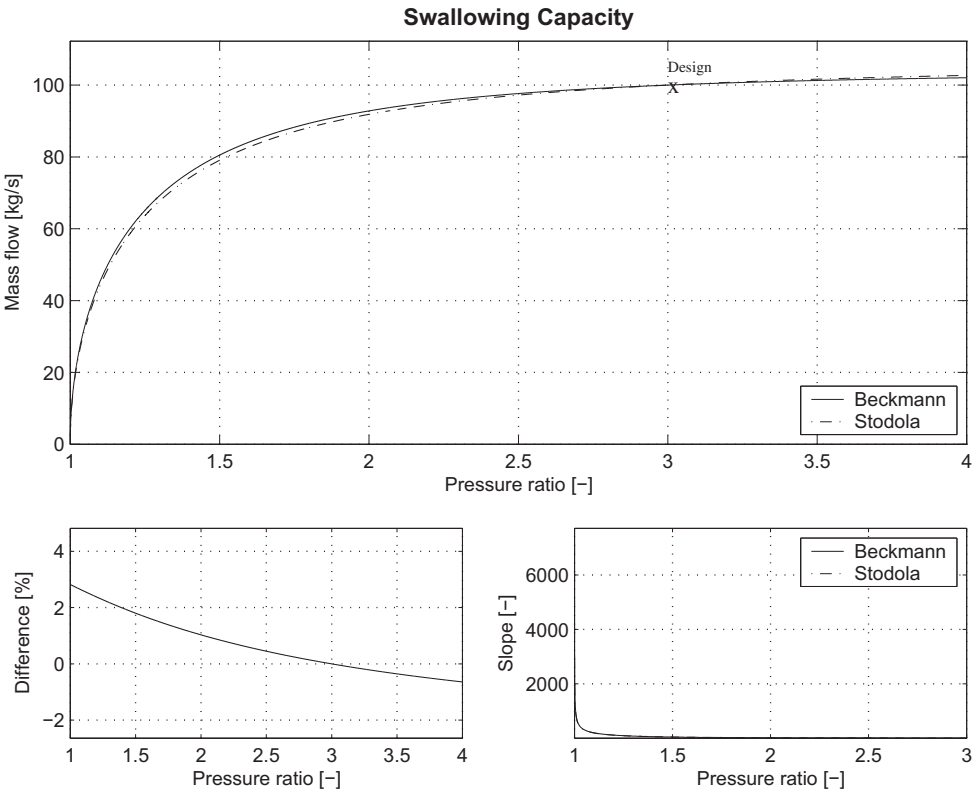

Fig. 4. Comparison between the Stodola cone rule and the more advanced Beckmann model for lightely loaded stages (stage pressure ratio approx 1.25).

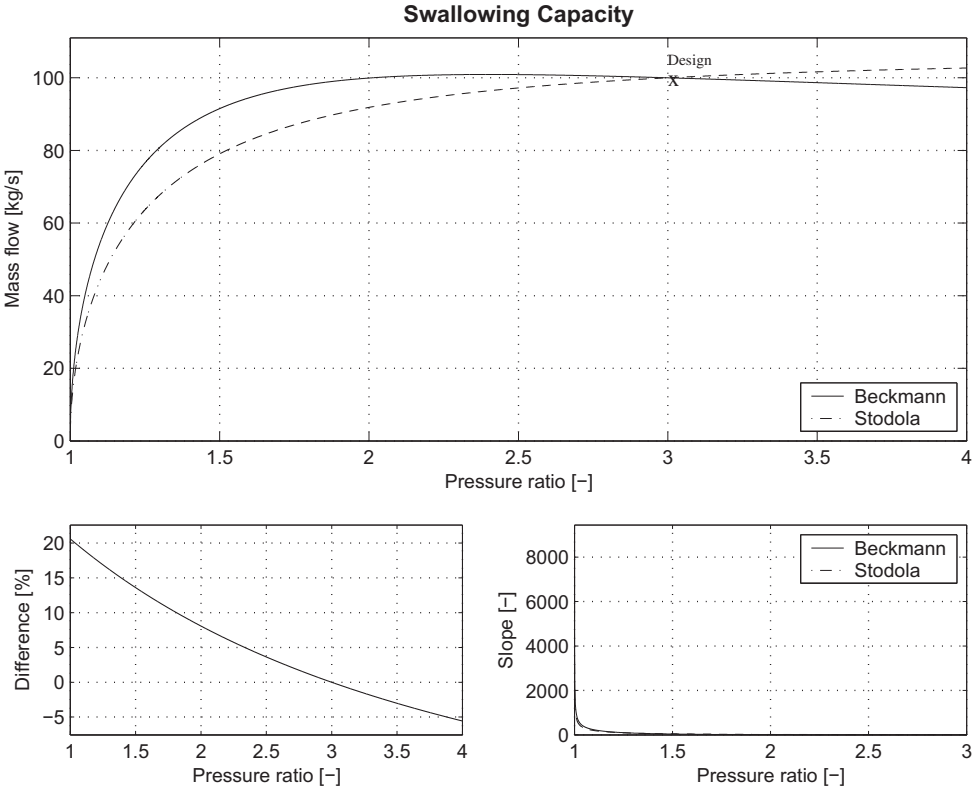

Fig. 5. Comparison between the Stodola cone rule and the more advanced Beckmann model for a highly loaded stage (stage pressure ratio approx. 3).

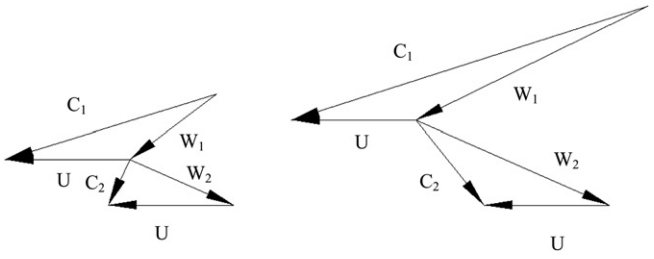

Fig. 6. Single-row control stage at design load (left) and approximately half turbine output (right).

individual stages. A partial turbine is a group of stages (typically n-stages) between two extraction/induction points. The situation is even better at higher pressure ratios such as those encountered if whole cylinders are calculated.

The capacity eq. (3) sets the pressure at the inlet of each turbine section and thus the isentropic enthalpy drop for each section. The Parson number ($\sum u^2/\Delta h_s$) is determined if speed and isentropic enthalpy drop are known and hence it is possible to calculate the efficiency. Since the outlet pressure is more or less fixed by the heat sink and condenser surface, all pressures in the turbine develop from the condenser. By adopting this principle, one can show that the isentropic enthalpy drop is more or less constant for all stages except the last. One other convenient feature is that the section efficiency is close to constant since the isentropic enthalpy drop and speed are constant. This reasoning leads to three types of steam turbine stages:

Control stage with varying pressure drop/efficiency
Single stages with constant pressure drop/efficiency
Final stage with varying pressure drop/efficiency

The rather large temperature span in district heating systems may reduce the efficiency loss in the last stage. The reason for this is the coupling between the lower pressures at lower temperatures at reduced heat load, causing the volume flow to be less affected compared to a condensing unit.

The control stage has, in a sense, a variable admission area and will therefore have a large variation in enthalpy drop. The pressure after the rotor will be proportional to the mass flow passing to the next turbine section. For example, if the mass flow is reduced to half the level the pressure is reduced in the same manner and hence the pressure drop in the admitted arcs is doubled. Fig. 6 shows the velocity triangles at full and 50 percent flow, respectively. The left hand triangle shows the full load point where the stage is lightly loaded ($\Delta h_0/u^2 = 1.5$, $\mathrm{Ma}_1 = 0.65$). The figure to the right shows the 50 percent flow case which is heavily loaded and choked ($\Delta h_0/u^2 = 3.4$, $\mathrm{Ma}_1 = 1.16$). The reason for this is that the pressure before the second stage decreases as the mass flow decrease in accordance with Eq. (2). Therefore the control stage pressure ratio and hence Δh_0 increase.

The best approach for modeling the control stage is to calculate the loading for each arc separately and then to use a mass flow weighted average. The design point efficiency of a control stage is typically in the range of 65–75 percent. Kostyuk and Frolov [10] present a correlation for calculating the efficiency of single-row control stages, based on statistical data:

$$\eta_{C-\mathrm{Stage}} = k_\nu \left(0.83 - \frac{2\cdot 10^{-4}}{\dot{m}}\sqrt{\frac{p}{\nu}}\right) \tag{6}$$

Where k_ν is a convex function of deviation from optimum stage loading.

6. Hybrid control

Both partial arc control and sliding pressure control have drawbacks in terms of efficiency and there is a potential gain in combining the methods. If they are combined to avoid both throttling- and elevated control stage velocity level simultaneously, then the performance can be improved. This combination is referred to as hybrid control mode.

Partial arc suffers from throttling losses whilst sliding pressure operation suffers from decreased thermal efficiency due to a reduced average temperature of heat addition to the cycle.

The losses in a valve are proportional to the pressure ratio over it. When the pressure ratio decreases, the mass flow will be reduced and the loss has less influence. Hence, at a certain point the pressure loss will peak. The points where no valves are partly closed i.e. all valves are either fully open or closed are called the valve points. At the valve points there will be no throttling losses and at these loads partial arc control achieves superior efficiencies.

The thermal efficiency of a Rankine cycle benefits from a high mean temperature of heat addition, $T_{\mathrm{Hot,\ avg}}$. In a Rankine cycle the mean temperature of heat addition is coupled to the pressure at which the heat addition occurs. Therefore, a decreased pressure will decrease the $T_{\mathrm{Hot,\ avg}}$ which in turn means that sliding pressure control reduces the cycle thermal efficiency potential.

In accordance with eq. (2) the pressure after the control stage decreases as the mass flow is reduced. Therefore, the pressure drop over the open arcs in the control stage will increase when reducing the load with partial arc control. This results in a low Parson number and therefore a reduced efficiency. If hybrid control is used, the pressure drop will decrease again when sliding pressure mode is adopted.

The α – value as a function of heat load is plotted in Fig. 7 where partial arc control and sliding pressure from each valve point is shown. The load curve of partial arc control is characterized by the throttling losses, where the discontinuities represent a valve point. At each valve point a new sliding pressure curve is initiated. Note that the last valve point represents where the final two valves are closed simultaneously in order to even out the shaft forces.

The expansion process at 70 percent heat load for regular partial arc mode and hybrid control from the first valve point is plotted in a Mollier-chart shown in Fig. 8. For the partial arc case (black) the second valve is partially closed (dotted) and valve 3 and 4 are open. After the control stage the flows are mixed before further expansion. For the sliding pressure case (red) the admittance pressure have been reduced with maintained temperature.

It can be shown that increased entropy at the control stage will manifest itself as a lower loss at the turbine exhaust. The relation between loss and increased entropy, at constant pressure, is given by the equation: $\Delta h_{\mathrm{loss}} = T\cdot\Delta S$. The behavior can be explained by the slope of the pressure lines in the Mollier-chart. This can be thought of as having the same increase in entropy at the turbine exhaust and expressing the loss ratio as:

$$\frac{\Delta h_{\mathrm{loss,exhaust}}}{\Delta h_{\mathrm{loss,control\ stage}}} = \frac{T_{\mathrm{exhaust}}}{T_{\mathrm{control\ stage}}} \tag{7}$$

For a certain district heating load, the DH-supply temperature is fixed and hence the hot condenser temperature is fixed. If the exhaust steam is saturated, which is the normal case, this results in that the condenser pressure is also fixed. Due to the larger enthalpy drop in the control stage for partial arc control the steam entering the condensers lower enthalpy compared with sliding pressure control (see Fig. 8). The effect of this is that for a certain heat load a larger mass and therefore slightly more fuel is required. Also, the distribution between the cold and hot condenser is shifted to the

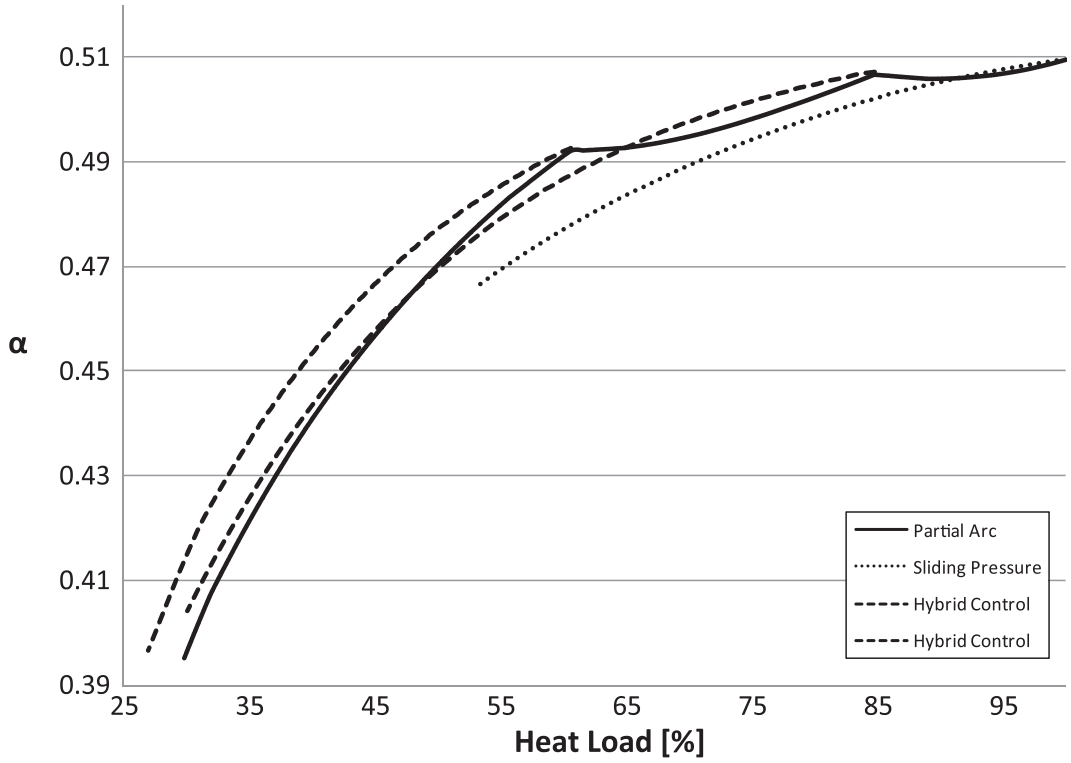

Fig. 7. Load curves for partial arc, sliding pressure and hybrid mode.

hotter side, hence relatively less steam flows through the final turbine stage. However, as shown in Eq. (7), a loss in the high pressure section is much smaller than in the low-pressure section and the difference in condenser flows is very small.

Sliding pressure control does not handle instant load changes due to the inertia of the boiler. By initially reducing the load by closing the first control valve and then switching to sliding pressure control, the closed valve gives the possibility to instantly increase the load without affecting the boiler pressure level.

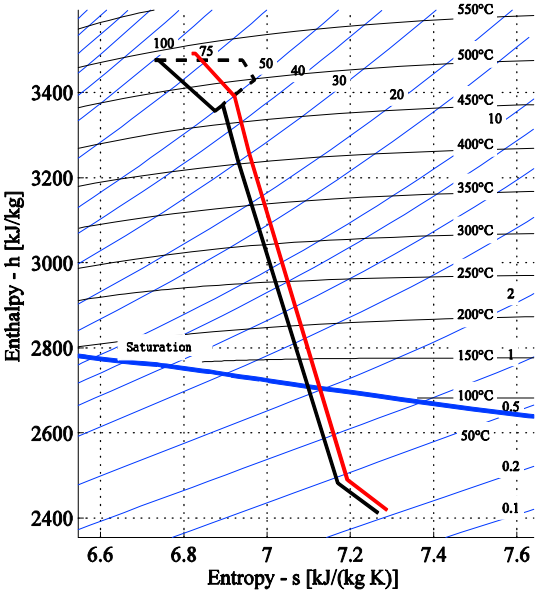

Fig. 8. Mollier-chart with the expansion at 70 percent heat load. The black line is partial arc control and the red represents hybrid control.

7. Analysis

By virtue of its design and operational philosophy, the amount of power produced is determined by the heat sink, i.e. the district heating load. Hence, an increased power to heat ratio increases the produced electricity – an indeed valuable commodity.

The load curve in Fig. 7 shows that there is a gain from changing to sliding pressure at each valve point. At full load the gain of sliding pressure only last for a short load period and thereafter it quickly falls below partial arc control. At the second valve point the gain is greater and last further down in the load range. It is suggested that sliding pressure should be used in this operating window and when the load decreases below the point where the load curves intersect the boiler should be brought up to full pressure and the second valve should be used to reduce the load. At the last valve point where the two remaining valves close simultaneously it is always advantageous to adopt sliding pressure control.

8. Conclusions

- Hybrid control increases the power to heat ratio in a significant part of the load range.
- Hybrid control offers a faster load response than a normal sliding pressure plant.
- Hybrid control will reduce the cyclic stresses from passing through the admitted and non-admitted sectors.

References

[1] Couchman RS, Robbins KE, Schofield PGE. Steam turbine design philosophy and technology programs, report no 3705. Schenectady, NY: GE Company; 1991.
[2] Cotton KC. Evaluating and improving steam turbine performance. 2nd ed. New York: Cotton Fact Inc.; 1998.

[3] Zhang C-F, Li Y-L, Wang H-J, Zhang B, Xie F, Huang Y. In: Selection of the optimal steam pressure for coal-fired power units, vol. 3. Guangzhou, China: ICMLC; 2005. p. 1835–8.
[4] Sengupta S, Datta A, Duttagupta S. Exergy analysis of a coal-based 210 MW thermal power plant. International Journal of Energy Research 2007;31(1): 14–28.
[5] Weber GE, Woek WM. Sliding pressure analysis using the second law. Heat Recovery Systes & CHP 1993;13(3):253–60.
[6] Fridh J. Partial admission in axial turbines, Report no. HPT/KTH 03/2003 [available at]. Stockholm, Sweden: Dept. of Energy Technology Div. of Heat and Power, http://www.energy.kth.se/index.asp?pnr=10&ID=188&lang=1; 2002.
[7] IPSEpro by SimTech Simulation Technology, Austria. Information [available at], http://www.simtechnology.com.
[8] Beckmann G. Eine allgemeine Theorie der Mengendruckgleichung. PhD-thesis, Technisches Universität Dresden; 1961.
[9] Cordes W. Strömungstechnik des gasbeaufschlagen Axialturbine. Springer Verlag; 1963.
[10] Kostyuk A, Frolov V. In: English, editor. Steam and gas turbines. Moscow: Mir Publishers; 1988.

VII

22nd International Conference on Efficiency, Cost, Optimization
Simulation and Environmental Impact of Energy Systems
August 31 – September 3, 2009, Foz do Iguaçu, Paraná, Brazil

Improved Load Control Strategy for Large Sized Combined Cycles

Klas Jonshagen, klas.jonshagen@energy.lth.se
Magnus Genrup, magnus.genrup@energy.lth.se
Department of Energy Sciences, Lund University, P.O. Box 118, SE-221 00 Lund, Sweden

Pontus Eriksson, pontus.eriksson@volvo.com
Volvo Powertrain, Sweden

Abstract. *The load of a single-shaft unit is usually controlled by the firing level and the engine mass flow, in concert. The mass flow is controlled by the variable inlet guide vanes (VIGV) setting, where one can control the axial velocity into the first stage of the compressor. The reduced compressor air flow and hence engine pressure ratio results in a higher exhaust gas temperature (EGT). A reduced firing temperature mainly reduces the power density. Life of hot section will, however, improve. A reduction in firing also have an influence on the emission performance and one can expect to have higher CO and, in some cases, increased NO_x. The latter is due to the relative increased pilot burner level to maintain stability.*
The widespread method of controlling the load of combined cycles is to use the VIGV's down to a certain load-point where maximum EGT is reached. From this threshold value, the firing temperature has to be reduced to limit the EGT, as the VIGV continues to close. At some low-load point the VIGV has reached its maximum setting and the load can only be controlled by the firing level towards idle. The vice-versa is applicable when the unit is brought up in load. This method gives good combined cycle part-load efficiency and is well-established in the gas turbine community.
Most steam turbines in this frame size are designed for a maximum admission of 565 °C and cannot be operated at elevated levels for more than very short periods. Hence, there is no margin in steam temperature from the mentioned design case and the increased EGT cannot be utilized in the steam turbine. Instead, the common practice is to use spray coolers between the super-heaters to limit the value at the nominal.
The benefit from the previously mentioned control strategy is eclipsed by the limitation in admission temperature. Instead, it is suggested to use the steam admission temperature, rather than the EGT, to set the firing in the gas turbine. The performance impact from having a lower EGT is indeed very small and one can maintain, more or less, the same performance and gain significant gas turbine hot component lifing. This is due to the fact that a fixed-speed unit will keep the same blading centrifugal stress levels regardless of the power level but at a lower temperature, hence less risk of oxidation and creep. The results indicated a efficiency drop on the order of 0.2 %-units.
The work is based on an in-house advanced off-design model within the software package IPSEpro.

Keywords*: Combined Cycle, Load control, Spray, Lifing*

1. INTRODUCTION

Combined-cycle power plants (CCPP) have low investment cost and short construction times compared to large coal fired stations and even more so compared with nuclear plants. This is an important factor in today's deregulated electric power market, where high investment cost is connected to a larger risk. CCPP also are benefit from their high efficiency and low environmental impact, especially if they are fired with natural gas. It is easier to get permission to build and operate a plant that emits less CO_2 per unit power. (Kehlhofer, et al. 1999)

Typically a power generation mix consists of a base including nuclear power plants and / or large coal fired power plants. Above this base the CCPP's are to be found. Above the CCPP's usually diesel engines and gas turbines handle the peak loads (Vuorinen 2009). Not operating as the base of the power generation mix makes the load of CCPP's vary widely and they will spend a great amount of their operational life time under part load conditions. Hence the load control strategy is of great importance.

Key parameters for successful power plant operation are; fuel burn and CO_2-emission and maintenance costs. A high efficiency plant has lower fuel burn, hence lower operational costs and less CO_2-fee. The driver for gas turbine efficiency is mainly pressure ratio, whilst a combined cycle unit requires high exhaust temperature for optimum cycle performance. These two cycle requirements renders in high firing level and hot components. The dominating turbine failure mechanisms are creep and hot corrosion, which both are heavily temperature dependent. This dependency is highly non-linear and a modern unit is typically operated at levels where the slopes are steep. A state-of-the-art engine is therefore quite delicate in terms of hot-section component lifing, with high replacement costs.

A path for reducing maintenance without an efficiency penalty should provide relief for the operating economics. With this in mind a novel part load strategy for CCPP's is studied at the department of Energy Sciences at Lund University. The strategy was first introduced by (Fredriksson-Möller, et al., 2005) and with this work the purpose is to test its feasibility in a regular CCPP.

2. NOMENCLATURE

Annulus Area	A	[m^2]
Constants	a,b,c	[-]
Blade stagger angel	ξ	[°]
Difference	Δ, δ	[-]
Efficiency	η	[-]
Heat transfer	Q	[kW/s]
Maintenance factor	M_f	[-]
Mass flow	$\dot{m}$	[kg/s]
Pressure Ratio	π	[-]
Shaft speed	N	[s^{-1}]
Specific Heat	C_p	[J/(kg·K)]

2.1. Abbreviations and acronyms

CCPP	Combined Cycle Power Plant
COT	Combustor Outlet Temperature
EGT	Exhaust Gas Temperature
GT	Gas Turbine
HRSG	Heat Recovery Steam Generator
HP	High Pressure
LP	Low Pressure
OEM	Original Equipment Manufacturer
SHT	Steam Superheating Temperature
VIGV	Variable Inlet Guide Vanes

2.2. Subscript and superscript

*	Normalized to ISO conditions
CHIC	Compressor Characteristics
rel	Relative

3. THE COMBINED CYCLE

The combined cycle power plant (CCPP) which is used as the basis for this work consist of a GE Frame-9 gas turbine and a standard three-pressure reheat (three admissions) steam turbine from Alstom. The cycle has no separate feedwater tank and the feedwater is degassed in the condenser and the low-pressure drum. The latter is posing limits in terms of temperature difference between the saturation level at the LP-pressure and the feedwater after the first economizer. There is a minimum LP drum pressure for good deaeration and the approach temperature should be at least 11°C. To control the superheat temperatures water from after the high - and intermediate-pressure feedwater pumps is sprayed in to the steam before the final superheaters of respectively pressure.

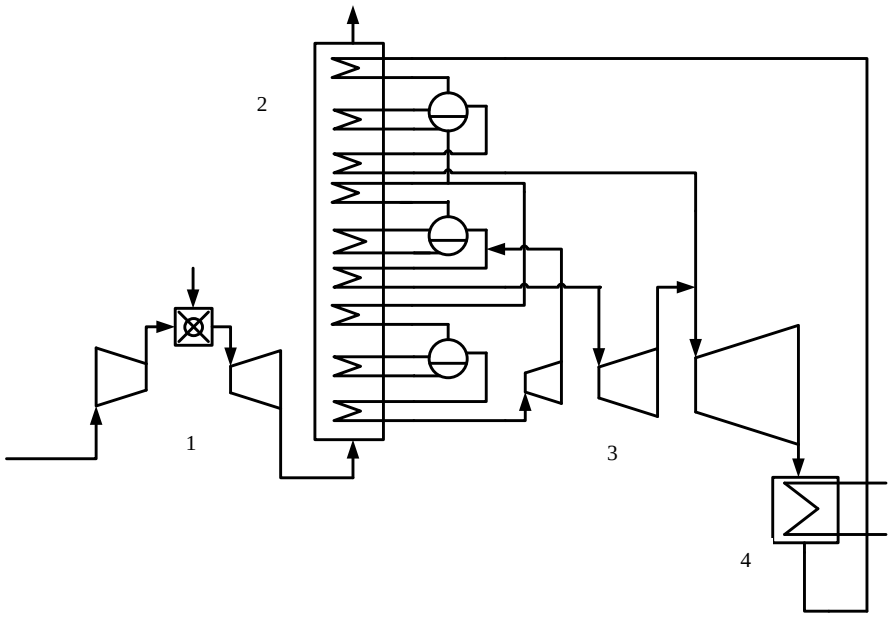

1. *Gas Turbine*
2. *HRSG*
3. *Three pressure Steam Turbine*
4. *Condenser*

Figure 1: Schematic figure of the plant

3.1 The gas turbine

The gas turbine is a General Electric Frame-9, a 300MW single shaft machine. The gas turbine is, by virtue of its size, directly connected to a 50 Hz generator running at a fixed speed of 3000 rpm. The exact details for the GE unit are not published but the model is based on available data. The compressor and turbine characteristics are normally not available outside the OEM's domains. In this case, the compressor map is based on a publication by General Electric (Gülen, et al., 2002). The map is actually for a Frame 7 unit, which is the 60 Hz version of the Frame 9 type. It is assumed that the Frame 9 compressor is a direct scale-up of the smaller Frame 7. There are only relative values on the published characteristics and the reference points are assumed to be the same for both cases and the actual values are based on the ISO condition. The used isentropic efficiency is based on an assumed polytropic design efficiency of 90 percent.

3.2 The calculation model

The calculations in this work have been performed with the commercially available heat and mass balance program IPSEpro. The off-design model consists of modified standard components and specially designed components developed at the division of thermal power engineering at Lund University. Gas turbine modeling is described in (Walsh, et al., 2004) this particular CCPP model is described in detail in (Jonshagen, et al., 2009).

The gas turbine is modeled with the refereed parameter groups on the rigorous form (in a sense that γ and R are included). This gives the possibility to calculate component performance under a wide range of operational conditions, i.e. changing media compositions.

The basis for the compressor model is either a generic- or a certain non-dimensional map, which can be parameterized for the specific engine. As mentioned earlier, the compressor map is based on a GE publication and should be more accurate than a generic map. The usage of generic maps may render in accuracy issues and should be

avoided when possible. Providing design levels parameterizes the map, where values of unity represent design values of: normalized flow, efficiency, pressure ratio and aerodynamic speed. The off-design calculation is highly recursive since all components have to be matched together to form a gas turbine unit. On a more detailed level, each point in the maps represents unique velocity triangles (based on Mach number). Hence, the aero-thermal behavior of the compressor and turbine is set if two dimensionless parameters are known for each of them. In order to avoid separate maps for each VIGV setting, influence coefficients are introduced. The influence coefficients are used according to the equations:

$$\dot{m}^*_{rel} = \dot{m}^*_{rel,CHIC}\left(1 + \frac{a_{VIGV}}{100}\Delta\xi\right),\ a_{VIGV} = \frac{\delta(\dot{m}^*_{rel})}{\delta(\Delta\xi)} \quad (1)$$

$$\pi_{rel} = \pi_{rel,CHIC}\left(1 + \frac{b_{VIGV}}{100}\Delta\xi\right),\ b_{VIGV} = \frac{\delta(\pi_{rel})}{\delta(\Delta\xi)} \quad (2)$$

$$\eta_{rel} = \eta_{rel,CHIC}\left(1 - \frac{c_{VIGV}}{100}[\Delta\xi]^2\right),\ c_{VIGV} = \frac{\delta(\eta_{rel})}{\{\delta(\Delta\xi)\}^2} \quad (3)$$

The preceding equations show a linear behavior for pressure ratio and mass flow, whilst the efficiency follows a quadratic behavior (Kurzke, 2007). Furthermore, this behavior is empirically shown by e.g. (Savic, et al., 2005) and (Lechner, et al., 2003). The gas turbine model has been tuned to fit published data of the actual engine (Fredriksson Möller, et al., 2005).

4. PART LOAD CONTROL

A single-shaft gas turbine has two parameters for controlling the load; the variable inlet guide vanes (VIGV) and the firing level. The VIGV controls the inlet flow angle of the compressor and thereby the axial velocity e.g. the mass flow. Decreasing the mass flow will reduce the pressure ratio of the turbine, especially when operating in the choked area. The VIGV will, by decreasing the expansion ratio, increase the exhaust gas temperature, this is a loss to the GT alone, but in a combined cycle all of the energy in the exhaust gas of the GT is recovered in the steam cycle.

Using the firing level as load control is not good for the combined cycle efficiency, both the Brayton and the Rankine cycle suffers from a reduced maximum temperature. However, the maximum temperature in the GT is crucial for the lifing of the hot parts and lowering it will extend the lifetime extensively.

In the steam cycle sliding pressure operation is used to cope with the decreasing flue gas flow, which is the source of heat. For further information on steam turbine control the reference (Cotton, 1998) is recommended. At full load the gas turbine accounts for two thirds of the total power output, however at low loads the gas turbine efficiency is poor and relatively more energy is available in the bottoming steam cycle. At about 40 – 50 % load half of the power output is produced in the steam cycle.

4.1. The high EGT strategy

The general method of controlling the load of combined cycles is to use VIGV down to a point where the maximum exhaust temperature is reached, where after the firing temperature is reduced as VIGV continues to close. When the VIGV has reached its fully closed position the firing temperature is the only option for further reduction in load. The method gives good part load efficiency and is well established.

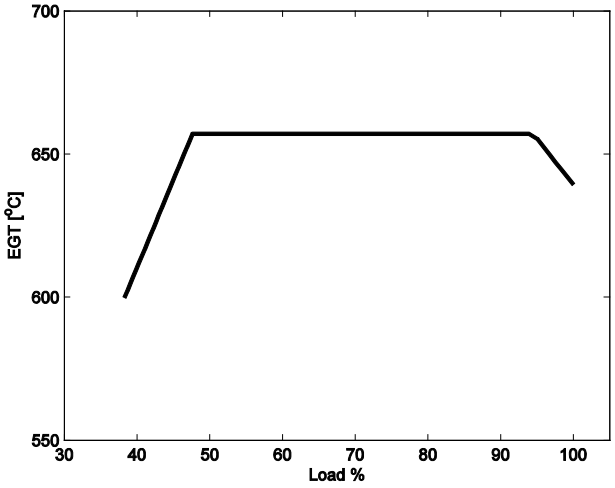

Figure 2. Load control with “high EGT” strategy

Figure 2 illustrates how the EGT increases when the VIGV decreases the compressor flow down to a certain load where the maximum EGT is reached. At what load this occurs is depending on the ambient conditions, Fig. 2 shows ISO-conditions. From here on the EGT is kept constant by reducing the firing level as VIGV continues to close. At approximately 50 % load the VIGV has reached its fully closed position and the firing level is reduced to decrease the load further.

Clearly the method keeps a very high EGT far down in the load range; therefore high graded heat is available for steam generation. To obtain the best efficiency in a steam turbine it should be operated at the highest possible steam temperature. Therefore the heat recovery steam generator (HRSG) is designed to deliver steam at this temperature at full load. To ensure that the steam temperature doesn't exceed this value, a spray in front of the final superheater is used to control the temperature. When the GT load is reduces with VIGV and the EGT is increased the spray mass flow will increase in order to keep down the superheat temperature. For this reason, the higher EGT cannot be utilized in the most optimal way.

4.2. The constant SHT strategy

This novel strategy was first introduced in (Fredriksson-Möller, et al., 2005). The foundation of this method is that the spray is thermodynamicly unsound for the steam cycle and heat recovery steam generator (HRSG). Since there are limitations in maximum steam temperature, the high exhaust temperature cannot be fully utilized in terms of admission temperature in the steam cycle. Hence, little is gained in performance at the expence of reduced lifing. To avoid spraying, the firing level is instead reduced in such a way that the steam superheating temperature (SHT) is kept constant as the VIGV reduces the load. The normal stategy when operated in a combined cycle, is to maintain a high exhaust temperature in order to have a high avarage temperature in the HRSG. This strategy is not sound in simple cycle mode since a high exhaust temperature means more unrecovered energy. This should be balanced by the gain in efficiency from having a better operational point in the compressor map when operated in high temperature mode. This could be visualized by studying a normal compressor map, where constant VIGV setting would result in more vertical movement in the map, hence, normally moving in a direction with steep efficiency gradients and potentially falling out of the high efficiency range. The high temperature strategy, with its usage of VIGVs, will shrink the compressor map. The result is a more favourable compressor operation.

Figure 3 shows how the EGT is increased with the constant SHT method wilst it is at the highest allowed level during a great part of the load range for the high EGT strategy.

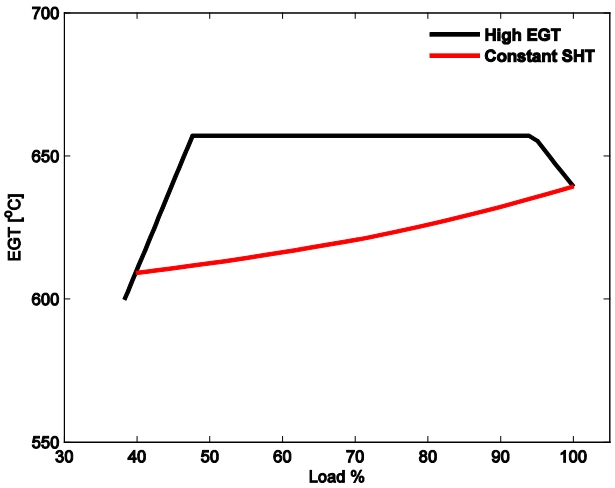

Figure 3: Comparison of EGT for the two strategies

5. THE SPRAY

In order to control the turbine admission temperature water is injected into the steam before the final high-pressure superheater and the reheat superheater. The spray water is extracted from just after the feedwater pumps i.e. this water will skip a great section of the HRSG making the heat recovery less optimal. The optimal TQ-diagram is fully reversible hence the flowing fluids must have the same temperature at all time. In accordance with the second law of thermodynamics one of the fluids must be warmer than the other in order for energy to be transferred. To optimize a HRSG the difference in temperature between the flue gas and the water/steam must be minimized within economic constraints.

$$Q = \dot{m} c_p \Delta T \tag{4}$$

In Fig. 3 a TQ-diagram of the HRSG's four last sections is shown, the sprays occur as vertical lines. Obviously vertical movement in a TQ-diagram is devastating for the heat recovery. Equation (4) indicates that the derivate in a TQ-diagram represents $\dot{m} c_p$. If the difference in derivates of the two lines can be minimized the area between the fluids can be reduced, hence more optimal heat recovery can be achieved. The spray mass flow, which for the worst case represents 12% of the total superheater mass flow, skips a great part of the HRSG. As seen in Fig. 3 the gradient of the steam before the spray is very steep and grounds in less optimal heat recovery. If the spray could be avoided, the mass flow in the section between the feedwater pump and the final superheater would increase, this would favor the heat recovery.

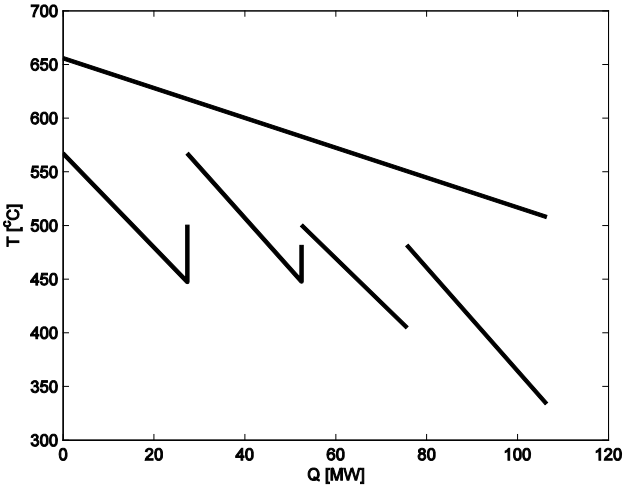

Figure 4. TQ-diagram for the last section of the HRSG, sprays occurs as vertical lines

6. LIFING AND MAINTENANCE

Key parameters for successful power plant operation are; fuel burn (and CO_2-emission) and maintenance costs. A high efficiency plant has lower fuel burn, hence lower operational costs and CO_2-fees. The driver for gas turbine efficiency is mainly pressure ratio, whilst a combined cycle unit requires high exhaust temperature for optimum cycle performance. These two cycle requirements result in high firing level and hot components. The dominating turbine failure mechanisms are creep and hot corrosion, which both are heavily temperature dependent. This dependency is highly non-linear and a modern unit is typically operated at levels where the slopes are steep, hence a small change in temperature will have a great affect. A state-of-the-art engine is therefore quite delicate in terms of hot-section component lifing, with high replacement costs.

6.1. General Gas Turbine

Depending on the service-duty of a gas turbine different failure mechanism will occur. Thermal fatigue is the dominant limiter for peaking machines, while creep and corrosion are the dominant limiters of life for continuous duty machines.

Thermal fatigue is caused by cyclic stresses, such as cycling the engine from idle to peak load. Cyclic operation is typical for peaking machines; these machines have a very varying operation. The temperature gradients within the airfoil will cause tension in the material. With cyclic operation the inertia of the system will increase the temperature gradients even more. Thermal fatigue weakening the material and will eventually initiates crack formation and propagation.

Creep is plastic deformation of the airfoil that occurs after a long period of exposure to stress at high temperature. Creep is not caused by extreme operation it is actually caused by moderate loads which normally only would cause elastic deformation, but when applied over long periods of time some plastic deformation is likely to occur. The amount of permanent deformation is depending on the material, the applied load, the temperature and time. Creep is very temperature dependent; a higher temperature will increase the rate of creep. As a rule of thumb, each 11 K increment will reduce the lifing by a factor of half.

Corrosion caused by oxidation or sulfidation consumes the walls of the airfoils making them thinner and weaker. Sulfidation is a low temperature phenomenon depends on the sulfur content of both the fuel and the intake air. Natural

gas is very clean and does not impose sulfidation. Sulfidation occurs when sodium sulfate condensates on the blade surface. Condensation occurs when the airfoil temperature is less than the boiling temperature of sodium sulfate, and the liquid attacks the metal surface. Oxidation on the other hand is a high temperature phenomenon. At the regions where the surface temperature is extremely high the metal reacts with the oxygen in the gas. Again, despite the fundamental difference between creep and oxidation, the relationship between lifing and firing level is about the same as for creep.

6.2. Fixed speed heavy frames

A single shaft design of this size is always operated non-geared at synchronous speed, since there are no gears available above 100 MW. These large sized gas turbines are always operated at 3000 and 3600 rpm, for 50 and 60 Hz, respectively. The blade/disc stress level can be thought of in terms of AN^2, which simply is the product between annulus area and the shaft speed squared. The normal range for AN^2 is $50\text{-}60 \cdot 10^6$. For fixed speed machines this factor is constant throughout the load range. At the last stage the stress levels are great due to a large annulus area. Therefore, the dominating life limiter for a last stage is creep. Since the creep rate is a function of the temperature, operation at elevated exhaust temperatures (with nominal firing) with closed VIGV, therefore affects the last stage lifing. The last rotor temperature environment i.e. inlet relative total temperature, sets the metal temp for the (normally) uncooled last rotor. If the engine is operated at part-load with nominal firing level, then the exhaust temperature is higher than at full load. It is intuitive to assume that the last rotor should experience the same increase in temperature. This is, however, not generally the case since the last stage vane which sets the relative inlet state is unaffected since the row pressure ratio is unchanged. The stage will off-load and have lower reaction level – but the inlet relative total temperature to the last rotor is unchanged. This reasoning is strictly valid for a choked rotor throat and all turbines will fulfill some kind of radial equilibrium (and 3D effects) that most likely will result in a subsonic rotor at the lower part of the blade.

For the front stage creep is a problem but here, where the temperature is much more extreme, oxidation is added as a further complication. This will have a great effect in high loads, especially from 90 to about 100 % load where the high EGT utilizes a maximum COT.

7. RESULTS

The main target was to extend the gas turbine lifing without suffering too much in terms of combined cycle efficiency. The cycle efficiency for the two strategies is plotted in Fig. 4. The difference between the two methods is very small, maximum 0.25 percentage points.

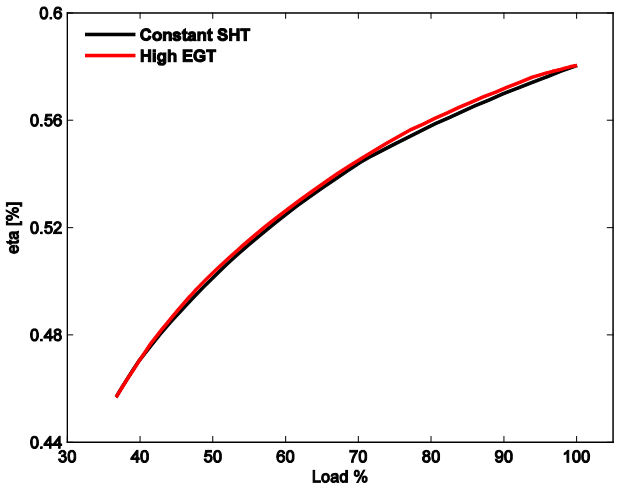

Figure 5. Efficiency comparison of the two methods

The lifing of machine parts is expected to be extended by decreasing temperatures. A lower COT will reduce the rate of oxidation, especially in the first stage. The reduction in EGT is expected to reduce the creep rate in the final rotor. In Fig. 6 both COT and EGT is plotted during the load range of the two control strategies. The high EGT method maintains the COT until maximum EGT is reached; at this point the difference in COT between the two methods is approximately 25 °C. From this point the difference increases all the way down to the point where the high EGT strategy has reached the maximum VIGV angle. Here the difference is 45 °C.

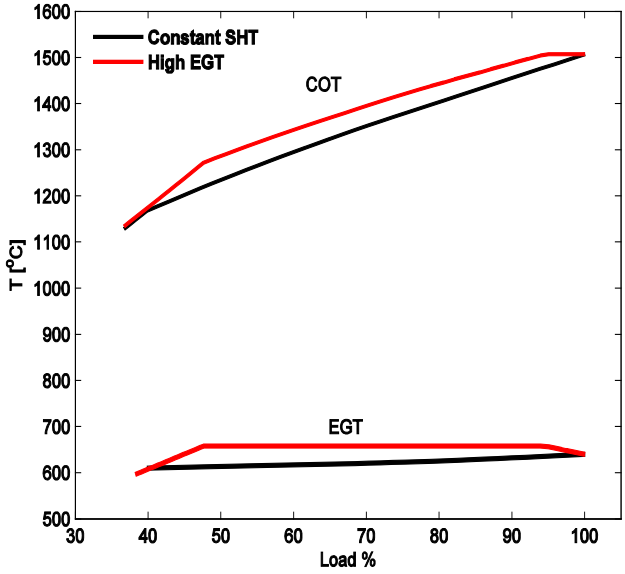

Figure 6. COT comparison of the two methods

In reference (Balevic, et al., 2004) the lifing penalty due to increased rating is given as: 1:1 at datum level, 6:1 at 56 K increase and 36:1 at 111 K increased firing. This can be thought of as 6 times shorter lifing interval at 56 K peak rating and 36 times at 111 K peak rating, respectively. In this interval the behavior is exponential but extrapolation may be dubious. An exponential fit to the mentioned values results in:

$$M_f = e^{0.0323\,\Delta COT} \tag{5}$$

Where M_f is the maintenance factor and ΔCOT is the change in COT compared to the base load level. The reduction in COT will have greatest effect on the lifing when it is reduced from a high starting point; therefore the point where maximum EGT just have been reached with the high EGT method is of great interest. The preceding equation shows the classic factor of two per 11 K increase in blade temperature, which translates into some 15 to 20 K COT for a cooled blade. Here the difference is 25 K, which if (1) is applied, will return a maintenance factor of 0.44 or an increased maintenance interval by 2.24 times.

Equation (5) only considers the influence of COT to the maintenance interval and is only valid in a range where the COT is not deviating much from the base load value. Further down in the load range the weight of COT is smaller. The standard method (high EGT) uses the maximum allowed EGT all the way down to somewhere around 50 % load, by applying the new method the final stage will experience a reduced temperature throughout almost the whole load range. Increasing the lifing of the last stage will probably not extend the maintenance of the whole machine but it will certainly affect the repair costs of the machine.

8. CONCLUSION

Heavy frame gas turbines are always operated at either 3000 or 3600 rpm, for 50 and 60 Hz, respectively. Blade and disc stress i.e. centrifugal scales with AN^2, hence constant throughout the load range. This means that the only primary variable, in terms of lifing, is the temperature. A common strategy for combined cycle power plant is to maintain the highest possible COT at part load by using the VIGV. This result in a decreased mass flow, hence a smaller pressure ratio and increased exhaust gas temperature. A higher firing level typically results in less unburnt and CO in the flue gas and there is normally no need for e.g. by-pass systems. A high COT increase both the rate of oxidation and creep and a high exhaust gas temperature increases the creep rate at the last rotor. In the steam generation large amount of water spray is needed to not exceed the maximum steam turbine admission temperature. Hence, the high graded available heat cannot be utilized in a thermodynamically good manner.

An alternative strategy for load control of combined cycle power plants has been evaluated and explained. By controlling the firing level in such a way that no spray is needed in order to keep the steam superheating below its maximum allowed level, the machine lifing can be increased. It is shown that by changing the strategy the maintenance interval can be extended with close to no efficiency penalty at all, due to a more optimal steam generation. At 90 % load the maintenance interval can be extended with a factor of about 2.2.

ACKNOWLEDGEMENTS

The authors wish to acknowledge Eon for supplying background material and funding for this research. The authors also acknowledge Dr Raik C. Orbay, Dr Andre Hildebrandt, Markus Truedsson and Marco Lorenz for the early development of the off-design models.

REFERENCES

Balevic David, R. Burger and D. Forry, Haevy-Duty gas turbine operating and maintenance considerations: GE Energy, 2004.

Cotton K. C., Evaluating and improving steam turbine performance. - New York, 1998. - Vol. Second Edition.

Fredriksson Möller B., M. Genrup and M. Assadi, On the off-design of a natural gas-fired combined cycle with CO_2 capture // Energy. - Lund, 2005.

Gülen S. C., P. R. Griffin and S. Paolucci, Real-time in-line performance diagnostics of heavy-duty industrial gas turbines. Journal of Engineering for Gas Turbine and Power, 2002. - 911 : Vol. 124.

Jonshagen Klas, Genrup Magnus and Eriksson Pontus, Low-calorific fuel mix in a large size combined cycle plant. - Lund : Asme Turbo Expo, 2009. - Vols. GT2009-59329.

Kehlhofer Rolf H., Combined-Cycle Gas & Steam Turbine Power Plants. - Tulsa, Oklahoma: PennWell Publishing company, 1999.

Kurzke Joachim, Manual for GasTurb 11. - Germany, 2007.

Lechner Christof and Seume Jörg, Stationäre Gasturbinen: Springer-Verlag Berlin Heidelberg, 2003.

Savic Sasha M., Micheli Marco A. and Bauer Andreas C., Redesign of a multistage axial compressor for heavy duty industrial gas turbine, Turbo Expo. - Nevada : ASME, 2005. - Vols. GT2005-68315.

Walsh Philip P. and Fletcher Paul, Gas Turbine Performance 2nd ed.: Blackwell Science Ltd. ISBN 0-632-06434-X, 2004.

Vuorinen Asko, Planing of optimal power systems. Vammala Kirjapaino Oy, Vammala, Finland. ISBN 978-952-67057-1-2, 2009.

RESPONSIBILITY NOTICE

The authors are the only responsible for the printed material included in this paper.